Gifford & Partners

The Mersey Gateway - A New Mersey Crossing Phase II Modelling: Construction Options

Date: July 2005

Project Ref: R/3411/1

Report No: R.1180

ABP mer
marine environmental research

Gifford & Partners

The Mersey Gateway - A New Mersey Crossing
Phase II Modelling: Construction Options

Date: July 2005

Project Ref: R/3411/1

Report No: R.1180

Version	Details of Change	Authorised By	Date
1	Draft for Comment	J M Harris	04.02.05
1.1	2nd Draft for Comment	J M Harris	04.03.05
2	Final	J M Harris	22.06.05
3	Client Revised Final	J M Harris	20.07.05

Document Authorisation		Signature	Date
Project Manager:	J M Harris	John Harris	20/07/2005
Quality Manager:	R H Swift	RH Swift	20/07/2005
Project Director:	W S Cooper	W.S. Cooper	20-7-5

ABP Marine Environmental Research Ltd
Pathfinder House
Maritime Way
SOUTHAMPTON
Hampshire
SO14 3AE

Tel: +44(0)23 8033 8100
Fax: +44(0)23 8033 8040
Web: www.abpmer.co.uk
Email: enquires@abpmer.co.uk

Summary

The aim of this report was to investigate possible construction schemes for the preferred Route 3A option. As in the previous modelling work undertaken for Phase II, two higher resolution models were applied. The set up for the model grids and the calibration and validation of these models is described in Appendix A of ABPmer (2004).

As previously, the main concerns to be addressed in the modelling study can be summarized within the following topics:

- Flood defence and intertidal habitats
- Channel morphology
- Scouring around bridge piers
- Potential impacts on the SSSI site downstream of Runcorn
- Potential impact on existing structures, in particular the Manchester Ship Canal

The use of two models was necessary so that the morphological modelling undertaken to assess longer-term changes could be carried out within a reasonable time-scale. The hydrodynamic model set up is computationally intensive with calculations taking the order of weeks to run a simulation over a 14 days spring-neap cycle. Such time-scales are not practical for the morphological runs (see ABPmer, 2004) as the introduction of morphology increases the model run times.

Three possible construction schemes have been modelled as given below:

(1) Island construction scheme - Spring-neap cycle
(2) Aligned jetty - Spring-neap cycle
(3) Spike Island jetty - Spring-neap cycle

The key hydrodynamic processes that have been investigated in this part of the study are water level, bed shear stress and velocity. In addition to this a morphological model has been run. The detailed hydrodynamic and morphological results are shown in Appendices A and B, respectively. For the purposes of comparison the hydrodynamic results have been run for a spring-neap cycle except for the extreme surge and fluvial event, which was run for a 4 days period. Similarly, the morphological model has been run for a spring-neap cycle, which has been scaled to represent a 1 year period for all results except for the extreme event scenarios, where no scaling factor was applied. Based on the results of the study the following key points have been made.

- Based on the results of the hydrodynamic and morphological modelling all the construction schemes tested have a greater impact on the upper estuary than during the “as built” operational phase.

- With reference to the hydrodynamic and morphological change of the construction schemes tested the two temporary jetty schemes show the least impact on the system.

In addition to these tests, additional modelling has been undertaken using the aligned jetty scheme. This has been assessed using the 2002 bathymetry for an extreme surge and fluvial event as well as a new bathymetric layout using bathymetry collected in 2005, which shows a different channel configuration in the upper estuary. For the 2005 bathymetry the model scenarios investigated a spring-neap tidal cycle and an extreme surge and fluvial event. Based on these scenarios the following conclusions can be made:

- Under extreme conditions (1:200 years return surge and fluvial event) the magnitude and extent of change as a result of the proposed crossing is increased. However, such events are infrequent and the extent of change is limited to about 2km upstream and downstream of the proposed crossing. In addition, backwater effects are generally limited between peak flood and high water and are low in magnitude and of limited duration.

- The causeway appears to have little impact on the hydrodynamics except around high water on spring tides when the water levels are high enough to extend onto this part of the intertidal shore. There is some indication of increased flows circulating along the side of the causeway during this period, which may lead to some scouring at this location.

- The use of the 2005 bathymetry in the modelling leads to in a change in dominance from the north to the south channel due to the change in channel configuration. In addition, whilst the overall pattern of change is different, the extent and magnitude of the change is of a similar order to that predicted using the 2002 bathymetry. Therefore, it is suggested that for different channel configurations, whilst the spatial pattern of change may vary, particularly local to the structures, the overall magnitude and extent of change remains similar.

Based on the additional modelling undertaken it is this latter point that is of key importance as it suggests that regardless of the position of the channels relative to the proposed crossing the magnitude and extent of change within the system will be of a similar order.

The Mersey Gateway - A New Mersey Crossing
Phase II Modelling: Construction Options

Contents

Appendices

Tables

Figures

1. Background

Halton Borough Council wishes to relieve the congestion at the existing road crossing, the Silver Jubilee Bridge, carrying the A557 across the Mersey at Runcorn, through the construction of a new bridge crossing over the estuary. ABP Marine Environmental Research Ltd. (ABPmer) was commissioned by Gifford & Partners on behalf of Halton Borough Council to carry out fieldwork and undertake a numerical modelling study. In Phase I of the study five possible route options were assessed, including different span designs. Eleven options were tested in total, excluding the baseline case (existing conditions). Under Phase II of the study, the preferred scheme was modelled in detail using a high-resolution model scheme. The aim of this part of the Phase II study was to investigate possible construction schemes for the preferred Route 3A option.

The Mersey Estuary is located in the north west of the UK. The outer estuary forms Liverpool Bay, a generally shallow region containing large areas of sandbanks that are exposed at low water. Liverpool Bay is bounded to the east by the Lancashire coast, from Seaforth to Formby Point; and to the south by the Wirral Peninsula, from Hilbre Point at the mouth of the Dee Estuary, to New Brighton at the mouth of the River Mersey. Within The Narrows at New Brighton the width of the Mersey is 1.5km, approximately, and at Pier Head the river narrows to about half this width (Figure 1). Beyond The Narrows is a large tidal basin, classified as the inner estuary, which widens to a maximum width of about 5.5km. The upper estuary extends for a distance of about 42km from the Dingle to Howley Weir. At low water almost all the tidal basin dries out leaving three channels, Garston, Middle Deep and Eastham. In the area of the proposed new bridge crossing (Runcorn Gap - Fiddler's Ferry) the low-water channel meanders through large areas of sand and mud banks (Figure 2).

The Mersey has been classified as a coastal plain estuary formed during the Holocene transgression through the flooding of pre-existing valleys in both glaciated and unglaciated areas. Typical characteristics of such estuaries are large width to depth ratios (dependent on rock type), low river flows compared with the volume of the tidal prism and low fluvial sediment transport. The geological constraints that exist in the Mersey basin mean that the large width to depth ratio is not a characteristic of large parts of the estuary. McDowell (1964) described the tidal mouth of the Mersey as a tidal inlet since the inner basin between Hale Head and The Narrows was not formed by the action of the rivers that discharged into it.

This report provides details of the modelling undertaken to assess several possible construction schemes for the Route 3A Medium Span Revised 3 Tower alignment. The report should be read in conjunction with ABPmer (2004) Report No R.1151. Section 2 provides a summary of the construction schemes tested whilst Section 3 summarises the main results from the numerical modelling study. The model results are discussed in more detail in Appendices A and B. Section 4 presents a discussion of the findings and Section 5 the main conclusions from the study.

2. Construction Schemes

This report provides details of the modelling undertaken to assess possible construction schemes for the proposed new bridge crossing over the Mersey Estuary. This detailed phase of modelling has only investigated the impact of the preferred scheme option Route 3A. Within the previous part of this modelling phase, reported in ABPmer (2004) Report No R.1151, several alternative pier/tower layout and alignment options have been tested. The various options tested are as follows:

(1) Route 3A Medium Span original alignment (Drawing No. B4027/2/B/361).

(2) Route 3A Medium Span modified alignment (Drawing No. B4027/3/H/G/3).

(3) Route 3A Medium Span 3 Tower alignment (Drawing No. B4027/3/B/300).

(4) Route 3A Medium Span Revised 3 Tower alignment (Drawing No. B4027/3/ B/300 Rev. A).

(5) Route 3A Short Span (Drawing No. B4027/3/B/301).

In the current work only one of these Route 3A alignment options has been tested with the proposed construction approaches, the Route 3A Medium Span Revised 3 Tower alignment (Drawing No. B4027/3/B/300 Rev. A) see also Figure 3. Therefore, from this point forward this alignment option will be referred to as the 'preferred option'.

ABPmer were instructed to undertake modelling on three possible construction schemes, which are described briefly below. For further details see Gifford(2005).

2.1 Island Construction Scheme

The island construction scheme requires hovercraft access to supply materials to site. Each island will be 60m x 58m, approximately, and aligned to minimize the impact on the hydrodynamics. Cofferdams, 30m in diameter, will be placed within the plan area of the island. It is envisaged that the islands will need to be in place for a period of 18 months. The layout of the island construction scheme is shown in Figure 4A.

Figure 4B shows the representation of the islands within the high-resolution hydrodynamic numerical model. The islands have been included as a change in the bathymetry. It is assumed that the islands cannot be flooded even on extreme water level events such as storm surges.

2.2 Aligned Jetty

The aligned jetty structure extends out into the estuary from both banks (see Figure 5A and 6) with no linkage between the two halves. The jetty structure itself consists of 6m wide deck on top of pairs of 0.5m diameter piles 5m apart at 12m centres. There will be finger jetties incorporated adjacent to each bridge tower. The towers will each be constructed within 30m diameter cofferdams. It is possible that these temporary structures will be in place for up to a period of one year. Access to the jetty across the intertidal area is provided by means of a stone haul road or causeway built across the saltmarsh at Widnes Warth.

2.3 Jetty from Spike Island

The temporary jetty structure from Spike Island extends into the estuary from the north bank only. The jetty structure provides access to all three bridge towers with finger piers servicing each tower structure. The towers will each be constructed within 30m diameter cofferdams. As with the temporary jetty, the structure consists of 6m wide deck on top of pairs of 0.5m diameter piles 5m apart at 12m centres. Again, it is possible that these temporary structures will be in place for up to a period of one year. Figure 5B shows the proposed layout of this construction scheme (see also Figure 6).

3. Modelling Results

A detailed description of the numerical modelling results is presented in Appendices A and B. The aim of this part of the Phase II study was to investigate possible construction schemes for the preferred Route 3A option. As in the previous modelling work undertaken for Phase II, two higher resolution models were applied. The set up for the model grids and the calibration and validation of these models is described in Appendix A of ABPmer (2004).

As previously, the main concerns to be addressed in the modelling study can be summarized within the following topics:

- Flood defence and intertidal habitats
- Channel morphology
- Scouring around bridge piers
- Potential impacts on the SSSI site downstream of Runcorn
- Potential impact on existing structures, in particular the Manchester Ship Canal

The use of two models was necessary so that the morphological modelling undertaken to assess longer-term changes could be carried out within a reasonable time-scale. The hydrodynamic model set up is computationally intensive with calculations taking the order of weeks to run a simulation over a spring-neap cycle. Such time-scales are not practical for the morphological runs, which would be the order of months just for a 15 days simulation (see ABPmer, 2004).

As previously, the bridge piers, towers and cofferdams in the two models have been simulated using a combination of approaches. Where bridge piers and towers are the same size as the model grid cells, the cells have been closed off as they are effectively blocked for the transmission of fluid flow. However, where the bridge piers are smaller than the grid cell size added friction terms have been used to represent the piers. In this manner there is an allowance for some flow transmission across the cell, even if that flow is low. Whilst the piers and towers are octagonal in shape their representation in the model when represented as solid structures is as rectangles. However, it is not considered that pier shape will have a significant impact on the results as flow separation and viscous effects are excluded from the model solution and only flow transmission effects as a result of blockage are simulated.

3.1 Hydrodynamic Modelling

3.1.1 Introduction

The detailed modelling has concentrated on investigating the impact of possible construction schemes with the preferred option as shown in drawing B4027/3/B/300 Rev. A. Below are listed the model runs undertaken:

- Preferred option (Drawing No. B4027/3/B/300 Rev. A):
  - Island construction scheme - Spring-neap cycle
  - Aligned jetty - Spring-neap cycle
  - Aligned jetty - High fluvial (1:200 year event) and corresponding 1:200 year surge event
  - Spike Island jetty - Spring-neap cycle
  - New bathymetry - aligned jetty spring-neap cycle

The key hydrodynamic processes that have been investigated in this part of the study are water level, bed shear stress and velocity. Results have been presented as changes relative to a baseline case. The bed shear stress is the frictional force exerted on an area of seabed or river bed by current flowing over it. Therefore, it is an important quantity in the study of sediment transport processes, because it represents the flow-induced force acting on the bed sediments. The detailed hydrodynamic and results are shown in Appendix A.

3.1.2 Water Level Changes

Changes in water level can impact on the ability of the estuary to discharge flood waters effectively, may have implications for quay/river wall stability and may also affect intertidal habitats. Therefore, to assess the various construction schemes proposed for the preferred option the various sets of results from the hydrodynamic model have been analysed.

For all the construction schemes considered, there is an observed backwater effect around peak flood tide as a result of the reduced cross-sectional area. This effect is greatest within the north channel. However, for the island construction scenario this backwater effect is not limited to the flood tide although the observed effects are greatest over this period (Figure 7A). The flood tide period creates the biggest changes due to the strong tidal asymmetry in the tidal curve with a very short flood period ($\approx$ 1.5 hours) and a much longer ebb period ($\approx$ 11 hours).

The results from the two jetty schemes are very similar as many of the piers are situated on the intertidal banks and, therefore, are only exposed to the flow at certain states of tide, reducing their overall impact on the system. However, for 2002 channel configuration the island construction scheme results in a greater reduction in cross-sectional area over the whole channel width, which may lead to a larger impact on water levels. However, this effect will be dependent on channel position and its approach to the temporary islands as well as the state of the tide.

As the flooding or ebbing tide moves onto or off the intertidal areas large differences can be manifested along the front of the tidal wave (for example Figure 7B). These differences do not, generally, represent a real change in height rather they are an artefact of phase differences in the propagation of the tidal wave. Figure 8 shows the variation in water level around high water between the baseline case and the island construction scheme. The figure shows both a difference in phase as well as magnitude. Table 1 shows a comparison of the maximum and minimum water level values at positions around the piers/cofferdams, within the channels, and over the intertidal areas. The maximum and minimum values found within the channels are the most appropriate indicator of change as it is more likely these represent a change in the main water body rather than a localized variation in water level. The preferred option as modelled under its operational phase is included for comparison purposes.

Regarding the jetty schemes, it is assumed that the deck of the jetty is high enough above the water surface to prevent it being inundated on high spring tides and tidal surges (pressure flow scour).

Table 1. Comparison of maximum and minimum changes in water level over a spring tide

Scenario	Position	Water Level (m)							
		Low Water		Peak Flood		High Water		Peak Ebb	
		Max	Min	Max	Min	Max	Min	Max	Min
Preferred option (operational phase)	Piers	0.08	-	0.02	-0.07	0.01	-0.02	0.08	-0.07
	Channels	-	-	-	-0.03	-	-	-	-
	Intertidal	0.14	-0.09	0.12	-0.10	-	-0.02	0.08	-0.06
Island construction scheme	Piers	0.12	-	0.15	-0.16	0.03	-0.05	0.11	-0.03
	Channels	-	-	0.09	-	0.01	-0.02	0.02	-
	Intertidal	0.03	-0.08	0.13	-0.09	0.02	-0.03	0.01	-
Aligned jetty	Piers	-	-	0.07	-0.04	0.03	-0.02	0.01	-
	Channels	-	-	0.03	-0.03	0.01	-	-	-
	Intertidal	-	-	0.08	-0.05	0.05	-	0.04	-0.08
Jetty from Spike Island	Piers	0.02	-0.04	0.08	-0.06	0.02	-0.05	0.02	-0.05
	Channels	-	-	0.02	-0.04	-	-	-	-
	Intertidal	0.07	-0.07	0.08	-0.16	0.07	-0.02	0.07	-0.10
Note: - = No change									

3.1.2.1 Summary

The proposed construction schemes all result in a degree of obstruction to the flow particularly on the flood tide as a result of the reduced cross-sectional area leading to some increase in water levels, particularly over the spring flood tide. The flood tide period creates the biggest changes due to the strong tidal asymmetry in the tidal curve and this effect is greatest within the north channel.

- Based on the modelling undertaken the greatest impact on water levels is observed with the island construction scheme with backwater effects predicted to occur over the peak flood to peak ebb period.

- For both of the jetty construction schemes backwater effects are limited to the flood tide period.

3.1.3 Speed Changes

3.1.3.1 Island construction scheme

The greatest changes in flow speed occur around peak flood with strong acceleration of flows past the island structure placed close to the north channel. There is also a change in flow speed within the channels. The largest extent of flow change is within the north channel. Around low water there is no significant change in speed. This is due to the fact that the island structures are outside of the channels at this state of tide.

Over the ebbing tide the island structures lead to increased flow speeds in the north channel in the vicinity of the island and on the south bank along the intertidal area downstream to Old Quay lock.

Around the time of high water there is a general change in flow speed across the whole width of the estuary due to the size of the islands, which extends over 1000m upstream from the island positions.

Maximum changes in speed along the intertidal area tend to occur on the front of the tidal wave as it propagates onto the intertidal areas However, where these observed changes occur along the edge of the propagating wave such changes are considered to be insignificant, as they are very short in duration (seconds) and affect a very limited area. In addition, such changes are considered to represent a phase change rather than an absolute change in speed.

3.1.3.2 Aligned jetty construction scheme

At low water there is some change in speed indicated to occur along the intertidal area, particularly in the region of Old Quay Lock. The increase in flow speed is caused by acceleration of the flow through the jetty structures due to reduced flow cross-sectional area, and small changes in phase of the flow due to the placement of the structures across the channel. The observed reduction in flow speed is primarily caused by the change in the phase of the flow.

At peak flood the greatest magnitude of change occurs within the north channel, with accelerated flow speeds along the intertidal areas of both the north and south channels. However, some of the changes in speed along the intertidal area tend to occur on the front of the tidal wave as it propagates onto these areas. As previously, where these observed changes occur along the edge of the propagating wave such changes are considered to be insignificant, as they are very short in duration (seconds) and affect a very limited area. In addition, such changes are considered to represent a change in phase rather than magnitude.

Around the time of high water there is a general change in flow speed across the whole width of the estuary due to the number of piers present and the 30m diameter cofferdams. There is a general acceleration of flow around the cofferdams and a reduction in flow speed in front of and behind the structures.

Over the ebbing tide the cofferdam and pier structures lead to increased flow speeds along much of the north bank along the intertidal area local to the bridge as well as along the south bank downstream of Old Quay Lock. There is also a reduction in flow speed upstream of the Runcorn Gap.

3.1.3.3 Spike Island jetty construction scheme

As with the aligned jetty construction scheme, around low water there is some change in speed indicated to occur along the intertidal area, particularly in the region of Old Quay Lock, caused by a residual change in the flow due to the presence of the jetty and cofferdam structures. This modification is an artefact of the reduced flow cross-sectional area, and small variations in phase of the flow due to the placement of the structures across the channel. The observed reduction in flow speed is primarily due to the change in the phase of the flow.

Around peak flood the greatest magnitude of change occurs within the north channel, with accelerated flow speeds along the intertidal areas of both the north and south channels. The greatest modifications occur within the north channel as this is where the greatest obstruction lies. However, some of the changes in speed along the intertidal area tend to occur on the front of the tidal wave as it propagates onto these areas. However, as previously, where these predicted variations occur along the edge of the propagating wave such changes are considered to be insignificant, as they are very short in duration (seconds) and affect a very limited area.

Table 2. Comparison of maximum and minimum changes in near-surface speed over a spring tide

Scenario	Position	Near-Surface Speed (m/s)							
		Low Water		Peak Flood		High Water		Peak Ebb	
		max	min	max	min	max	min	max	min
Preferred option (operational phase)	Piers	-	-	0.16	-0.21	0.10	-0.63	0.04	-0.23
	Channels	-	-	0.04	-0.06	0.02	-	-	-
	Intertidal	-	-	0.25	-0.28	0.03	-0.08	-	-
Island construction scheme	Piers	0.02	-0.04	1.03	-1.08	0.44	-0.90	0.43	-0.56
	Channels	-	-	0.21	-0.24	0.14	-0.15	0.02	-0.03
	Intertidal	-	-	0.33	-0.49	0.19	-0.13	0.11	-0.07
Aligned jetty	Piers	-	-	0.79	-0.79	0.14	-0.76	0.15	-0.45
	Channels	-	-	0.06	-0.06	0.03	-0.05	-	-
	Intertidal	0.11	-0.14	0.66	-0.41	0.12	-0.16	0.37	-0.11
Jetty from Spike Island	Piers	-	-	0.43	-0.71	0.69	-0.88	0.11	-0.55
	Channels	-	-	0.01	-0.02	0.05	-0.05	0.02	-0.05
	Intertidal	0.18	-0.08	0.65	-0.43	0.09	-0.05	0.35	-0.23
Note: - = No change									

Around the time of high water there is a general change in flow speed across the whole width of the estuary due to the number of piers present and the 30m diameter cofferdams. There is a general acceleration of flow around the cofferdams and a reduction in flow speed in front of and behind the structures.

Over the ebbing tide the cofferdam and pier structures lead to increased flow speeds along much of the north bank along the intertidal area local to the bridge as well as along the south bank downstream of Old Quay Lock. There is a reduction in flow speed upstream of Runcorn Gap.

3.1.3.4 Summary

The results described above represent changes over a spring tide and, therefore, as such provide a conservative view of the modification in the flow over a full spring-neap cycle by representing the period of greatest change over an average tidal cycle. The maximum and minimum variations in near-surface speed differences given in Table 2 also represent the largest change within a vertical section through the water column.

Of all the construction schemes tested the island construction scheme shows the greatest impact with maximum increases in flow speed local to the structures of the order of 1.0m/s (north channel island position).

Both of the temporary jetty construction schemes show varying degrees of change over a spring tidal cycle and, as such, have a similar order of impact within the upper estuary.

In general, the greatest differences in speed occur around the island/cofferdam structures as a result of the changes in flow transmission due to the presence of the structure.

3.1.4 Bed Shear Stress Changes

3.1.4.1 Island construction scheme

For the proposed island construction scheme the largest difference in bed shear stress occurs around peak flood with the greatest increase occurring in the north channel. In general, the largest changes are confined to the immediate locality of the bridge. The difference in bed shear stress along the front of the tidal wave as it propagates onto the intertidal banks is considered to represent a phase change between the baseline case and scheme rather than an absolute increase. Although Table 3 indicates large changes in bed shear stress along the intertidal area many of these changes are due to this change in the phase of the flow propagation. However, some of these large changes are real and are caused by the obstruction across the channel that this scheme represents.

Around peak ebb the modelling indicates that there is a reduction in bed shear stress within the north channel and an increase in bed stress in the south channel. This is likely to be due the greater blockage effect observed in the north channel leading to an

increase in flow within the south channel. This may lead to a change in the channel dominance at least for the duration of the island placements.

3.1.4.2 Aligned jetty construction scheme

Around low water the greatest extent of change in bed shear stress for the proposed aligned jetty construction scheme occurs along the southern bank between the proposed crossing and Runcorn.

Around peak flood the largest changes are confined to the immediate locality of the cofferdam and pier structures. As the front of the tidal wave propagates onto the intertidal banks the difference in bed shear stress is considered to represent a phase change between the baseline case and scheme as discussed previously.

Around high water the greatest increases in bed shear stress occur around the temporary structures. However, the largest predicted change is a reduction in bed shear stress along the intertidal area. This is probably caused by a combination of blockage effects from the structures together with a phase change between the baseline case and the scheme.
Around peak ebb the modelling indicates that there is a general increase in bed shear stress within the north and south channels particularly along the intertidal area. This is likely to be due to the acceleration of flows around the temporary structures and the greater blockage effect within the channels. Between Old Quay Lock and Runcorn Gap there is a reduction in bed shear stress, which might lead to a build up of sediment over the banks in this area.

3.1.4.3 Spike Island jetty construction scheme

For the proposed temporary jetty from Spike Island around low water the greatest extent of change in bed shear stress occurs along the southern bank between the proposed crossing and Runcorn Gap due to a residual change in the flow caused by the presence of the jetty and cofferdam structures. This change is a result of the reduced flow cross-sectional area, and small changes in phase of the flow due to the placement of the structures across the channel.

Around peak flood the largest changes are confined to the immediate locality of the cofferdam and pier structures. The largest changes in bed shear stress along the intertidal areas are located in the north channel. Many of these changes in bed shear stress along the intertidal area are due to a change in the phase of the flow propagation.

A round high water the greatest increases in bed shear stress occur around the temporary structures. However, the largest predicted change is a reduction in bed shear stress around the structures. This is primarily caused by the blockage effect from the temporary structures.

Table 3. Comparison of maximum and minimum changes in bed shear stress over a spring tide

Scenario	Position	Bed Shear Stress (N/m²)							
		Low Water		Peak Flood		High Water		Peak Ebb	
		max	min	max	min	max	min	max	min
Preferred option (operational phase)	Piers	-	-	2.68	-4.95	0.82	-2.02	0.28	-0.67
	Channels	-	-	0.17	-0.12	0.09	-0.02	-	-
	Intertidal	-	-	0.84	-0.72	0.14	-0.09	-	-
Island construction scheme	Piers	0.09	-0.07	11.20	-8.33	1.91	-2.51	2.11	-1.08
	Channels	-	-	0.32	-0.54	0.53	-0.47	0.12	-0.15
	Intertidal	-	-	3.17	-2.56	1.16	-2.56	0.35	-0.24
Aligned jetty	Piers	0.04	-0.09	8.40	-3.85	0.78	-2.45	0.61	-1.37
	Channels	-	-	0.92	-0.49	0.03	-0.04	0.12	-0.28
	Intertidal	0.93	-0.59	6.78	-3.20	0.35	-8.43	2.02	-0.35
Jetty from Spike Island	Piers	0.10	-	3.51	-6.93	1.99	-2.48	0.99	-0.93
	Channels	-	-	0.17	-0.24	0.13	-0.12	0.14	-0.24
	Intertidal	0.69	-0.27	9.26	-6.00	0.34	-0.48	1.91	-0.48
Note: - = No change									

Around peak ebb the modelling indicates that there is a general increase in bed shear stress within the north and south channels particularly along the intertidal area. This is likely to be due to the acceleration of flows around the temporary structures and the greater blockage effect within the channels. Between Old Quay Lock and Runcorn Gap there is a reduction in bed shear stress, which might lead to a build up of sediment over the banks in this area (see Table 3).

3.1.4.4 Summary

The results described above represent changes over a spring tide and, therefore, as such provide a conservative solution over a full spring-neap cycle as they are representative of the period over which greatest impact on the system is likely to occur.

From the modelling of the proposed construction schemes the Island construction scheme has the greatest impact. However, both of the temporary jetty construction schemes may result in a build up of sediment over the banks between Old Quay Lock and Runcorn Gap.

For all of the construction schemes tested the greatest changes observed are local to the island/cofferdam structures.

The difference in bed shear stress along the front of the tidal wave as it propagates onto the intertidal banks is considered to represent a phase change between the baseline case and scheme rather than an absolute increase.

3.1.5 Aligned Jetty Extreme Fluvial and Surge Event - 1:200 Return Period

From the analysis of the results from the simulations for the various construction schemes the jetty schemes demonstrated the least impact on the system. After discussions with Giffords it was decided to undertake some additional simulations using the aligned jetty scheme. The scenario applied corresponded to the extreme fluvial and surge event (with a 1:200 years return period) used previously and defined in Appendix B ABPmer (2004). The shape of the surge tide was determined from a surge event recorded at Gladstone Dock. The recorded tidal curve was 'stretched' to fit the 1:200 years return event as quoted in Environment Agency (1998).

3.1.5.1 Results

Table 4 summarizes the maximum and minimum changes for the aligned jetty scenario for an extreme fluvial and surge event. In general, the changes in water level are minimal. However, over a spring tide around peak flood there is a small backwater effect observed in the north channel as a result of the strong tidal asymmetry. There is a residual effect from this, which carries into the high water period, but which has dissipated by the time of peak ebb.

In terms of the speeds predicted by the modelling the largest changes are associated with the cofferdam structures and, in particular, the structure within the north channel. The causeway appears to have little impact on the hydrodynamics except around high water on spring tides when the water levels are high enough to extend onto this part of the intertidal shore. There is some indication of increased flows circulating along the side of the causeway during this period.

The bed shear stresses follow a similar pattern as that of the speeds. The largest increases are local to the structures. In addition, in the lee of the cofferdams there is a blocking effect, which leads to a reduction in the shear stress.

3.1.6 Aligned Jetty - 2005 Bathymetry

In early 2005 a limited survey of the estuary local to the proposed crossing was undertaken. This captured the significant movement of the channels between this new survey and the previous 2002 survey used to date in all modelling undertaken in the project. The new bathymetry allowed a modelling assessment of the hydrodynamic response to the proposed bridge with a completely different channel configuration and to assess the significance of this. The detailed modelling only carried out this assessment for the preferred option using the aligned jetty construction scheme. As with previous scenarios run with the aligned jetty a causeway was included over the intertidal area joining with the jetty.

3.1.6.1 Results

Table 4 provides a summary of the maximum and minimum changes for the aligned jetty using the 2005 bathymetry and a spring-neap tidal cycle. The greatest changes in water level are associated with the flood tide and are a result of the strong tidal asymmetry in this part of the estuary. Around peak flood there is a small backwater effect occurring in the south channel. This effect has dissipated by around high water.

The main changes in speed are predicted to occur local to the cofferdam structures. Changes along the intertidal area tend to occur on the front of the tidal wave as it propagates onto these areas and these are generally considered to be insignificant due to the fact that they are very short in duration (seconds) and affect a limited area. In addition such changes are considered to represent a change in phase rather than magnitude.

As previously, the bed shear stress results follow a similar pattern to the changes in speed, with the maximum changes occurring local to the cofferdam structures (See Table 4).

Table 4. Maximum and minimum changes for Route 3a preferred option - Aligned Jetty: for extreme fluvial and surge event - 1:200 return period and 2005 bathymetry

Scenario	Position	Low Water		Peak Flood		High Water		Peak Ebb	
		Max	Min	Max	Min	Max	Min	Max	Min
Aligned Jetty: for extreme fluvial and surge event - 1:200 return period									
Water level (m)	Piers	0.02	-	0.06	-0.08	0.02	-	0.03	-
	Channels	-	-	0.04	-	-	-	-	-
	Intertidal	-	-	0.01	-	-	-	-	-
Near-surface speed (m/s)	Piers	0.24	-0.65	0.89	-1.40	0.59	-0.85	0.96	-1.07
	Channels	-	-	0.09	-0.06	0.06	-0.08	-	-
	Intertidal	-	-	0.16	-0.14	0.05	-0.07	0.04	-0.04
Bed shear stress (N/m^2)	Piers	1.03	-1.04	7.17	-5.89	3.82	-1.61	1.55	-1.81
	Channels	-	-	0.32	-0.39	0.20	-0.20	0.09	-
	Intertidal	-	-	3.02	-0.36	0.46	-0.48	0.19	-0.10
Aligned Jetty: for 2005 bathymetry									
Water level (m)	Piers	0.28	-	0.06	-0.14	0.06	-0.05	0.04	-0.06
	Channels	-	-	0.02	-0.02	-	-	0.02	-
	Intertidal	0.01	-	0.03	-0.09	0.03	-0.03	-	-
Near-surface speed (m/s)	Piers	0.11	-0.13	0.63	-1.16	0.39	-1.16	0.79	-0.87
	Channels	0.01	-	0.08	-0.09	0.07	-0.15	0.05	-
	Intertidal	-	-0.09	0.07	-0.30	0.11	-0.15	0.09	-0.15
Bed shear stress (N/m^2)	Piers	0.56	-1.63	8.42	-4.88	4.38	-3.39	6.71	-2.01
	Channels	0.16	-	0.68	-1.25	0.15	-0.15	0.11	-0.34
	Intertidal	0.20	-0.64	1.85	-3.02	0.82	-0.45	0.25	-2.31
Note: - = No change									

3.2 Morphological Modelling

3.2.1 Introduction

The morphological modelling has been used to investigate a wider range of construction scenarios. Below are listed the model runs undertaken:

- Preferred option (Drawing No. B4027/3/B/300 Rev. A):
  - Island construction scheme - Spring-neap cycle
  - Aligned jetty - Spring-neap cycle
  - Aligned jetty - High fluvial (1:200 year event) and corresponding 1:200 year surge event
  - Spike Island jetty - Spring-neap cycle
  - New bathymetry - aligned jetty spring-neap cycle
  - New bathymetry - aligned jetty High fluvial (1:200 year event) and corresponding 1:200 year surge event

Appendix B presents the results of the morphological modelling. The bed shear stress values described above and quoted in detail in Appendix A represent maximum changes of the instantaneous stress and may not be sustained for any length of time. The bed shear stresses give an indication of potential change in erosion/accretion based on the hydrodynamic equations. Changes in sedimentation patterns can be identified from the morphological modelling.

For river beds consisting of sands (non-cohesive sediments) the movement of these particles depends on the physical properties of the individual grains, such as size shape and density. For river beds made up of silty and muddy materials, the cohesive forces between the sediment particles become important, leading to a significant increase in sediment resistance to erosion. Flocculation of sediment particles is the result of particles adhering together as they come into contact with each other and the resulting aggregations are called flocs. Biological activity at the bed may also influence the critical shear stress values required to initiate sediment movement (ABPmer, 2003). Seasonal variations in sedimentation are considered sufficiently small to be masked by the variances arising from the acknowledged limitations of sediment transport models.

The other important factor relating to the erodibility of cohesive sediments is the consolidation rate. Mud recently deposited consists of low-density mud flocs possessing a relatively loose structure. The cohesive forces in this deposit are not very strong at this early stage. If the deposit is not eroded again, then the density will increase gradually, as the interstitial water (water between the flocs) is expelled from the deposit as a result of its own weight. As the deposit is compacted so its resistance to erosion increases.

Whilst changes to the hydrodynamic regime are important, what is most important to the intertidal areas is erosion and deposition. The following discussion will concentrate on results from the morphological modelling. Based on the complexity of sediments as discussed above, the results from the morphological model need to be interpreted with care, taking into account the various factors affecting sediment transport, and considering the effects of processes not included as parameters within the model (for example biological activity. The morphological modelling of the Mersey Estuary has been undertaken using the predominant sediment type found across the study area (sand d_{50} = 150 μm), ABPmer (2003).

3.2.2 Island Construction Scheme

For the island construction scheme the following comments highlight the key changes in sedimentation patterns:

Changes are seen upstream of the proposed temporary island structures with increased sedimentation over intertidal banks (> 0.05m).

In the vicinity of the temporary islands adjacent to the north and south channels there is an increase in erosion is predicted (erosion > 1m). Some deposition is predicted local to the scour around the island structures.

In the vicinity of the Runcorn Gap and the existing bridge crossings there is an area of predicted erosion of 1.18m. A high level of deposition is also predicted along the north bank with an increase of 0.3m.

Within the main flood and ebb channels there is a slight change in sediment deposition along the margins ($\pm$0.02m).

3.2.3 Aligned Jetty Construction Scheme

For the Aligned jetty construction scheme the following comments highlight the key changes in sedimentation patterns:

In general the greatest changes are local to the cofferdams and in particular the structure located close to the north channel with predicted erosion of 1.4m. Local to this area of erosion is a large area of accretion (>0.05m) extending around the area of predicted erosion.

No change in bed elevation is predicted adjacent to the central tower structure.

Less significant is the extent of change in bed elevation in the vicinity of the cofferdam close to the southern channel with predicted erosion < 0.06m local to the structure.

No significant changes in sedimentation are observed downstream of the proposed bridge crossing and upstream of the proposed bridge crossing the changes in bed elevation are small.

3.2.4 Spike Island Jetty Construction Scheme

For the temporary jetty from Spike Island the following comments highlight the key changes in sedimentation patterns:

There is a predicted increase in erosion local to the cofferdam structures adjacent to the north and south channels (≈ 1.4m and 0.06m, respectively). The greatest extent of erosion occurs within the north channel.

There is no predicted change in bed elevation adjacent to the central cofferdam.

Changes in bed elevation upstream of the proposed bridge crossing are small (0.04m ±0.02m).

There are no significant changes predicted to occur downstream of the proposed bridge crossing.

3.2.5 Cross-sections

Table 5 summarizes the cross-sectional bed level changes for the various construction schemes with values given relative to the baseline condition. From the table it demonstrates that overall the island construction approach produces the greatest change over the largest area. The cross-sections are shown in Appendix B, Figures B7-B13.

Table 5. Summary of cross-sectional bed level changes for the various construction schemes. Description of changes compared against the existing 'baseline' condition

Cross-Section	Preferred Option - Construction Scenarios		
	Temporary Island Scheme	Spike Island Jetty	Aligned Jetty
A	No Change	No Change	No Change
B	No Change	No Change	No Change
C	Erosion over intertidal bank (max ≈ 0.3m) and some accretion on margin of north channel (max ≈ 0.14m)	No Change	No Change
D	No Change	No Change	No Change
E	Slight accretion in south channel (max ≈ 0.04m) and some erosion (max ≈ 0.06m) and accretion (max ≈ 0.07m) within the north channel	Slight accretion (max ≈ 0.02m) and erosion (max ≈ 0.01m) in north channel	Slight accretion (max ≈ 0.02m) and erosion (max ≈ 0.01m) in north channel
F	Sedimentation along margins of north channel margin (max ≈ 0.35m -0.5m)	Significant erosion within north channel (max ≈ 1.4m) and some accretion along channel margin (max ≈ 0.3m)	Significant erosion within north channel (max ≈ 1.4m) and some accretion along channel margin (max ≈ 0.3m)
G	Slight erosion on shoulder of south channel (max ≈ 0.05m). In the north channel there is erosion (max ≈ 0.3m) and accretion (max ≈ 0.14m) predicted	Slight accretion in north channel (max ≈ 0.06m)	Slight accretion in north channel (max ≈ 0.06m)
H	Accretion (max ≈ 0.11m) at the shoulder of the south channel. Small area of accretion in north channel (max ≈ 0.07m)	Both erosion (max ≈ 0.3m) and accretion (max ≈ 0.09m) on shoulder of the south channel. Small area of accretion in north channel (max ≈ 0.03m)	Both erosion (max ≈ 0.3m) and accretion (max ≈ 0.09m) on shoulder of the south channel. Small area of accretion in north channel (max ≈ 0.03m)
I	General accretion over cross-section (max ≈ 0.17m)	General accretion over cross-section (max ≈ 0.07m)	General accretion over cross-section (max ≈ 0.07m)
J	Accretion and erosion in southern channel (max ≈ 0.03m). Migration of northern channel towards north bank with accretion (max ≈ 0.1m) and erosion (max ≈ 0.08m)	Accretion and erosion in southern channel (max ≈ 0.01m). Within the north channel modelling predicts both areas of erosion (max ≈ 0.03m) and accretion (max ≈ 0.04m)	Accretion and erosion in southern channel (max ≈ 0.01m). Within the north channel modelling predicts both areas of erosion (max ≈ 0.03m) and accretion (max ≈ 0.04m)
K	Some accretion in south channel (max ≈ 0.08m). Also accretion predicted in the north channel (max ≈ 0.06m)	Slight accretion in southern channel (max ≈ 0.01m). In addition some accretion in north channel (max ≈ 0.03m)	Slight accretion in southern channel (max ≈ 0.01m). In addition some accretion in north channel (max ≈ 0.03m)
L	Slight accretion in north channel (≈ 0.03m) and minor erosion on banks between north and south channels	Slight accretion in north channel (max ≈ 0.01m)	Slight accretion in north channel (max ≈ 0.01m)

3.3 Aligned Jetty: Extreme Fluvial and Surge Event - 1:200 Return Period

3.3.1 Spatial Change

For the aligned jetty the following comments highlight the key changes in sedimentation patterns:

There is a predicted increase in erosion local to the cofferdam structures adjacent to the north and south channels. The greatest extent of deposition and erosion occurs within the north channel ($\approx$ 0.9m and 1.8m, respectively)

There is no predicted change in bed elevation adjacent to the central cofferdam. This is due to its limited exposure to the tidal flow.

Runcorn Gap is the limit of downstream changes as a result of the crossing and changes are small ($< \pm$0.05m). The total extent of change is approximately 2km either side of the proposed crossing.

3.3.2 Cross-sections

Table 6 summarizes the cross-sectional bed level changes for the aligned jetty for an extreme fluvial and surge event, with values given relative to the corresponding baseline condition. The greatest changes are observed at section F, which is located close to the proposed bridge alignment and the north bridge tower, in particular. The cross-sections are shown in Appendix B, Figures B14-B19.

Table 6. Summary of cross-sectional bed level changes for the Aligned Jetty: extreme fluvial and surge event - 1:200 return period. Description of changes compared against a comparable 'baseline' condition

Cross-Section	Preferred Option - Extreme Fluvial and Surge Event Scenario	Preferred Option - Construction Scenarios
	Aligned Jetty Scheme	Aligned Jetty
A	No Change	No Change
B	No Change	No Change
C	Erosion over intertidal bank (max ≈ 0.04m) and some accretion on margin bank (max ≈ 0.02m)	No Change
D	No Change	No Change
E	Slight erosion in south channel (max ≈ 0.03m) and some erosion (max ≈ 0.24m) and accretion (max ≈ 0.09m) within the north channel	Slight accretion (max ≈ 0.02m) and erosion (max ≈ 0.01m) in north channel
F	Within the north channel modelling predicts both areas of erosion (max ≈ 1. 8m) and accretion (max ≈ 0.9m). No significant change in bed elevation is predicted in the south channel.	Significant erosion within north channel (max ≈ 1.4m) and some accretion along channel margin (max ≈ 0.3m)
G	There is some slight erosion in the south channel (max = 0.06m) and deposition on the lower slope of the channel adjacent the intertidal bank (max = 0.32m). within the north channel there is erosion (max = 0.48m) predicted along the side of the intertidal bank and deposition within the central part of the channel (max = 0.54m).	Slight accretion in north channel (max ≈ 0.06m)
H	In the south channel there is a slight deepening of the channel along the shoreline (max = 0.11m) and accretion along the lower slopes of the channel (max = 0.10m). Some deposition (max = 0.07m) and erosion (max =0.05m) on shoulder of intertidal bank. In the north channel there is some erosion (max = 0.08m) and accretion (max = 0.03m) predicted.	Both erosion (max ≈ 0.3m) and accretion (max ≈ 0.09m) on shoulder of the south channel. Small area of accretion in north channel (max ≈ 0.03m)
I	Changes in bed level over cross-section are small with maximum differences in deposition and erosion of ±0.03m.	General accretion over cross-section (max ≈ 0.07m)
J	Changes in bed level over cross-section are small with maximum differences in deposition (max = 0.02m) and erosion of (max = 0.03m).	Accretion and erosion in southern channel (max ≈ 0.01m). Within the north channel modelling predicts both areas of erosion (max ≈ 0.03m) and accretion (max ≈ 0.04m)
K	There is minor deposition predicted in the south channel (max = 0.03m) and over the intertidal bank (max = 0.02m). There are also some small areas of erosion over the banks (max = 0.02m).	Slight accretion in southern channel (max ≈ 0.01m). In addition some accretion in north channel (max ≈ 0.03m)
L	There is some slight accretion (max = 0.02m) and erosion (max = 0.03m) within the south channel. There is also erosion (max = 0.03m) and deposition (max = 0.02m) predicted within the north channel towards the intertidal bank.	Slight accretion in north channel (max ≈ 0.01m)

3.4 New Bathymetry

After undertaking the above modelling and the subsequent analysis it was decided to assess one of the jetty schemes for a new bathymetric layout. After discussion it was decided that the aligned jetty layout would be used. In early 2005 a limited survey of the estuary local to the proposed crossing was undertaken. This captured the significant movement of the channels between this new survey and the previous survey in 2002 (Figure 11).

3.4.1 Aligned Jetty - 2005 Bathymetry

3.4.1.1 Spatial change

For the aligned jetty using a new bathymetric dataset the following comments highlight the key changes in sedimentation patterns:

There is a predicted increase in erosion local to all the cofferdam structures. Compared to previous scenarios using the 2002 bathymetry there is now a change in dominance from the north channel to the south channel with a similar order of scour being predicted around the cofferdam structures in both channels (≈ 1.5m). The results also reveal the dominance of the flood tide in the upper estuary under normal flow conditions with most changes in bed level occurring upstream of the crossing. Along the intertidal margins of the north channel there is deposition (≈ 0.2m).

The largest changes are local to the crossing, with no significant changes in bed elevation predicted downstream of the proposed bridge crossing.

3.4.1.2 Cross-sections

Table 7 summarizes the cross-sectional bed level changes for the aligned jetty and using 2005 bathymetry. Values are given relative to the corresponding baseline condition. The greatest changes are observed at section F, and section H that correspond to pier positions in the north and south channels, respectively. At cross-section H there is a change in profile within the south channel and along the flank of the intertidal bank. Towards the shoreline there is some deepening of the channel (max = 0.06m). Along the flank of the bank a small channel is formed (max erosion = 1.4m) and deposition along the shoulder of the bank (max = 0.6m), see Table 7. The cross-sections are shown in Appendix B, Figures B20 - 25.

Table 7. Summary of cross-sectional bed level changes for the Aligned Jetty - 2005 bathymetry. Description of changes compared against a comparable 'baseline' condition

Cross-Section	Preferred Option - 2005 Bathymetry	Preferred Option - 2002 Bathymetry
	Aligned Jetty	Aligned Jetty
A	No Change	No Change
B	No Change	No Change
C	Minor deposition (max = 0.01m) and erosion (max = 0.01m) predicted over the intertidal bank and some slight erosion (max = 0.01m) within the north channel.	No Change
D	No Change	No Change
E	Some erosion over the intertidal bank (max = 0.01m). Some deposition (max = 0.05m) in the north channel.	Slight accretion (max ≈ 0.02m) and erosion (max ≈ 0.01m) in north channel
F	Small changes in south channel (max deposition = 0.02m; max erosion = 0.02m) with some slight deepening of the channel and some erosion and deposition over the lower slopes of the channel, adjacent to the central intertidal bank. Within the north channel significant erosion (max = 1.01m) and deposition (max = 0.35m).	Significant erosion within north channel (max ≈ 1.4m) and some accretion along channel margin (max ≈ 0.3m)
G	In the south channel deepening of the channel (max = 0.03m) and accretion (max = 0.02m) on bank side. Along the flank of the bank there is some erosion (max = 0.06m). Over top of the bank there is a change in profile with erosion (max = 0.36m) and deposition (max = 0.21m) occurring. Within the north channel there is accretion occurring along the sides of the channel (max = 0.11m).	Slight accretion in north channel (max ≈ 0.06m)
H	In south channel towards the shoreline there is deepening of the channel (max = 0.06m). Along the flank of the bank a small channel is formed (max erosion = 1.4m) and deposition along the shoulder of the bank (max = 0.6m). In the north channel there is some erosion along the sides of the channel (max = 0.04m).	Both erosion (max ≈ 0.3m) and accretion (max ≈ 0.09m) on shoulder of the south channel. Small area of accretion in north channel (max ≈ 0.03m)
I	Movement of the south channel profile deposition within the deep channel (max = 0.18m). Along the flanks of bank there is erosion on the slopes forming a shallow channel (max = 0.26m) then above this is an area of deposition (max =0.2m).	General accretion over cross-section (max ≈ 0.07m)
J	Deposition occurring in south channel (max = 0.3m). Along the flank of the intertidal bank there is some erosion (max = 0.04m) and above this an area of accretion (max = 0.15m).	Accretion and erosion in southern channel (max ≈ 0.01m). Within the north channel modelling predicts both areas of erosion (max ≈ 0.03m) and accretion (max ≈ 0.04m)
K	In south channel there is accretion within the deepest section (max = 0.1m) and on the upper shoulder of the intertidal bank (max = 0.15m).	Slight accretion in southern channel (max ≈ 0.01m). In addition some accretion in north channel (max ≈ 0.03m)
L	In south channel accretion close to the shoreline (max = 0.2m). Also, accretion over the side of the bank (max = 0.07m).	Slight accretion in north channel (max ≈ 0.01m)

3.4.2 Aligned Jetty - 2005 Bathymetry: Extreme Fluvial and Surge Event

3.4.2.1 Spatial extent

For the aligned jetty and using 2005 bathymetry under extreme fluvial and surge conditions the following comments highlight the key changes in sedimentation patterns:

There is a predicted increase in erosion local to the cofferdam structures adjacent to the north and south channels. The greatest extent of erosion and deposition occurs within the south channel (≈ 1.4m and 0.4m, respectively). Within the north channel the erosion around the cofferdam has a maximum scour depth of 1.2m, approximately.

There is no significant change in bed elevation adjacent to the central cofferdam. The new channel configuration results in a change in dominance from the north channel to the south channel as observed for the construction scheme under normal flow conditions. The total extent of change is the order of 2km either side of the crossing with downstream changes not extending beyond Runcorn Gap, although the greatest spatial extent of change occurs upstream of the proposed crossing (see Figure B6a).

There are some slight increases in bed elevation <0.05m adjacent to the margins of the north channel downstream of the proposed bridge crossing as well as some changes over the upper intertidal area of Wigg Island. However, these latter changes are due to the elevated water levels as a result of the surge event allowing the flow to flood onto these areas.

3.4.2.2 Cross-sections

Table 8 summarizes the cross-sectional bed level changes for the aligned jetty and using 2005 bathymetry for an extreme surge and fluvial event (1:200 years return period). Values are given relative to the corresponding baseline condition. The greatest changes are observed at section F, which is located close to the proposed bridge alignment. The largest changes due to the location of the cofferdam in the south channel are not picked up by the cross-sections. The cross-sections are shown in Appendix B, Figures B20 - 25 and their positions are shown in Figure B7.

Table 8. Summary of cross-sectional bed level changes for the Aligned Jetty - 2005 bathymetry: extreme fluvial and surge event. Description of changes compared against a comparable 'baseline' condition

Cross-Section	Preferred Option - 2005 Bathymetry - Extreme Fluvial and Surge Event Scenario	Preferred Option - 2005 Bathymetry
	Aligned Jetty	Aligned Jetty
A	No Change	No Change
B	No Change	No Change
C	Erosion and deposition predicted over the flanks and the top of the intertidal bank (max deposition = 0.05m; max erosion = 0.02m). Within the north channel there is erosion predicted in the deepest section (max = 0.02m).	Minor deposition (max = 0.01m) and erosion (max = 0.01m) predicted over the intertidal bank and some slight erosion (max = 0.01m) within the north channel.
D	Some minor erosion in the north channel (max = 0.02m).	No Change
E	Erosion over the top of the intertidal bank (max = 0.02m) and minor deposition (max = 0.04m) and erosion (max = 0.02m) within the north channel.	Some erosion over the intertidal bank (max = 0.01m). Some deposition (max = 0.05m) in the north channel.
F	In the south channel a deepening of the channel towards the intertidal bank (max = 0.1m) and deposition (max 0.15m) and some erosion (max = 0.04m) along the lower flanks of the bank. In the north channel there is a deepening of the channel (max = 1.2m) and deposition along the slopes of the channel (max = 0.7m).	Small changes in south channel (max deposition = 0.02m; max erosion = 0.02m) with some slight deepening of the channel and some erosion and deposition over the lower slopes of the channel, adjacent to the central intertidal bank. Within the north channel significant erosion (max = 1.01m) and deposition (max = 0.35m).
G	In the south channel there is deepening of the channel (max = 0.2m) and deposition towards the intertidal bank (max = 0.25m). Over the top of the bank there is some minor erosion (max = 0.02m). In the north channel there is erosion (max = 0.04m) in the deep section and deposition on the lower slopes of the channel (max = 0.01m).	In the south channel deepening of the channel (max = 0.03m) and accretion (max = 0.02m) on bank side. Along the flank of the bank there is some erosion (max = 0.06m). Over top of the bank there is a change in profile with erosion (max = 0.36m) and deposition (max = 0.21m) occurring. Within the north channel there is accretion occurring along the sides of the channel (max = 0.11m).
H	Deepening of the south channel (max = 0.08m) an some deposition on the lower slope on the inshore side (max = 0.01m). On the flanks of the bank a shallow channel is forming (max erosion = 0.16m) with deposition either side (max = 0.37m). In the north channel there is a reduction in the channel depth (max erosion = 0.04m) and some deposition on the lower slopes of the channel (max = 0.01m).	In south channel towards the shoreline there is deepening of the channel (max = 0.06m). Along the flank of the bank a small channel is formed (max erosion = 1.4m) and deposition along the shoulder of the bank (max = 0.6m). In the north channel there is some erosion along the sides of the channel (max = 0.04m).
I	Within the centre of the south channel is an area of deposition (max = 0.45m). On the lower flank of the intertidal bank is an area of erosion (max = 0.12m). Across the remaining part of the section differences in bed level are small (max erosion = 0.02m; max deposition = 0.01m).	Movement of the south channel profile deposition within the deep channel (max = 0.18m). Along the flanks of bank there is erosion on the slopes forming a shallow channel (max = 0.26m) then above this is an area of deposition (max =0.2m).
J	Accretion within the south channel (max = 0.06m). Over the remaining part of the cross-section the changes are small (max erosion = 0.01m; max deposition = 0.03m).	Deposition occurring in south channel (max = 0.3m). Along the flank of the intertidal bank there is some erosion (max = 0.04m) and above this an area of accretion (max = 0.15m).
K	Some erosion and deposition predicted in the north channel (max = $\pm$0.03m)	In south channel there is accretion within the deepest section (max = 0.1m) and on the upper shoulder of the intertidal bank (max = 0.15m).
L	Some minor deposition (max = 0.02m) and erosion (max = 0.04m) in the south channel.	In south channel accretion close to the shoreline (max = 0.2m). Also, accretion over the side of the bank (max = 0.07m).

4. Discussion

A range of construction schemes have been tested for the Route 3A preferred option. The variations have consisted of an island construction scheme and two temporary jetty schemes, one of which consists of two sections, which extend out from both the north and south banks of the estuary and the other scheme consisting of a single jetty extending from Spike Island. In addition to these initial tests, additional scenarios have been run for the aligned jetty under an extreme surge and fluvial event as well as for a new channel alignment based on a survey conducted in 2005. All runs have also included a causeway over the saltmarsh to link the aligned jetty with the intertidal area.

Looking at the three construction schemes assessed first, hydrodynamically, all the schemes tested lead to an increased impact on the upper estuary, particularly when compared to the operational phase. This is demonstrated by comparing Figures 10A and 10B. However, between the various construction methodologies the temporary island construction scheme has the greater impact. In addition, the ability to maintain a stable rock bund in such a dynamic system is questionable. Rapid channel movement could easily destabilize a structure of this type. The size of the structures and the fact that they need to be placed close to or within both of the main channels along the north and south banks means that they will result in significant blockage of the flow at least at peak times of the flow and this may lead to more persistent residual effects at slack periods in the tidal cycle, for example around high water.

For the two temporary jetty schemes tested the modelling results suggest a similar order of impact within the upper estuary. There are some subtle differences between the two schemes due to the different jetty pile configurations, but generally the cofferdams dominate the changes in morphology observed in the model results. This is likely to be due to the small diameter piles (0.5m) being used and the spacing between each span (12m). The reason for the close similarity in results is due to the fact that for a large period of time many of the piles for the aligned jetty are not exposed to the flow being on the intertidal banks.

As a general consideration the deck of the jetty should be high enough above the water surface to prevent it being inundated on high spring tides and tidal surges (pressure flow scour). Such effects have not been modelled currently as it is assumed that the bridge deck is far enough above the water surface for this to be neglected.

In addition to ensuring that the deck of the temporary jetty structures are high enough to prevent pressure flow scour, navigation considerations should be taken into account to ensure that yachts are able to navigate upstream and downstream of the construction works without undue delays in normal passage time. This might be particularly important for the aligned jetty scheme extending out from both the north and south banks. To minimize impact on the upper estuary, the length of time that the large temporary structures are in place should be minimized.

The aligned jetty scheme has been used in additional model runs as this enables the investigation of a causeway over the saltmarsh to link the jetty with the intertidal foreshore. This scheme has been tested with the 2002 bathymetry and also a new bathymetric layout derived from a survey undertaken in 2005.

The upper estuary is highly dynamic (see Figure 11) and this has implications for scouring around the temporary structures. As was discussed previously in ABPmer (2004) the use of scour countermeasures may require extensive coverage, which may in turn have a greater impact on channel movement than the structures themselves. However, assuming no countermeasures are applied the maximum scour depth based on a range of empirical formulae for the circular cofferdams is in the range of about 2m - 4m (See Appendix A). The temporary island structures exhibit more scour than the circular cofferdams. This is both a function of size and shape. For further details see Appendix A.

Under extreme conditions the aligned jetty shows a slightly reduced impact downstream in terms of the extent of change, whilst this increases upstream of the crossing. Around the structures the magnitude and extent of change is increased due to the higher flows. Such events are infrequent and generally short in duration although it is considered that the high fluvial flow events are key to major channel movement in the upper estuary.

The use of a new channel configuration based on the 2005 survey results (Figure 12) in different patterns of change particularly local to the structures. However, the magnitude and extent of the change is of a similar order, which is an important result, since it suggests that for different channel configurations the impact of the proposed crossing will lead to no significant variation in change over those predicted to date from all the modelling undertaken in terms to the extent and magnitude of the change.

The placement of a causeway over the intertidal area appears to have little impact on the hydrodynamics except around high water on spring tides when the water levels are high enough to extend onto this part of the intertidal shore. There may be some scouring along the side of the causeway as a result of some increase in the flow at this location, but such changes will be localized and limited in extent as well as dependent on the erosion threshold of the bed material.

5. Conclusions

A detailed numerical modelling study has been undertaken to assess possible construction methodologies for the Route 3A preferred option (Drawing No. B4027/3/B/300 Rev. A). Three possible construction schemes have been tested in total as detailed below:

- Island construction scheme - Spring-neap cycle
- Aligned jetty - Spring-neap cycle
- Spike Island jetty - Spring-neap cycle

Based on the results of the hydrodynamic and morphological modelling all the construction schemes tested have a greater impact on the upper estuary than during the "as built" operational phase. However, of the construction schemes tested the two temporary jetty schemes show the least impact on the system.

The highly dynamic nature of the upper estuary and, in particular, the movement of the position of the channels makes the temporary island scheme impractical. The rapid movement of the channels could destabilize any rock bund structure. In addition, scour around the large temporary islands is likely to be greater than that for the large circular cofferdams.

In addition to these tests, additional modelling has been undertaken using the aligned jetty scheme. This has been assessed using the 2002 bathymetry for an extreme surge and fluvial event as well as a new bathymetric layout using bathymetry collected in 2005, which shows a different channel configuration in the upper estuary. For the 2005 bathymetry the model scenarios investigated a spring-neap tidal cycle and an extreme surge and fluvial event. Based on these scenarios the following conclusions can be made:

- Under extreme conditions (1:200 years return surge and fluvial event) the magnitude and extent of change as a result of the proposed crossing is increased. However, such events are infrequent and the extent of change is limited to about 2km upstream and downstream of the proposed crossing. In addition, backwater effects are generally limited between peak flood and high water and are low in magnitude and of limited duration.

- The causeway appears to have little impact on the hydrodynamics except around high water on spring tides when the water levels are high enough to extend onto this part of the intertidal shore. There is some indication of increased flows circulating along the side of the causeway during this period, which may lead to some scouring at this location.

- The use of the 2005 bathymetry in the modelling leads to in a change in dominance from the north to the south channel. In addition, whilst the overall pattern of change is different, the extent and magnitude of the change is of a similar order to that predicted using the 2002 bathymetry. Therefore, it is suggested that for different channel configurations, whilst the spatial pattern of change may vary, particularly local to the structures, the overall magnitude and extent of change remains similar.

Based on the additional modelling undertaken it is this latter point that is of key importance as it suggests that regardless of the position of the channels relative to the proposed crossing the magnitude and extent of change within the system will be of a similar order.

6. References

ABPmer (2003). *New Mersey Crossing*. ABP Marine Environmental Research Ltd, Report No. R.1007, May.

ABPmer (2004). *New Mersey Crossing - Phase II Modelling Study*. ABP Marine Environmental Research Ltd, Report No. R.1151, November.

Environment Agency (1998). *Extreme Sea Levels for Section 105 Surveys.* Final report, JBA Ltd., July, 9pp (+Tables and Figures).

McDowell, D.M. (1964) In: *Field and model investigation into the reasons for siltation in the Mersey estuary*, Price, W.A. and Kendrick M.P., Reply to the Discussions, Proc. Inst. Of Civil Engrs., Vol. 27, March, pp. 613-647.

Figures

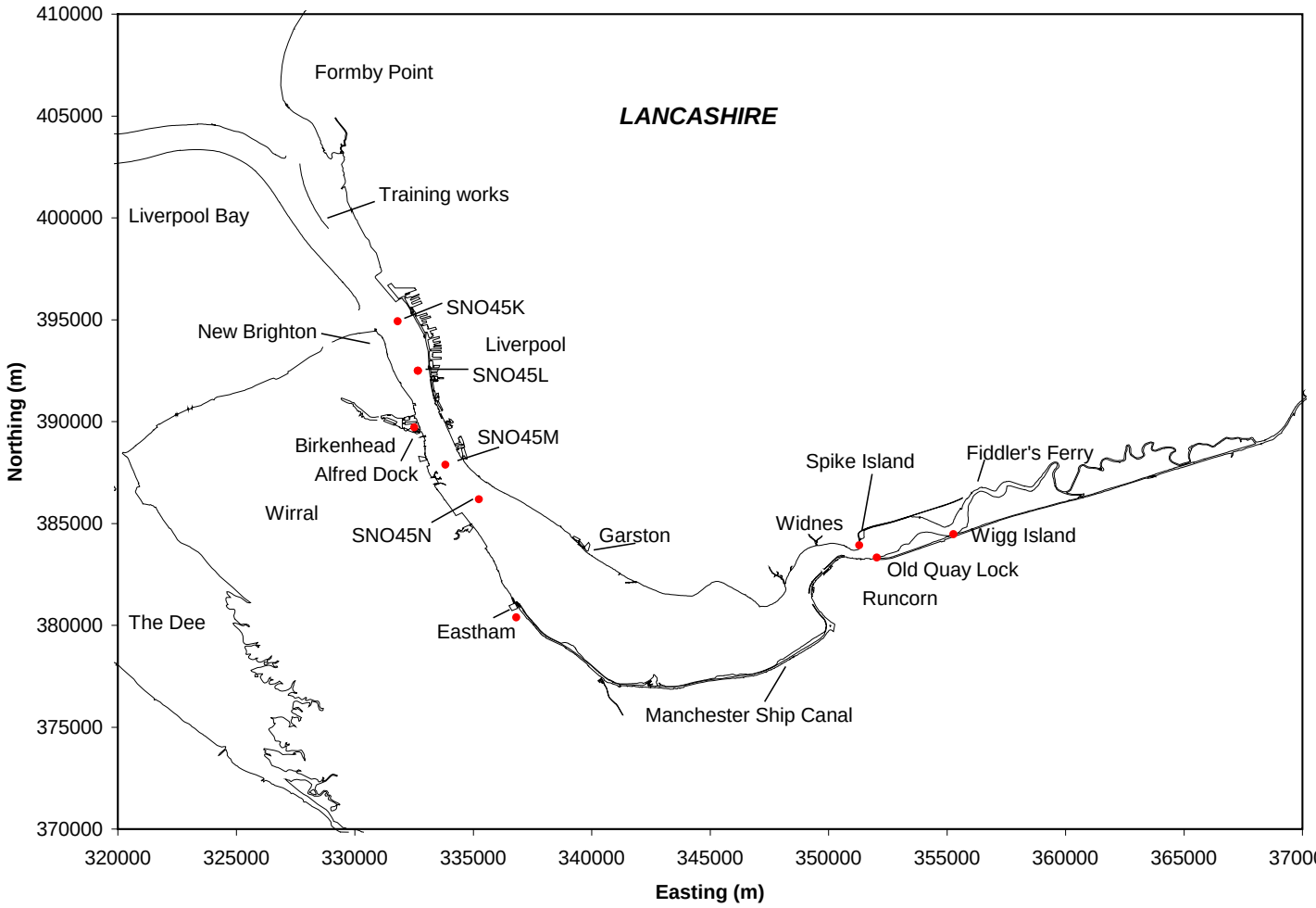

Plan of the Mersey Estuary

Figure 1

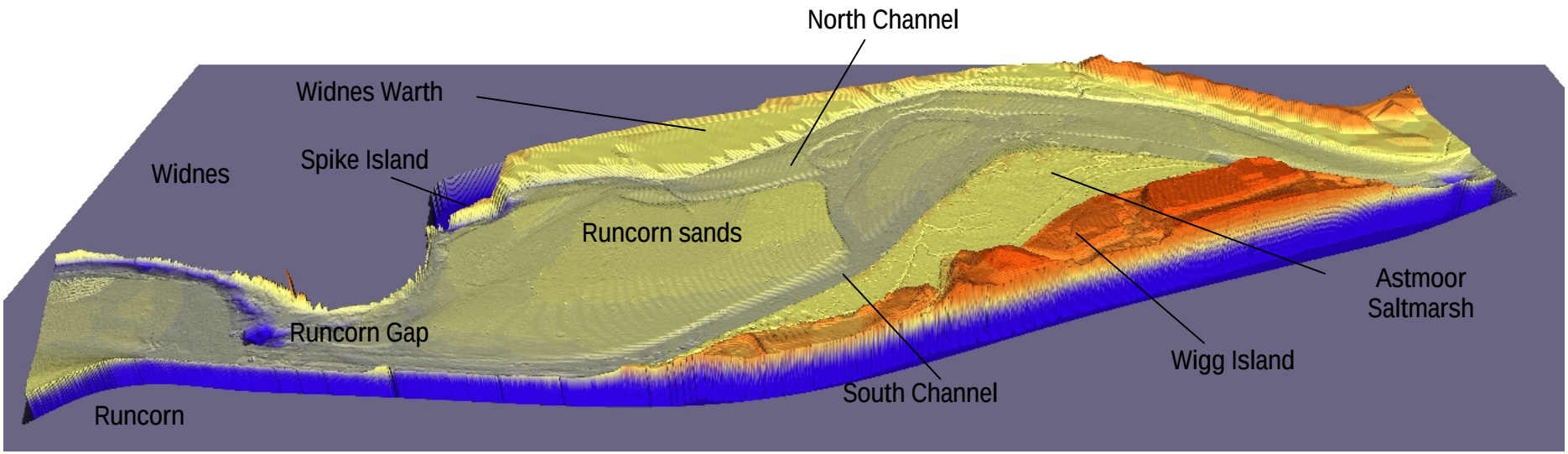

ABP mer marine environmental research	Figure showing the bathymetry as derived from data collected by the Environment Agency, 2002	Figure 2

Figure showing the Route 3A medium - 3 tower option revised alignment ('preferred option')

Figure 3

A.

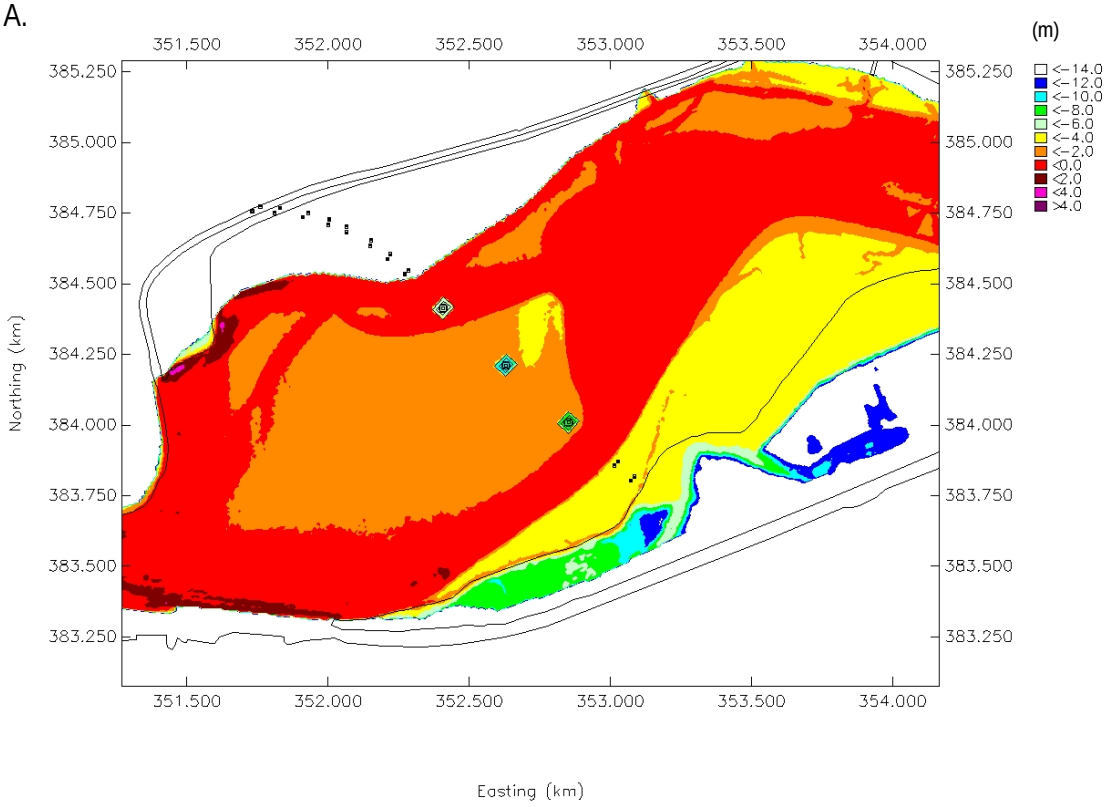

B.

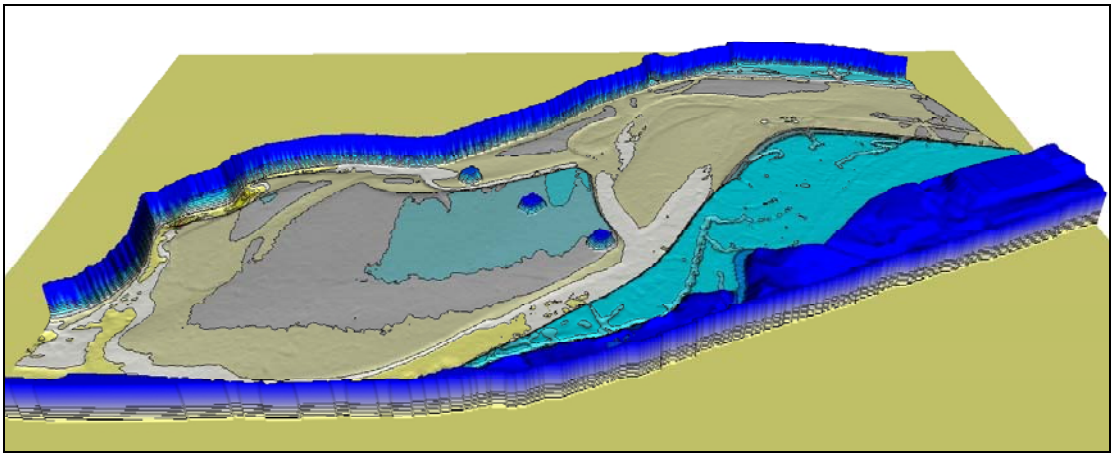

ABP mer marine environmental research	The layout of the Island construction scheme (A) and its representation within the high-resolution hydrodynamic model (B)	Figure 4

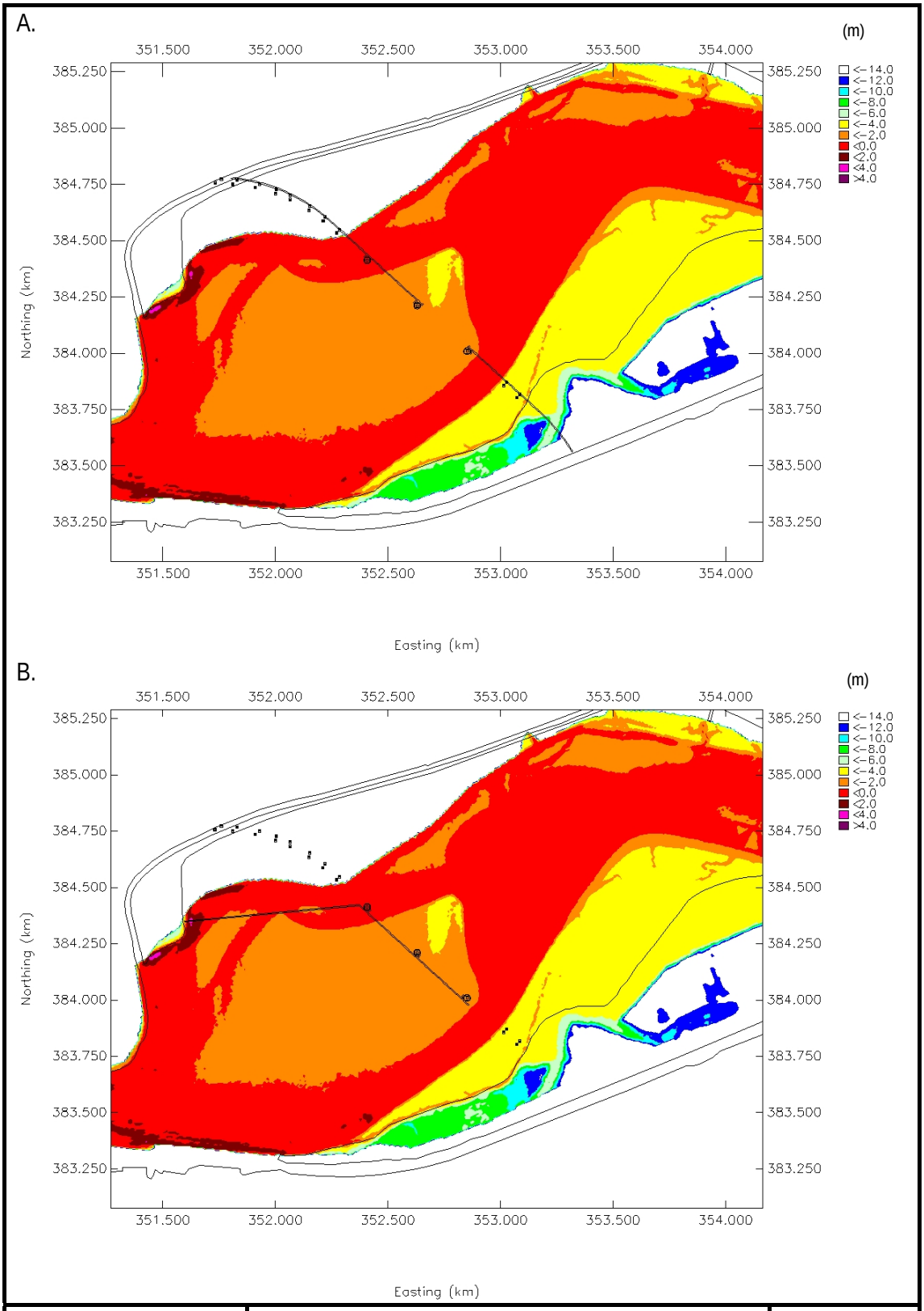

The layout of the aligned jetty scheme (A) and the jetty from Spike Island (B)

Figure 5

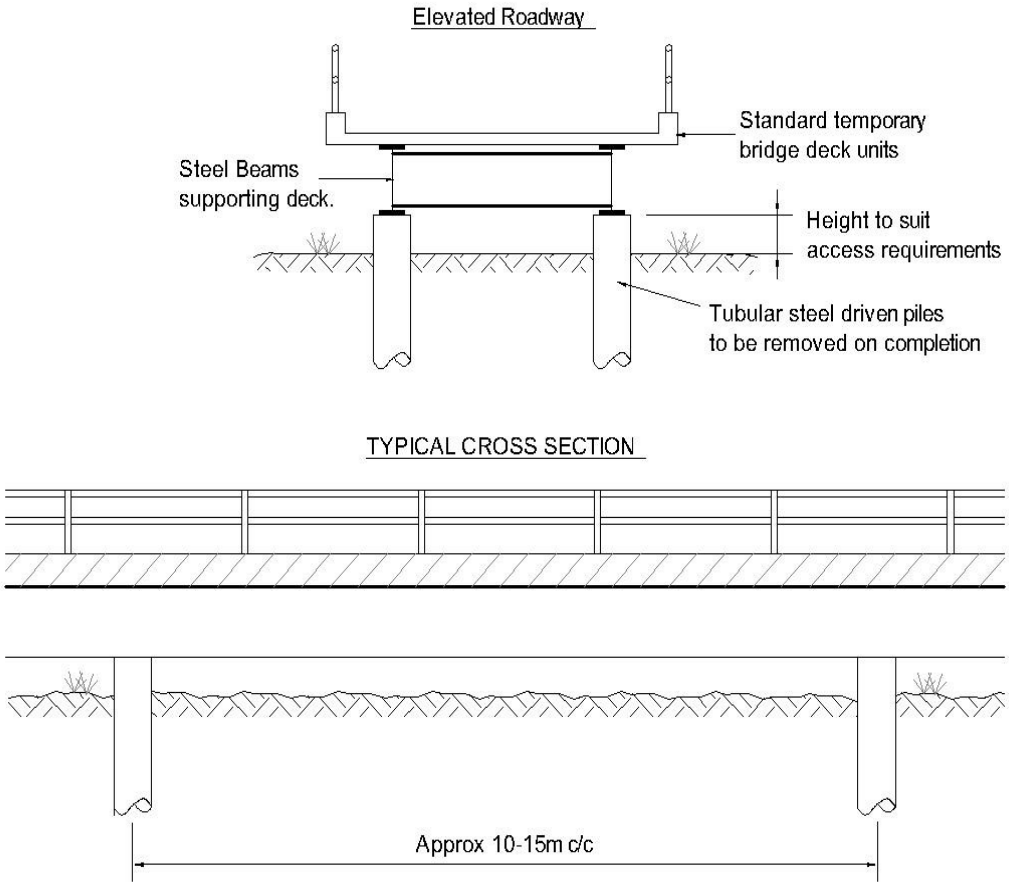

Note: As an alternative support may be provided by discrete pontoons resting on the salt marsh.

ABP mer marine environmental research	Jetty dimensions	Figure 6

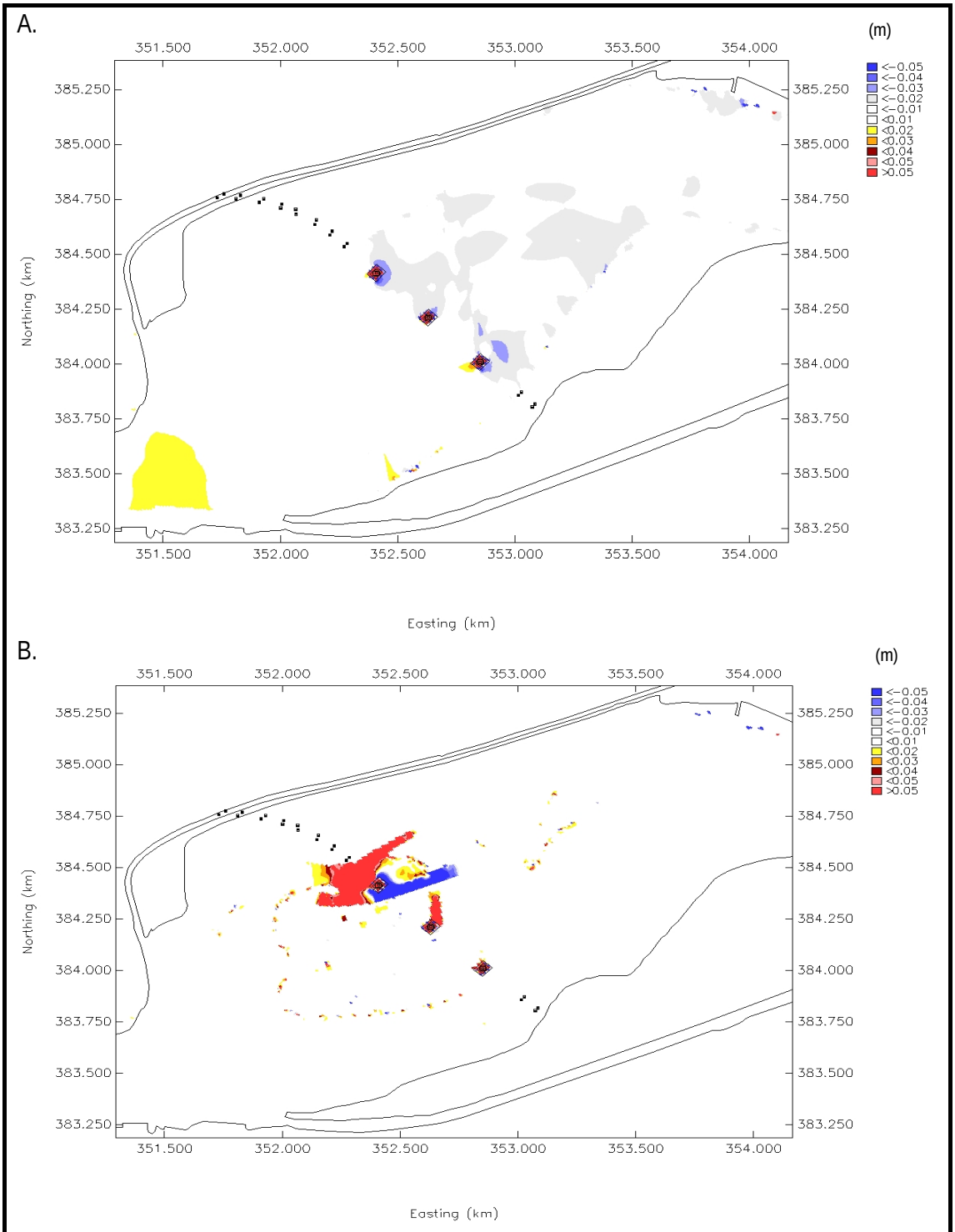

ABP mer marine environmental research	Differences in water level (m) between the preferred option and the baseline case for high water (A) and peak flood (B) on a spring tide - island construction scheme	Figure 7

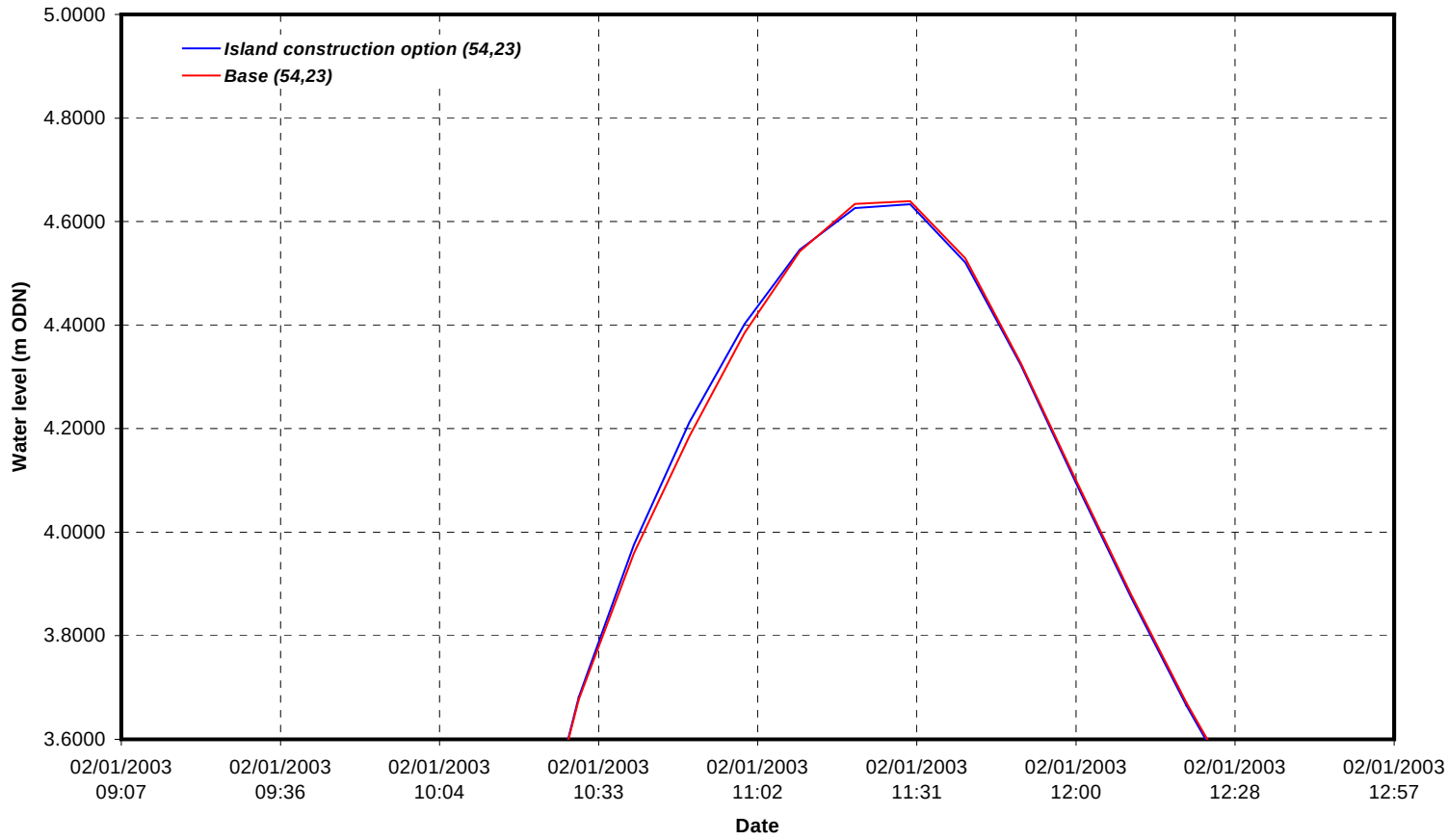

Figure showing the variation in water level around high water for the baseline case and the island construction scheme. The figure shows both a variation in phase as well as magnitude.

Figure 8

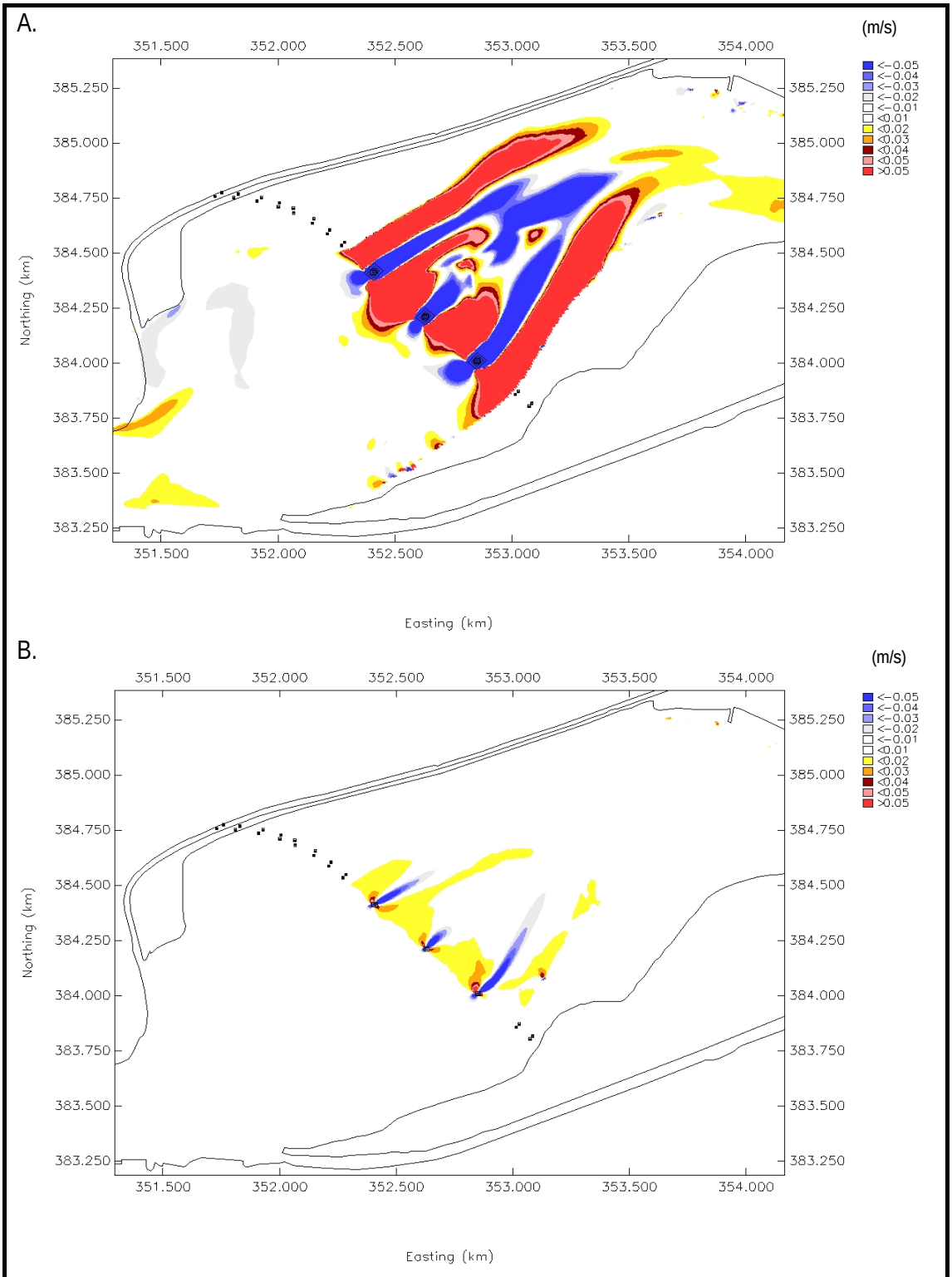

ABP mer marine environmental research	Differences in near-surface speed (m/s) between the preferred option and the baseline case for high water on a spring tide - island construction (A) and operational phase (B)	Figure 9

A.

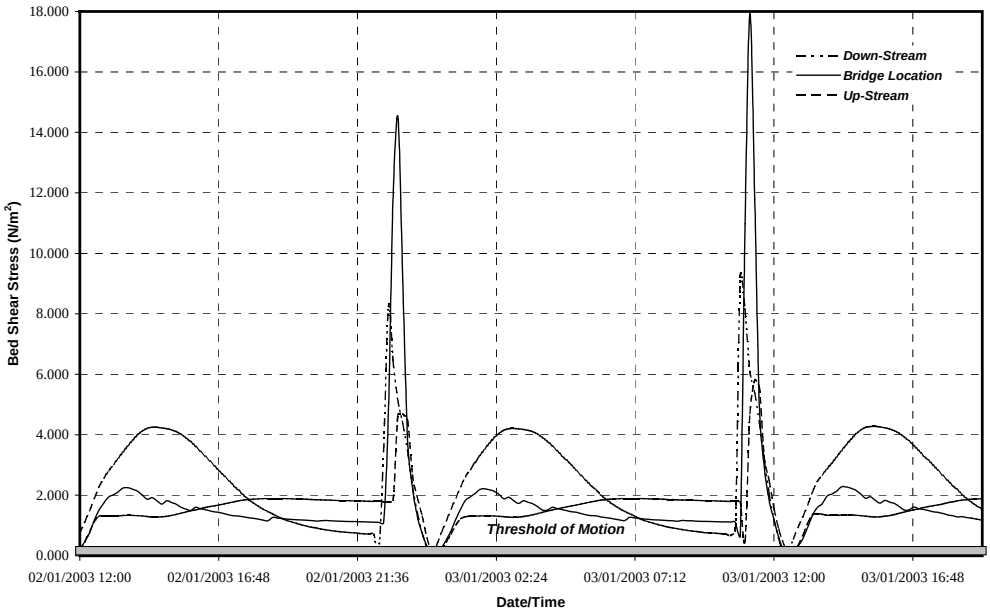

B.

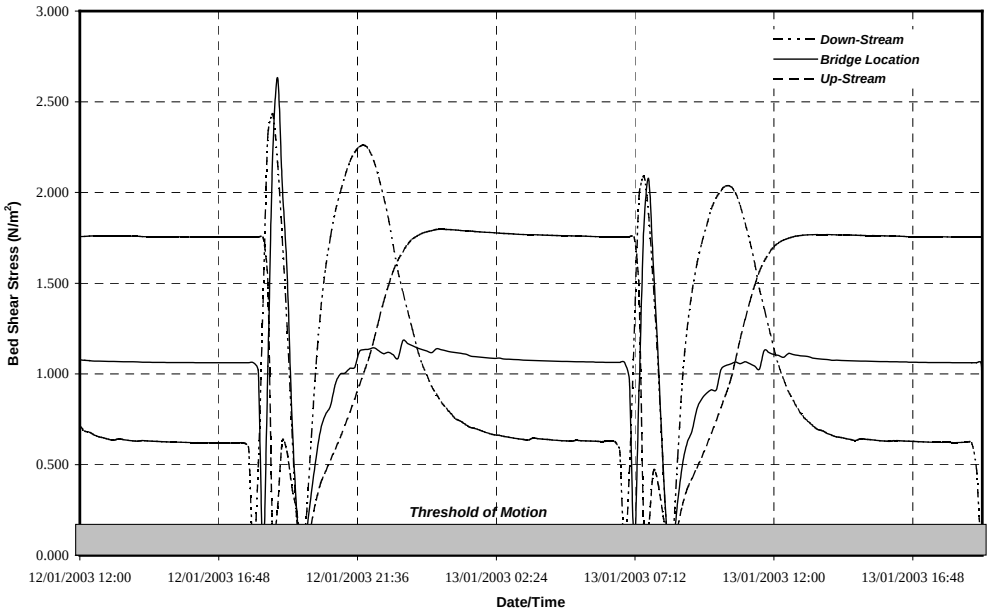

ABP mer marine environmental research	Plot of bed shear stress across the study area showing the threshold of sediment motion for 150μm grain size over spring (A) and neap (B) tides	Figure 10

A.

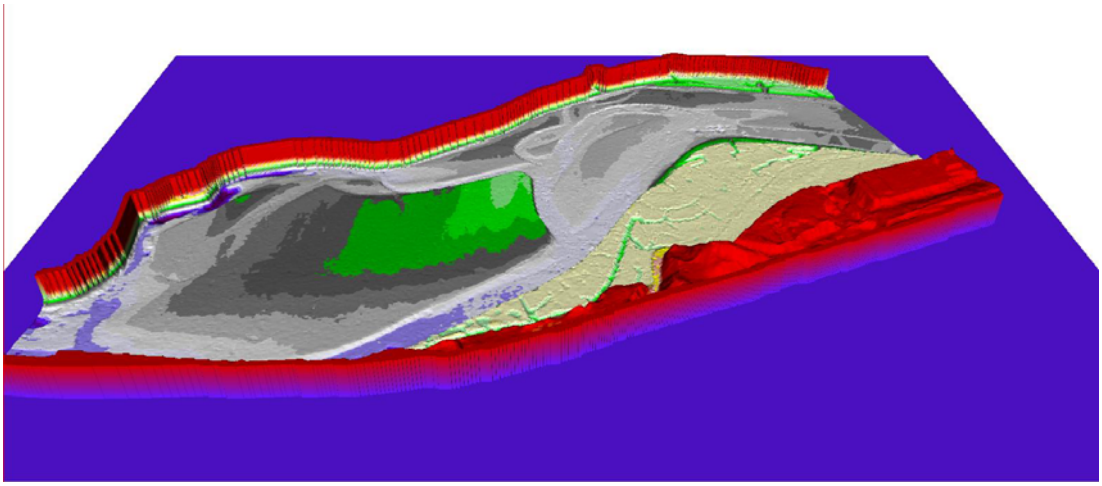

B.

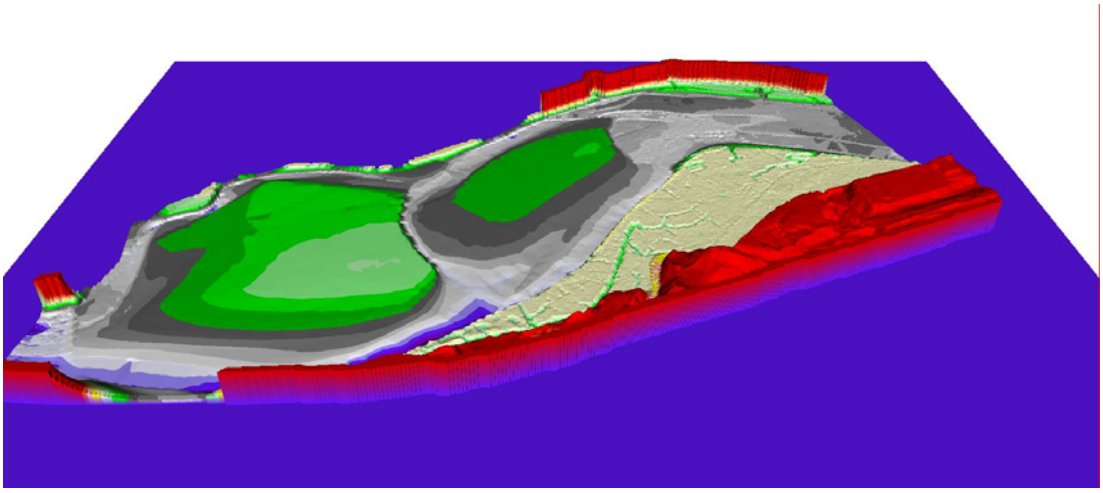

ABP mer marine environmental research	Bathymetry within the upper estuary; 2002 survey (A) 2005 survey (B).	Figure 11

Appendices

Appendix A

Detailed Hydrodynamic Assessment
of Construction Schemes

Appendix A. Detailed Hydrodynamic Assessment of Construction Schemes

A1. Introduction

This appendix presents the results from the detailed hydrodynamic numerical modelling undertaken to assess the impact of possible construction schemes with the Route 3A preferred option as shown in drawing B4027/3/B/300 Rev. A.

- Preferred option (Drawing No. B4027/3/B/300 Rev. A):
  - Island construction scheme - Spring-neap cycle
  - Aligned jetty - Spring-neap cycle
  - Aligned jetty - High fluvial (1:200 year event) and corresponding 1:200 year surge event
  - Spike Island jetty - Spring-neap cycle
  - New bathymetry - aligned jetty

Tables A1.1 and A1.2 provide a schedule of the model runs undertaken for each scenario with their respective figure numbers for high water and peak ebb (Table A1.1) and low water and peak flood (Table A1.2).

The previous modelling study undertaken in Phase I of the work used an additional quadratic friction term in the momentum equations to represent the effect of bridge piers in the model. Further details on this approach are given in Appendix A and ABPmer (2003a). In the current modelling bridge piers have been simulated using a combination of approaches. Where bridge piers and towers are the same size as or larger than the model grid cells the cells have been closed off as they are effectively blocked for the transmission of fluid flow. However, where the bridge piers are smaller than the grid cell size added friction terms have been used to represent the piers. In this manner there is an allowance for some flow transmission across the cell, even if that flow is low. Therefore, in the high-resolution grid it is possible to model both the 10m diameter bridge towers and the 5m diameter bridge piers as closed off model cells as the smallest cell size in this grid is of the order of 3m x 3m. It is only necessary to use the quadratic friction term to simulate the 0.5m diameter piles.

The key hydrodynamic processes that have been investigated in this part of the study are water level, bed shear stress and velocity. Results are presented as changes relative to a baseline case. The bed shear stress is the frictional force exerted on an area of seabed or river bed by current flowing over it. Therefore, it is an important quantity in the study of sediment transport processes, because it represents the flow-induced force acting on the bed sediments.

For the various construction schemes modelled the results are shown in the figures as a difference between the scenario and the baseline case. Therefore, an increase in a quantity appears as a positive value whilst negative values represent a reduction. Changes in water

level of less than ±0.01m are considered to represent no change. Similarly, changes in speed of less than ±0.01m/s and bed shear stress of ±0.02N/m² are considered insignificant.

The vertical direction in the numerical model uses a scaled co-ordinate system called σ-co-ordinates. The σ-co-ordinate system is boundary fitted both to the bottom and to the moving free surface. The numbers of vertical layers used in the model are defined as a percentage of the total depth. Therefore, the actual value of the total depth that each of these layers represents varies through any given tidal cycle. The near-surface speed represents the uppermost layer in the model and provides an indication of the speeds likely to impact on shallow drafted vessels, whilst the near-bed speeds are more representative of the forces acting on the river bed/seabed.

For comparison purposes the results for the operational phase of the Route 3A preferred option are provided in a summary table (Table A2.1).

Table A1.1 Schedule of scenario model runs for high water and peak ebb of the spring tide

Scenario	High Water Spring				Peak Ebb Spring			
	Water Levels	Near-Surface Speed	Near-Bed Speed	Bed Shear Stress	Water Levels	Near-Surface Speed	Near-Bed Speed	Bed Shear Stress
Island scheme	A2A	A4A	A6A	A8A	A2B	A4B	A6B	A8B
Aligned jetty	A10A	A12A	A14A	A16A	A10B	A12B	A14B	A16B
Jetty - Spike Island	A18A	A20A	A22A	A24A	A18B	A20B	A22B	A24B
Aligned jetty - extreme	A26A	A28A	A30A	A32A	A26B	A28B	A30B	A32B
Aligned jetty - new bathymetry	A34A	A36A	A38A	A40A	A34B	A36B	A38B	A40B

Table A1.2 Schedule of scenario model runs for low water and peak flood of the spring tide

Scenario	Low Water Spring				Peak Flood Spring			
	Water Levels	Near-Surface Speed	Near-Bed Speed	Bed Shear Stress	Water Levels	Near-Surface Speed	Near-Bed Speed	Bed Shear Stress
Island scheme	A1A	A3A	A5A	A7A	A1B	A3B	A5B	A7B
Aligned jetty	A9A	A11A	A13A	A15A	A9B	A11B	A13B	A15B
Jetty - Spike Island	A17A	A19A	A21A	A23A	A17B	A19B	A21B	A23B
Aligned jetty - extreme	A25A	A27A	A29A	A31A	A25B	A27B	A29B	A31B
Aligned jetty - new bathymetry	A33A	A35A	A37A	A39A	A33B	A35B	A37B	A39B

A2. Route 3A Preferred Option

This section provides a summary of the hydrodynamic simulation undertaken for the operational phase for the Route 3A preferred option as shown in Drawing No. B4027/3/B/300 Rev A. This scheme consists of 3 towers and several sets of smaller piers. The bridge piers are octagonal (5m x 5m) and the towers are also octagonal (10m x 10m). The towers are all located with the main channel of the upper estuary whilst the pier groups are located either on or above the intertidal area.

Table A2.1 Maximum and minimum changes for Route 3a preferred option

Scenario	Position	Low Water		Peak Flood		High Water		Peak Ebb	
		Max	Min	Max	Min	Max	Min	Max	Min
Water level (m)	Piers	0.08	-	0.02	-0.07	0.01	-0.02	0.08	-0.07
	Channels	-	-	-	-0.03	-	-	-	-
	Intertidal	0.14	-0.09	0.12	-0.10	-	-0.02	0.08	0.06
Near-surface speed (m/s)	Piers	-	-	0.16	-0.21	0.10	-0.63	0.04	-0.23
	Channels	-	-	0.04	-0.06	0.02	-	-	-
	Intertidal	-	-	0.25	-0.28	0.03	-0.08	-	-
Near-bed speed (m/s)	Piers	-	-	0.18	-0.40	0.12	-0.46	0.06	-0.21
	Channels	-	-	0.01	-0.02	0.02	-	-	-
	Intertidal	-	-	0.21	-0.21	0.03	-0.07	-	-
Bed shear stress (N/m^2)	Piers	-	-	2.68	-4.95	0.82	-2.02	0.28	-0.67
	Channels	-	-	0.17	-0.12	0.09	-0.02	-	-
	Intertidal	-	-	0.84	-0.72	0.14	-0.09	-	-

A3. Island Construction Scheme

Section 2 in the main report outlines the island construction approach and layout. Within the high-resolution hydrodynamic model the islands have been included as a change in the bathymetry.

A3.1 Water Level

Figures A1-A2 show differences in water level between the baseline case and the island construction scheme over a spring tide. The figures show that as a result of the placement of islands there is a backwater effect. Some of the observed differences are due to small phase changes as the tide propagates over the intertidal areas. Changes in water level local to the island structures show the maximum change to be around 0.15m at peak flood. However, around low water minor changes in flow propagation may manifest themselves as apparent large differences. Similarly, as the flooding or ebbing tide moves onto the intertidal areas large differences can be manifested along the edge of the tidal wave. These differences do not provide a real indication of change as they are an artefact of phase differences in the propagation of the front of the tidal wave (see Figure A1B). In addition, changes in water level observed on intertidal areas which are dry at that particular state of the tide are caused by the

inability of the model to resolve the small drainage channels (< 1m in width) in these areas leading to 'ponding' of water which in reality would be able to drain away.

The backwater effect is due to the reduction in flow cross-sectional area, with the extent of this blockage effect greatest in the north channel. This backwater effect is not limited to the flood tide although the observed effects are greatest in magnitude over this period and is caused by the strong asymmetry in the tidal curve with a very short flood period (≈1.5 hours) and a much longer ebb period (≈11 hours). The maximum change around the piers is 0.15 m and within the channel this reduces to 0.09 m (Table A3.1). Around peak ebb there is a general raising of the water level by between 0.01 - 0.02m upstream of the structures due to the reduced cross-sectional area.

A3.2 Speed

Figures A3 - A6 show differences in near-bed and near-surface flow speeds between the proposed island construction scheme and the baseline case over a spring tide. Around peak flood the model shows accelerated flow speeds around the island structure along the north channel. The maximum increase in flow speed local to the structure is of the order of 1.0m/s. Further, around peak flood there is a localized increase in flow speed within the channels (0.2m/s). The largest extent of flow change is within the north channel.

Over the ebbing tide the island structures lead to increased flow speeds in the north channel in the vicinity of the island and on the south bank along the intertidal area downstream to Old Quay lock. The maximum increase in speed around the structures is about 0.4m/s (see Table A3.1)

Around the time of high water there is a general change in flow speed across the whole width of the estuary due to the size of the islands. This effect is reduced on neap tides (not shown) due to the lower water levels. However, the magnitude of the change is still quite large with a maximum increase in speed around the structures of about 0.4m (see Table A3.1). The extent of the change is over 1000m extend upstream from the island positions.

Maximum changes in speed along the intertidal area tend to occur on the front of the tidal wave as it propagates onto the intertidal areas (see Table A3.1 and Figure A3B). However, as previously observed in the water level results, where these changes occur along the edge of the propagating wave such changes are considered to be insignificant, as they are very short in duration (seconds) and affect a very limited area. In addition, such changes are considered to represent a positional change in value rather than an absolute change.

A3.3 Bed Shear Stress

Figures A7 - A8 show differences in bed shear stress between the proposed island construction scheme and the baseline case over a spring tide. Figure A7B shows the difference in bed shear stress around peak flood with the greatest increase occurring in the north channel. In

general, the largest changes are confined to the immediate locality of the bridge structures with maximum increases of around 1.9 - 11.2N/m² and maximum reduction in bed shear stress of around 1.1 - 8.3N/m².

Figure A7B also shows the difference in bed shear stress along the front of the tidal wave as it propagates onto the intertidal banks. This effect is considered to represent a phase change between the baseline case and scheme and shows a positional change in bed shear stress rather than an absolute increase.

Although Table A3.1 indicates large changes in bed shear stress along the intertidal area (up to 3.2N/m²) many of these changes are due to the positional change in bed shear stress as a result of a change in the flow propagation. However, Figure A8B also reveals that some of these large changes are real and are caused by the obstruction across the channel that this scheme represents.

Around peak ebb the modelling indicates that there is a reduction in bed shear stress within the north channel and an increase in bed stress in the south channel. This is likely to be due the greater blockage effect observed in the north channel leading to an increase in flow within the south channel. This may lead to a change in the channel dominance at least for the duration of the island placements.

Table A3.1 Maximum and minimum changes for Route 3a preferred option - island construction scheme

Scenario	Position	Low Water		Peak Flood		High Water		Peak Ebb	
		Max	Min	Max	Min	Max	Min	Max	Min
Water level (m)	Piers	0.12	-	0.15	-0.16	0.03	-0.05	0.11	-0.03
	Channels	-	-	0.09	-	0.01	-0.02	0.02	-
	Intertidal	0.03	-0.08	0.13	-0.09	0.02	-0.03	0.01	-
Near-surface speed (m/s)	Piers	0.02	-0.04	1.03	-1.08	0.44	-0.90	0.43	-0.56
	Channels	-	-	0.21	-0.24	0.14	-0.15	0.02	-0.03
	Intertidal	-	-	0.33	-0.49	0.19	-0.13	0.11	-0.07
Near-bed speed (m/s)	Piers	0.01	-0.03	0.78	-0.62	0.38	-0.59	0.34	-0.36
	Channels	-	-	0.12	-0.13	0.08	-0.09	0.01	-0.02
	Intertidal	-	-	0.21	-0.28	0.15	-0.15	0.09	-0.04
Bed shear stress (N/m²)	Piers	0.09	-0.07	11.20	-8.33	1.91	-2.51	2.11	-1.08
	Channels	-	-	0.32	-0.54	0.53	-0.47	0.12	-0.15
	Intertidal	-	-	3.17	-2.56	1.16	-2.56	0.35	-0.24

A4. Aligned Jetty Construction Scheme

A brief description of the scheme layout for the aligned jetty scheme is given in Section 2 of the main report. The 0.5m diameter piles for the jetty have been included as added friction terms and represent a reduction in flow transmission through a model cell. The cofferdams are represented in the model by closing off cells.

A4.1 Water Level

Figures A9-A10 show differences in water level between the baseline case and the temporary jetty construction scheme over a spring tide. The model results show that around peak flood (Figure A9B) the aligned jetty scheme shows a general elevation of water levels in both the south and north channels. The extent and magnitude of this blockage effect is greatest in the north channel. This backwater effect is limited to the flood tide and is caused by the strong asymmetry in the tidal curve with a very short flood period (≈1.5 hours) and a much longer ebb period (≈11 hours). The maximum change around the piers is 0.07 m and within the channel this reduces to 0.03 m (Table A4.1).

At other states of the tide the backwater effect is not observed and this is probably due to the small diameter piles (0.5m). It is assumed that the deck of the jetty is high enough above the water surface to prevent it being inundated on high spring tides and tidal surges (pressure flow scour).

A4.2 Speed

Figures A11 - A14 show differences in near-bed and near-surface flow speeds between the aligned jetty construction scheme and the baseline case over a spring tide. At low water there is some change in speed indicated to occur along the intertidal area, particularly in the region of Old Quay Lock. The increase in flow speed (maximum 0.11m/s) is caused by acceleration of the flow through the jetty structures due to reduced flow cross-sectional area, and small changes in phase of the flow due to the placement of the structures across the channel. The observed reduction in flow speed is primarily caused by the change in the phase of the flow.

At peak flood the greatest magnitude of change occurs within the north channel, with maximum increases in flow speed local to the structure of 0.8m/s. At peak flood the model shows the aligned jetty construction scheme to accelerate the flows speeds along the intertidal areas of both the north and south channels. Some of the changes in speed along the intertidal area tend to occur on the front of the tidal wave as it propagates onto these areas (see Table A4.1 and Figure A11B). However, as previously, where these observed changes occur along the edge of the propagating wave such changes are considered to be insignificant, as they are very short in duration (seconds) and affect a very limited area. In addition, such changes are considered to represent a positional change in value rather than an absolute change.

Around the time of high water there is a general change in flow speed across the whole width of the estuary due to the number of piers present and the 30m diameter cofferdams. On neap tides this effect is reduced, as the upper levels of the intertidal area remain uncovered at high water (not shown). There is a general acceleration of flow around the cofferdams (maximum increase in speed 0.15m/s) and a reduction in flow speed in front of and behind the structures (maximum decrease in speed 0.45m/s). Within the channel the maximum increase in flow speed is 0.03m/s and the maximum reduction in speed is 0.05m/s. Along the banks the greatest increase in speed is 0.15m/s.

Over the ebbing tide the cofferdam and pier structures lead to increased flow speeds along much of the north bank along the intertidal area local to the bridge as well as along the south bank downstream of Old Quay lock. There is also a reduction in flow speed upstream of the Runcorn Gap.

A4.3 Bed Shear Stress

Figures A15 - A16 show differences in bed shear stress between the aligned jetty construction scheme and the baseline case over a spring tide. Around low water (Figure A15A) the greatest extent of change in bed shear stress occur along the southern bank between the proposed crossing and Runcorn Gap (maximum changes along the intertidal area 0.93 N/m²).

Figure A15B shows the difference in bed shear stress around peak flood. In general, the largest changes are confined to the immediate locality of the cofferdam and pier structures, with maximum increases of around 0.92 - 8.40N/m² and maximum reduction in bed shear stress of around 0.49 - 3.85N/m². Figure A15B also shows the difference in bed shear stress along the front of the tidal wave as it propagates onto the intertidal banks. This effect is considered to represent a phase change between the baseline case and scheme and shows a positional change in bed shear stress rather than an absolute increase.

Around high water the greatest increases in bed shear stress occur around the temporary structures (maximum increase 0.78N/m²). However, the largest predicted change is a reduction in bed shear stress along the intertidal area (8.43N/m²). This is probably caused by a combination of blockage effects from the structures together with a phase change between the baseline case and the scheme.

Table A4.1 Maximum and minimum changes for Route 3a preferred option - Aligned Jetty

Scenario	Position	Low Water		Peak Flood		High Water		Peak Ebb	
		Max	Min	Max	Min	Max	Min	Max	Min
Water level (m)	Piers	-	-	0.07	-0.04	0.03	-0.02	0.01	-
	Channels	-	-	0.03	-0.03	0.01	-	-	-
	Intertidal	-	-	0.08	-0.05	0.05	-	0.04	-0.08
Near-surface speed (m/s)	Piers	-	-	0.79	-0.79	0.14	-0.76	0.15	-0.45
	Channels	-	-	0.06	-0.06	0.03	-0.05	-	-
	Intertidal	0.11	-0.14	0.66	-0.41	0.12	-0.16	0.37	-0.11
Near-bed speed (m/s)	Piers	-	-	0.56	-0.45	0.12	-0.50	0.10	-0.27
	Channels	-	-	0.02	-0.05	0.01	-0.03	-	-
	Intertidal	0.08	-0.12	0.43	-0.23	0.06	-0.10	0.23	-0.08
Bed shear stress (N/m²)	Piers	0.04	-0.09	8.40	-3.85	0.78	-2.45	0.61	-1.37
	Channels	-	-	0.92	-0.49	0.03	-0.04	0.12	-0.28
	Intertidal	0.93	-0.59	6.78	-3.20	0.35	-8.43	2.02	-0.35

Around peak ebb the modelling indicates that there is a general increase in bed shear stress within the north and south channels particularly along the intertidal area. This is likely to be due to the acceleration of flows around the temporary structures and the greater blockage effect within the channels. Between Old Quay Lock and Runcorn Gap there is a reduction in bed shear stress, which might lead to a build up of sediment over the banks in this area.

A5. Jetty from Spike Island

A brief description of the scheme layout for the jetty scheme from Spike Island is given in Section 2 of the main report. As with the previously described aligned jetty scheme the 0.5m diameter piles for the jetty have been included as added friction terms and represent a reduction in flow transmission through a model cell. The cofferdams are represented in the model by closing off cells.

A5.1 Water Level

Figures A17-A18 show differences in water level between the baseline case and the jetty from Spike Island over a spring tide. The model results show that around peak flood (Figure A9B) the Spike Island scheme shows a general elevation of water levels in the north channel. This backwater effect is limited to the flood tide and is caused by the strong asymmetry in the tidal curve with a very short flood period (≈1.5 hours) and a much longer ebb period (≈11 hours). The maximum change around the piers is 0.08 m and within the channel this reduces to 0.02 m (Table A2.4).

At other states of the tide the backwater effect is not observed and this is probably due to the small diameter piles (0.5m).

A5.2 Speed

Figures A19 - A22 show differences in near-bed and near-surface flow speeds between the proposed Spike Island jetty scheme and the baseline case over a spring tide. At low water there is some change in speed indicated to occur along the intertidal area, particularly in the region of Old Quay Lock. The increase in flow speed (maximum 0.18m/s) is caused by a residual change in the flow due to the presence of the jetty and cofferdam structures. This change is caused by the reduced flow cross-sectional area, and small changes in phase of the flow due to the placement of the structures across the channel. The observed reduction in flow speed is primarily caused by the change in the phase of the flow.

At peak flood the greatest magnitude of change occurs within the north channel, with maximum increases in flow speed local to the structure of about 0.43m/s. At peak flood the model shows the jetty from Spike Island accelerates the flow speeds along the intertidal areas of both the north and south channels. The greatest changes occur within the north channel as this is where the greatest obstruction lies. However, some of the changes in speed along the intertidal area

tend to occur on the front of the tidal wave as it propagates onto these areas (see Table A2.4 and Figures A19B and A21B). However, as previously, where these observed changes occur along the edge of the propagating wave such changes are considered to be insignificant, as they are very short in duration (seconds) and affect a very limited area. In addition, such changes are considered to represent a positional change in value rather than an absolute change.

Around the time of high water there is a general change in flow speed across the whole width of the estuary due to the number of piers present and the 30m diameter cofferdams. There is a general acceleration of flow around the cofferdams (maximum increase in speed 0.69m/s) and a reduction in flow speed in front of and behind the structures (maximum decrease in speed 0.88m/s). Within the channel the maximum increase in flow speed is 0.05m/s and the maximum reduction in speed is 0.05m/s. Along the banks the greatest increase in speed is 0.09m/s.

Over the ebbing tide the cofferdam and pier structures lead to increased flow speeds along much of the north bank along the intertidal area local to the bridge as well as along the south bank downstream of Old Quay lock. There is a reduction in flow speed upstream of Runcorn Gap (see Table A2.4 and Figure A20).

A5.3 Bed Shear Stress

Figures A23 - A24 show differences in bed shear stress between the proposed Spike Island jetty construction scheme and the baseline case over a spring tide. Around low water (Figure A23A) the greatest extent of change in bed shear stress occur along the southern bank between the proposed crossing and Runcorn Gap (maximum changes along the intertidal area 0.69 N/m^2) due to a residual change in the flow due to the presence of the jetty and cofferdam structures. This change is caused by the reduced flow cross-sectional area, and small changes in phase of the flow due to the placement of the structures across the channel.

Figure A23B shows the difference in bed shear stress around peak flood. In general, the largest changes are confined to the immediate locality of the cofferdam and pier structures, with maximum increases of around 0.17 - 3.51N/m^2 and maximum reduction in bed shear stress of around 0.24 - 6.93N/m^2. Figure A23B also shows the difference in bed shear stress along the front of the tidal wave as it propagates onto the intertidal banks. This effect is considered to represent a phase change between the baseline case and scheme and shows a positional change in bed shear stress rather than an absolute increase. The largest changes in bed shear stress along the intertidal area are located in the north channel.

Around high water the greatest increases in bed shear stress occur around the temporary structures (maximum increase 1.99N/m^2). However, the largest predicted change is a reduction in bed shear stress around the structures (2.48N/m^2). This is primarily caused by the blockage effect from the temporary structures.

Table A5.1 Maximum and minimum changes for Route 3a preferred option - Spike Island Jetty

Scenario	Position	Low Water		Peak Flood		High Water		Peak Ebb	
		Max	Min	Max	Min	Max	Min	Max	Min
Water level (m)	Piers	0.02	-0.04	0.08	-0.06	0.02	-0.05	0.02	-0.05
	Channels	-	-	0.02	-0.04	-	-	-	-
	Intertidal	0.07	-0.07	0.08	-0.16	0.07	-0.02	0.07	-0.10
Near-surface speed (m/s)	Piers	-	-	0.43	-0.71	0.69	-0.88	0.11	-0.55
	Channels	-	-	0.01	-0.02	0.05	-0.05	0.02	-0.05
	Intertidal	0.18	-0.08	0.65	-0.43	0.09	-0.05	0.35	-0.23
Near-bed speed (m/s)	Piers	-	-	0.28	-0.39	0.47	-0.54	0.11	-0.28
	Channels	-	-	0.01	-0.02	0.03	-0.03	-	-
	Intertidal	0.09	-0.12	0.44	-0.34	0.06	-0.04	0.27	-0.17
Bed shear stress (N/m^2)	Piers	0.10	-	3.51	-6.93	1.99	-2.48	0.99	-0.93
	Channels	-	-	0.17	-0.24	0.13	-0.12	0.14	-0.24
	Intertidal	-0.69	-0.27	9.26	-6.00	0.34	-0.48	1.91	-0.48

Around peak ebb the modelling indicates that there is a general increase in bed shear stress within the north and south channels particularly along the intertidal area. This is likely to be due to the acceleration of flows around the temporary structures and the greater blockage effect within the channels. Between Old Quay Lock and Runcorn Gap there is a reduction in bed shear stress, which might lead to a build up of sediment over the banks in this area (see Table A2.4).

A6. Aligned Jetty: Extreme Fluvial and Surge Event - 1:200 Return Period

From the analysis of the results from the simulations for the various construction schemes the jetty schemes demonstrated the least impact on the system. After discussions with Giffords it was decided to undertake some additional simulations using the aligned jetty scheme. The scenario applied corresponded to the extreme fluvial and surge event (with a 1:200 years return period) used previously and defined in Appendix B ABPmer (2004). The shape of the surge tide was determined from a surge event recorded at Gladstone Dock. The recorded tidal curve was 'stretched' to fit the 1:200 years return event as quoted in Environment Agency (1998).

The extreme fluvial flows were calculated from freshwater flow data obtained from the Environment Agency and the National Flow Archive. 1:200 years return events were calculated for the following stations:

- River Gowy
- River Weaver
- River Mersey
- Sankey Brook
- Ditton Brook

A6.1 Water Level

Figures A25 - A26 show differences in water level between the baseline case and the aligned jetty scheme for an extreme fluvial and surge event. Around low water changes are primarily limited to the channel area around the jetty and tower structures (max 0.02m). Any changes observed along the intertidal area are due to minor phase changes in the timing of the movement of the tide as it propagates within the channel.

Around peak flood the model shows a small backwater effect occurring in the north channel. This effect is generally limited to the flood tide and is caused by the strong asymmetry in the tidal curve with a very short flood period (≈1.5 hours) and a much longer ebb period (≈11 hours). The maximum change around the piers is 0.06 m and within the channel this reduces to 0.04 m (Table A6.1). There is a residual effect around high water as shown in Figure A26A, but this has dissipated by around peak ebb flows.

A6.2 Speed

Figures A27 - A30 show differences in near-bed and near-surface flow speeds between the baseline case and the aligned jetty scheme for an extreme fluvial and surge event. Around low water the greatest changes are predicted to occur local to the bridge towers (cofferdams) and jetty structures. Maximum increases in speed local to the structures are up to 0.24m/s, approximately. The largest predicted change is a reduction in speed as a result of the 'blockage' effect of the cofferdams (-0.65m/s).

Around peak flood the greatest predicted changes in speed are local to the jetty and bridge structures in both the north and south channels (Table 6.1). The speckled pattern in the Figure A27B represents the changes in speed along the intertidal area, which tend to occur on the front of the tidal wave as it propagates onto these areas. However, as previously, where these observed changes occur along the edge of the propagating wave such differences are considered to be insignificant, as they are very short in duration (seconds) and affect a very limited area. In addition, such changes are considered to represent a phase change rather than a change in magnitude.

Figures A28A and A30A show the differences in near-surface and near-bed speed around high water. The cofferdam around the bridge tower in the north channel reduces the flow transmission and, thus, the speed within the channel (max reduction -0.08m/s). The flow is increased between the three tower/cofferdam structures with the maximum increase in flow local to these structures predicted to be 0.59m/s, approximately.

The causeway appears to have little impact on the hydrodynamics except around high water on spring tides when the water levels are high enough to extend onto this part of the intertidal area. There is an indication that there is an increase in flow circulating along the side of the causeway during this period (Figure A28A). Table 6.1 shows the maximum and minimum changes in speed local to the structures, within the channels and along the intertidal areas.

Around peak ebb, the changes in speed are limited to the vicinity of the structures in the north and south channels. Maximum increases in near-surface speed around the towers/cofferdams are 0.96m/s, approximately, with the maximum reduction in flows of about 1.07m/s (Table 6.1).

A6.3 Bed Shear Stress

Figures A31 - A32 show differences in bed shear stress between the baseline case and the aligned jetty scheme for an extreme fluvial and surge event. Around low water the largest changes in bed shear stress are local to the cofferdam and jetty structures. Downstream of the proposed crossing the flows are confined with in relatively narrow channels with much of the intertidal banks exposed. Maximum changes local to the cofferdams are $\pm$1.0N/m², approximately (Table 6.1).

Table A6.1 Maximum and minimum changes for Route 3a preferred option - Aligned Jetty: extreme fluvial and surge event - 1:200 return period

Scenario	Position	Low Water		Peak Flood		High Water		Peak Ebb	
		Max	Min	Max	Min	Max	Min	Max	Min
Water level (m)	Piers	0.02	-	0.06	-0.08	0.02	-	0.03	-
	Channels	-	-	0.04	-	-	-	-	-
	Intertidal	-	-	0.01	-	-	-	-	-
Near-surface speed (m/s)	Piers	0.24	-0.65	0.89	-1.40	0.59	-0.85	0.96	-1.07
	Channels	-	-	0.09	-0.06	0.06	-0.08	-	-
	Intertidal	-	-	0.16	-0.14	0.05	-0.07	0.04	-0.04
Near-bed speed (m/s)	Piers	0.20	-0.41	0.54	-0.96	0.56	-0.65	0.69	-0.90
	Channels	-	-	0.06	-0.06	0.06	-0.06	-	-
	Intertidal	-	-	0.08	-0.05	0.05	-0.10	0.04	-
Bed shear stress (N/m²)	Piers	1.03	-1.04	7.17	-5.89	3.82	-1.61	1.55	-1.81
	Channels	-	-	0.32	-0.39	0.20	-0.20	0.09	-
	Intertidal	-	-	3.02	-0.36	0.46	-0.48	0.19	-0.10

Around peak flood the largest differences are local to the tower/cofferdam structures with a maximum increase in bed shear stress of 7.17N/m² and a maximum reduction of 5.89N/m², approximately. Changes within the channel, whilst more wide spread are relatively small compared with underlying values (see Table 6.1 and Figure 9).

Figure A32A shows the differences in bed shear stress around high water. There is a general increase in the bed stress along the line of the proposed crossing except in the lee of the cofferdams where their 'blocking' effect reduces the flow speed and hence the bed shear stress. The cofferdam around the bridge tower in the north channel reduces the bed stress within the channel over a large area, although the magnitude of the change is small relative to the background values (max reduction -0.20N/m²). The largest changes are again local to the structures (max increase 3.82N/m²)

Around peak ebb the modelling indicates that the changes in bed shear stress are relatively confined to the vicinity of the structures. The maximum increase in shear stress in the channel is 0.09N/m², approximately (see Table A6.1).

A7. Aligned Jetty: New Bathymetry

As stated in Section A6, from the subsequent analysis of modelling results the two temporary jetty construction schemes showed the least overall impact on the system. And following from discussions with Giffords it was decided that the aligned jetty layout would be used in subsequent scenarios.

In early 2005 a limited survey of the estuary local to the proposed crossing was undertaken. This captured the significant movement of the channels between this new survey and the previous 2002 survey used to date in all modelling undertaken in the project. The new bathymetry allowed a modelling assessment of the hydrodynamic response to the proposed bridge with a completely different channel configuration and to assess the significance of this. The detailed modelling only carried out this assessment for the preferred option using the aligned jetty construction scheme. As with the extreme scenario run with the aligned jetty a causeway was included over the intertidal area joining with the jetty.

A7.1 Water Level

Figures A33 - A34 show differences in water level between the baseline case and the aligned jetty scheme for the new channel configuration. Around low water changes are primarily limited to the channel area around the jetty and tower structures (max 0.28m). Any changes observed along the intertidal area are due to minor phase changes in the timing of the movement of the tide as it propagates within the channel.

Table A7.1 Maximum and minimum changes for Route 3a preferred option - Aligned Jetty: new bathymetry

Scenario	Position	Low Water		Peak Flood		High Water		Peak Ebb	
		Max	Min	Max	Min	Max	Min	Max	Min
Water level (m)	Piers	0.28	-	0.06	-0.14	0.06	-0.05	0.04	-0.06
	Channels	-	-	0.02	-0.02	-	-	0.02	-
	Intertidal	0.01	-	0.03	-0.09	0.03	-0.03	-	-
Near-surface speed (m/s)	Piers	0.11	-0.13	0.63	-1.16	0.52	-1.16	0.79	-0.87
	Channels	0.01	-	0.08	-0.09	0.07	-0.15	0.05	-
	Intertidal	-	-0.09	0.07	-0.30	0.11	-0.15	0.09	-0.15
Near-bed speed (m/s)	Piers	0.09	-0.09	0.56	-0.81	0.39	-0.84	0.51	-0.54
	Channels	-	-	0.03	-0.06	0.06	-0.09	0.03	-
	Intertidal	-	-	0.03	-0.26	0.07	-0.11	0.07	-0.09
Bed shear stress (N/m²)	Piers	0.56	-1.63	8.42	-4.88	4.38	-3.39	6.71	-2.01
	Channels	0.16	-	0.68	-1.25	0.15	-0.15	0.11	-0.34
	Intertidal	0.20	-0.64	1.85	-3.02	0.82	-0.45	0.25	-2.31

Around peak flood the model shows a small backwater effect occurring in the south channel (<0.02m). This effect is generally limited to the flood tide and is caused by the strong asymmetry in the tidal curve with a very short flood period (≈1.5 hours) and a much longer ebb period (≈11 hours). The maximum change around the piers is 0.06 m with a maximum reduction in water level of about 0.14m (Table A7.1). The effect extends downstream of the proposed crossing.

Around high water this backwater effect has dissipated and changes are mostly local to the structures with some small changes observed along the intertidal area (max ±0.03m) due to minor phase changes in the timing of the movement of the tide as it propagates within the channel (Figure A26A and Table A7.1).

Around the time of peak ebb changes are primarily confined to the channel area around the jetty and tower structures (max 0.04m). Any changes observed along the intertidal area are due to minor phase changes in the timing of the movement of the tide as it propagates within the channel.

A7.2 Speed

Figures A35 - A38 show differences in near-bed and near-surface flow speeds between the baseline case and the aligned jetty scheme with the revised channel configuration. Around low water the largest changes occur locally to the cofferdam and jetty structures (max 0.11m/s; min -0.13m/s). Changes in speed within the channel are insignificant with maximum differences of about 0.01m/s. Along the intertidal area changes are mostly due to minor phase changes in the timing of the movement of the tide as it propagates within the channel.

Around peak flood (Figures A35B and A37B) the great changes are predicted to occur local to the cofferdam and jetty structures with maximum increase in speed of 0.63m/s and a reduction in speed due to the 'blockage' effect of the cofferdams of 1.16m/s. Within the channels the largest increase in speed is of the order of 0.03m/s, whilst the largest reduction in speed is about 0.8m/s. Within the channels the largest increase in speed is of the order of 0.03m/s, with the largest reduction in speed of -0.06m/s. Along the intertidal areas changes tend to occur on the front of the tidal wave as it propagates onto these areas. However, as previously, where these observed changes occur along the edge of the propagating wave such differences are considered to be insignificant, as they are very short in duration (seconds) and affect a very limited area. In addition, such changes are considered to represent a phase change rather than a change in magnitude.

Figures A36A and A38A show the changes in speed around high water. The higher water levels ensure that the central tower/cofferdam structure is now exposed to the flow, with changes in speed predicted across the width of the estuary corresponding to the position of the proposed bridge alignment. As at other states of the tide the greatest changes occur locally to the cofferdam and jetty structures and are of similar order to those observed around peak flood,

with maximum increases in speed of 0.52m/s, approximately (see Table A7.1). Differences in speed along the intertidal area are small (max 0.07m/s; min -0.11m/s).

Around peak ebb changes in speed are generally localized to the proposed crossing with maximum and minimum changes (max 0.79m/s; min -0.87m/s) predicted to occur local to the cofferdam and jetty structures (Table A7.1). Changes in speed within the channel are small with maximum differences of about 0.05m/s. Along the intertidal area changes are mostly due to minor phase changes in the timing of the movement of the tide as it propagates within the channel.

A7.3 Bed Shear Stress

Figures A39 - A40 show differences in bed shear stress between the baseline case and the aligned jetty scheme with the revised channel configuration. Around low water the greatest changes occur local to the cofferdam and jetty structures with maximum differences of 0.56N/m² and -1.63N/m², approximately. Changes along the intertidal areas are localized as the flow is confined to the low water channels.

Around peak flood the largest changes occur local to the cofferdams with maximum increases in bed stress of 8.42N/m² and maximum reduction of bed stress, due to the blocking effect of the cofferdams, of -4.88N/m². Within the channels the largest predicted changes are a reduction in bed stress of -1.25N/m². However, background levels of bed shear stress around peak flood on a spring tide are between 6 - 18N/m² and, therefore, differences of this magnitude may not impact significantly on sediment transport rates. Along the intertidal area many of the predicted changes are due to minor phase changes in the timing of the movement of the tide as it propagates within the channel.

Around high water maximum changes in stress local to the cofferdams reduce to 4.38N/m² and -3.39N/m². Within the channels the largest predicted changes are of the order of $\pm$0.2N/m². Along the intertidal area the greatest changes are local to the bridge and jetty structures. In addition the speckled patterns of changes represent a phase change rather than a change in magnitude (see Figure A40A and Table A7.1).

Figure A40B shows the difference in bed shear stress around peak ebb. The falling water levels limits the spatial extent of change across the upper estuary. The largest changes are local to the cofferdams with a maximum increase of 6.71N/m², approximately. Within the channels the greatest increases in bed stress are of the order of 0.11N/m². However, generally the bed stress is reduced within the channels (max -0.34N/m²). Along the intertidal area there is some increase in bed stress local to the jetty structures, but generally there is a reduction in stress (Table A7.1).

A8. Bridge Scour Assessment

A8.1 Introduction

Whilst the theory behind the structural design of bridges is well founded, the mechanisms for flow and erosion in channels consisting of mobile sediments is not well defined. This makes the river boundary changes that occur at a bridge, due to a given flow condition, difficult to estimate with confidence.

In the context of the current report, scour is defined as the lowering of a river bed by erosion due to water turbulence such that there is a tendency to expose the bridge foundations. The extent of this reduction in the natural level of the river bed is the scour depth or depth of scour. The natural level of the bed is generally considered to be the level of the river bed prior to the onset of scour. The types of scour that can occur at a bridge crossing are normally referred to as general scour, contraction scour and local scour. These different types of scour may occur simultaneously, in combination or separately. In addition, in tidal estuaries scour development will take place in two directions due to the ebbing and flooding of the tide.

General scour occurs irrespective of the bridge being located within the river and can take place as long-term or short-term scour. Long-term scour is typically of the order of several years or longer, whilst short-term scour can occur over a single flood event. Long-term scour results in progressive degradation and lateral bank erosion. Progressive degradation is the general lowering of the river bed due to geomorphological changes, anthropogenic changes, or hydrometeorological changes.

Contraction scour and local scour are a direct consequence of the bridge being located in the river bed. The flow at a bridge usually converges as it approaches the bridge due to the bridge or the approach roads causing a constriction of the flow. As the flow contracts within the opening it accelerates. This accelerated flow induces scour across the contracted section of river and is, thus, termed contraction scour.

Local scour is caused by the interference of the bridge piers and abutments with the flow and manifests itself by the formation of scour holes immediately around these structures. Localized scour can occur either as clear-water scour or live-bed scour. Clear-water scour occurs when the bed sediment upstream of the areas of scour is at rest. Live-bed scour occurs when there is general sediment transport within the river. The maximum local scour depth is achieved when the flow is no longer able to remove bed material from the area of scour. The equilibrium scour depth occurs when the time-averaged transport of bed material into the scour hole equals that removed from it. Melville and Coleman (2000) give a detailed review of bridge scour.

The local scour around bridge piers is largely dependent on their geometry and, generally, will occur quite rapidly. Therefore, of most import is the maximum scour depth developed within the equilibrium phase.

The flow pattern near a bridge pier is quite complex, for example, Breusers and Raudkivi (1991), Melville and Coleman (2000). The principal features of scour round a circular pier are well defined, the downflow at the upstream face of the pier, the horseshoe vortex at the base of the pier, a surface roller (or bow wave) at the upstream face of the pier and wake vortices downstream of the pier (Figure 25).

The downflow is a result of flow deceleration in front of the pier. The associated stagnation pressures on the face of the pier are greatest near the surface, where the deceleration is largest, and decrease downwards. This resulting downwards pressure gradient at the face of the pier leads to the downflow. This downflow impinges on the bed, acting like a vertical jet and eroding a groove immediately adjacent to the pier face. The creation of the groove undermines the scour hole slope above and this slope then collapses bringing sediment into the erosion zone. The development of the scour hole around the pier creates a lee eddy, known as the horseshoe vortex. The horseshoe vortex develops as a result of separation flow at the upstream rim of the scour hole and is, therefore, a consequence of the scour not the cause of it. The horseshoe vortex is effective at transporting sediment away from the scour hole. It is the downflow and horseshoe vortex that are the primary mechanisms in the scour hole development.

The wake vortices are a consequence of flow separation at the sides of the pier. These vortices travel downstream due to the mean flow. Raudkivi (1991) describes these cast-off vortices as having vertical low pressure centres lifting sediment from the bed like miniature tornados. Melville and Coleman (2000) describe the vortices as acting like vacuum cleaners sucking sediment from the bed as well as transporting sediment entrained by the downflow and horseshoe vortex.

A8.2 Timescale

Scour around bridge piers can be divided into several stages (Hoffmans and Verheij, 1997): the initial phase, development phase, stabilization phase and equilibrium phase. The initial phase of the scour process can be characterized as the period in which the erosion capacity is greatest. The development phase is represented by a significant increase in the scour depth, whilst the shape of the scour hole remains the same. During the equilibrium phase the rate of development of the maximum scour depth reduces. In addition, the erosion capacity in the deepest part of the scour hole is small compared to the erosion capacity downstream of the point of reattachment. This leads to a greater increase in the longitudinal dimensions of the scour hole than in the vertical depth. The equilibrium phase is defined as the period during which the dimensions of the scour hole remain significantly unaltered.

Under live-bed conditions, the equilibrium depth is reached more quickly than under clear-water scour conditions. Thereafter, the scour depth will fluctuate due to the movement of sediment/bedforms past the pier.

A8.3 Effect of Flow Depth

Melville and Coleman (2000) define flow shallowness as representing the effect of flow depth relative to the pier width. For deep flows, that is, for narrow piers, the scour depth increases proportionately with foundation size and is independent of flow depth. Whereas, for shallow flows, relative to the pier size, the scour depth increases proportionately with flow depth and is independent of pier width. While for intermediate flow depths the depth of scour is dependent on both. In addition, the depth of the bed material is also important as this may limit the scour development.

A8.4 Effect of Tidal Flow

Relatively little work has been undertaken to investigate flow at bridges in tidal rivers in comparison to studies undertaken for unidirectional flow. Since the flow reverses direction with the tide consequently the scour development will take place in two directions. The local scour depth can be estimated using the same equations as for unidirectional river flow, although scour development is typically reduced due to sediment eroded during the first phase of the tide being deposited on the reversing part of the tidal cycle. Breusers (1966) suggested the following equation for local scour depth at piers.

$$d_s = 1.4b$$

where

b = the pier width

The equation was developed using measurements of scour depths in tidal estuaries. In addition to the astronomical variation of the tide, other factors that may affect local scour in tidal estuaries are meteorological effects such as storm surges and the relative magnitudes of the fluvial and tidal flows.

Numerous equations have been proposed for the estimation of the depth of local scour at bridge piers (Melville and Coleman, 2000), however, in the current study only the formulas of Breusers (1966), Breusers *et al.* (1977), Johnson (1992) and Richardson and Davis (2001) have been used for comparison purposes.

$$d_s = 1.5K_i b \tanh\left(\frac{h_0}{b}\right) \qquad \text{(Breusers } et\ al.,\ 1977\text{)}$$

$$d_s = 2.02K_i h_0 F_r^{0.21} \sigma_d^{-0.24} \left(\frac{b}{h_0}\right)^{0.98} \qquad \text{(Johnson, 1992)}$$

$$d_s = 2.0K_1K_2K_3K_4 h_0 F_r^{0.43} \left(\frac{b}{h_0}\right)^{0.65} \qquad \text{(Richardson and Davis, 2001)}$$

in which:

b	= the pier width (m)
h_0	= flow depth (m)
K_i	= correction factor
K_1	= correction factor for pier nose shape
K_2	= correction factor for angle of attack of flow
K_3	= correction factor for bed condition
K_4	= correction factor for size of bed material
F_r	= Froude number
d_s	= equilibrium scour depth

The local scour depth can be estimated using the same equations as for unidirectional river flow, although scour development is typically reduced due to sediment eroded during the first phase of the tide being deposited on the reversing part of the tidal cycle. Therefore, assuming that the depth of scour with time, *d(t)*, can be defined by the following formula (Sumer and Fredsøe, 2002):

$$d(t) = d_S\left[1 - \exp\left(-\frac{t}{T}\right)\right]$$

The Richardson and Davis (2001) expression has a tendency to over-predict scour depth. However, it is likely that based on the calculation the depth of scour around the bridge piers/towers can be expected to reach the order of metres unless scour countermeasures are applied. The width of the scour hole can be approximated to 3 - 4 times the width of the structure. Therefore, for the tower structures the width will be between 30 and 40m.

However, for the present study the structures have a large depth to structure diameter (b/h_0 > 0.5) and, therefore, the principal mechanism for scour is different than the slender pile case. Physical modelling studies by Torsethaugan (1975) for large diameter cylinders suggested that the maximum scour depth in a steady current does not occur at the upstream face of the cylinder but at about 45° from the axis of the oncoming flow. The maximum scour depth is dependent on the diameter of the structure as well as the ratio of the water depth to pile diameter. Rance (1980) reported results from physical model tests for scour around a large circular cylinder, as well as hexagonal and square structures both under waves alone as well as for one combined wave and current condition. For co-linear waves and currents Rance suggested that the maximum scour depth for the cylinder was 0.064b, with accretion of 0.028D in some adjacent areas to the cylinder.

Table A8.1 Maximum predicted scour depths for temporary structures under a spring tide

Formula	Cofferdam		Island		Jetty pile	
	Scour Depth d_s (m)		Scour Depth d_s (m)		Scour Depth d_s (m)	
	Flood	Ebb	Flood	Ebb	Flood	Ebb
Breusers *et al.* (1977)	4.2	3.2	5.5	4.2	0.5	0.5
Richardson and Davis (2001)	-	-	-	-	2.96	1.83
Rance (1980) wave + current	1.92	1.92	7.68	7.68	-	-

Table A3.1 shows the results of estimated maximum scour depth based on a range of formulae for the various temporary structures. Whilst the approach of Rance (1980) is strictly valid for combined waves and currents it provides an additional assessment of the scour depth around large structures and, therefore, an envelope for the likely possible maximum scour depth. May and Willoughby (1990) measured scour depths significantly smaller than that predicted by the Breusers *et al.* (1977) formula. The Richardson and Davis (2001) expression also has a tendency to over-predict scour depth. Figure 26 shows the variation of scour depth with time for the circular cofferdam and temporary island structure. The maximum scour attained under a spring tidal cycle is 4.0m, approximately. From the results the scour around the square island structure is clearly worse than for the circular cofferdam. This is both a function of size and shape.

The scour analysis undertaken is based on recognised empirical relationships, but remains simplistic in its approach and is based on calculated time-series of depths and speeds found at the various proposed bridge crossing locations. It assumes that the flow is aligned to the pier. However, more detailed analysis should be undertaken at the design stage once a preferred construction methodology has been selected.

A9. References

Breusers, H.N.C. (1966). Conformity and time scale in two-dimensional local scour. *Proc. Symp. On Model and Prototype Conformity.* Poona, pp. 1 - 8.

Breusers, H.N.C, Nicollet, G. and Shen, H.W. (1977). Local scour around cylindrical piers. *J. of Hydraulic Res.,* IAHR, Vol 15, No. 3, pp. 211-252.

Breusers, H.N.C. and Raudkivi, A.J. (1991). *Scouring*. IAHR Hydraulic structures design manual (2), A.A.Balkema, Rotterdam, 143pp.

Johnson, P.A. (1992). Reliability-based pier scour engineering. *J. of Hydr. Engng.*, ASCE, Vol. 118, HY8, pp. 626-629.

May, R.P. and Willoughby, I.R. (1990). *Local scour around large obstructions*. HR Wallingford Report SR 240.

Melville, B.W. and Coleman, S.E. (2000). *Bridge Scour*. Water Resources Publications, LLC, Colorado, USA, 550 pp.

Rance, P.J. (1980). The potential for scour around large objects. In: *Scour Prevention Techniques around Offshore Structures*, Proc. of a one day seminar, 16 Dec 1980, Society for Underwater Technology, London, pp. 41 - 53.

Richardson, E.V. and Davis, S.R. (2001). *Evaluating Scour at Bridges*. Hydr. Engng. Circular No. 18, US Department of Transport, Federal Highway Administration, Pub. No. FHWA NHI 01-001.

Sumer, B.M. & Fredsøe, J., 2002. *The mechanics of scour in the marine environment*. Advanced series in Ocean Engineering - Volume 17, pp536.

Torsethaugen, K. (1975). *Lokalerosjen ved store knostruksjoner. Modellforsøk*. SINTEF Report STF60 A75055, Norwegian Hydrotechnical Lab., Trondheim (in Norwegian).

Appendix A
Figures

A.

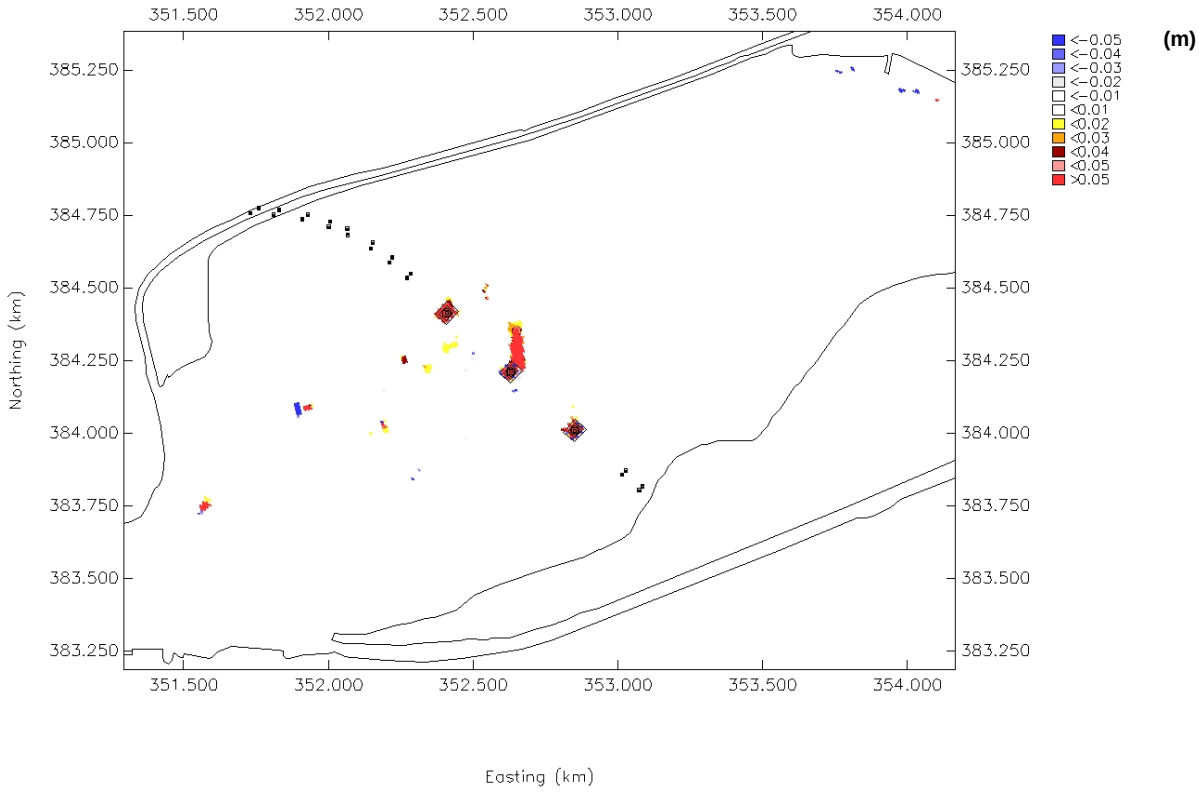

B.

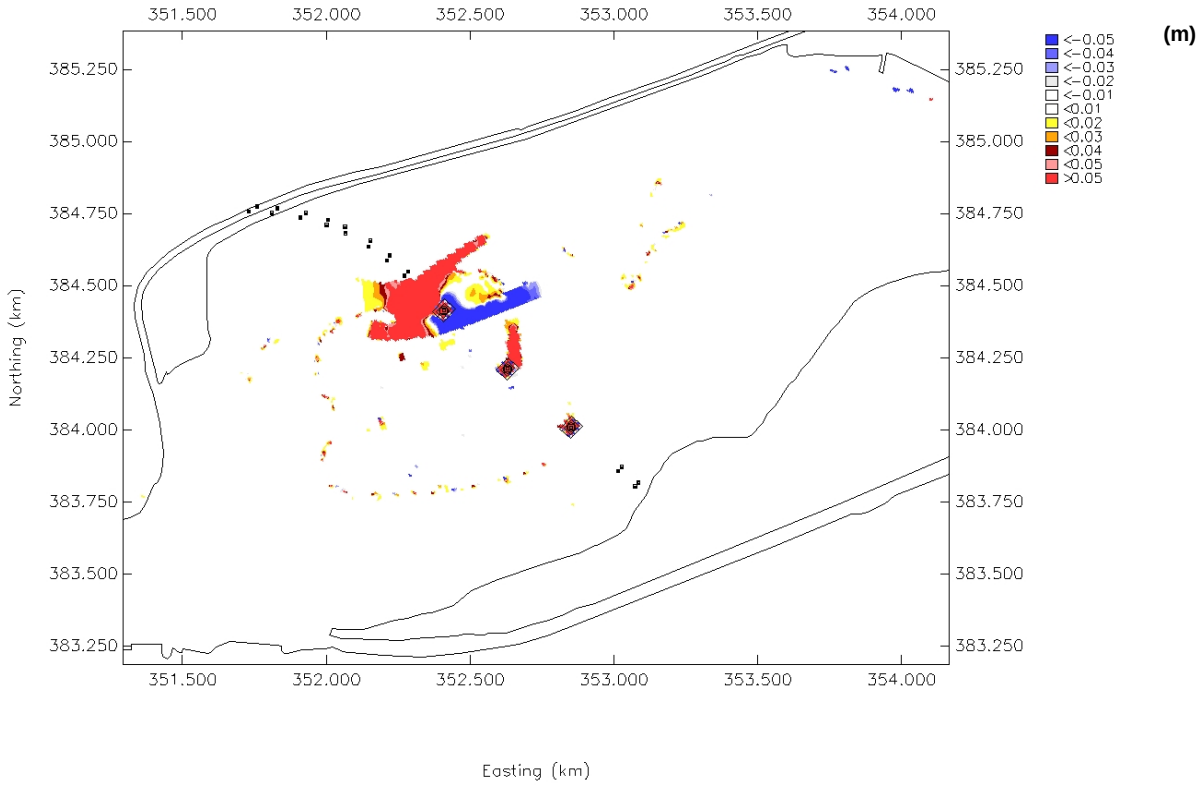

ABP mer marine environmental research	Differences in water level (m) between the proposed bridge scheme Route 3A Medium 3 Tower revised option and the baseline case for low water (A) and peak flood (B) on a spring tide – island construction option	Figure A1

A.

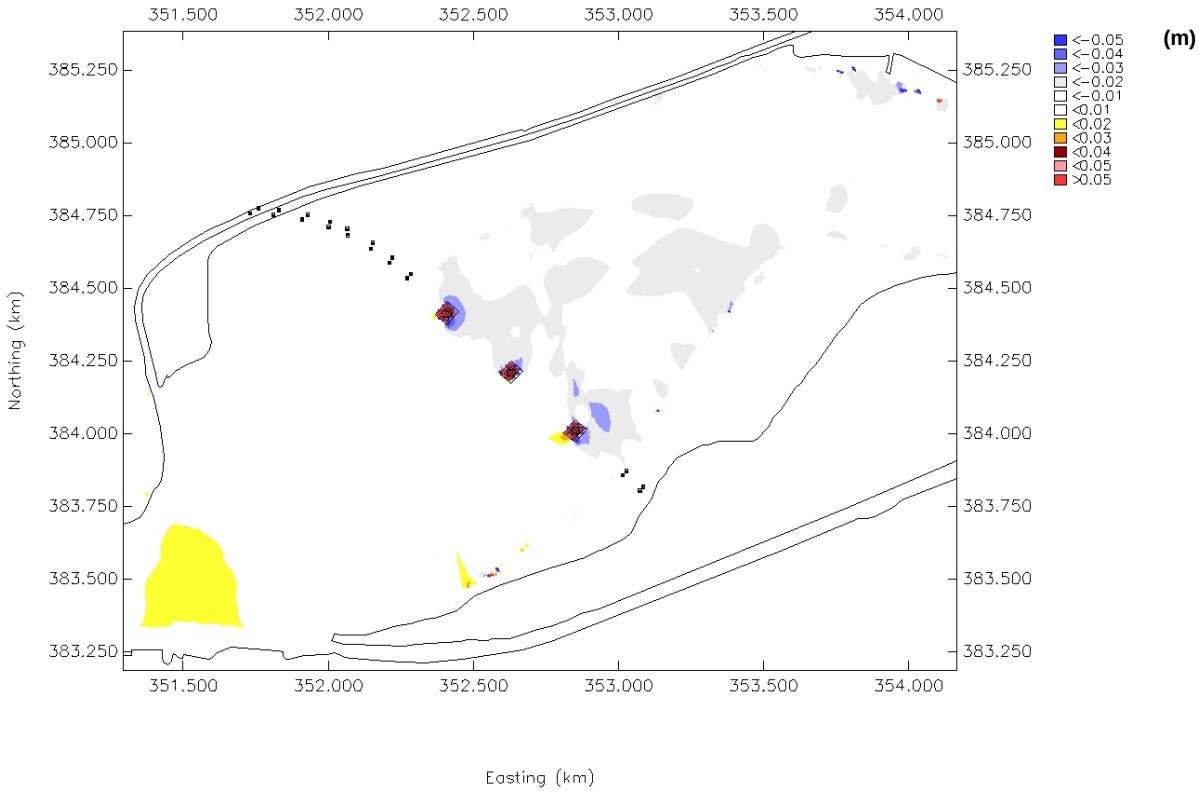

B.

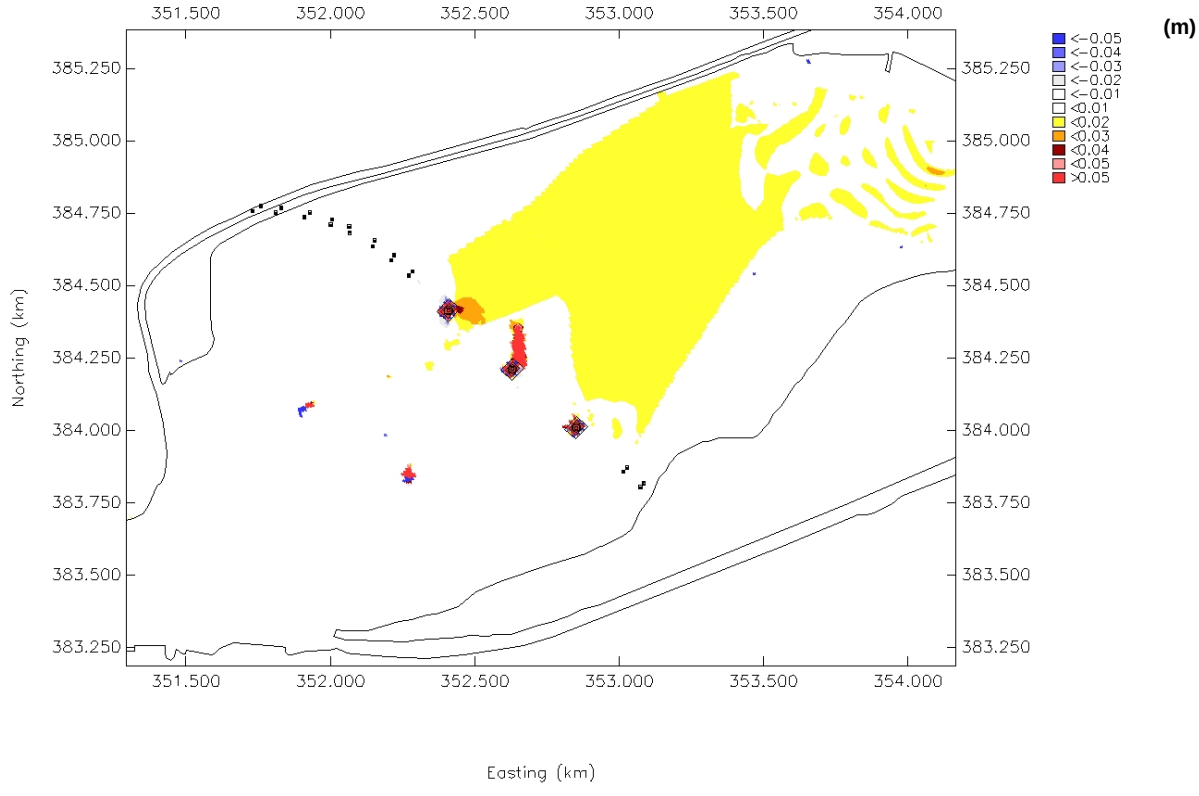

ABP mer marine environmental research

Differences in water level (m) between the proposed bridge scheme Route 3A Medium 3 Tower revised option and the baseline case for high water (A) and peak ebb (B) on a spring tide – island construction option

Figure A2

A.

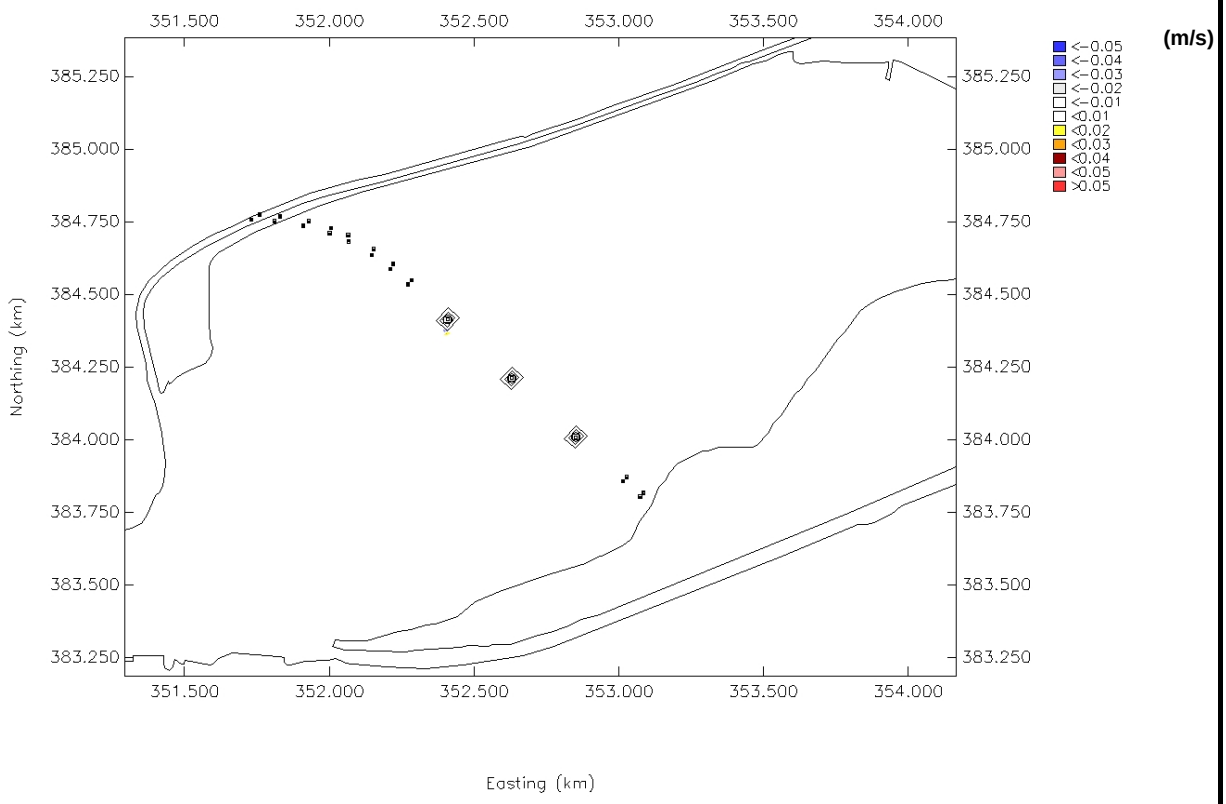

B.

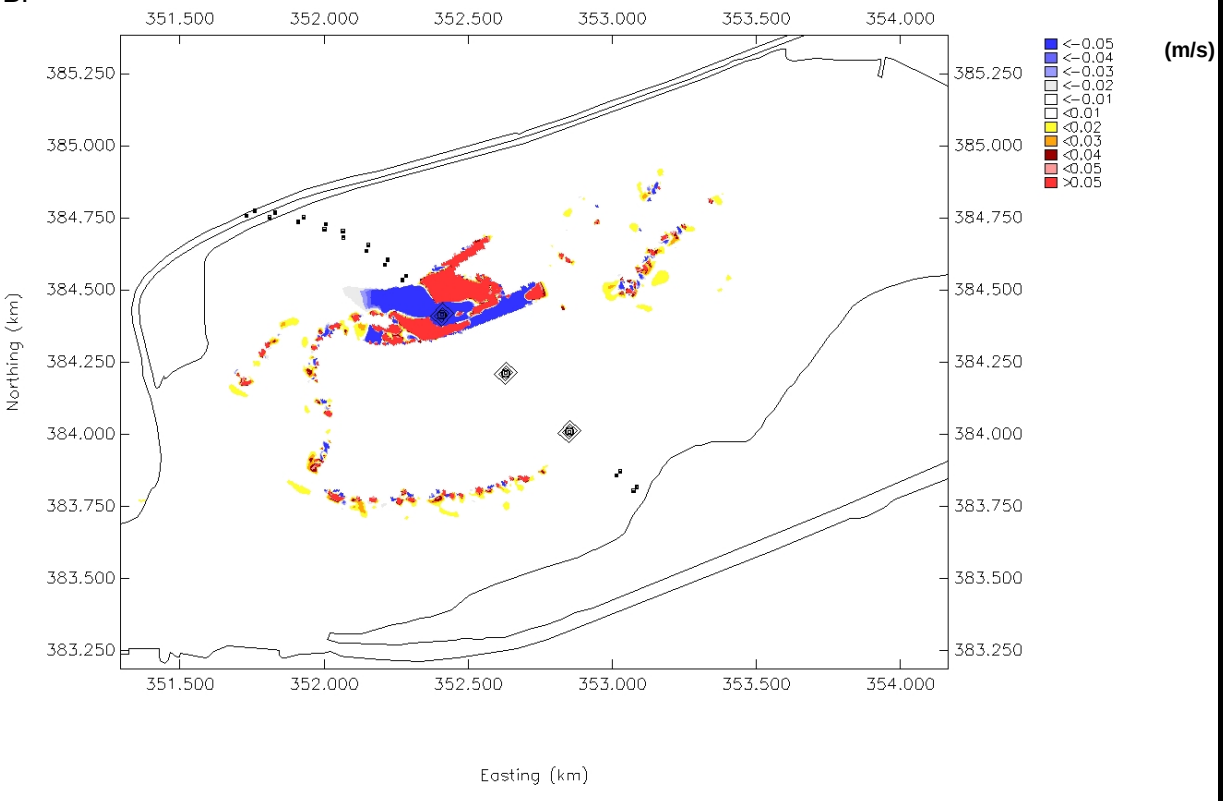

ABP mer marine environmental research

Differences in near-surface speed (m/s) between the proposed bridge scheme Route 3A Medium 3 Tower revised option and the baseline case for low water (A) and peak flood (B) on a spring tide – island construction option

Figure A3

A.

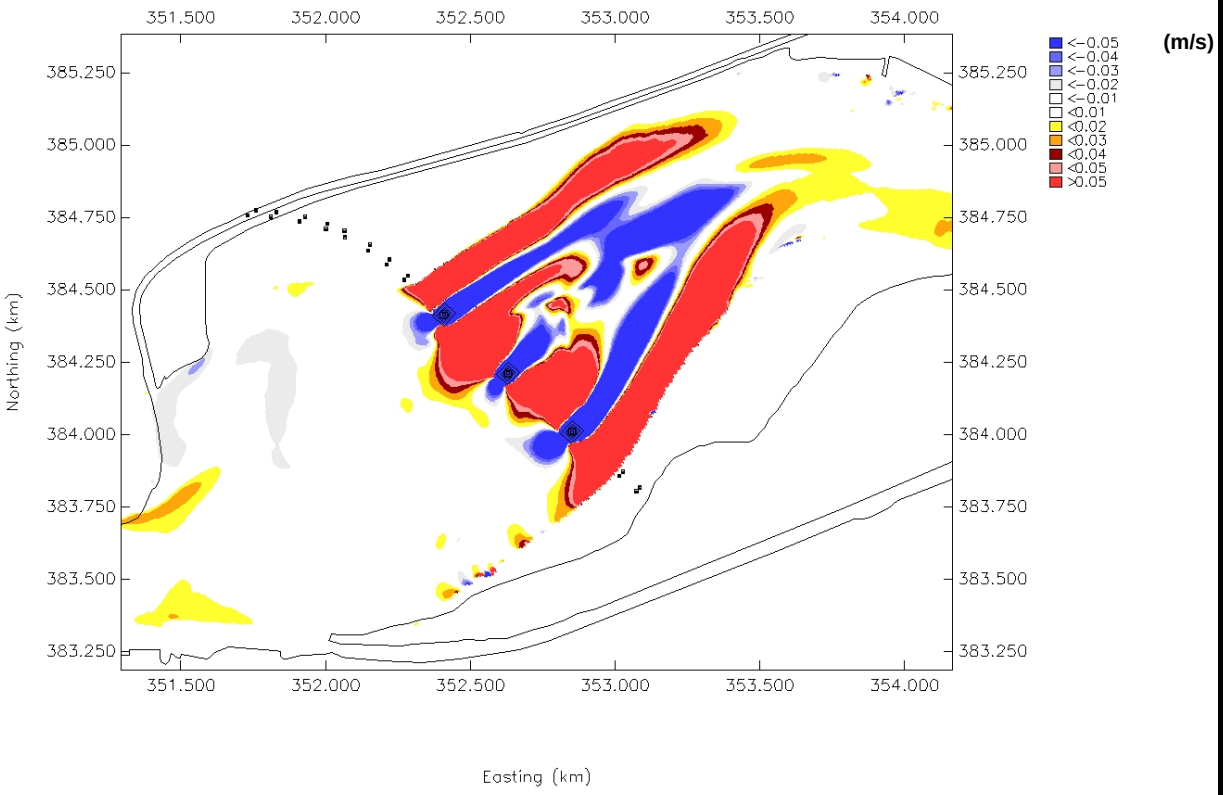

B.

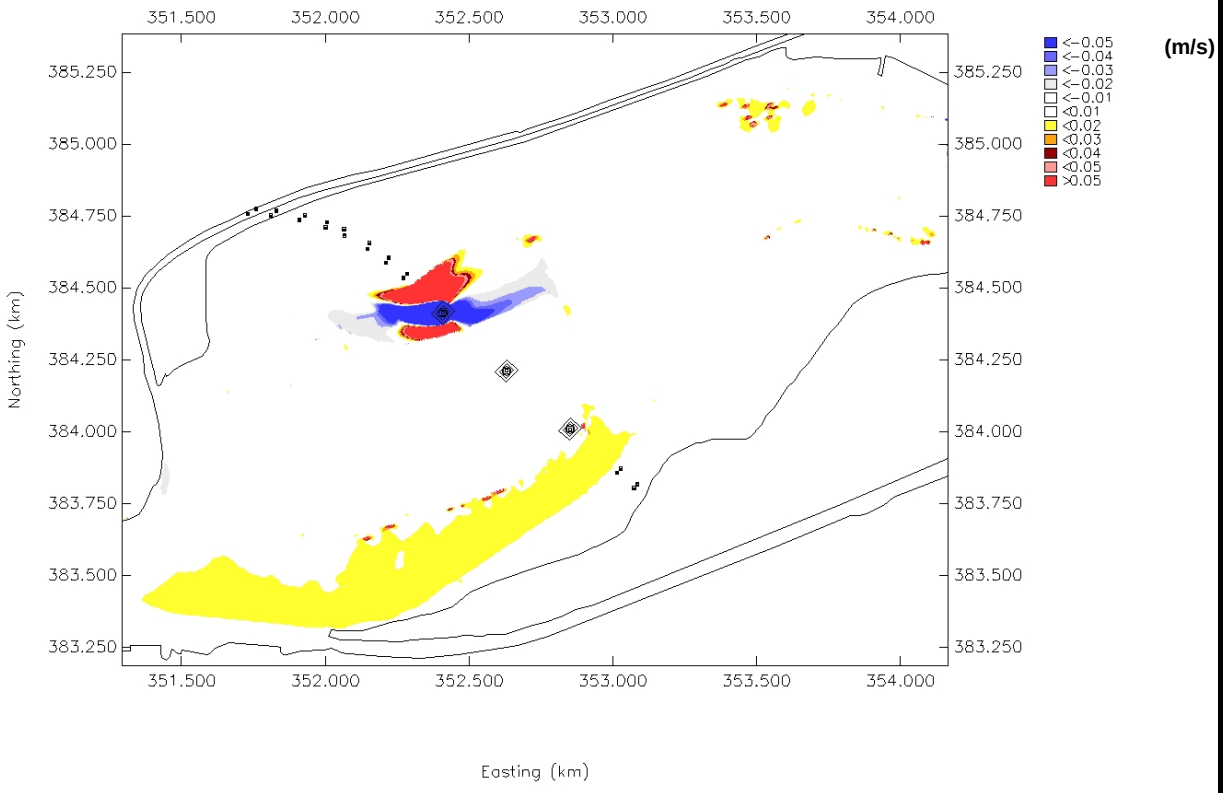

ABP mer marine environmental research	Differences in near-surface speed (m/s) between the proposed bridge scheme Route 3A Medium 3 Tower revised option and the baseline case for high water (A) and peak ebb (B) on a spring tide – island construction option	Figure A4

A.

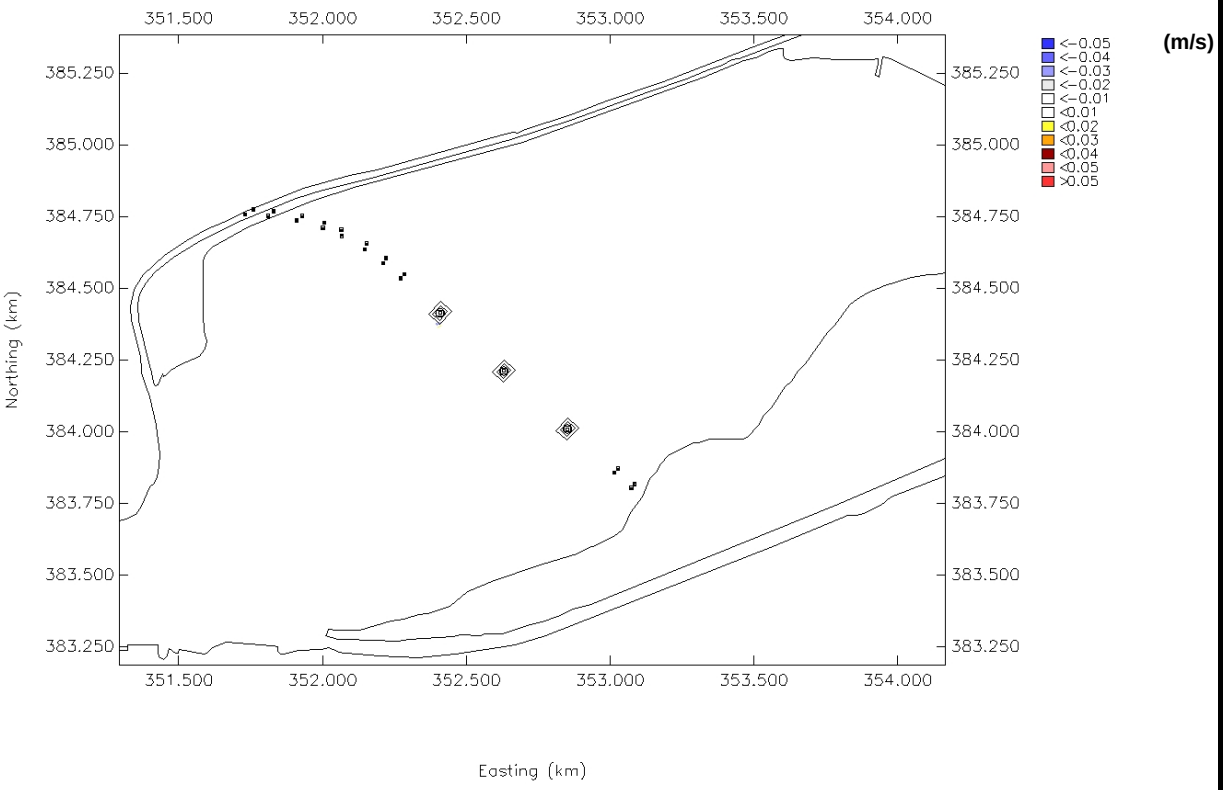

B.

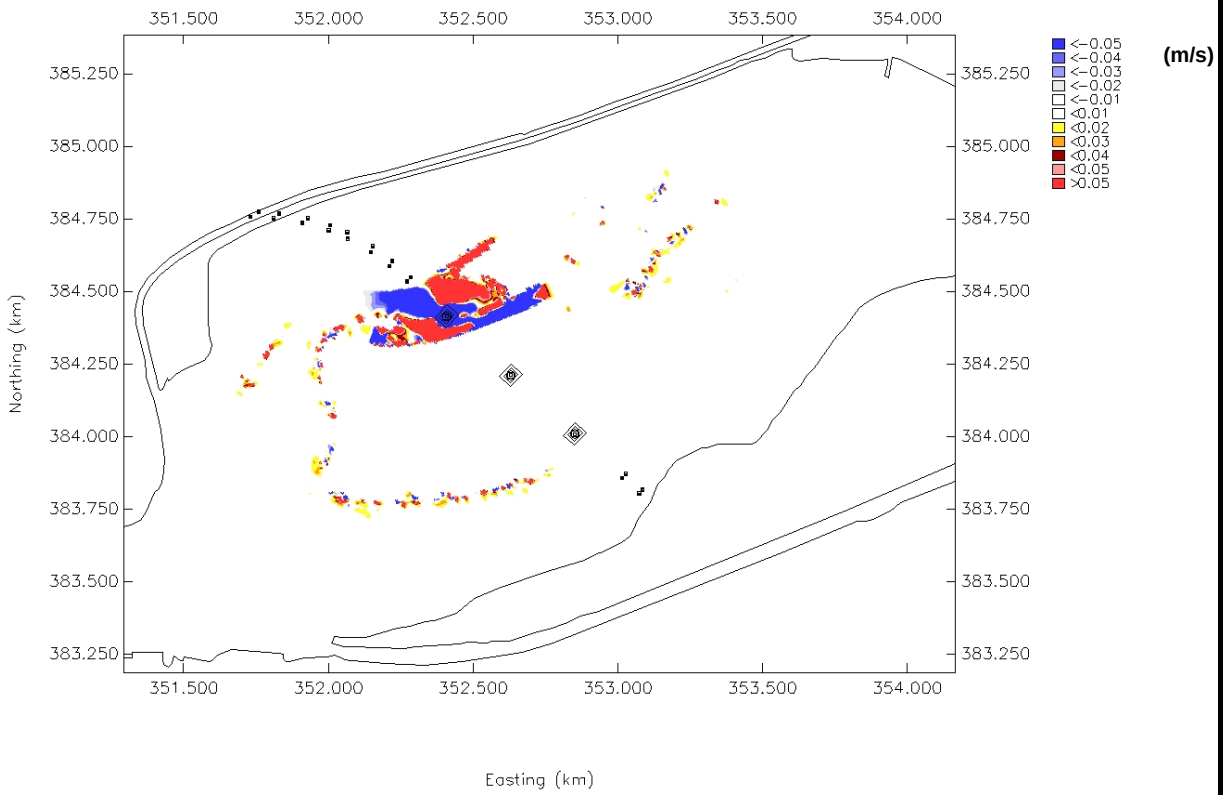

ABP mer marine environmental research	Differences in near-bed speed (m/s) between the proposed bridge scheme Route 3A Medium 3 Tower revised option and the baseline case for low water (A) and peak flood (B) on a spring tide – island construction option	Figure A5

A.

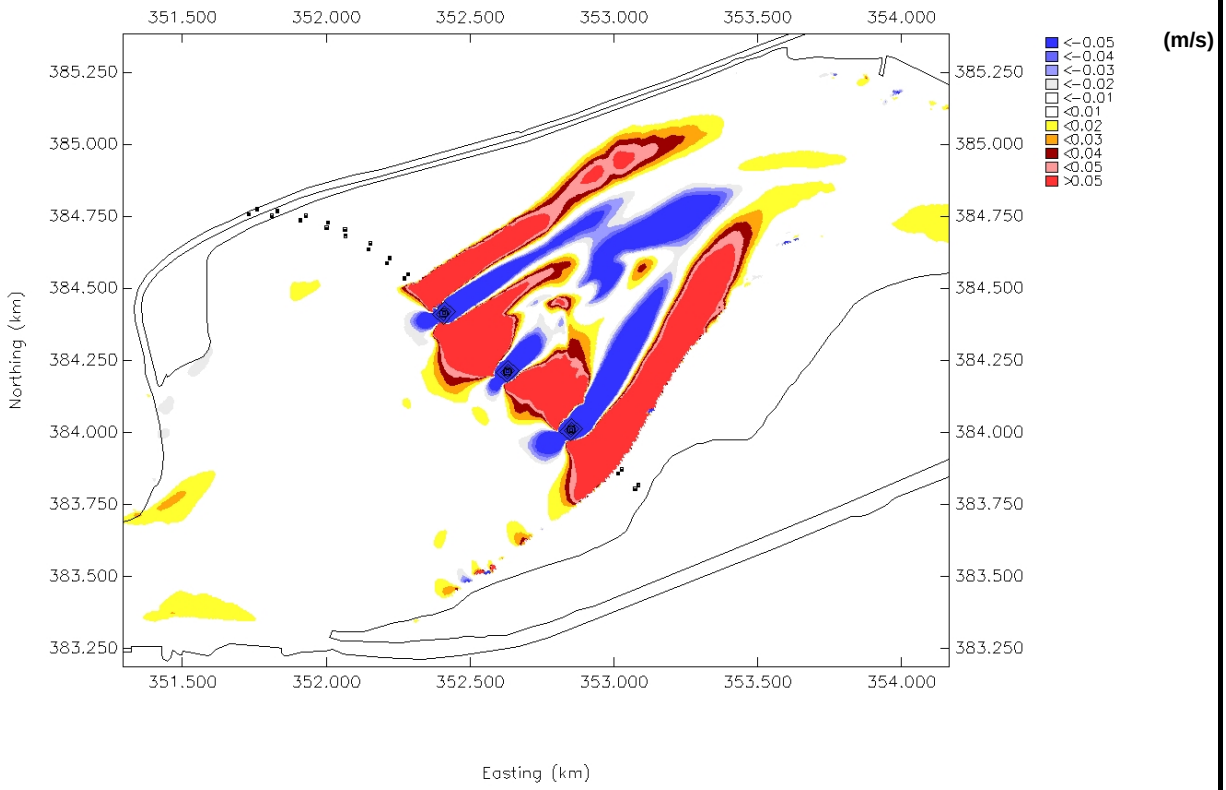

B.

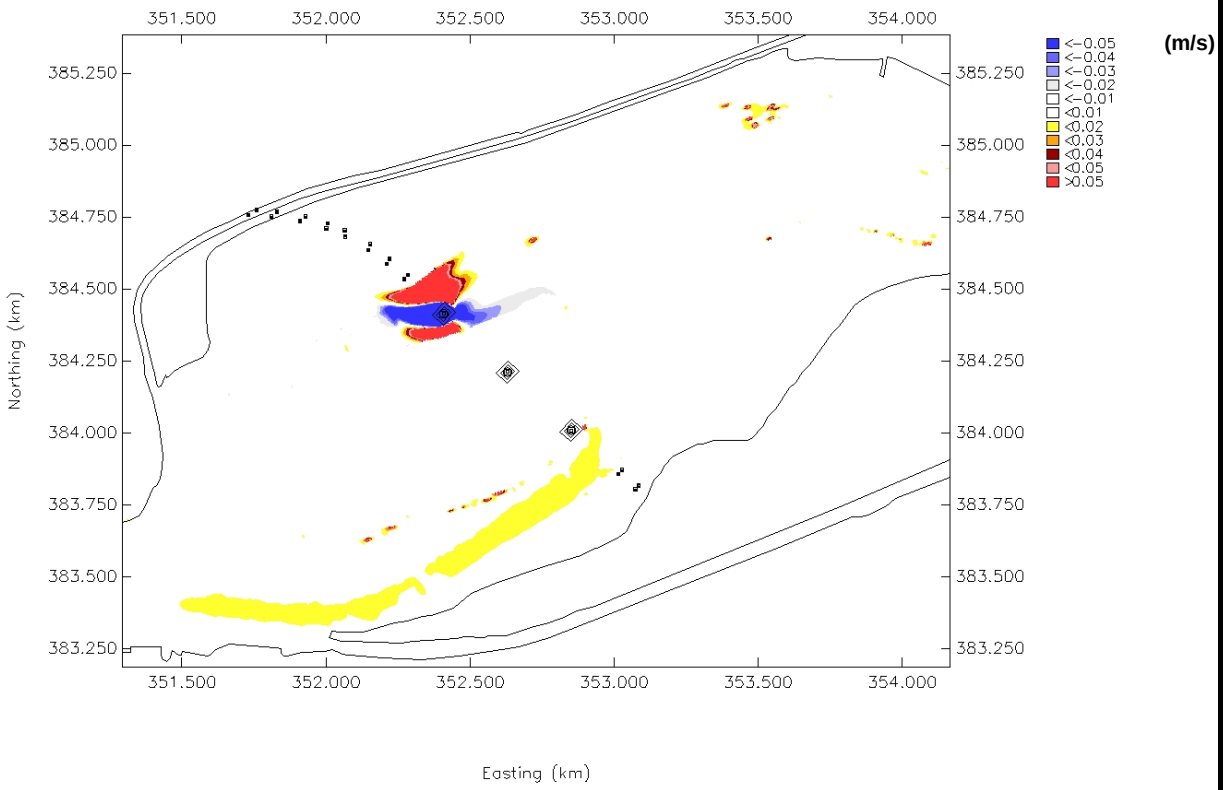

ABP mer marine environmental research

Differences in near-bed speed (m/s) between the proposed bridge scheme Route 3A Medium 3 Tower revised option and the baseline case for high water (A) and peak ebb (B) on a spring tide – island construction option

Figure A6

A.

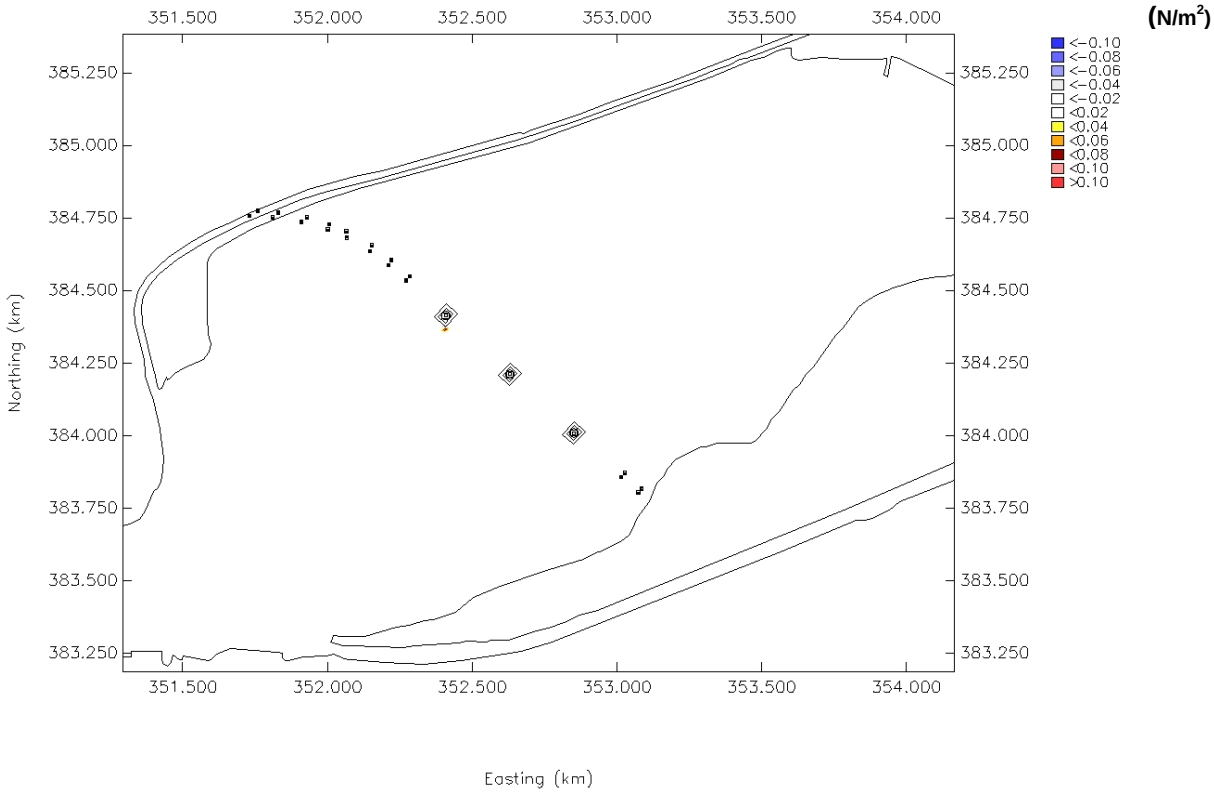

B.

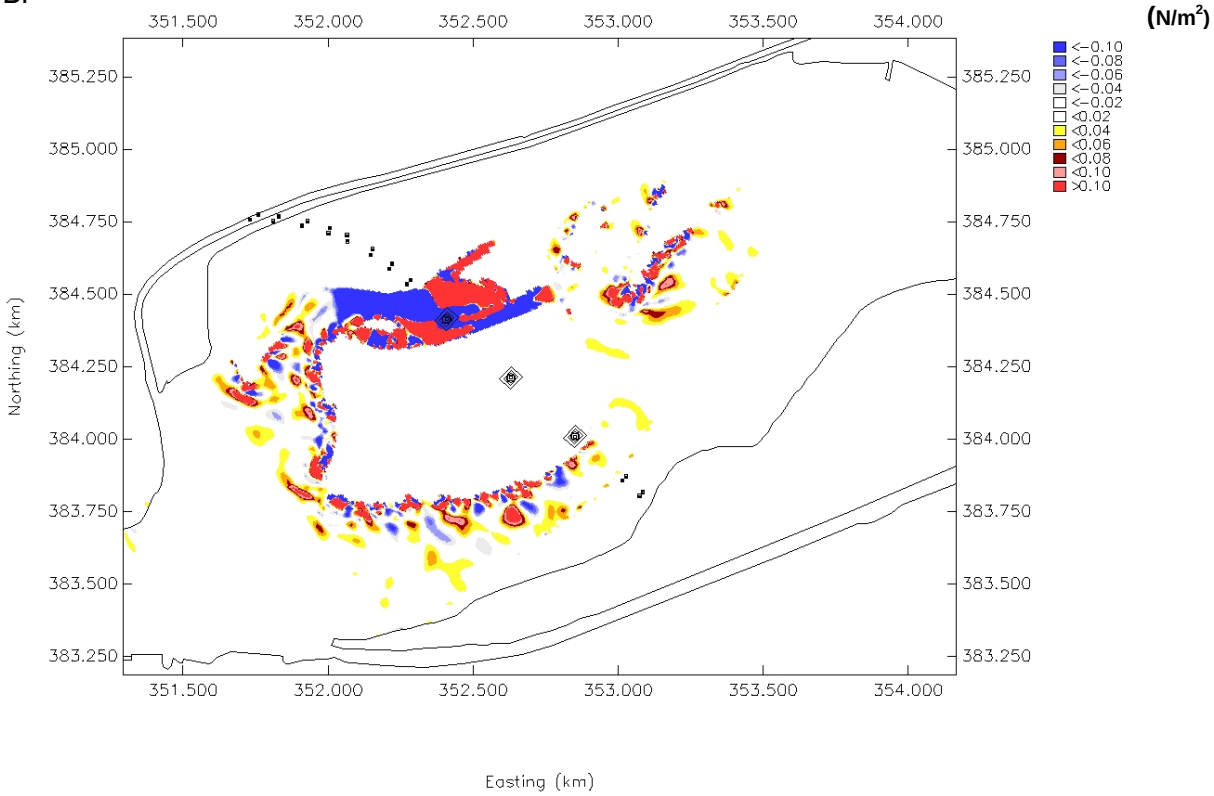

ABP mer marine environmental research	Differences in bed shear stress (N/m²) between the proposed bridge scheme Route 3A Medium 3 Tower revised option and the baseline case for low water (A) and peak flood (B) on a spring tide – island construction option	Figure A7

A.

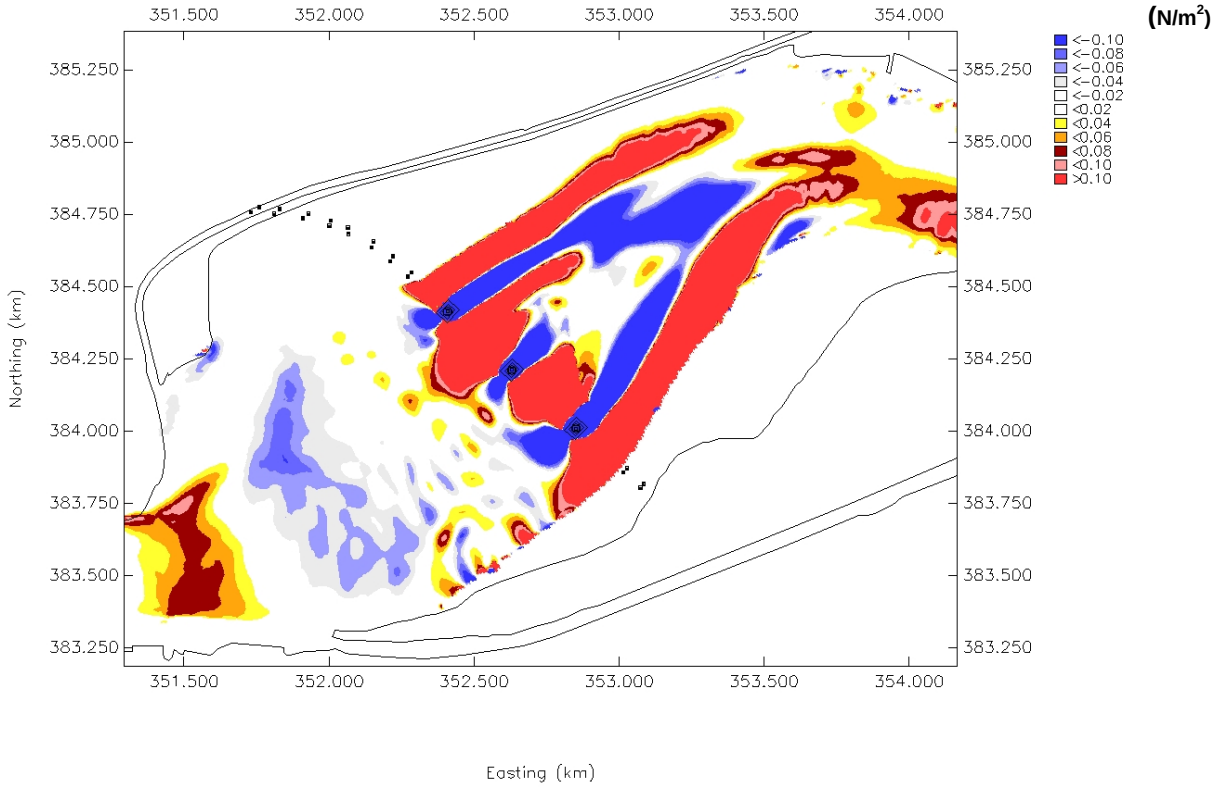

B.

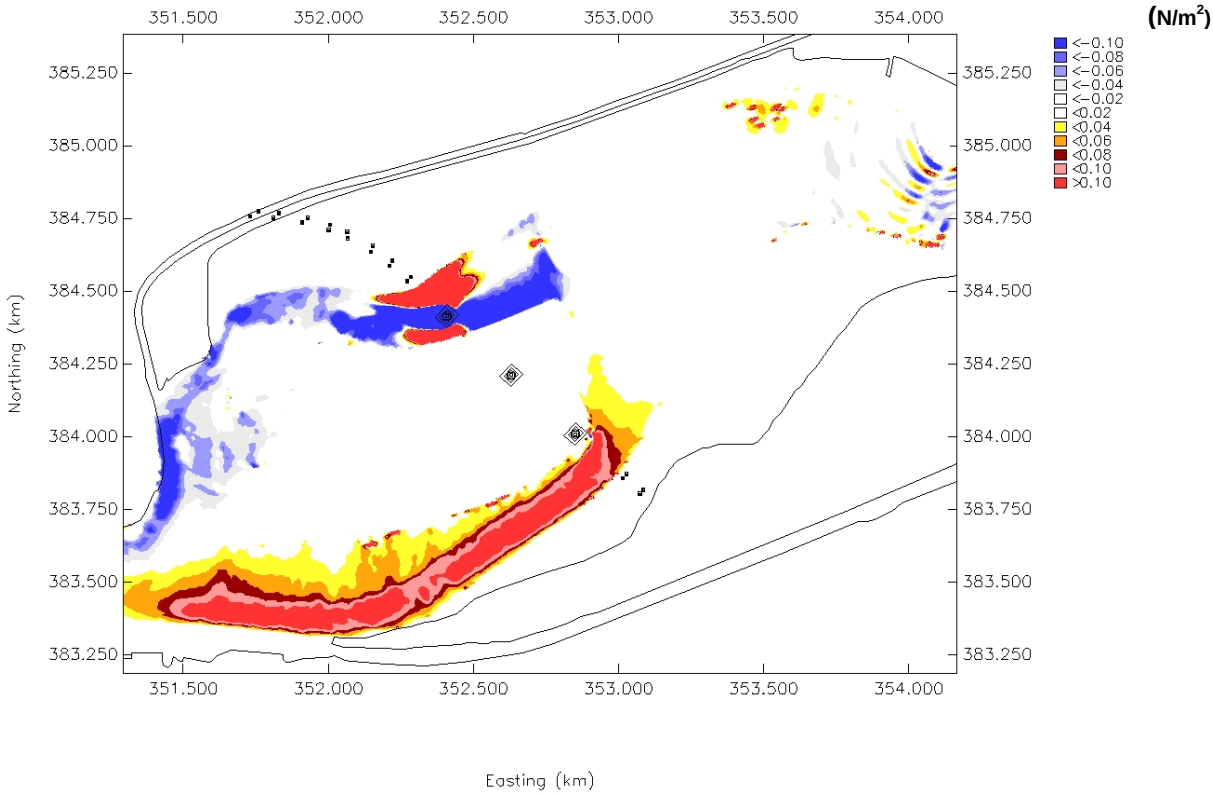

Differences in bed shear stress (N/m²) between the proposed bridge scheme Route 3A Medium 3 Tower revised option and the baseline case for high water (A) and peak ebb (B) on a spring tide – island construction option

Figure A8

A.

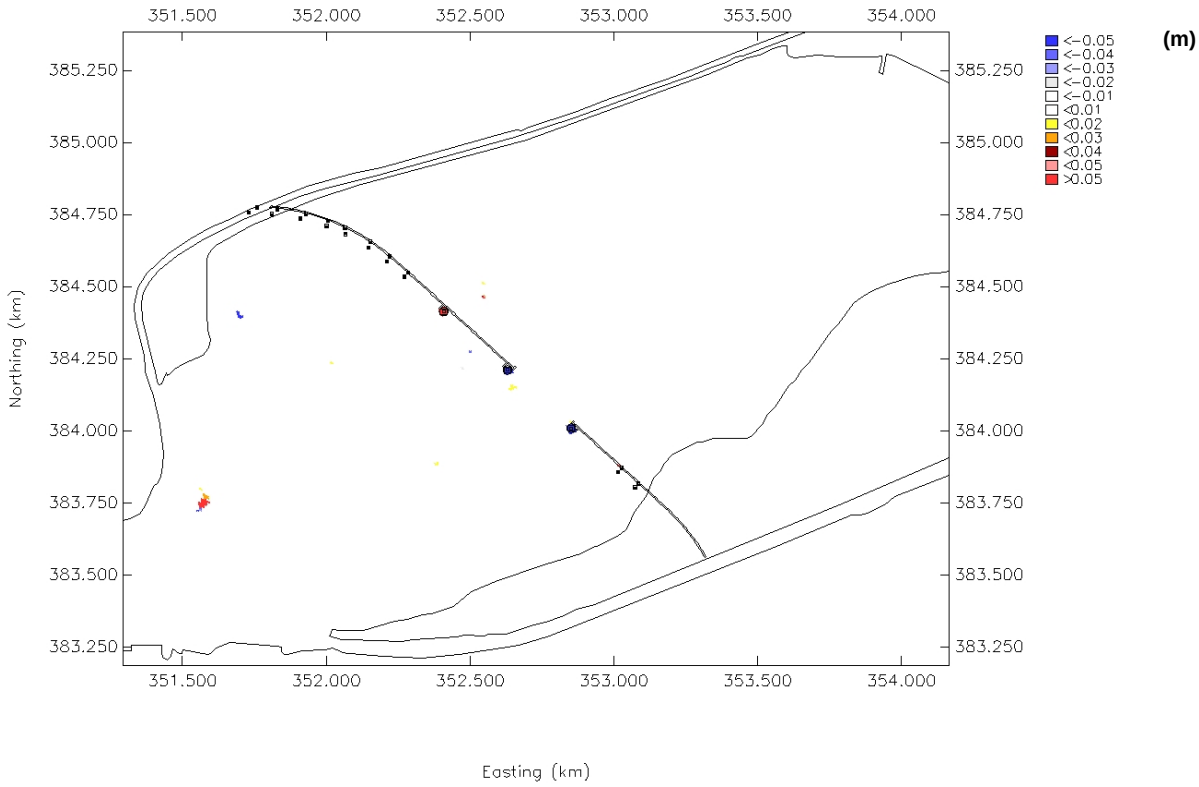

B.

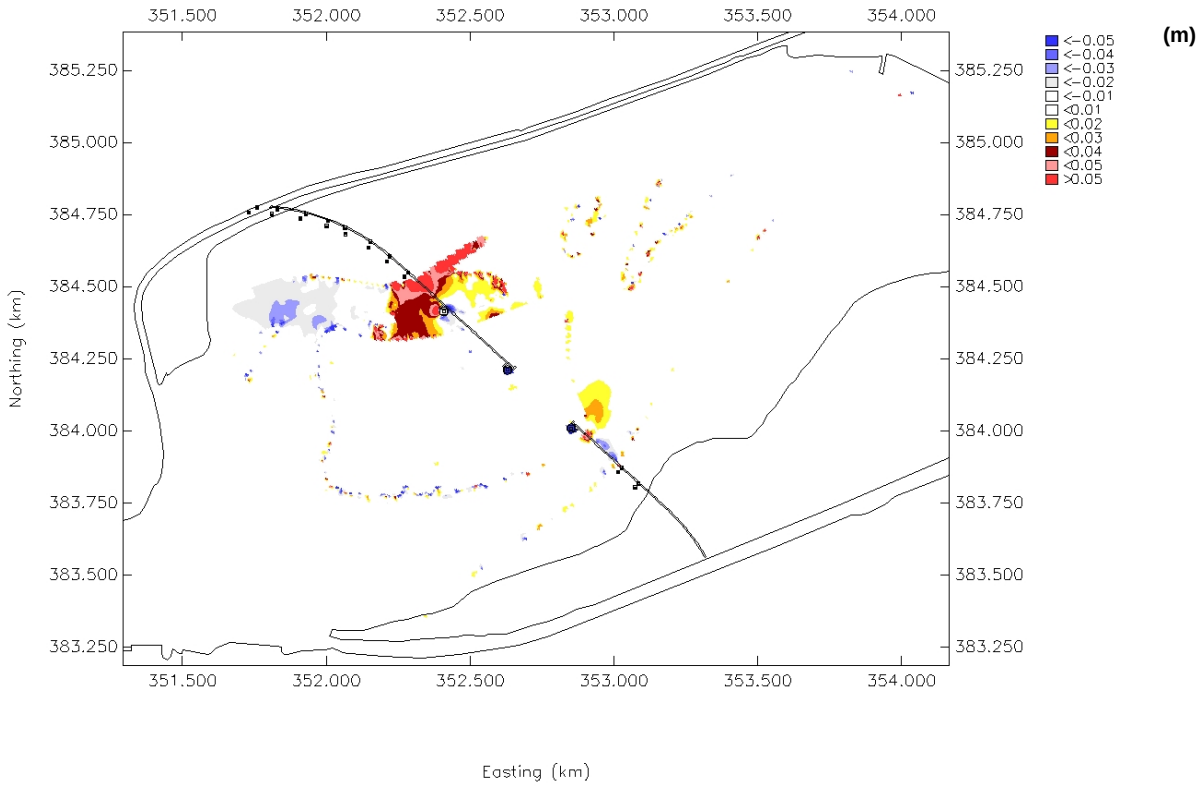

ABP mer marine environmental research

Differences in water level (m) between the proposed bridge scheme Route 3A Medium 3 Tower revised option and the baseline case for low water (A) and peak flood (B) on a spring tide – jetty construction option

Figure A9

A.

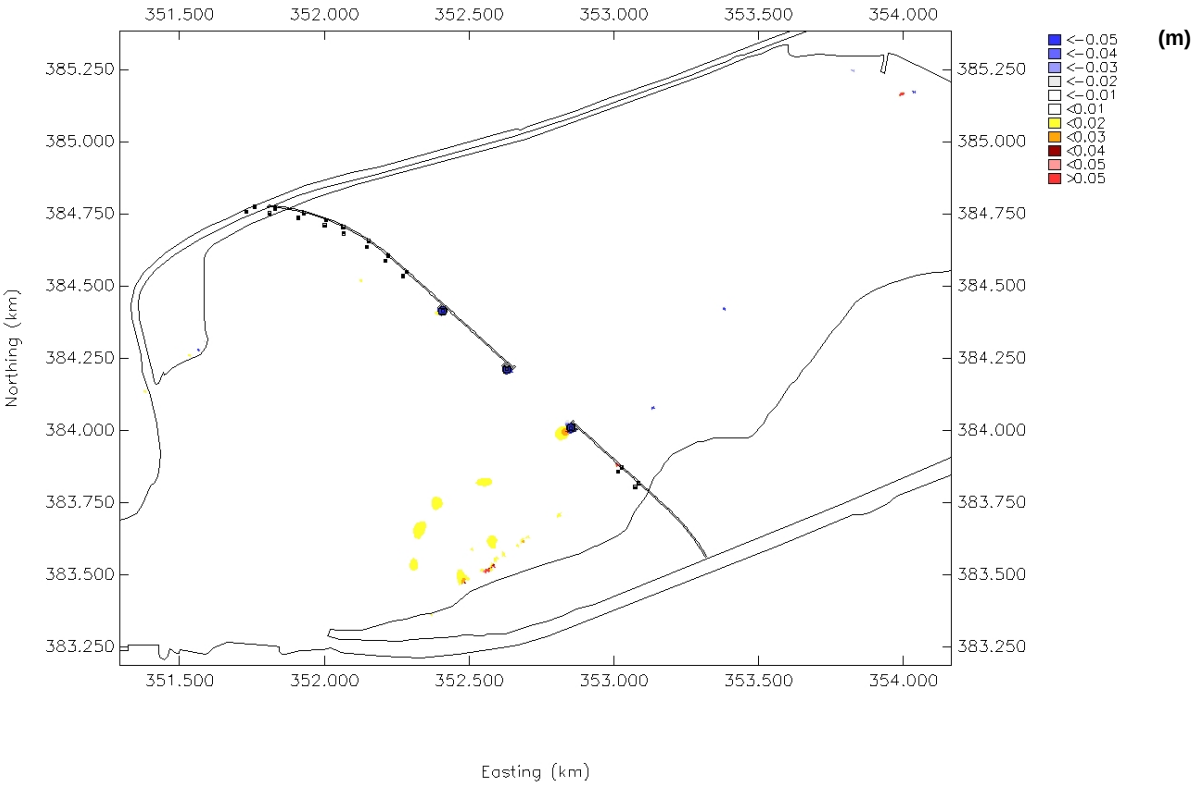

B.

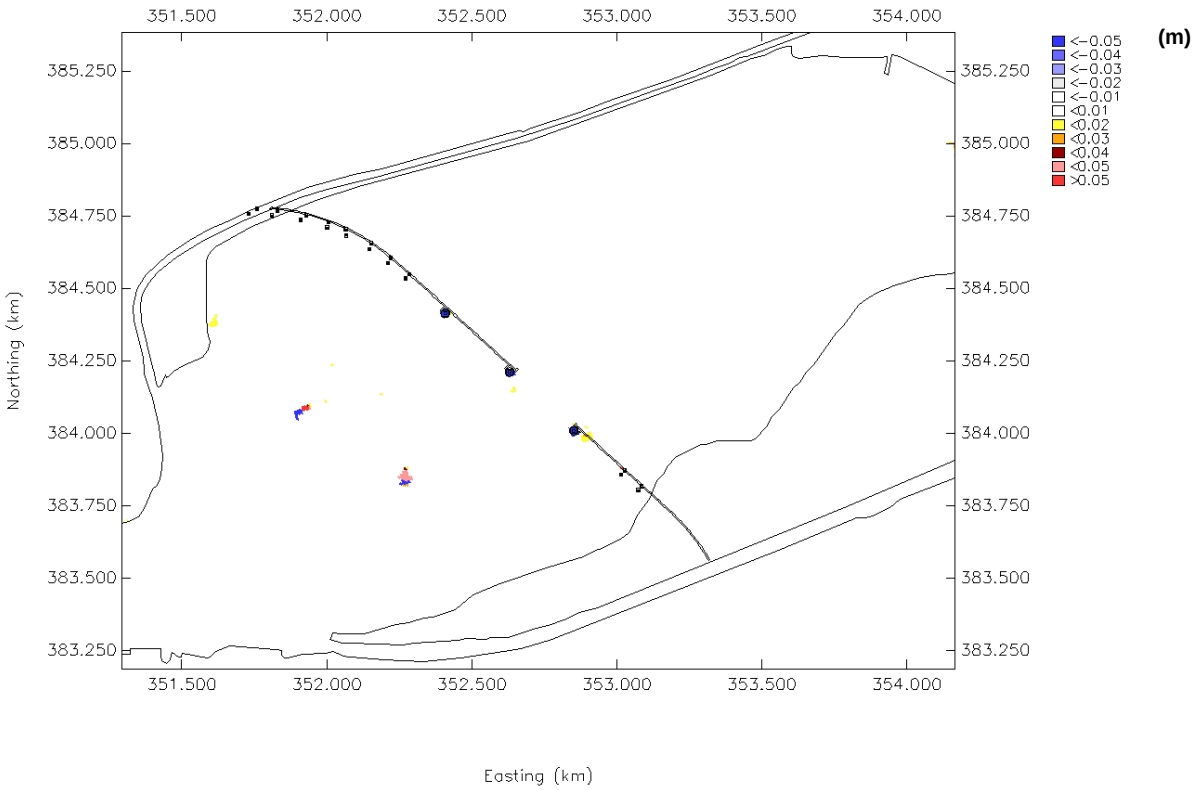

ABP mer marine environmental research

Differences in water level (m) between the proposed bridge scheme Route 3A Medium 3 Tower revised option and the baseline case for high water (A) and peak ebb (B) on a spring tide – jetty construction option

Figure A10

A.

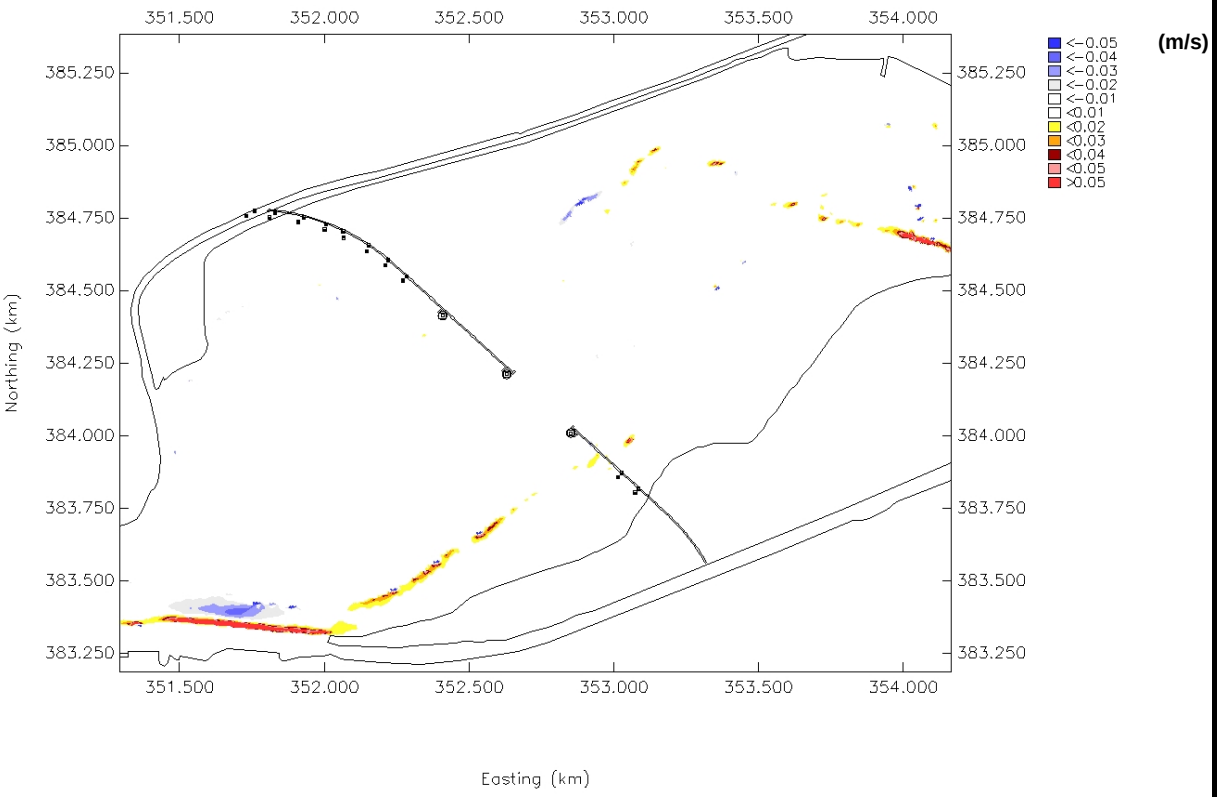

B.

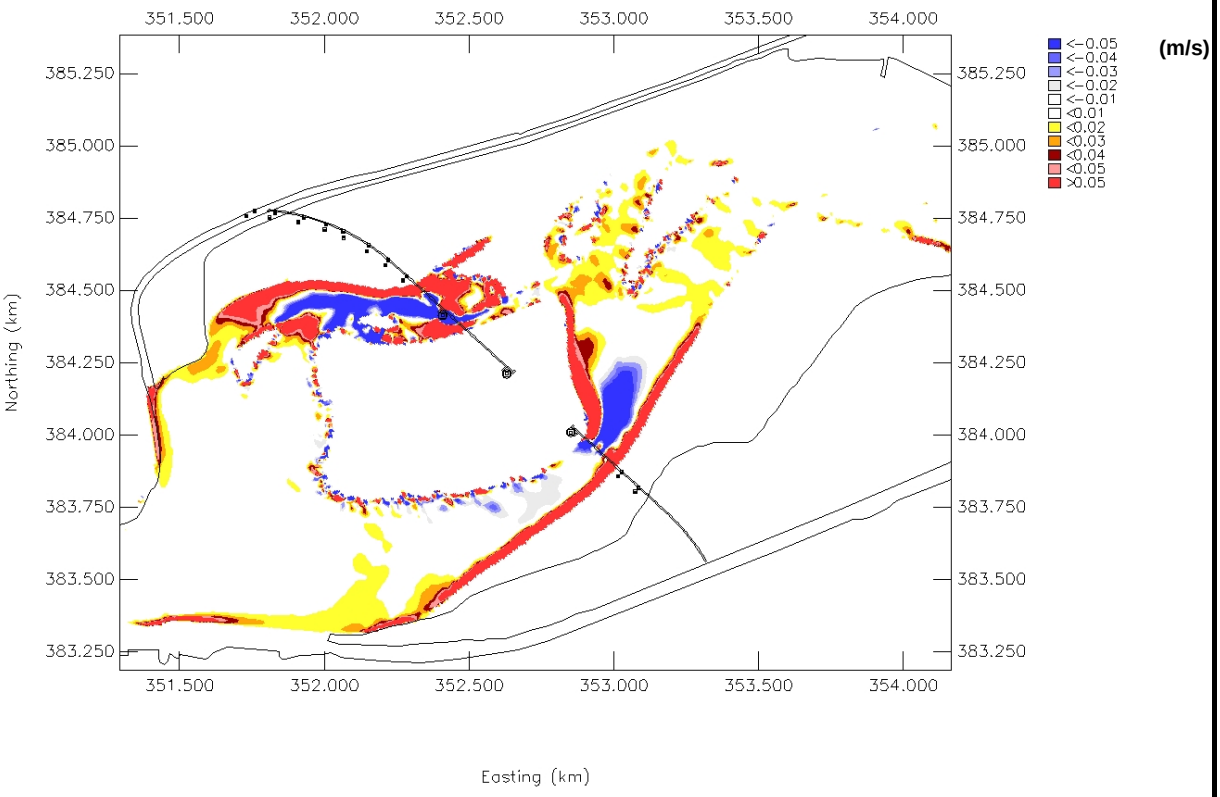

Differences in near-surface speed (m/s) between the proposed bridge scheme Route 3A Medium 3 Tower revised option and the baseline case for low water (A) and peak flood (B) on a spring tide – jetty construction option

Figure A11

A.

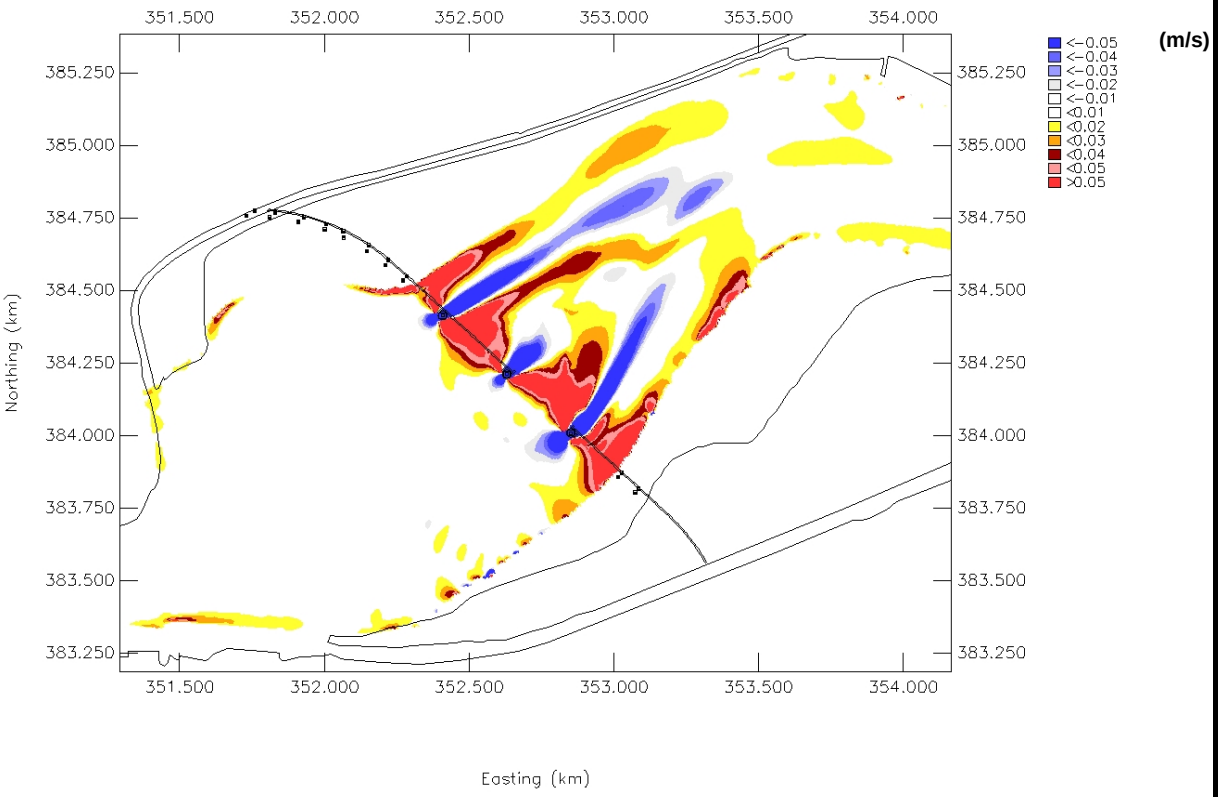

B.

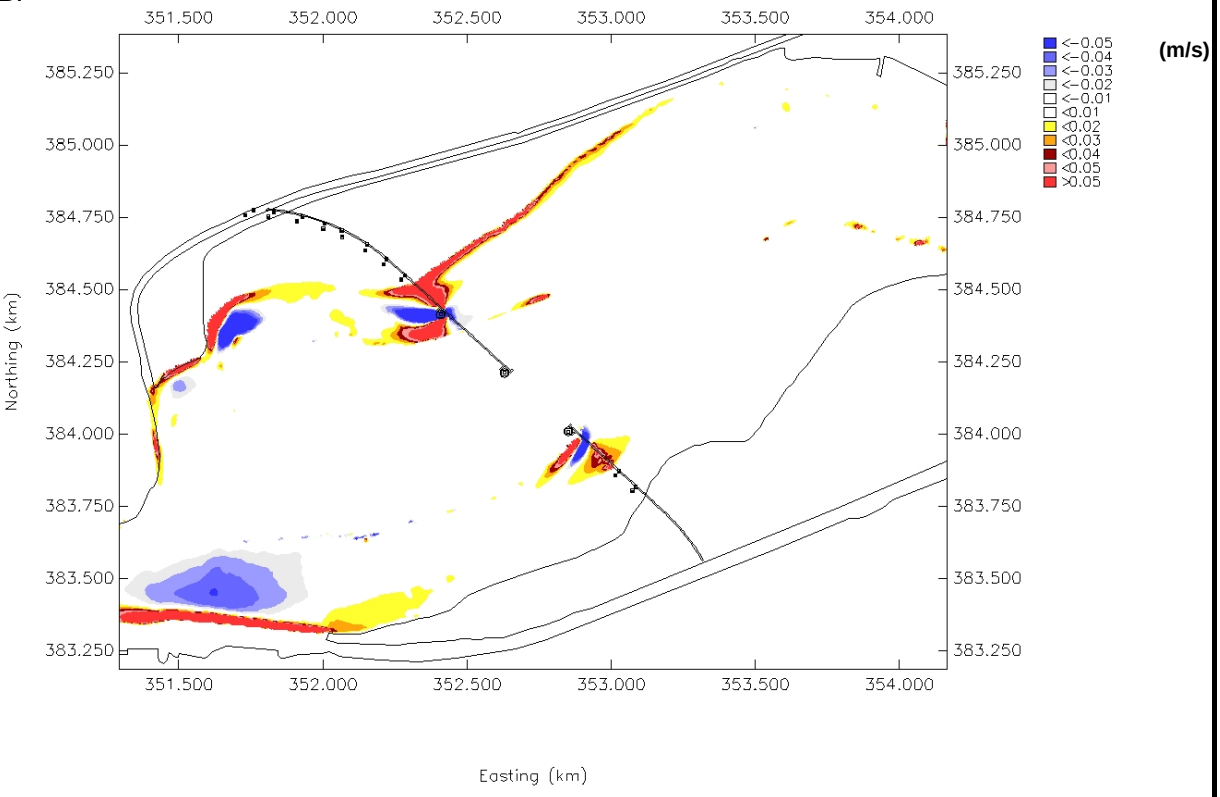

ABP mer marine environmental research	Differences in near-surface speed (m/s) between the proposed bridge scheme Route 3A Medium 3 Tower revised option and the baseline case for high water (A) and peak ebb (B) on a spring tide – jetty construction option	Figure A12

A.

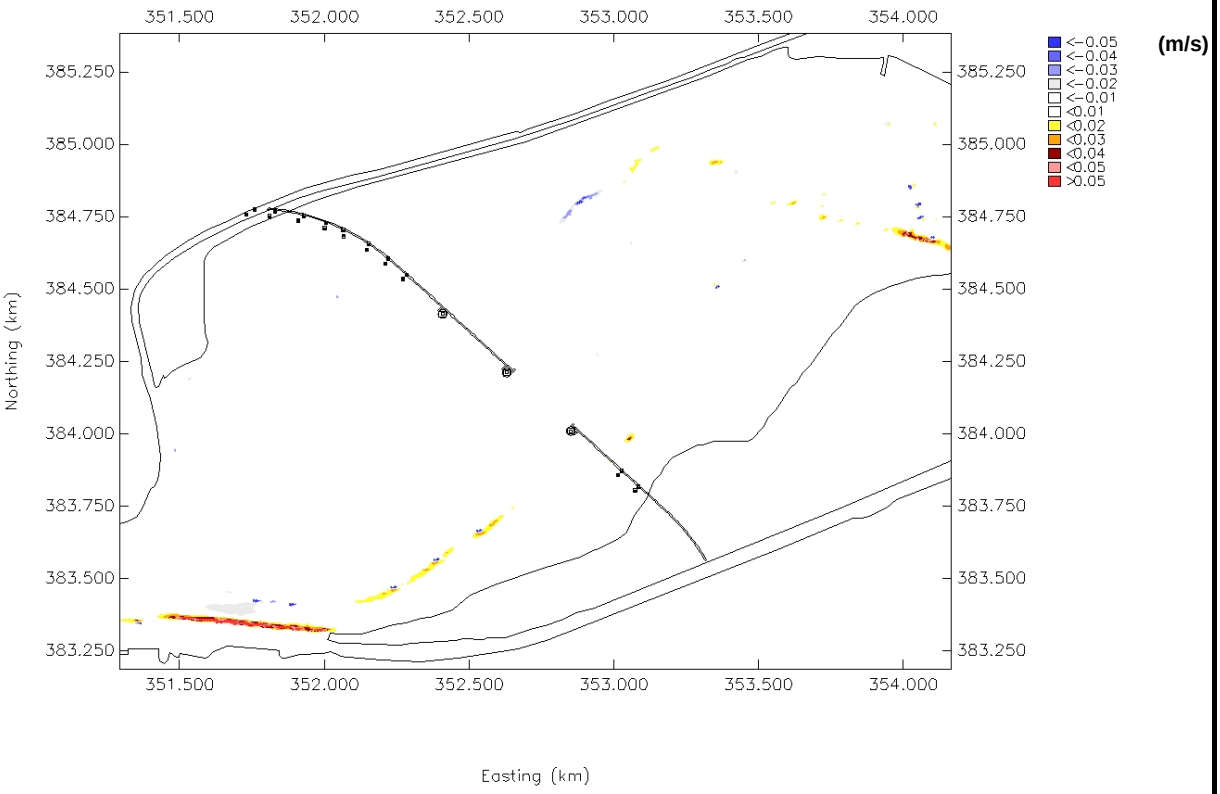

B.

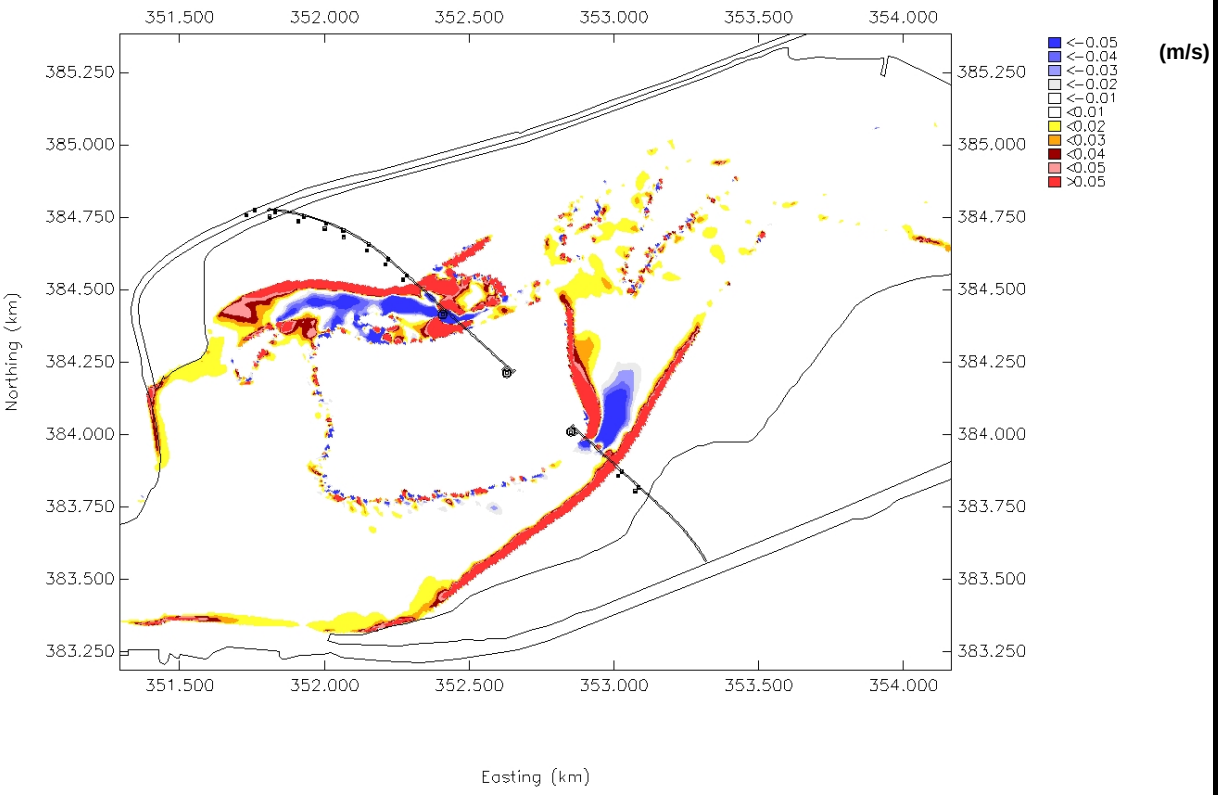

ABP mer marine environmental research	Differences in near-bed speed (m/s) between the proposed bridge scheme Route 3A Medium 3 Tower revised option and the baseline case for low water (A) and peak flood (B) on a spring tide – jetty construction option	Figure A13

A.

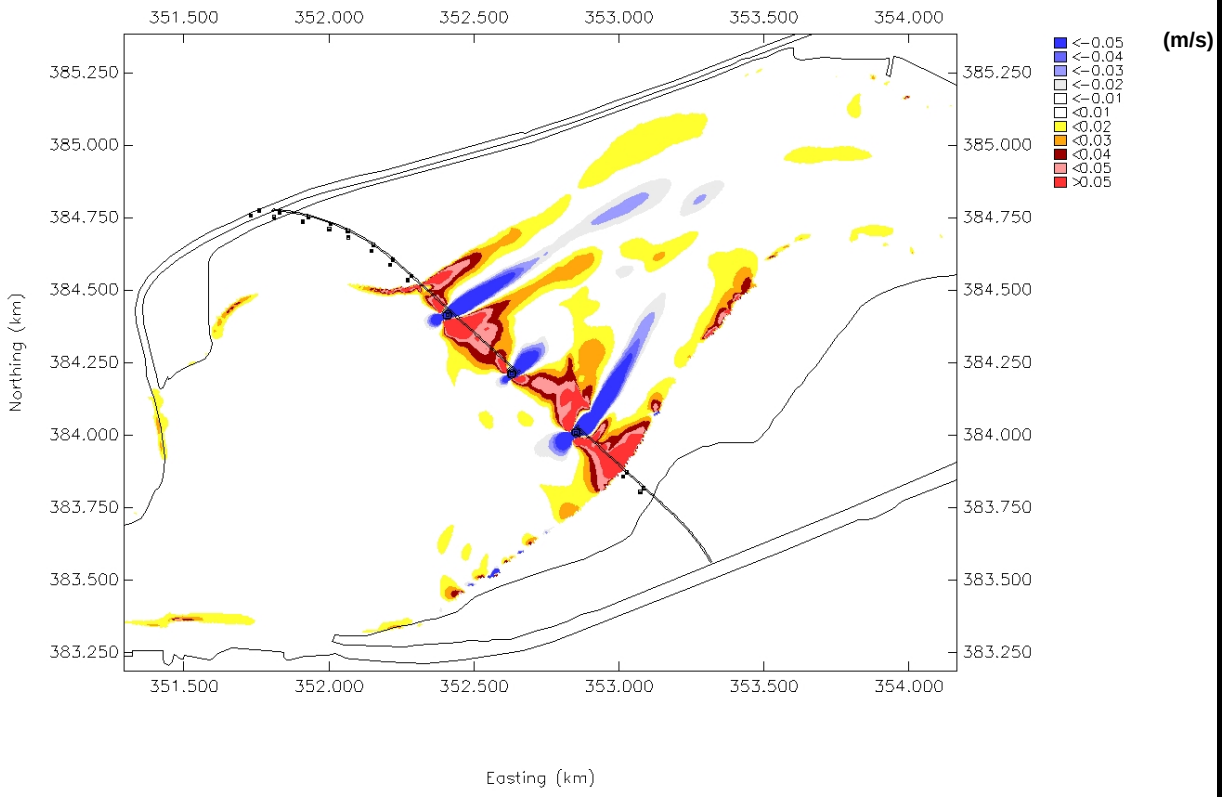

B.

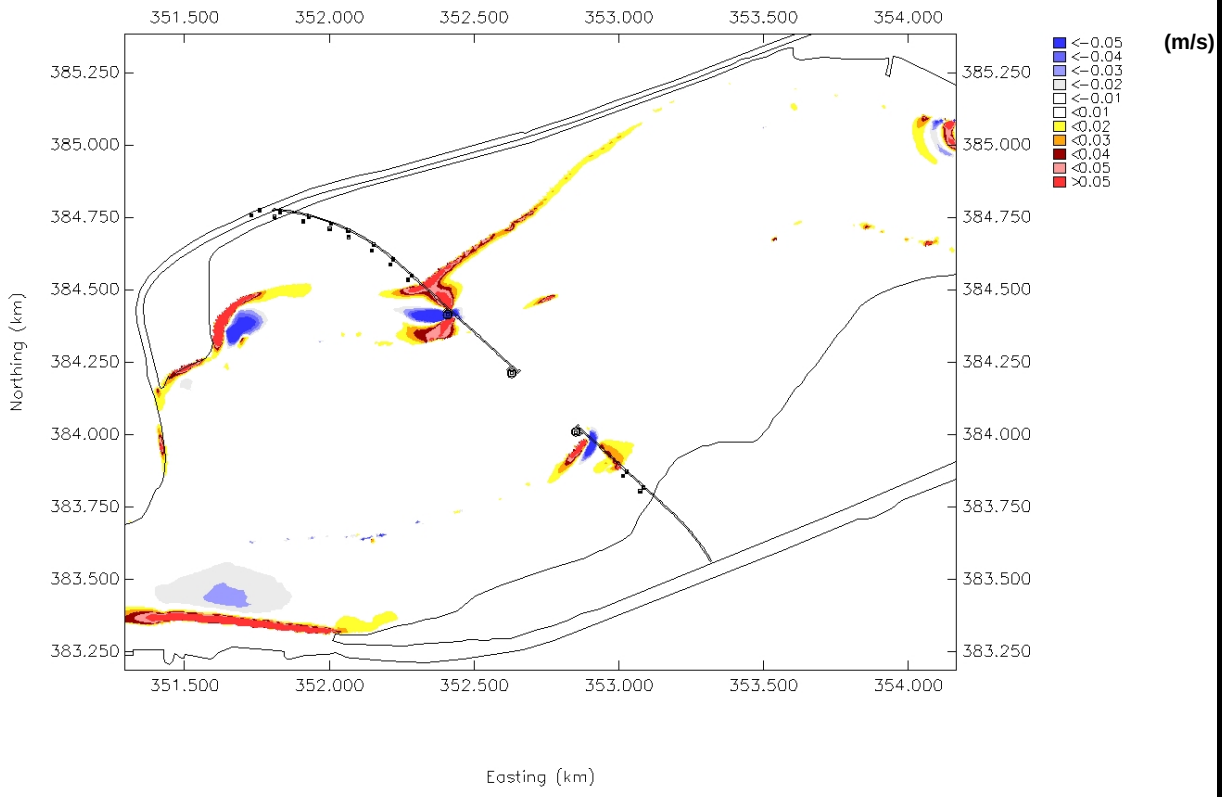

ABP mer marine environmental research

Differences in near-bed speed (m/s) between the proposed bridge scheme Route 3A Medium 3 Tower revised option and the baseline case for high water (A) and peak ebb (B) on a spring tide – jetty construction option

Figure A14

A.

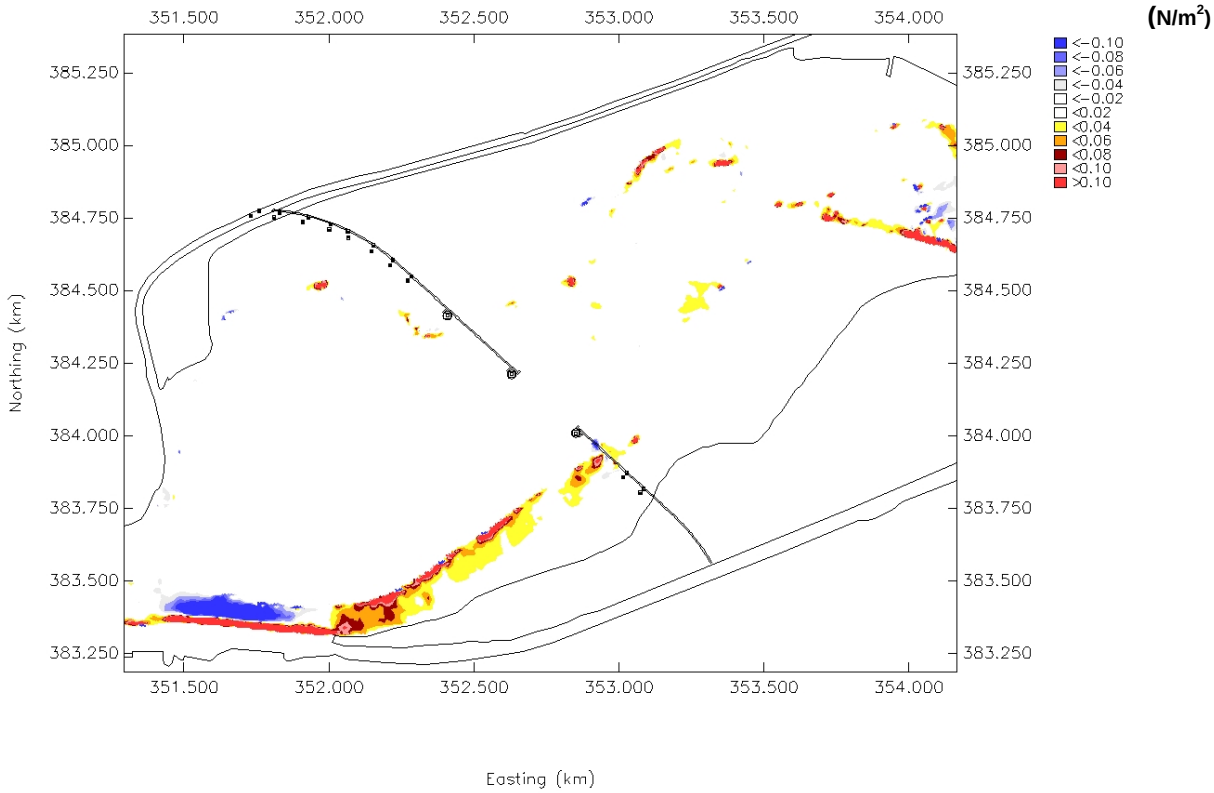

B.

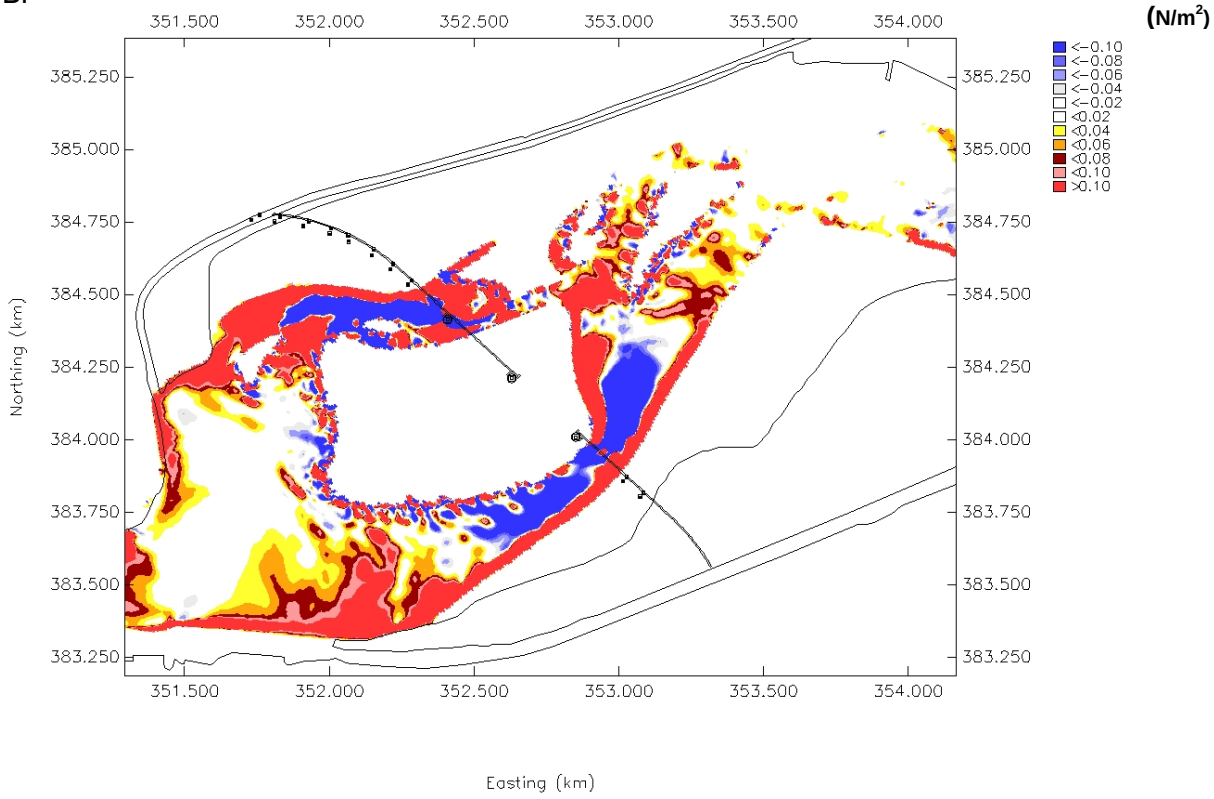

Differences in bed shear stress (N/m²) between the proposed bridge scheme Route 3A Medium 3 Tower revised option and the baseline case for low water (A) and peak flood (B) on a spring tide – jetty construction option

Figure A15

A.

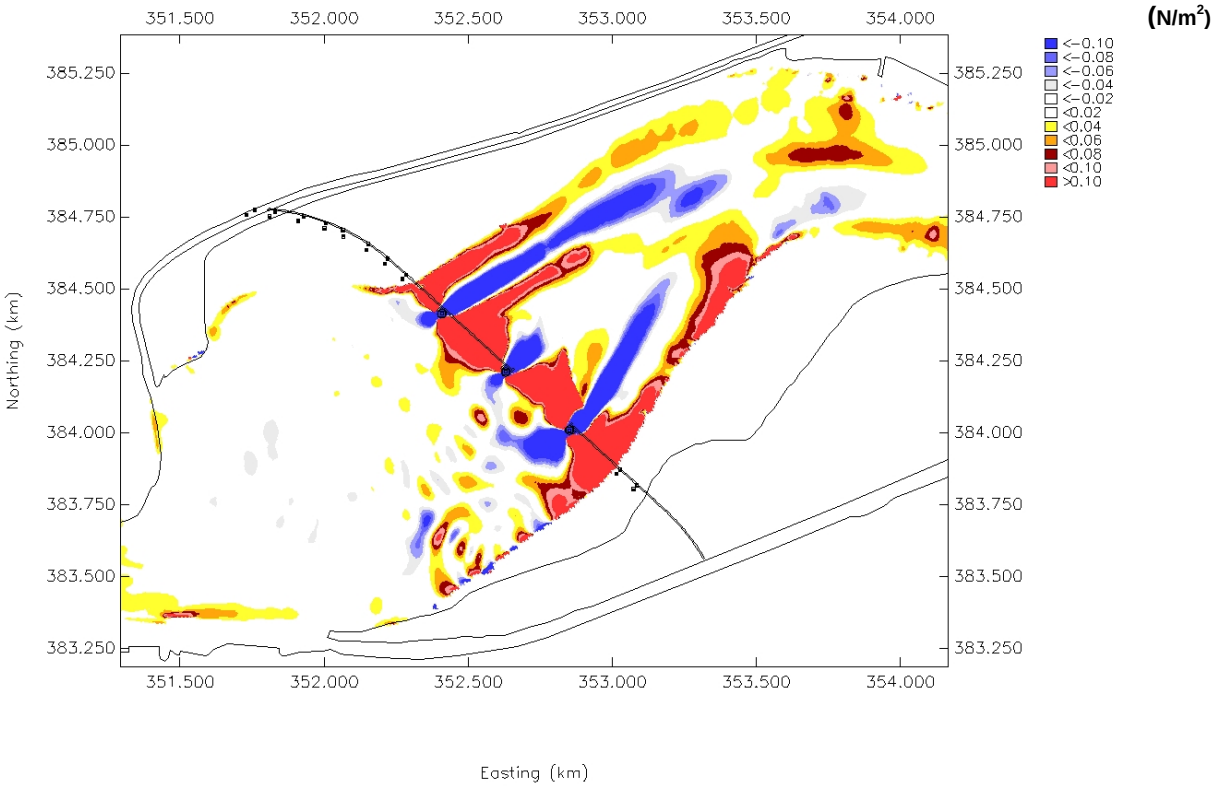

B.

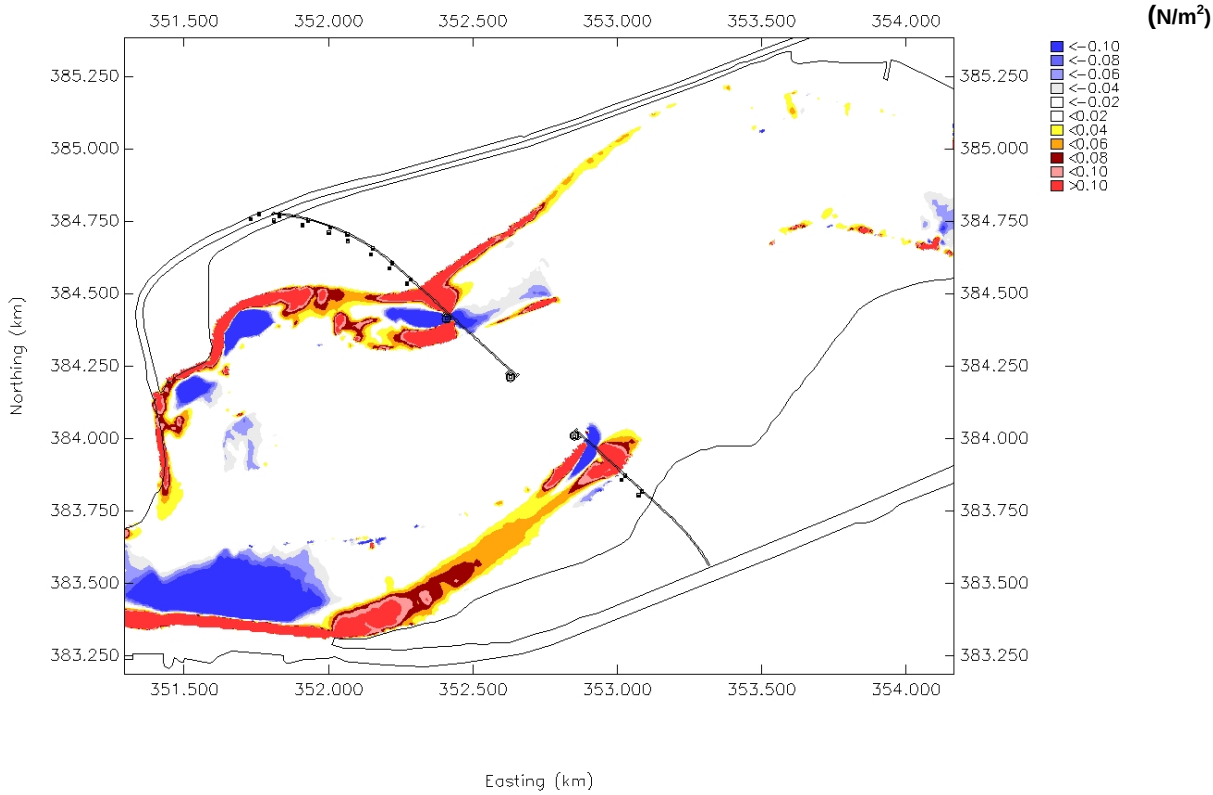

Differences in bed shear stress (N/m²) between the proposed bridge scheme Route 3A Medium 3 Tower revised option and the baseline case for high water (A) and peak ebb (B) on a spring tide – jetty construction option

Figure A16

A.

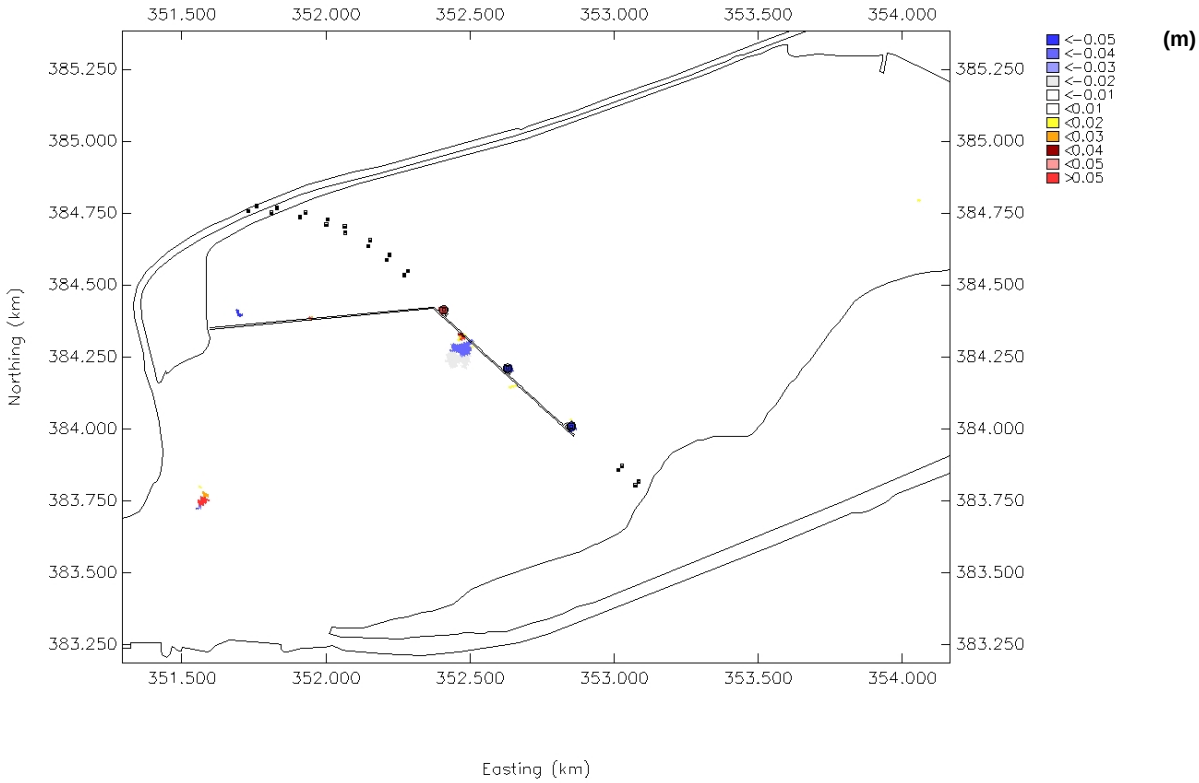

B.

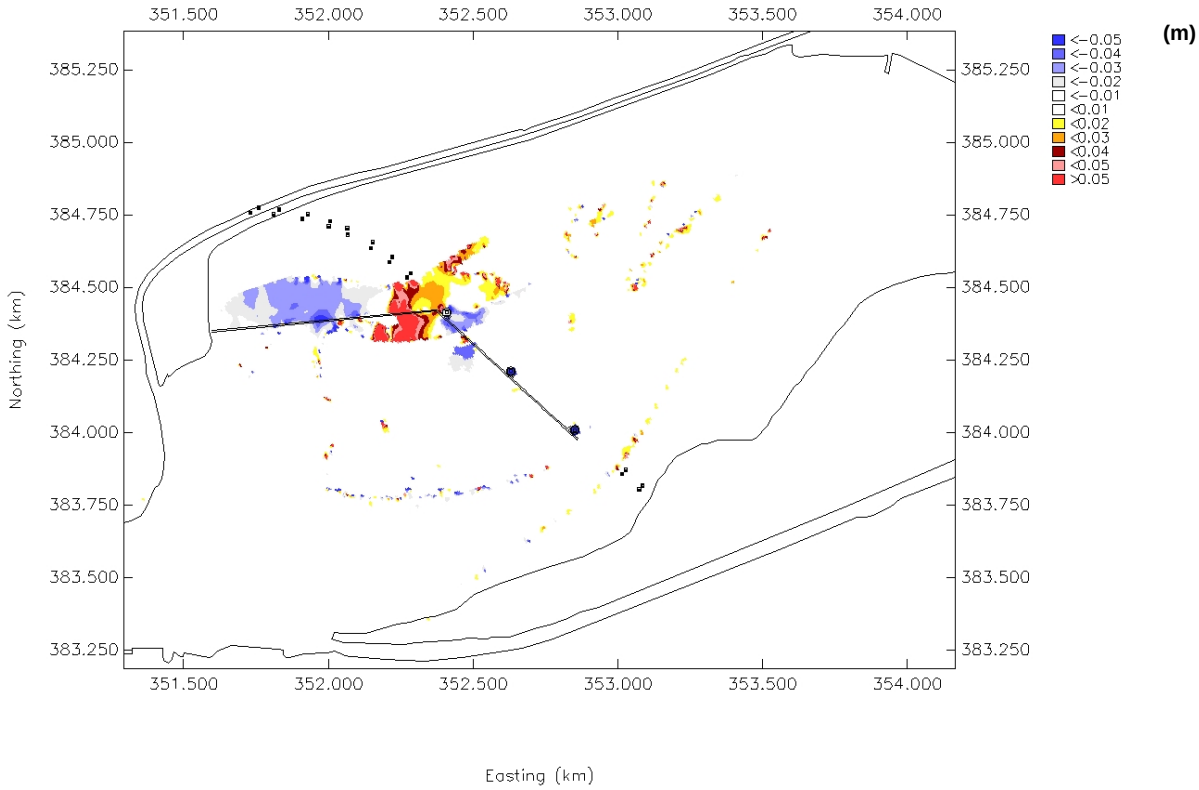

ABP mer marine environmental research

Differences in water level (m) between the proposed bridge scheme Route 3A Medium 3 Tower revised option and the baseline case for low water (A) and peak flood (B) on a spring tide – Spike Island jetty construction option

Figure A17

A.

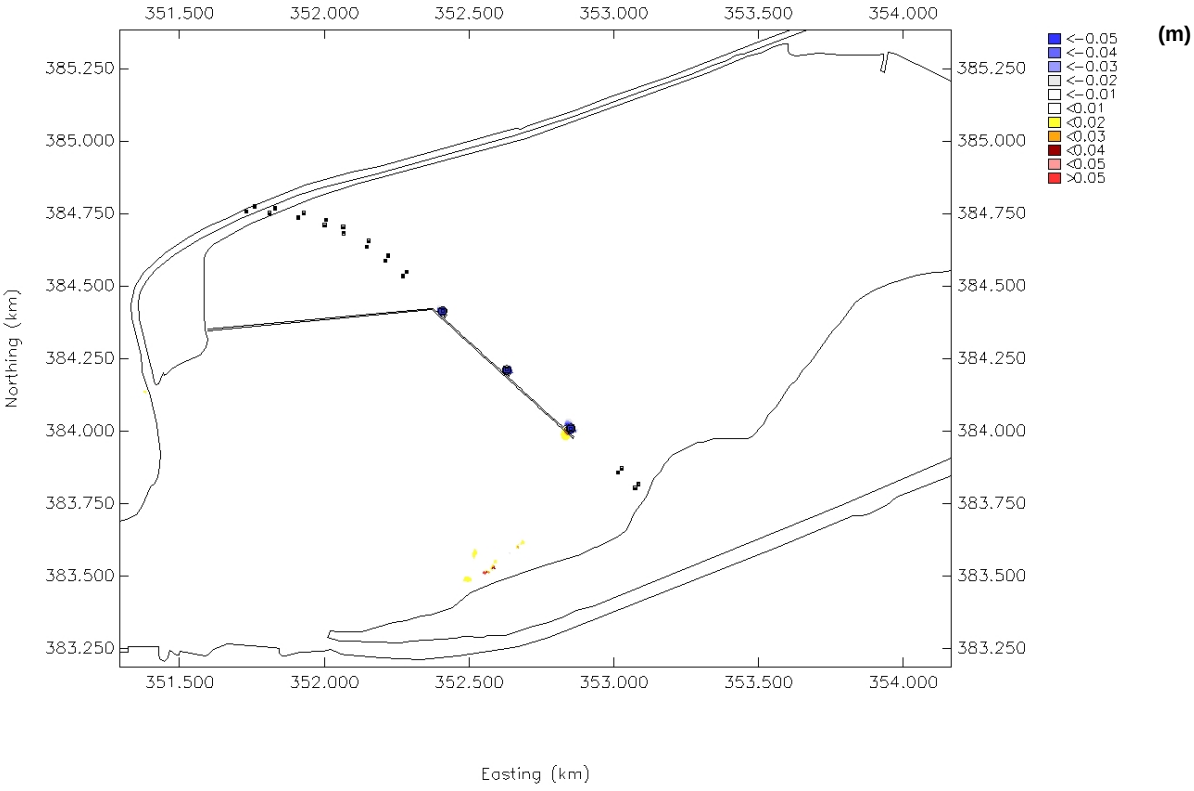

B.

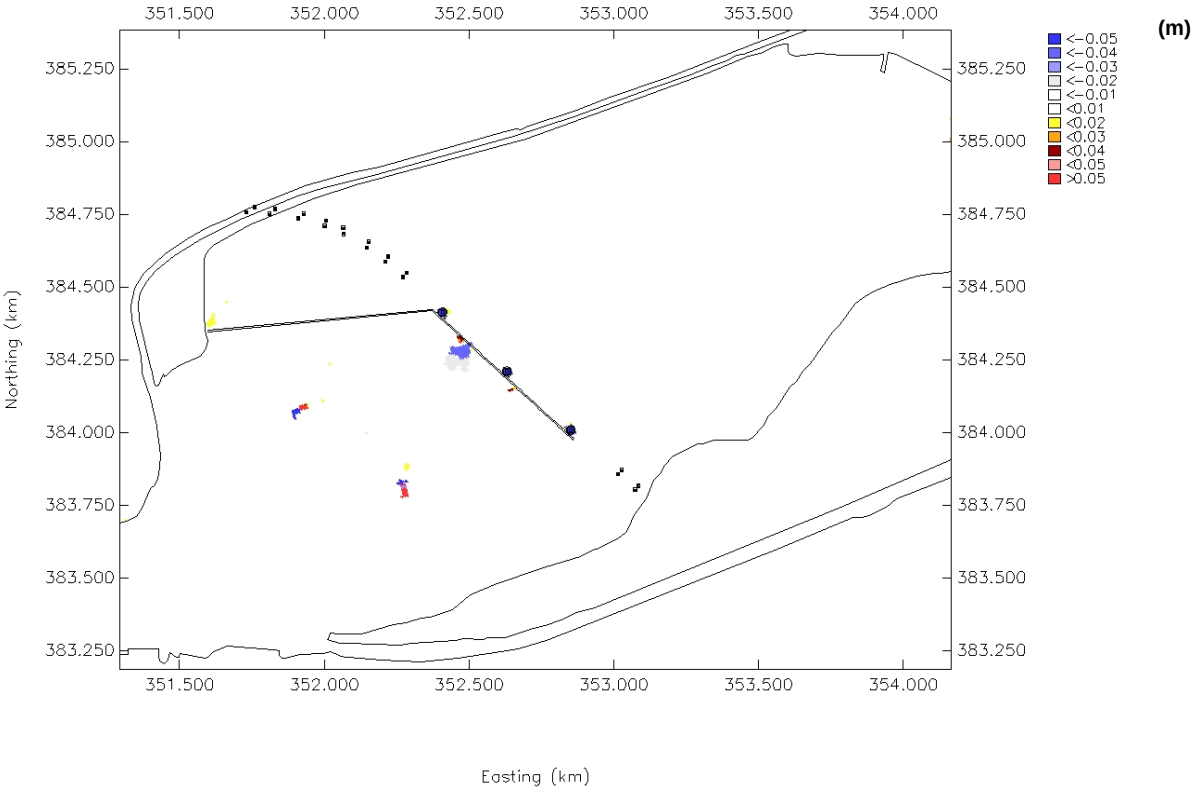

ABP mer marine environmental research

Differences in water level (m) between the proposed bridge scheme Route 3A Medium 3 Tower revised option and the baseline case for high water (A) and peak ebb (B) on a spring tide – Spike Island jetty construction option

Figure A18

A.

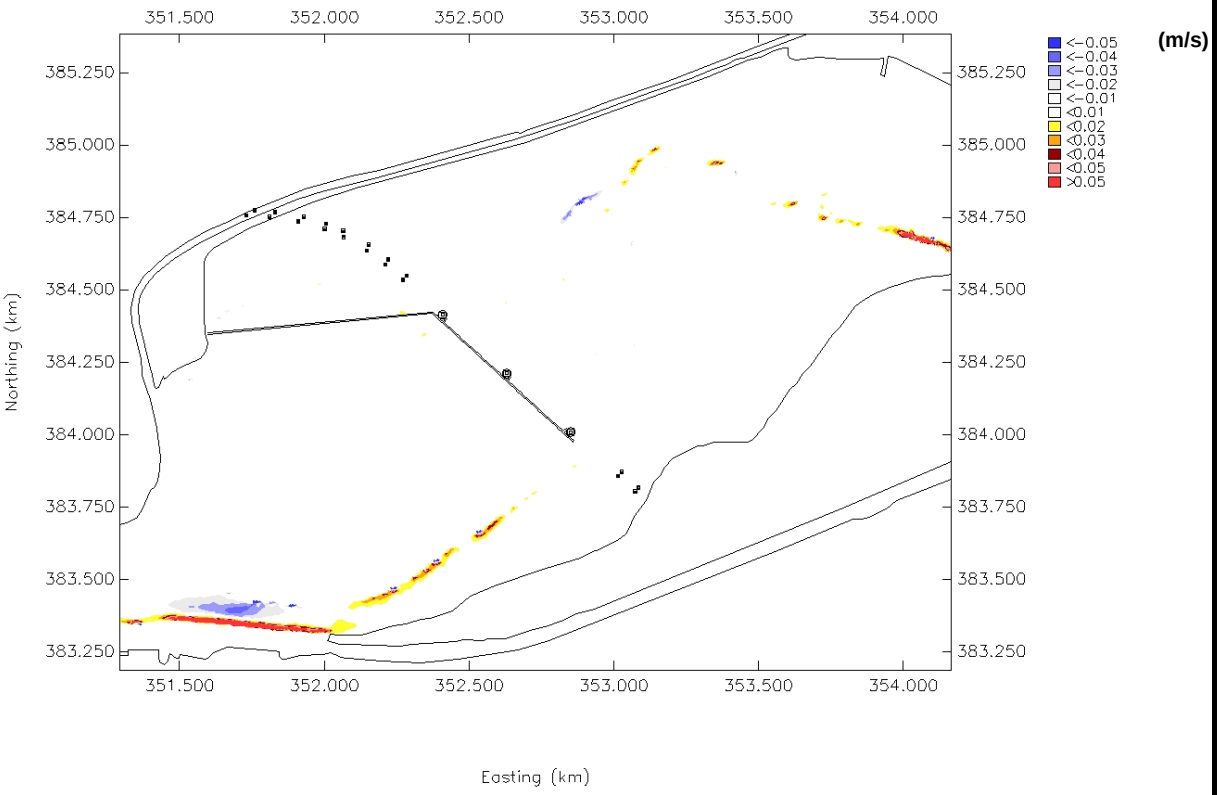

B.

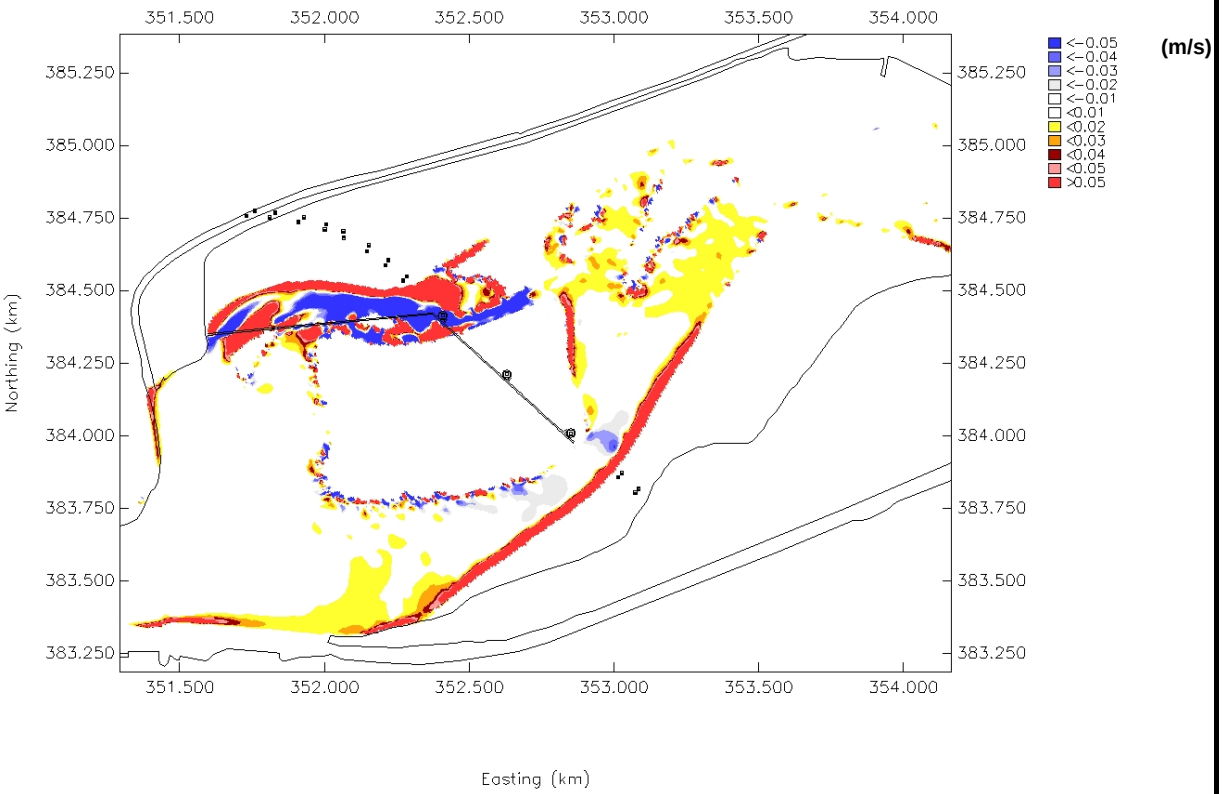

ABP mer marine environmental research	Differences in near-surface speed (m/s) between the proposed bridge scheme Route 3A Medium 3 Tower revised option and the baseline case for low water (A) and peak flood (B) on a spring tide – Spike Island jetty construction option	Figure A19

A.

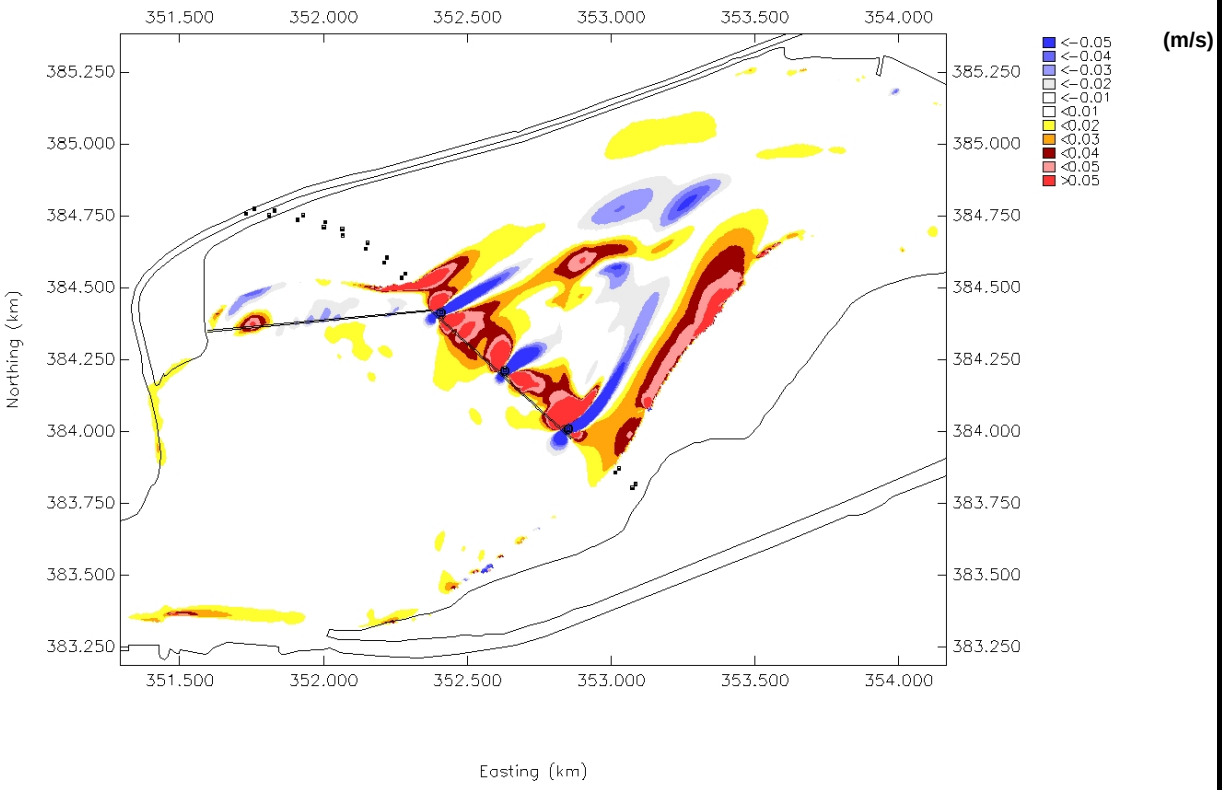

B.

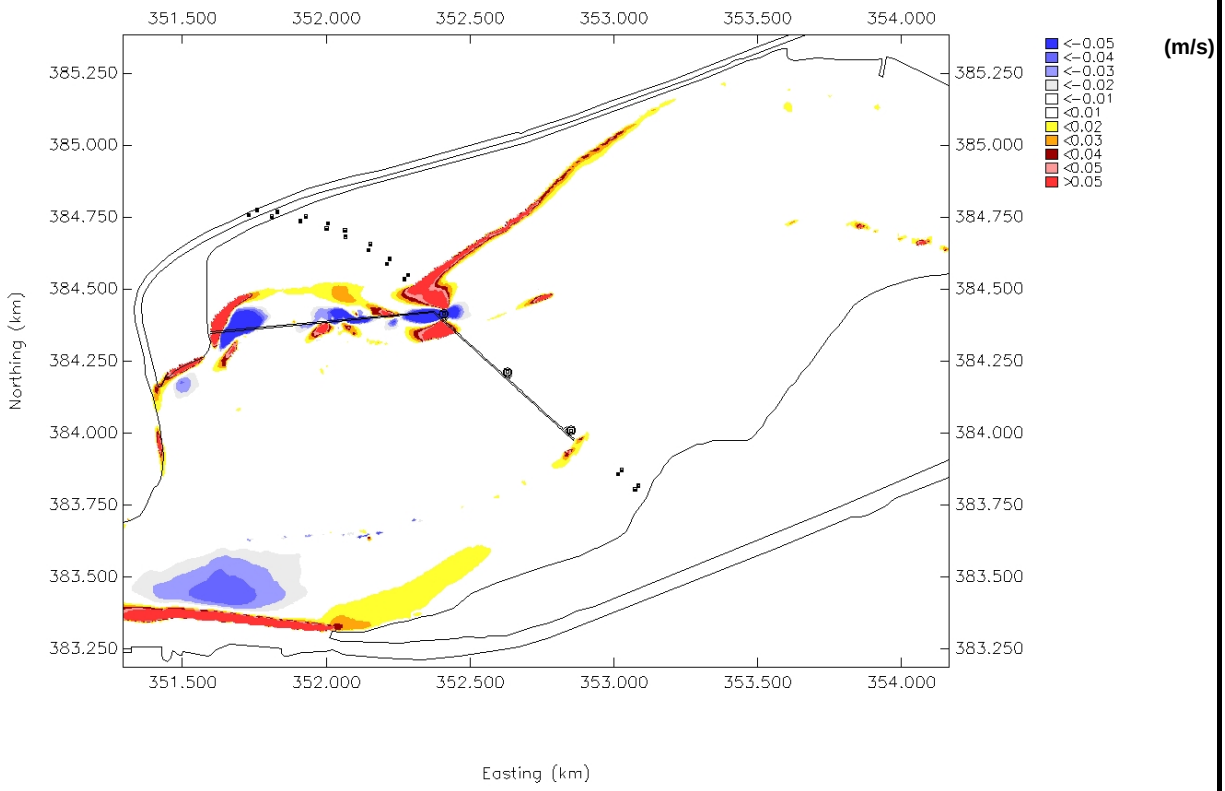

ABP mer marine environmental research

Differences in near-surface speed (m/s) between the proposed bridge scheme Route 3A Medium 3 Tower revised option and the baseline case for high water (A) and peak ebb (B) on a spring tide – Spike Island jetty construction option

Figure A20

A.

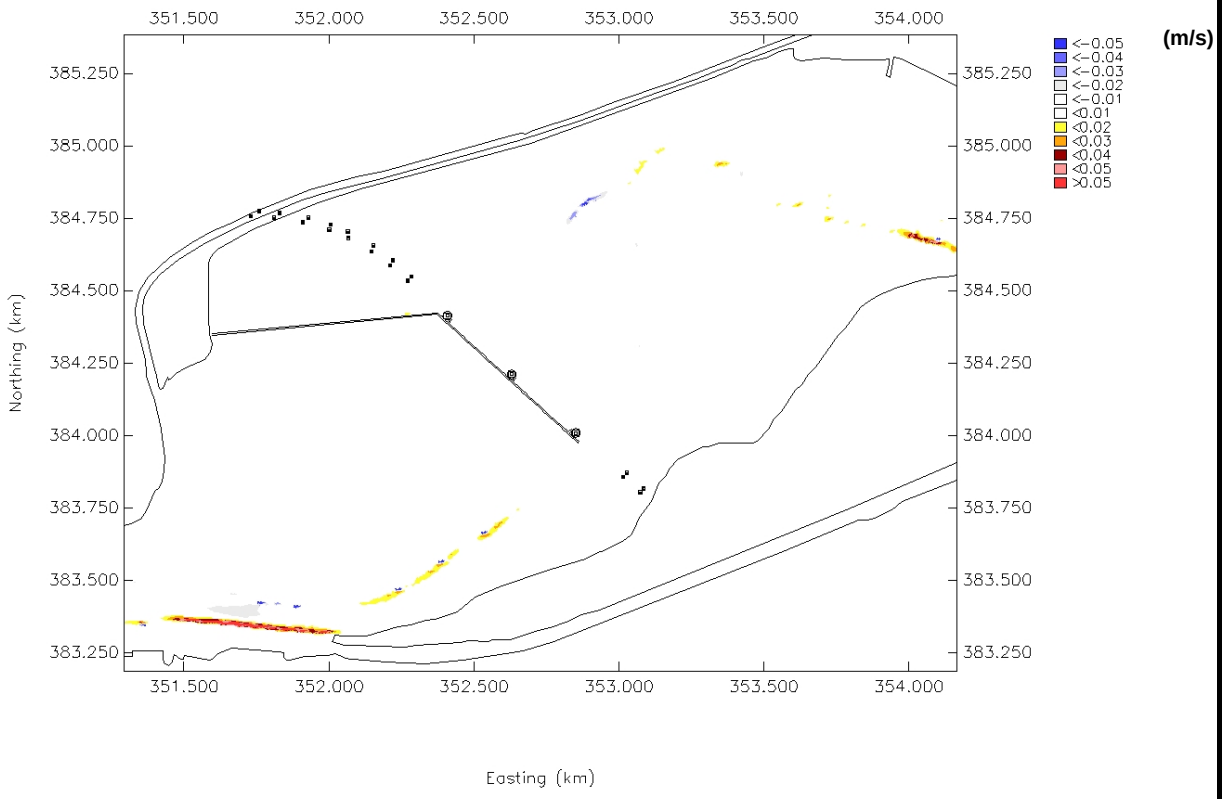

B.

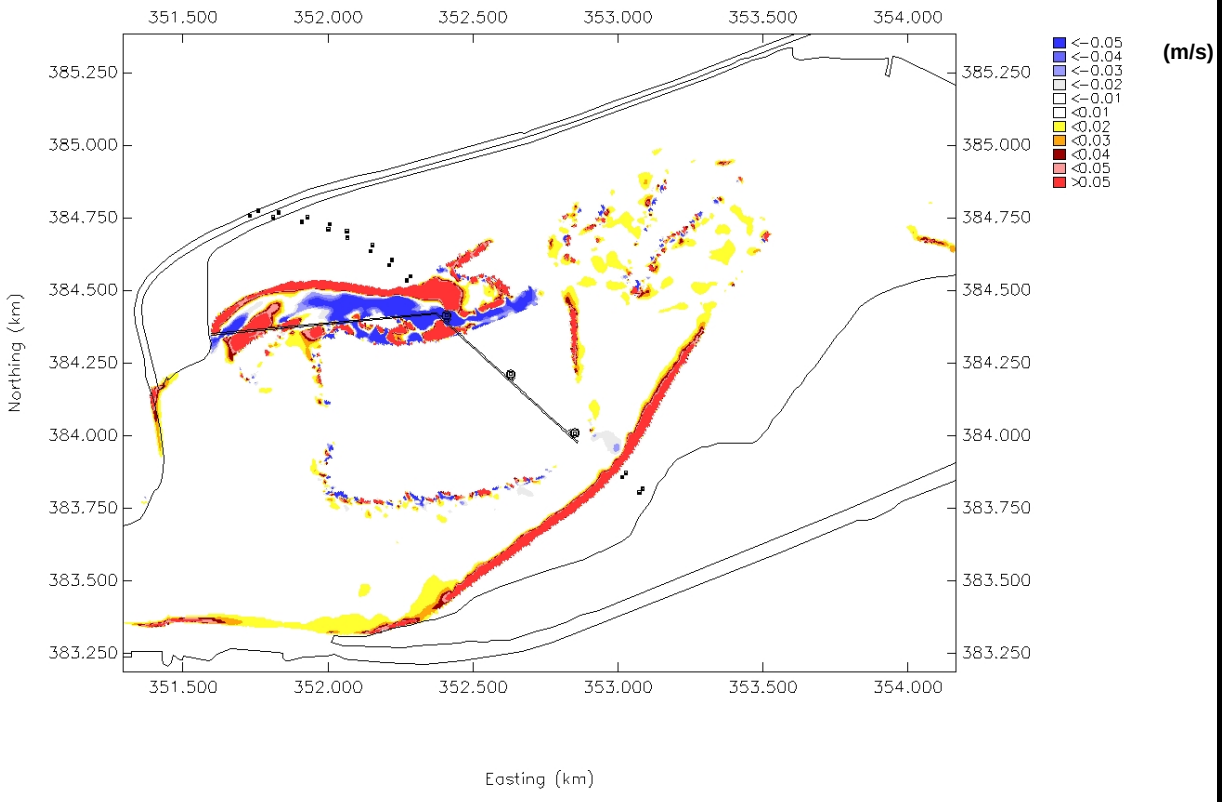

ABP mer marine environmental research

Differences in near-bed speed (m/s) between the proposed bridge scheme Route 3A Medium 3 Tower revised option and the baseline case for low water (A) and peak flood (B) on a spring tide – Spike Island jetty construction option

Figure A21

A.

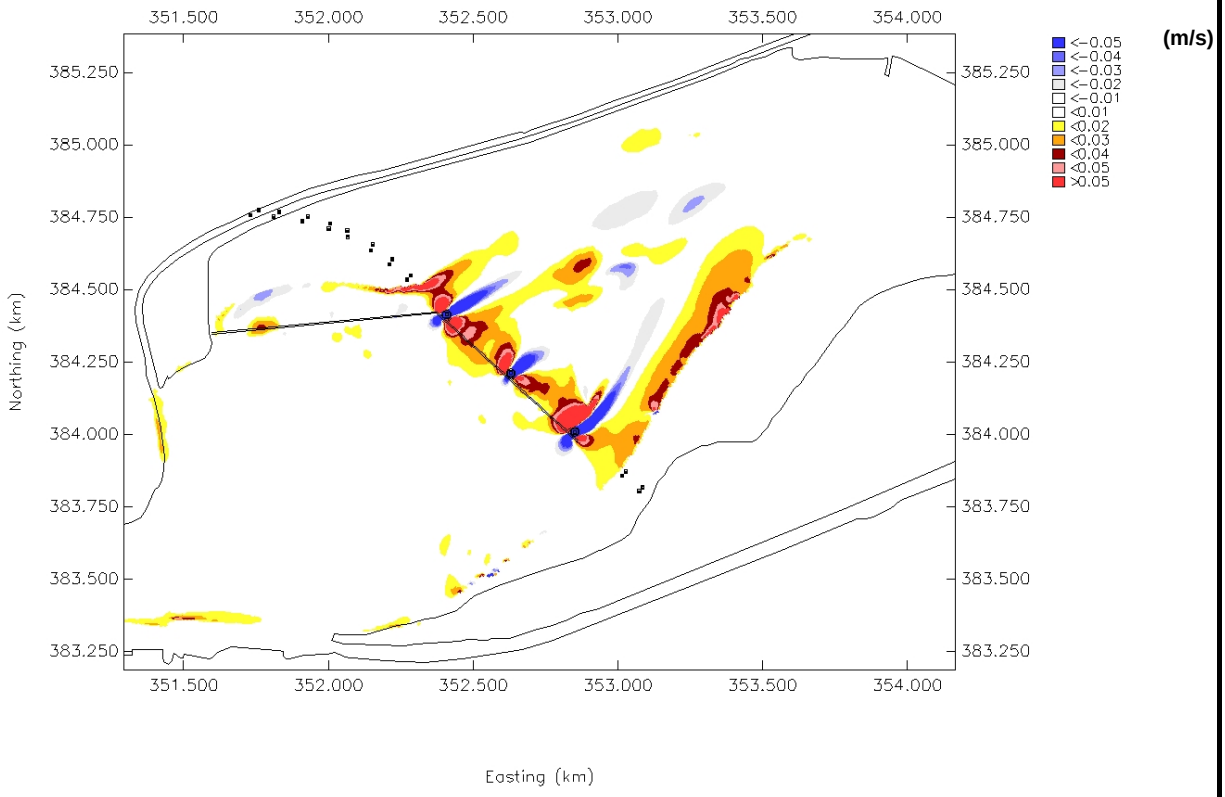

B.

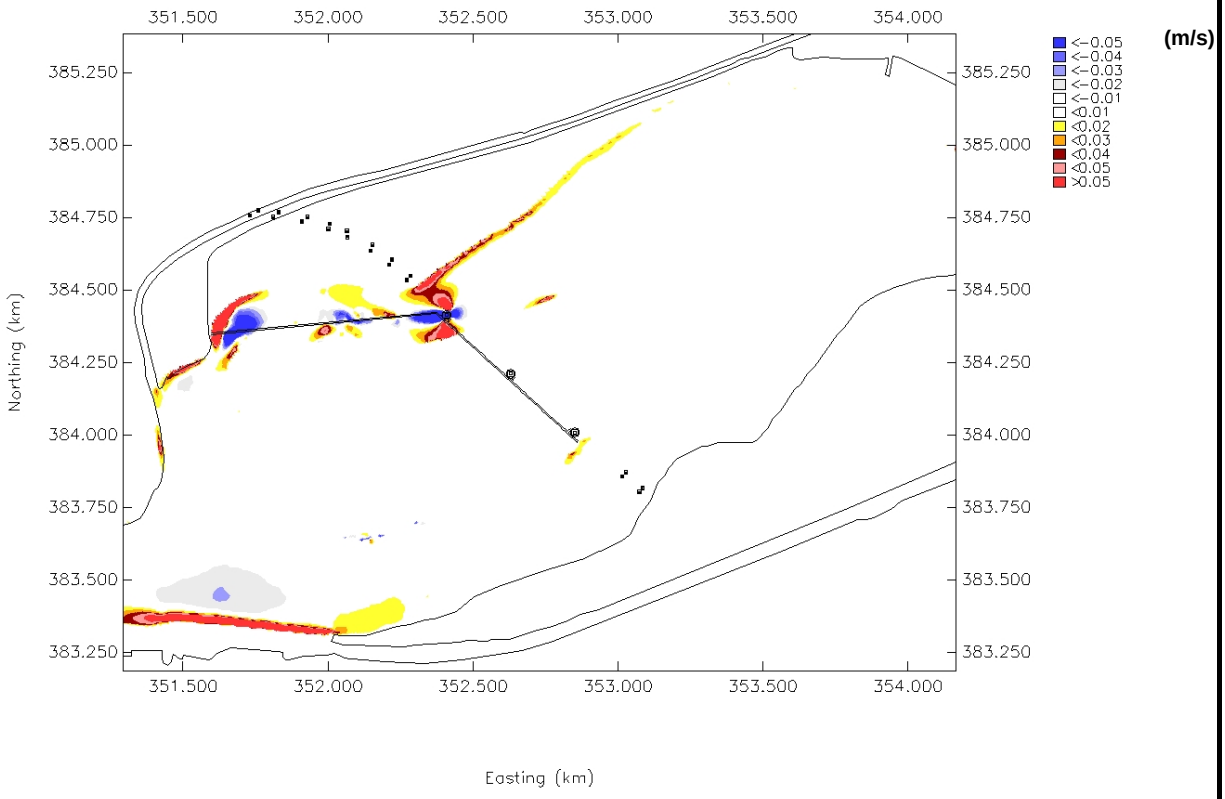

ABP mer marine environmental research

Differences in near-bed speed (m/s) between the proposed bridge scheme Route 3A Medium 3 Tower revised option and the baseline case for high water (A) and peak ebb (B) on a spring tide – Spike Island jetty construction option

Figure A22

A.

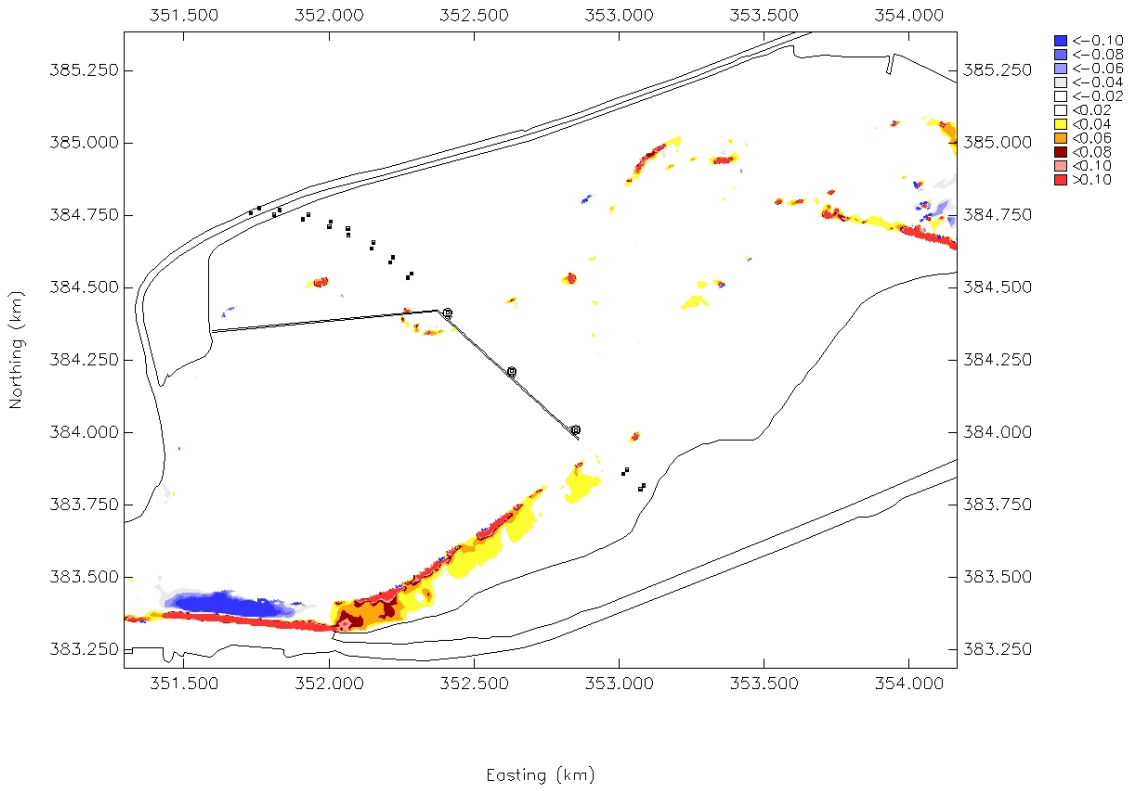

B.

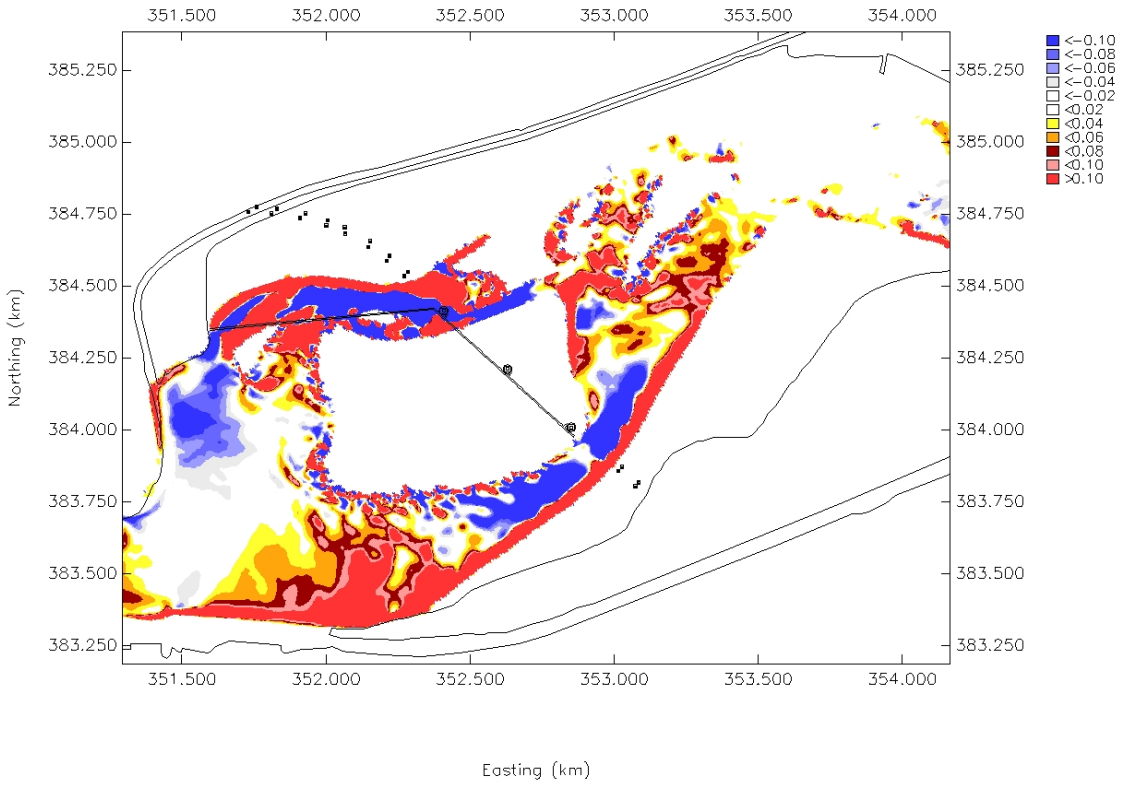

ABP mer marine environmental research

Differences in bed shear stress (N/m²) between the proposed bridge scheme Route 3A Medium 3 Tower revised option and the baseline case for low water (A) and peak flood (B) on a spring tide – Spike Island jetty construction option

Figure A23

A.

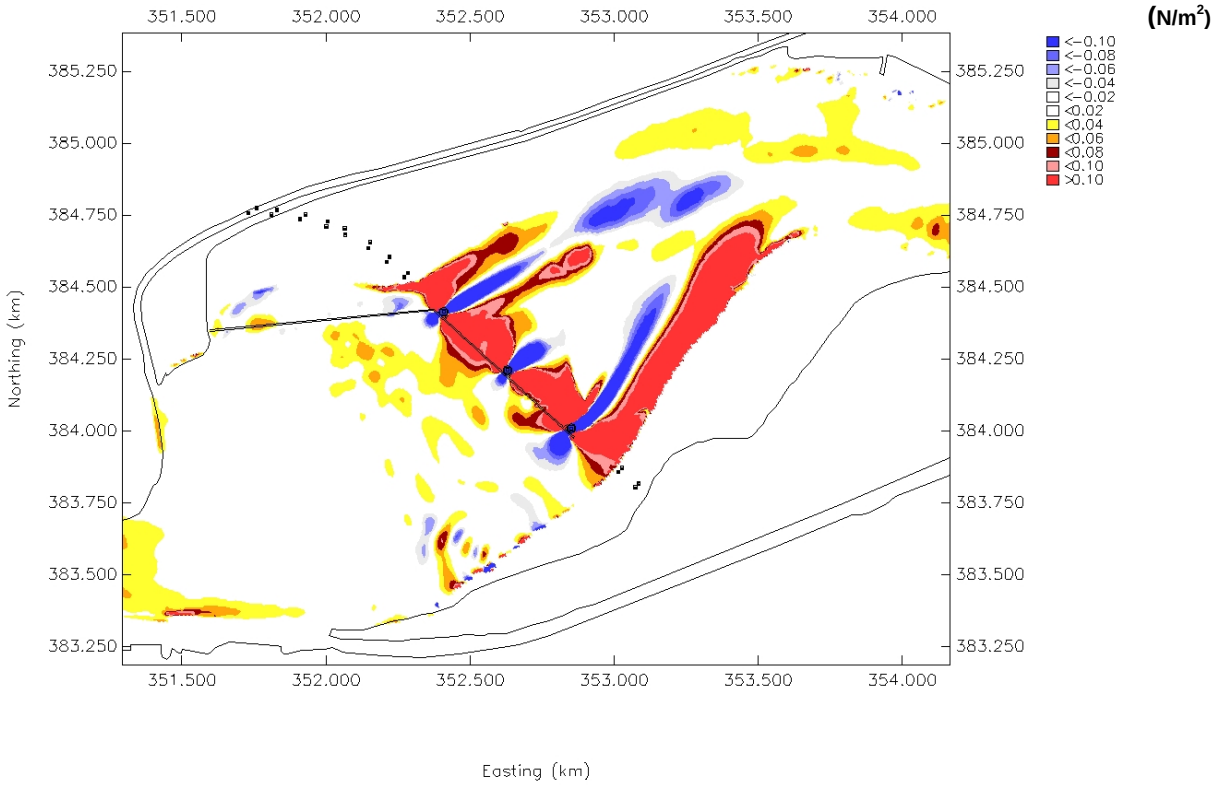

B.

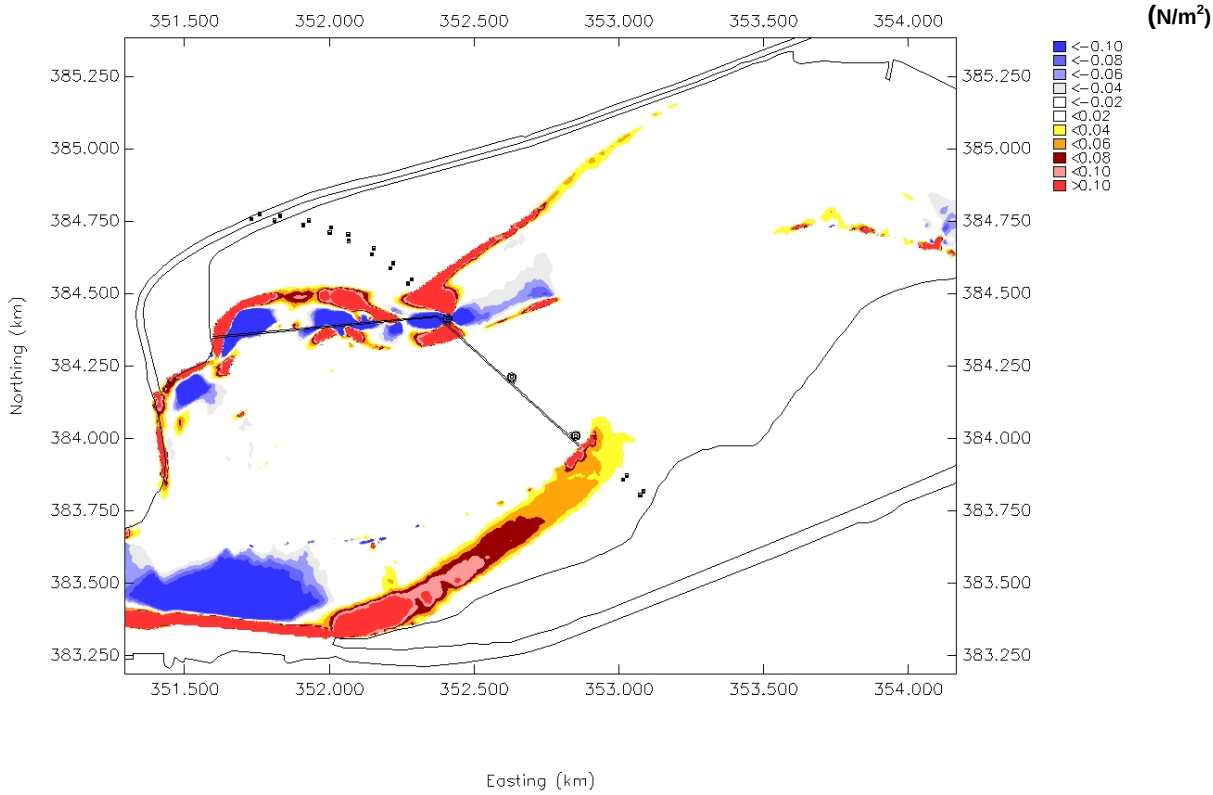

ABP mer marine environmental research

Differences in bed shear stress (N/m²) between the proposed bridge scheme Route 3A Medium 3 Tower revised option and the baseline case for high water (A) and peak ebb (B) on a spring tide – Spike Island jetty construction option

Figure A24

A.

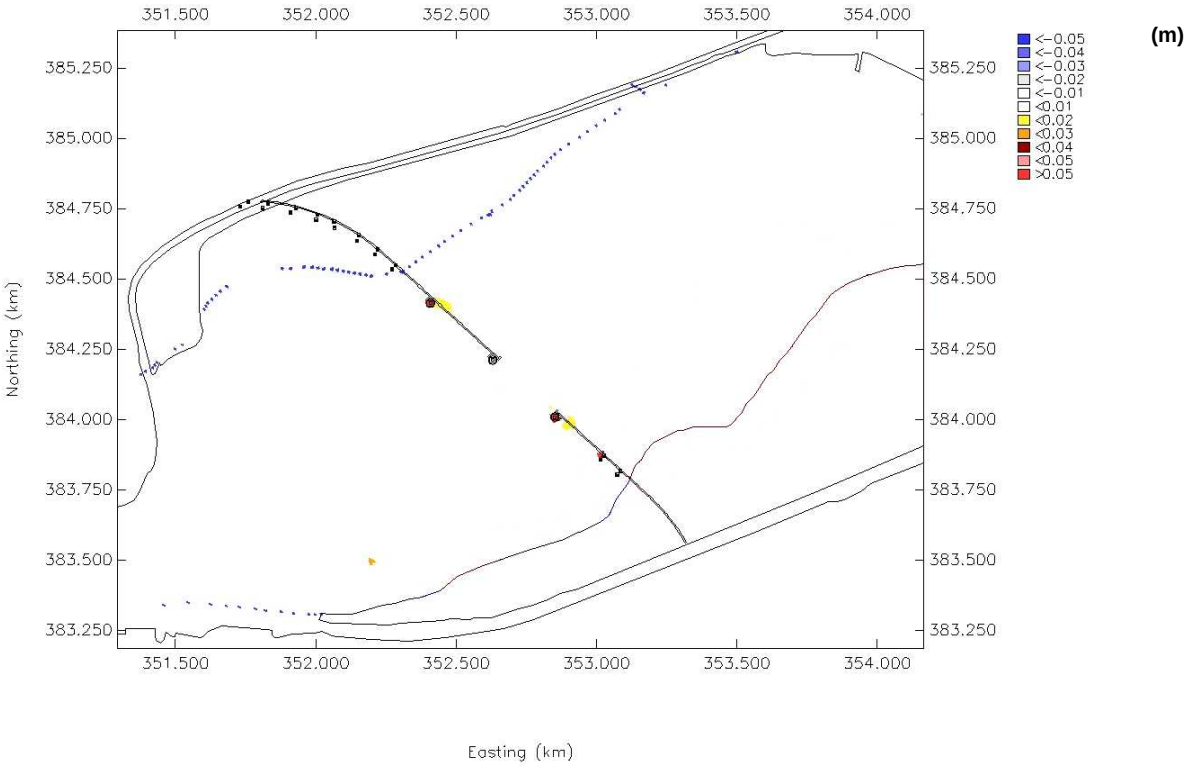

B.

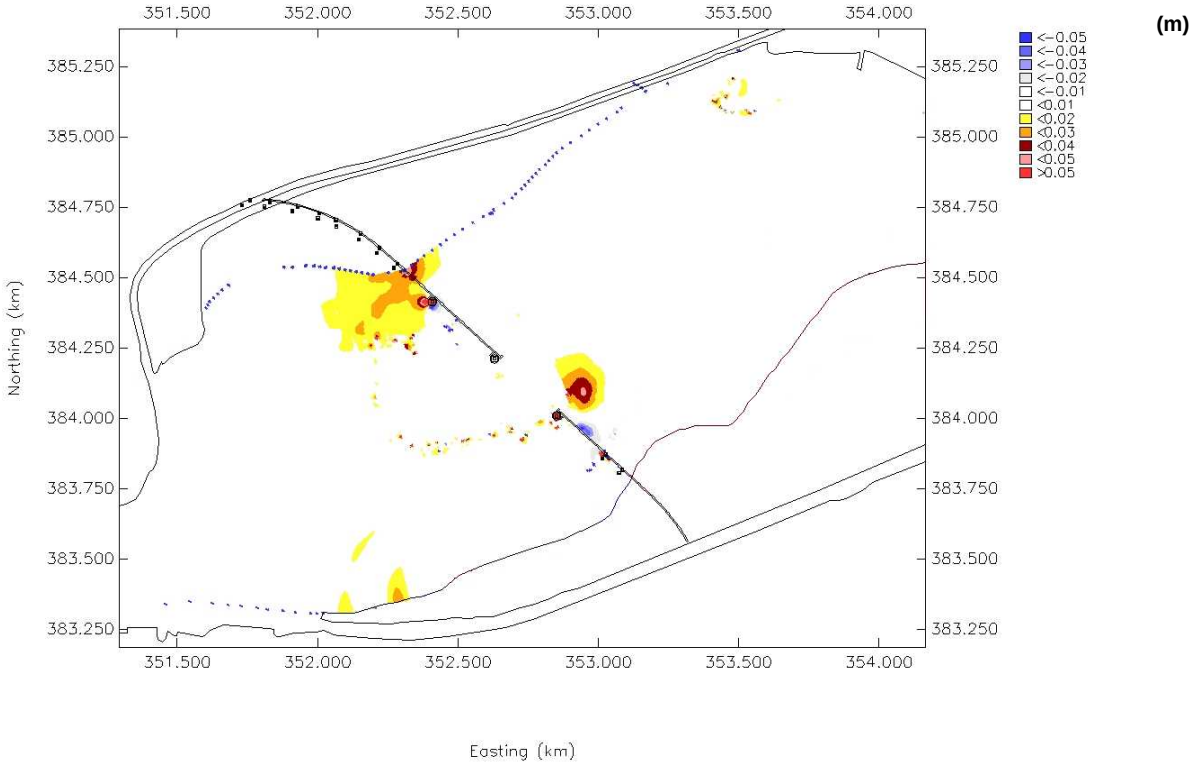

Differences in water level (m) between the Route 3A Preferred Option and the baseline case for an extreme fluvial and surge event at low water (A) and peak flood (B) on a spring tide

Figure A25

A.

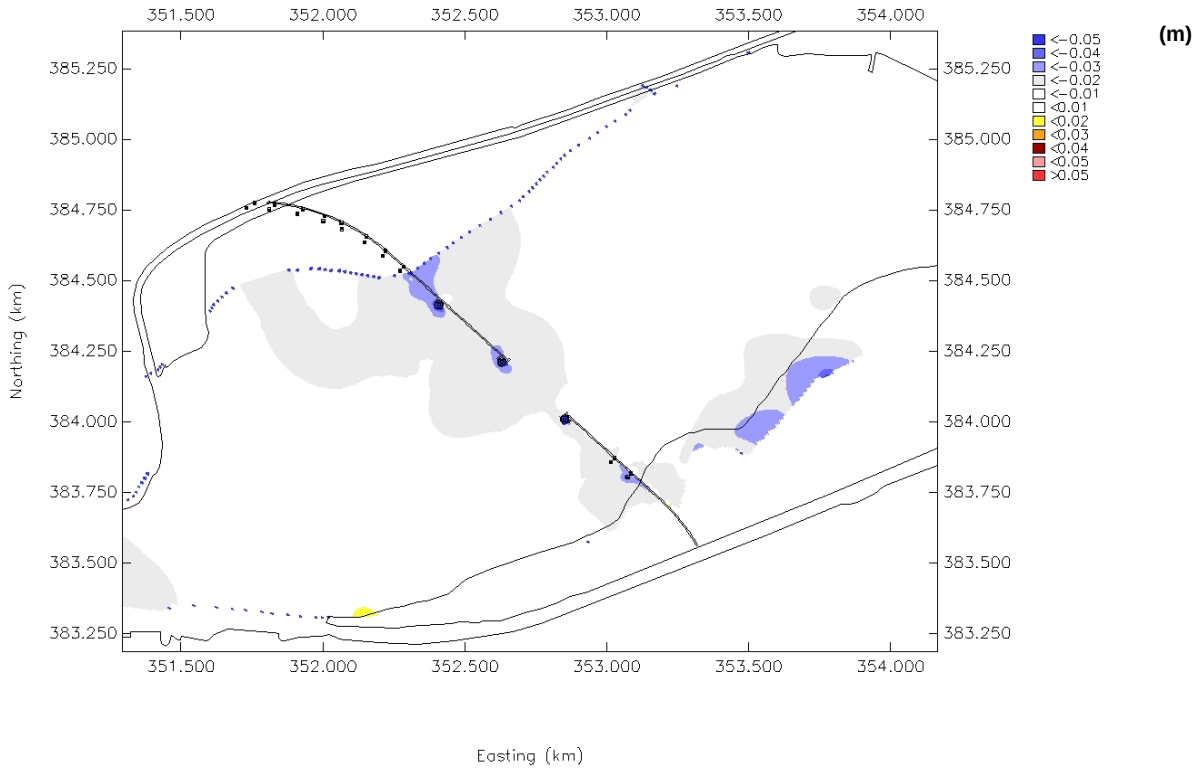

B.

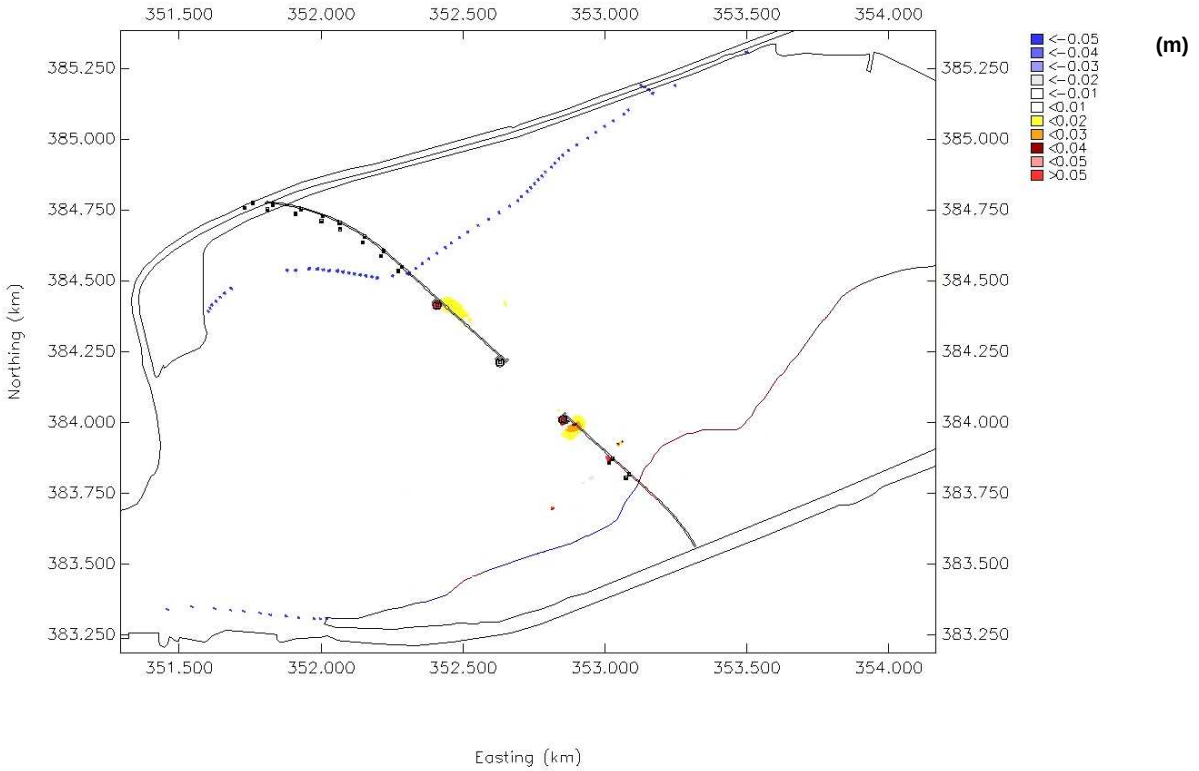

Differences in water level (m) between the Route 3A Preferred Option and the baseline case for an extreme fluvial and surge event at high water (A) and peak ebb (B) on a spring tide

Figure A26

A.

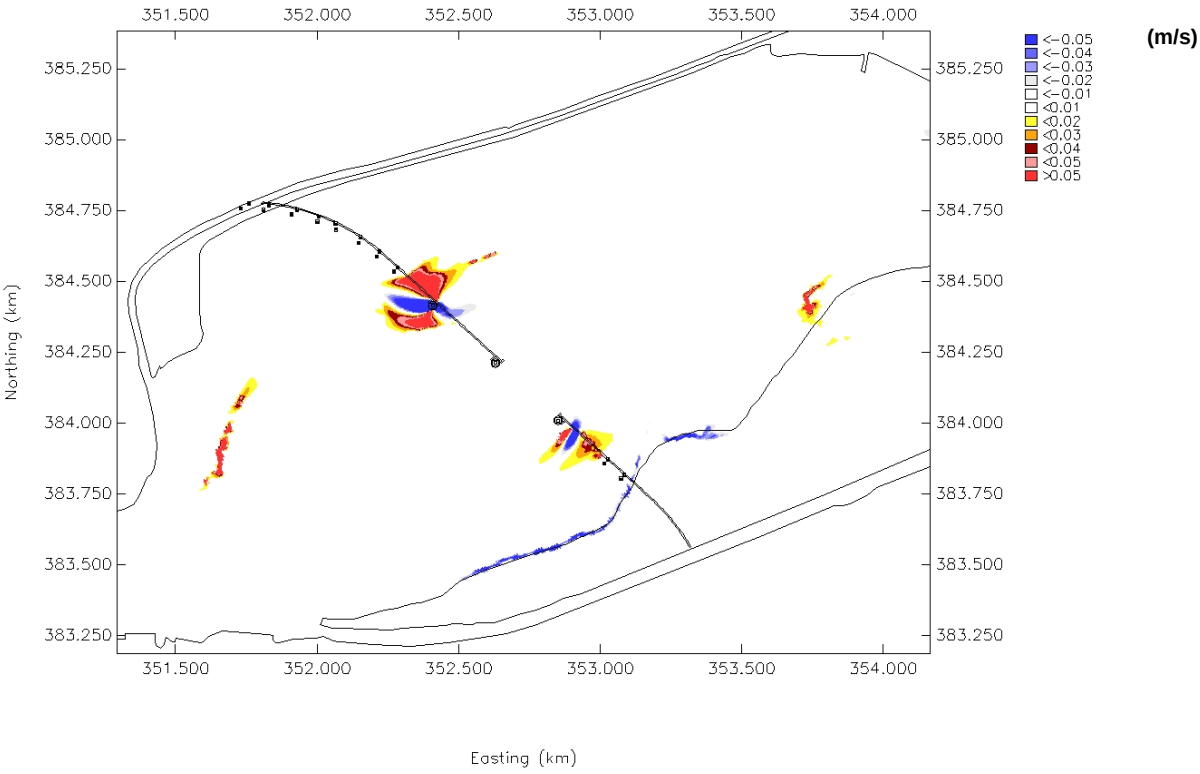

B.

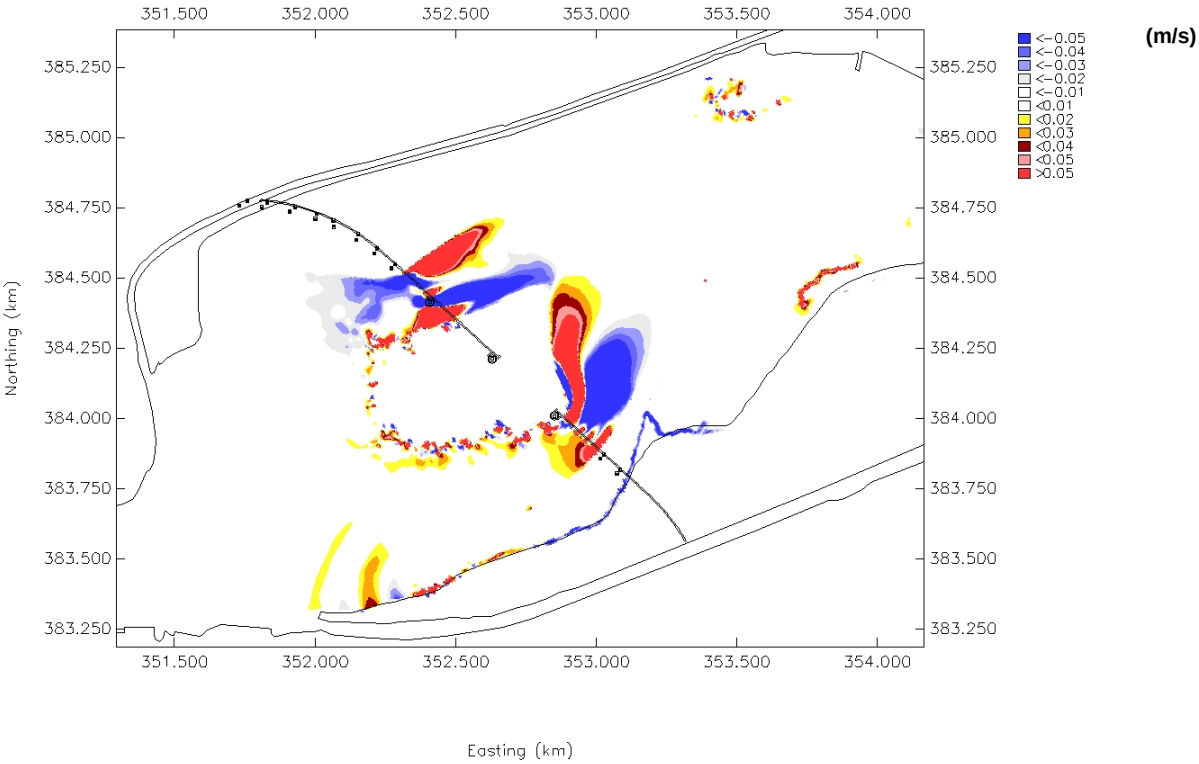

ABP mer marine environmental research

Differences in near-surface speed (m/s) between the Route 3A Preferred Option and the baseline case for an extreme fluvial and surge event at low water (A) and peak flood (B) on a spring tide

Figure A27

A.

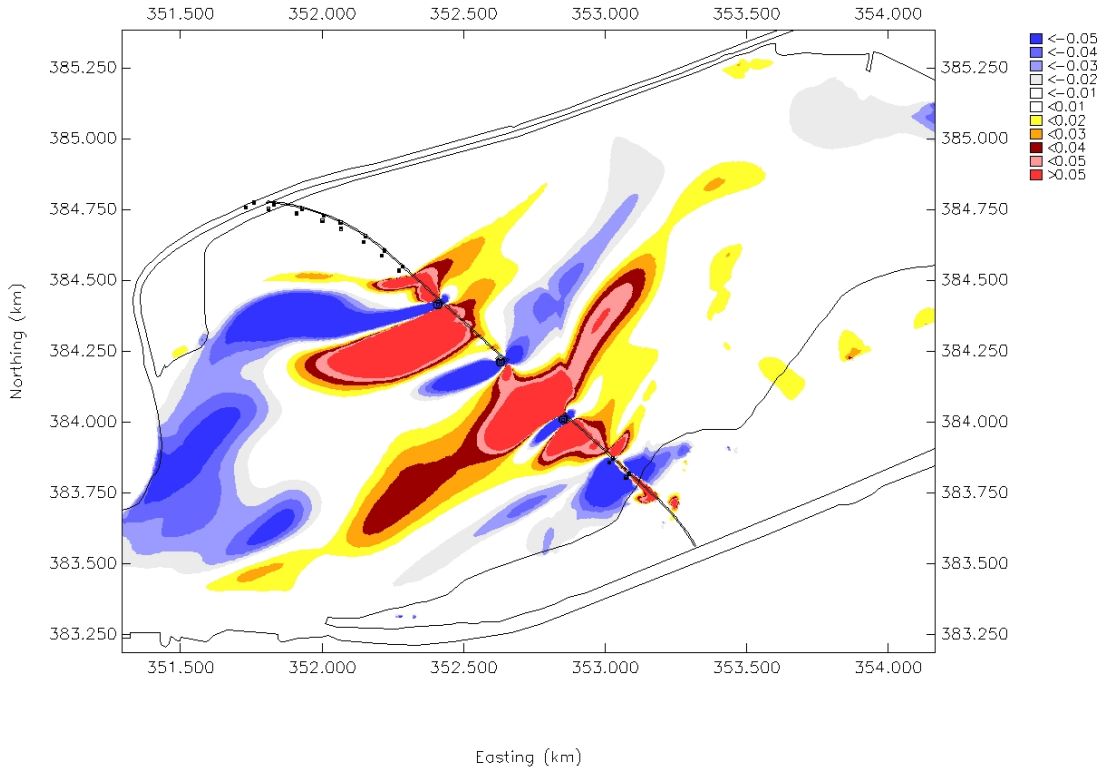

B.

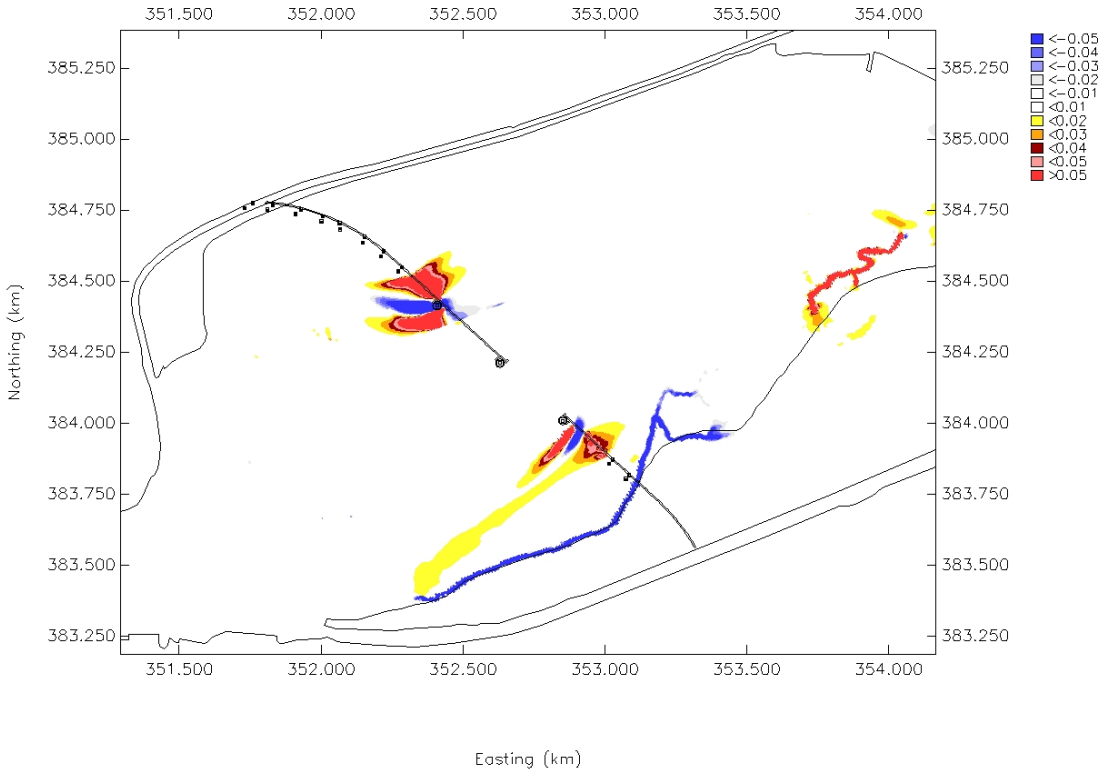

ABP mer marine environmental research

Differences in near-surface speed (m/s) between the Route 3A Preferred Option and the baseline case for an extreme fluvial and surge event at high water (A) and peak ebb (B) on a spring tide

Figure A28

A.

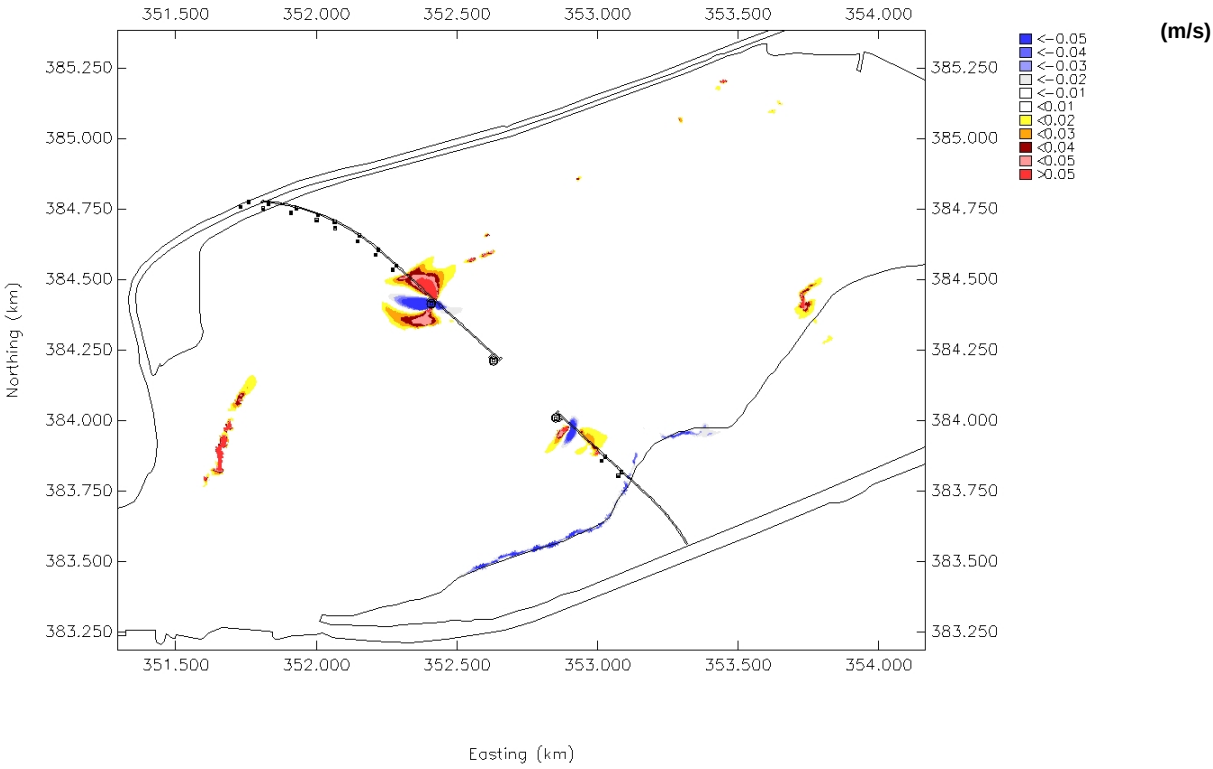

B.

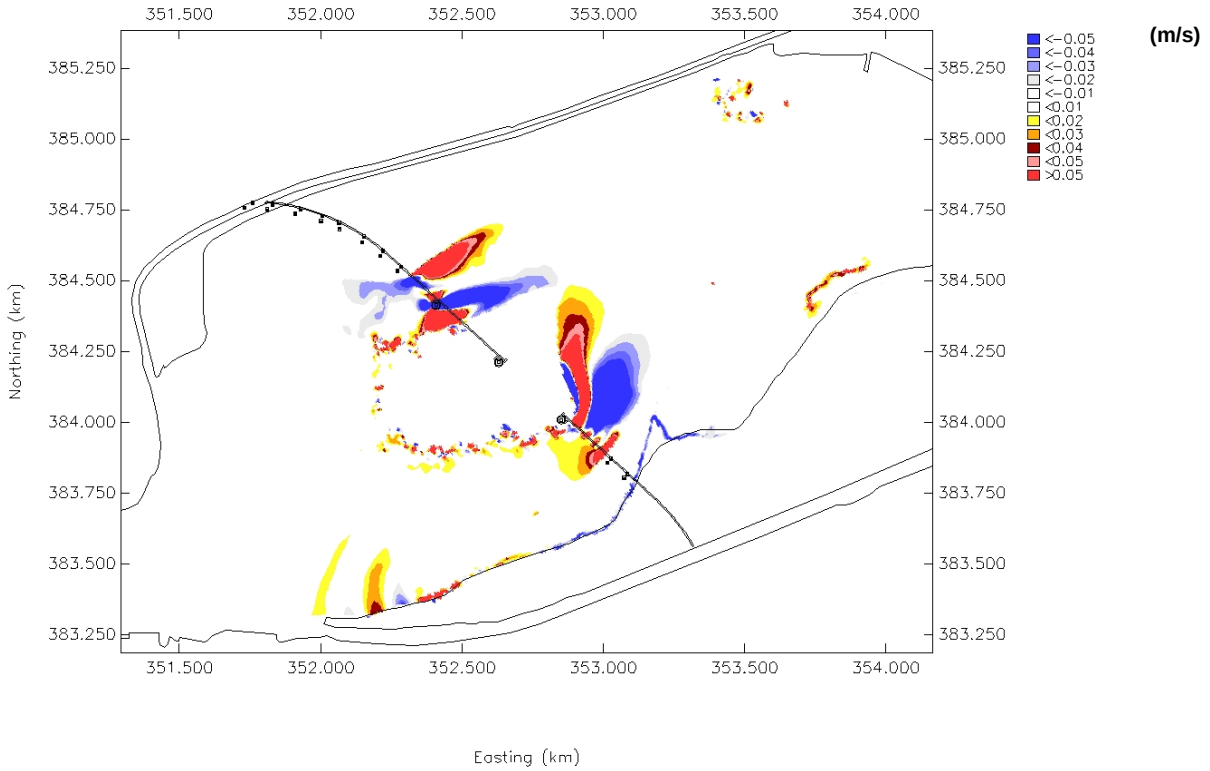

Differences in near-bed speed (m/s) between the Route 3A Preferred Option and the baseline case for an extreme fluvial and surge event at low water (A) and peak flood (B) on a spring tide

Figure A29

A.

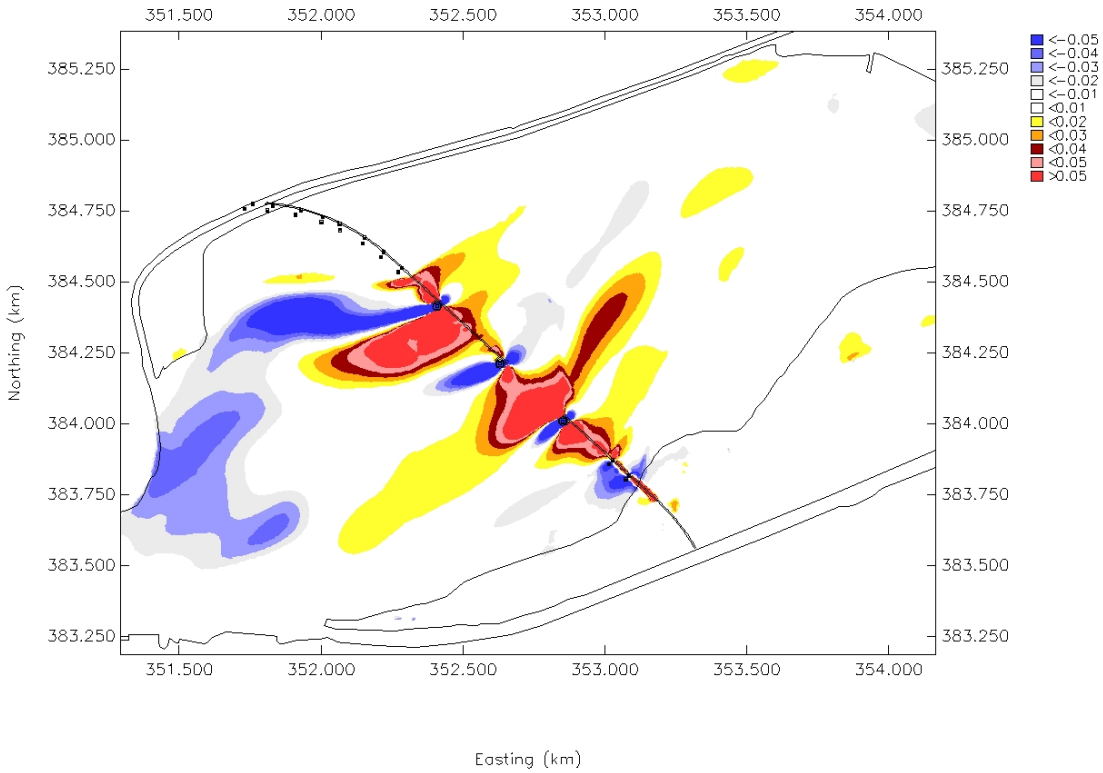

B.

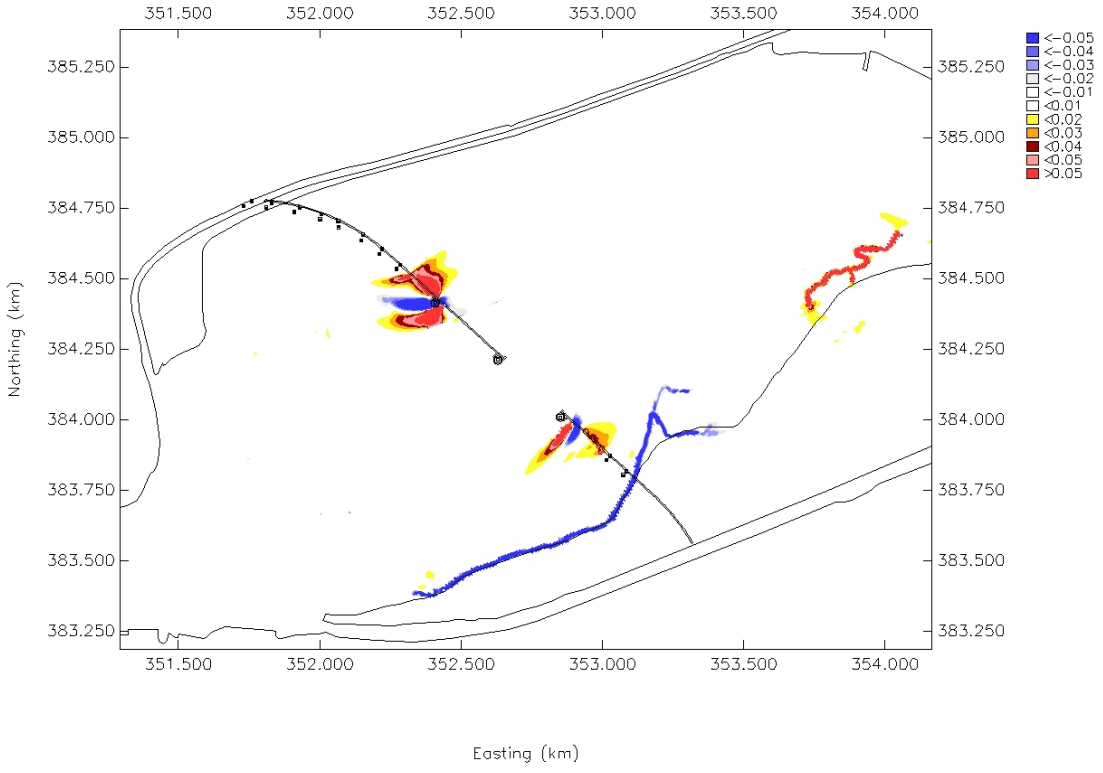

ABP mer marine environmental research

Differences in near-bed speed (m/s) between the Route 3A Preferred Option and the baseline case for an extreme fluvial and surge event at high water (A) and peak ebb (B) on a spring tide

Figure A30

A.

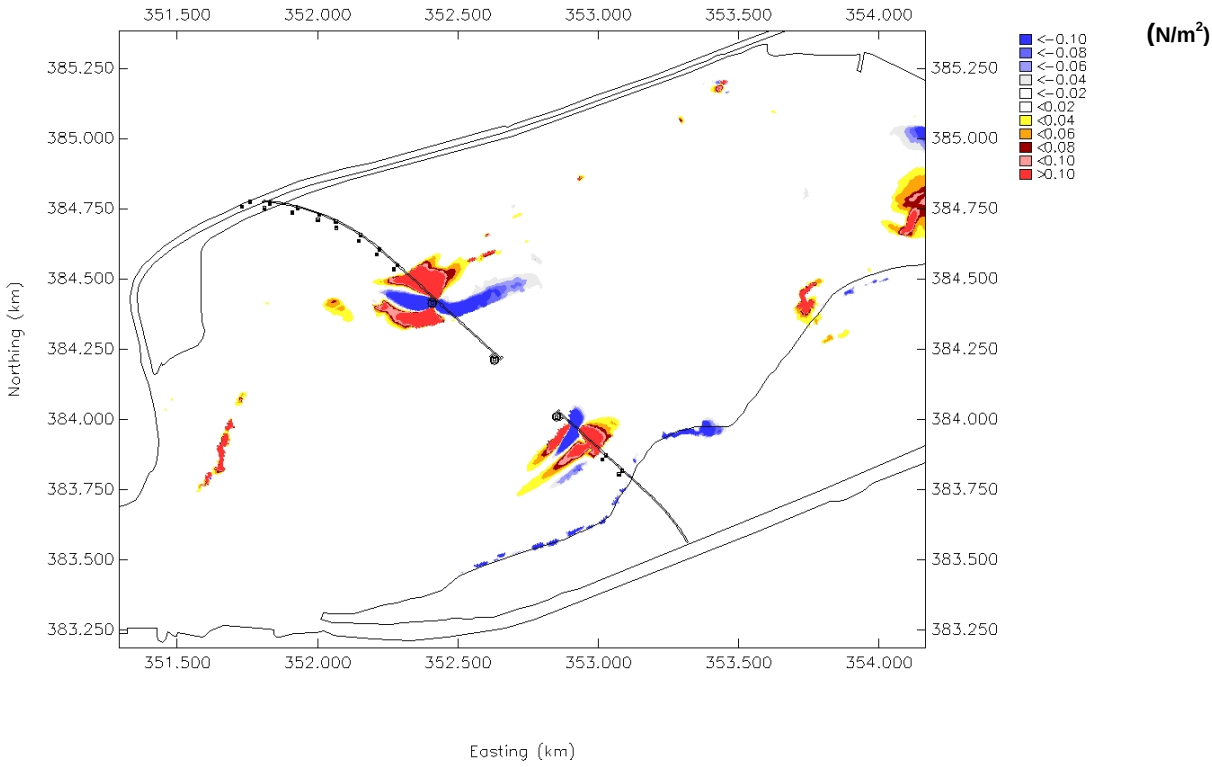

B.

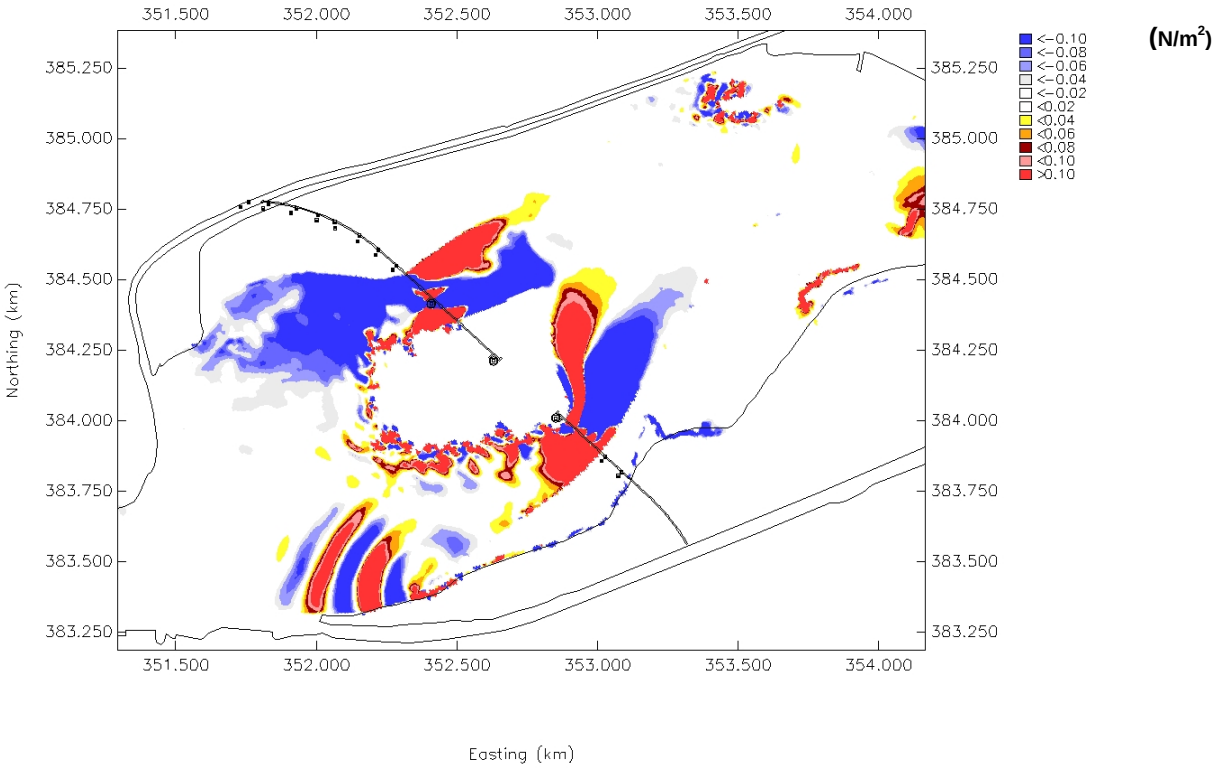

Differences in bed shear stress (N/m²) between the Route 3A Preferred Option and the baseline case for an extreme fluvial and surge event at low water (A) and peak flood (B) on a spring tide

Figure A31

A.

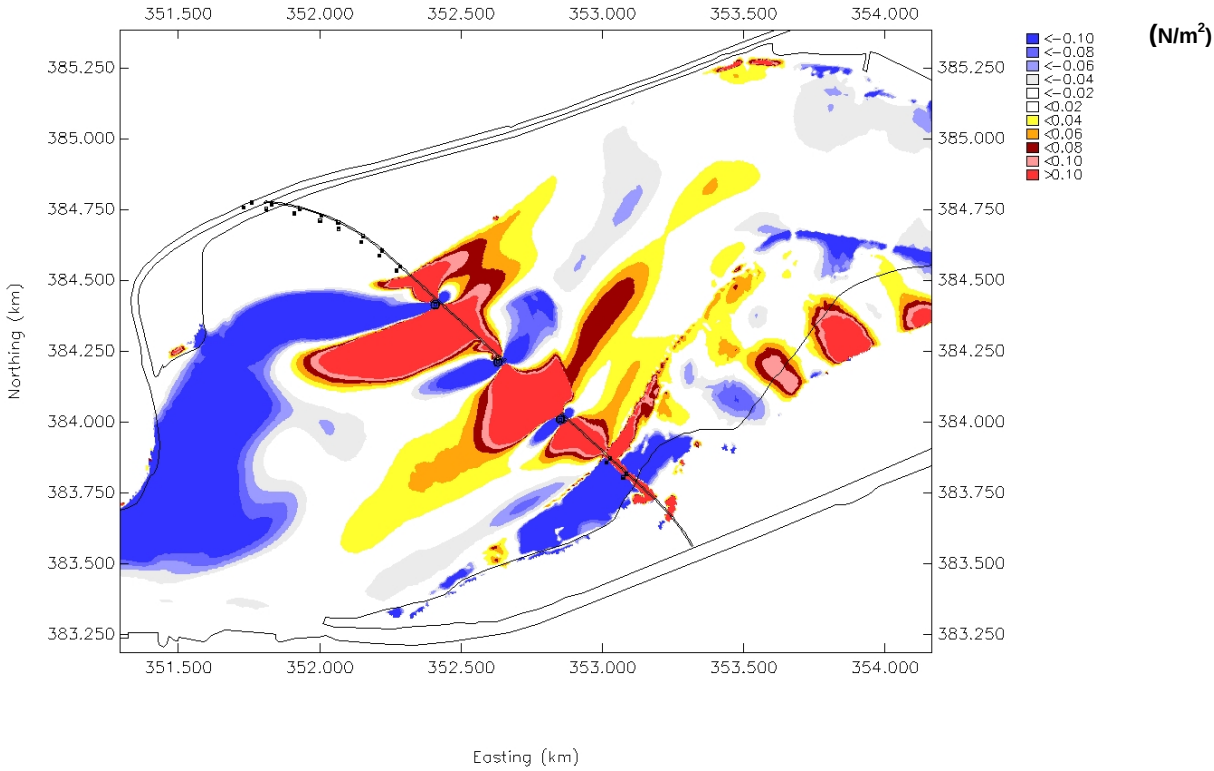

B.

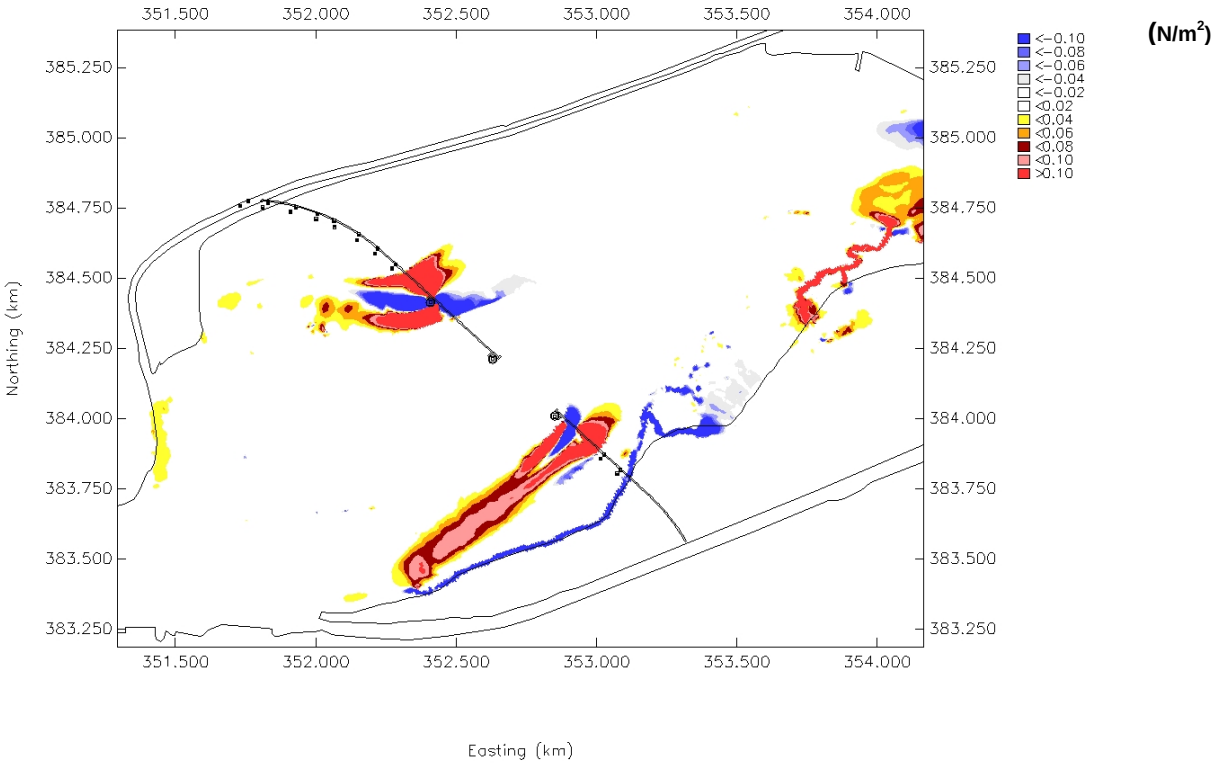

ABP mer
marine environmental research

Differences in bed shear stress (N/m²) between the Route 3A Preferred Option and the baseline case for an extreme fluvial and surge event at high water (A) and peak ebb (B) on a spring tide.

Figure A32

A.

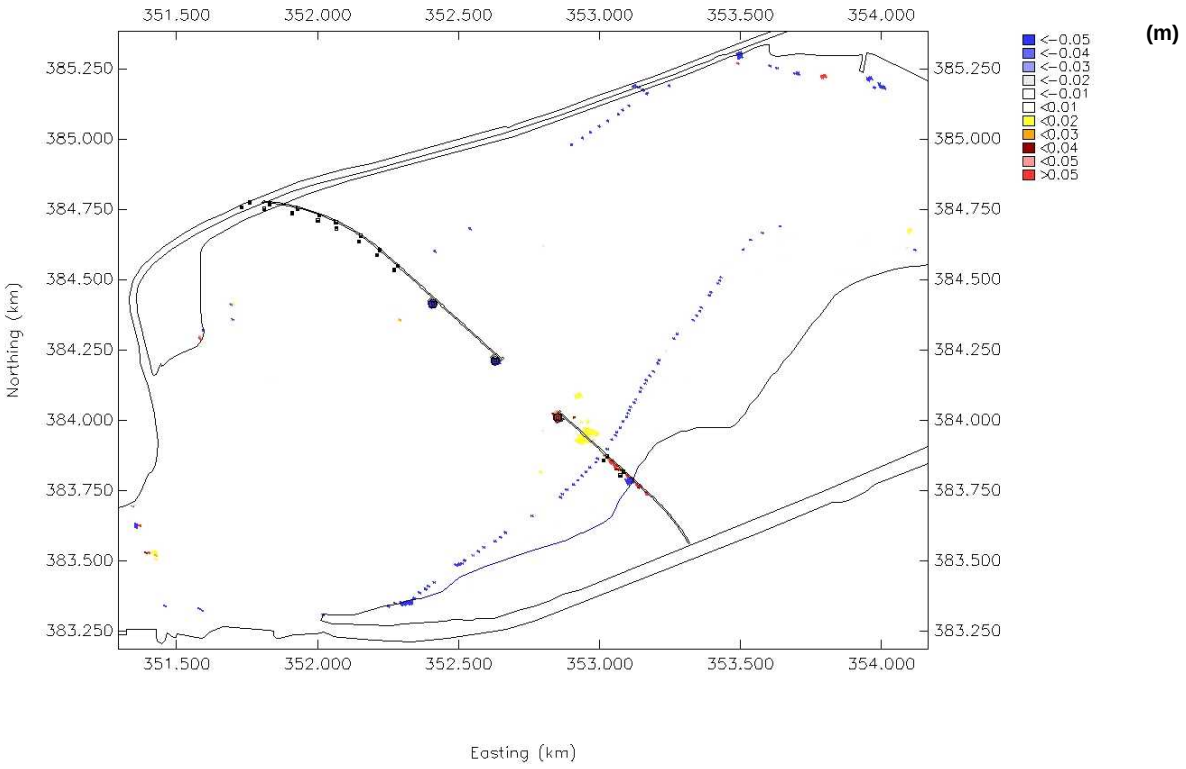

B.

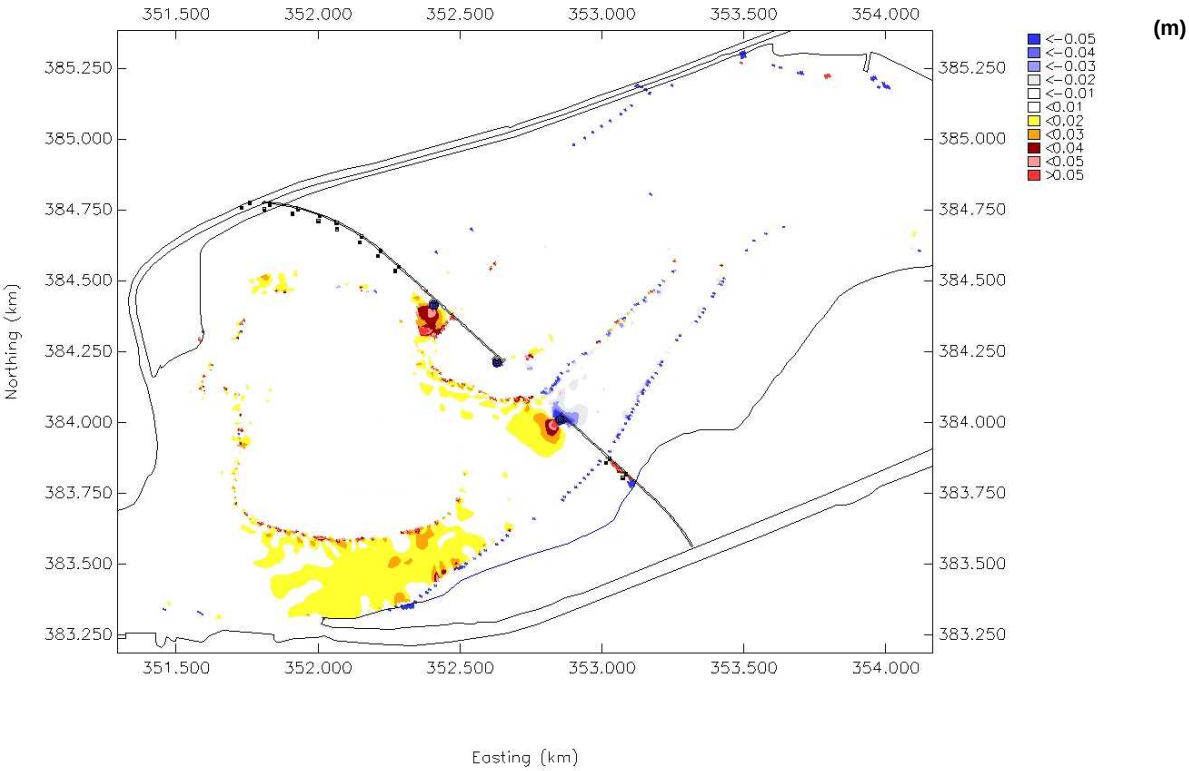

ABP mer marine environmental research	Differences in water level (m) between the Route 3A Preferred Option and the baseline case for low water (A) and peak flood (B) on a spring tide (2005 bathymetry)	Figure A33

A.

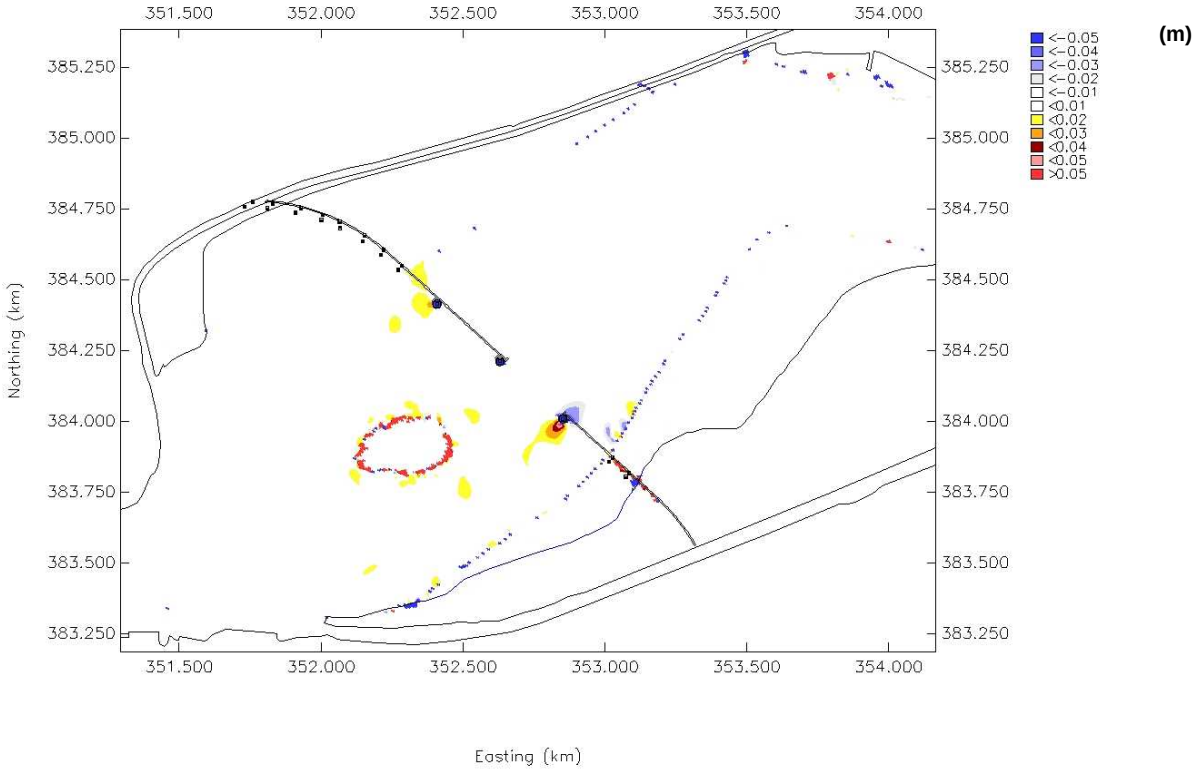

B.

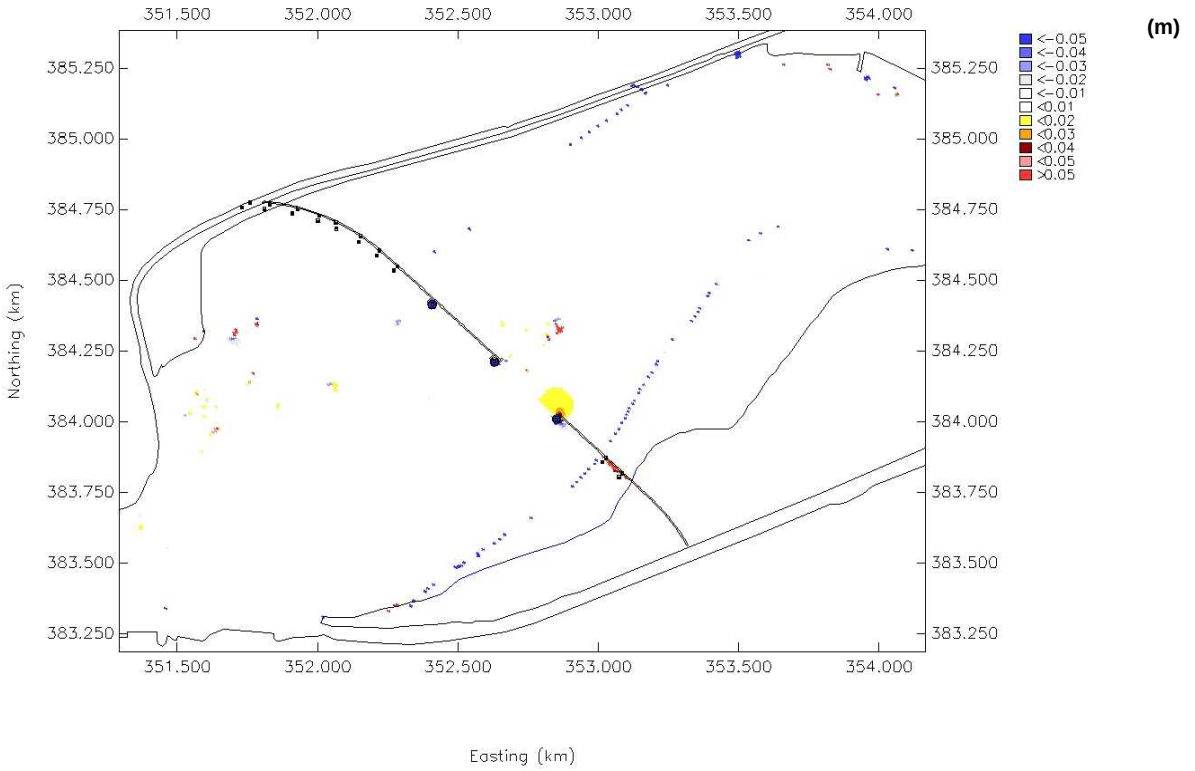

ABP mer marine environmental research

Differences in water level (m) between the Route 3A Preferred Option and the baseline case for high water (A) and peak ebb (B) on a spring tide (2005 bathymetry)

Figure A34

A.

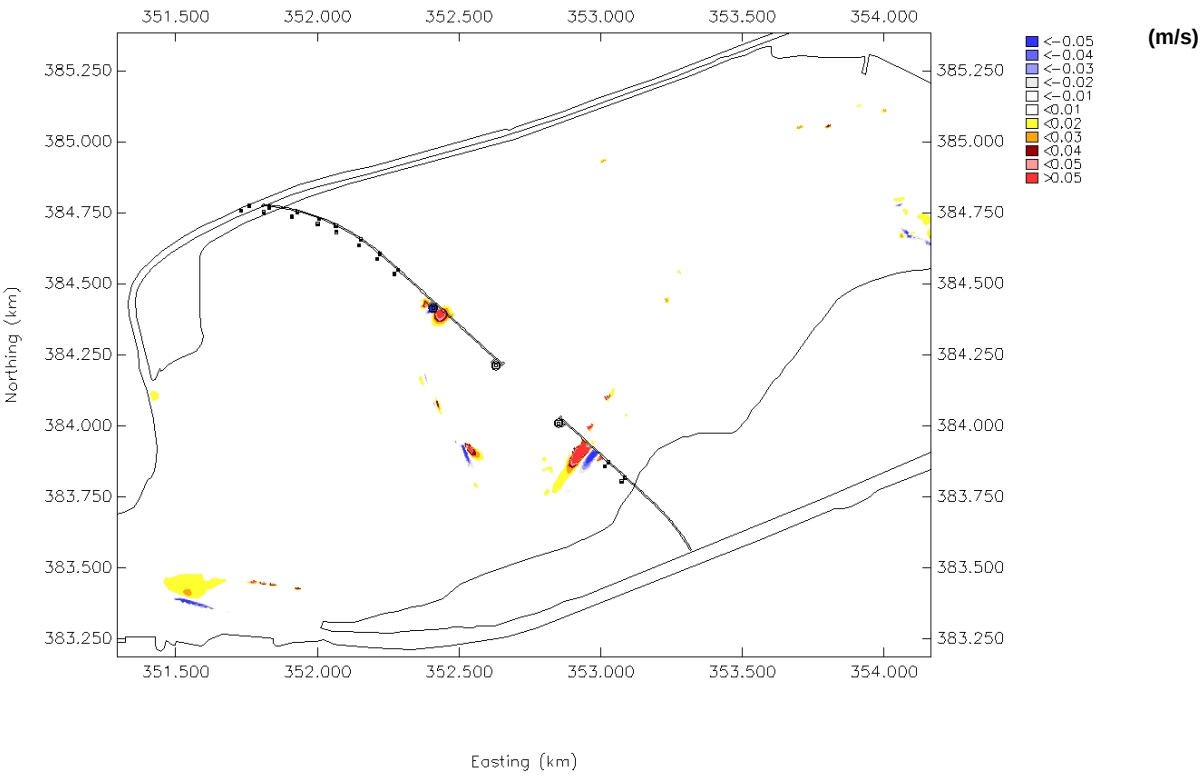

B.

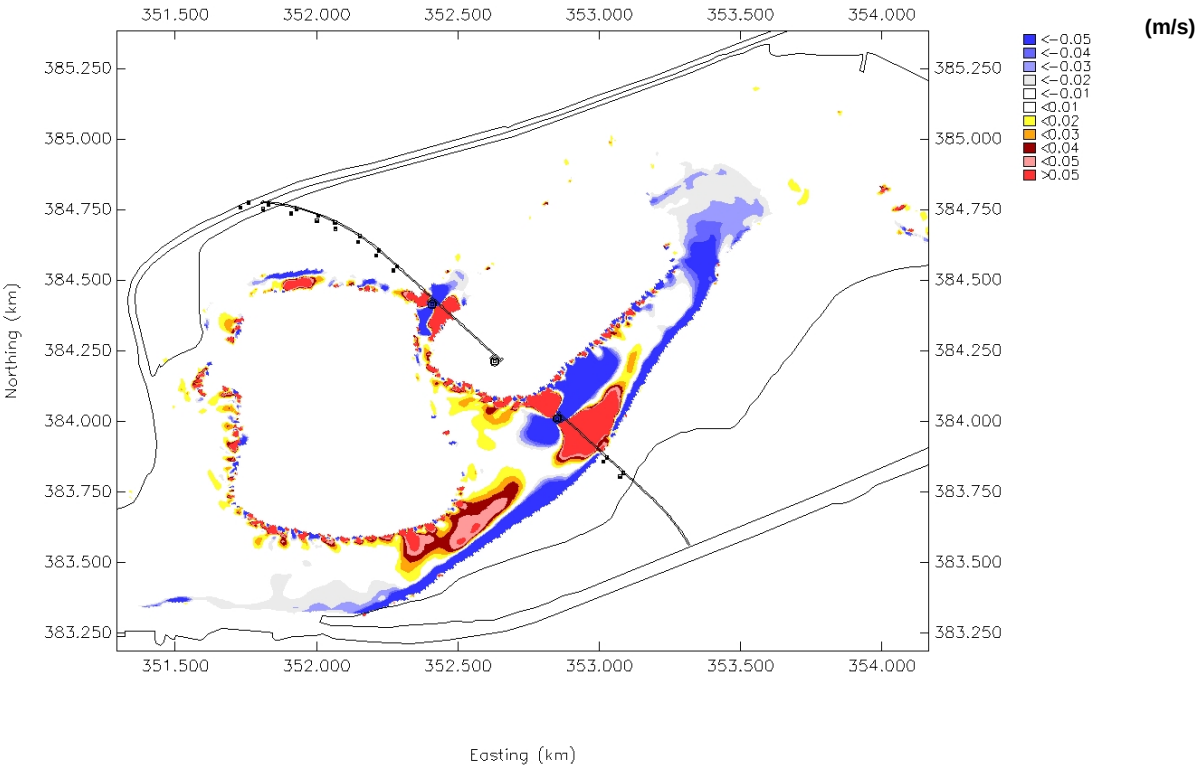

ABP mer marine environmental research

Differences in near-surface speed (m/s) between the Route 3A Preferred Option and the baseline case for low water (A) and peak flood (B) on a spring tide (2005 bathymetry)

Figure A35

A.

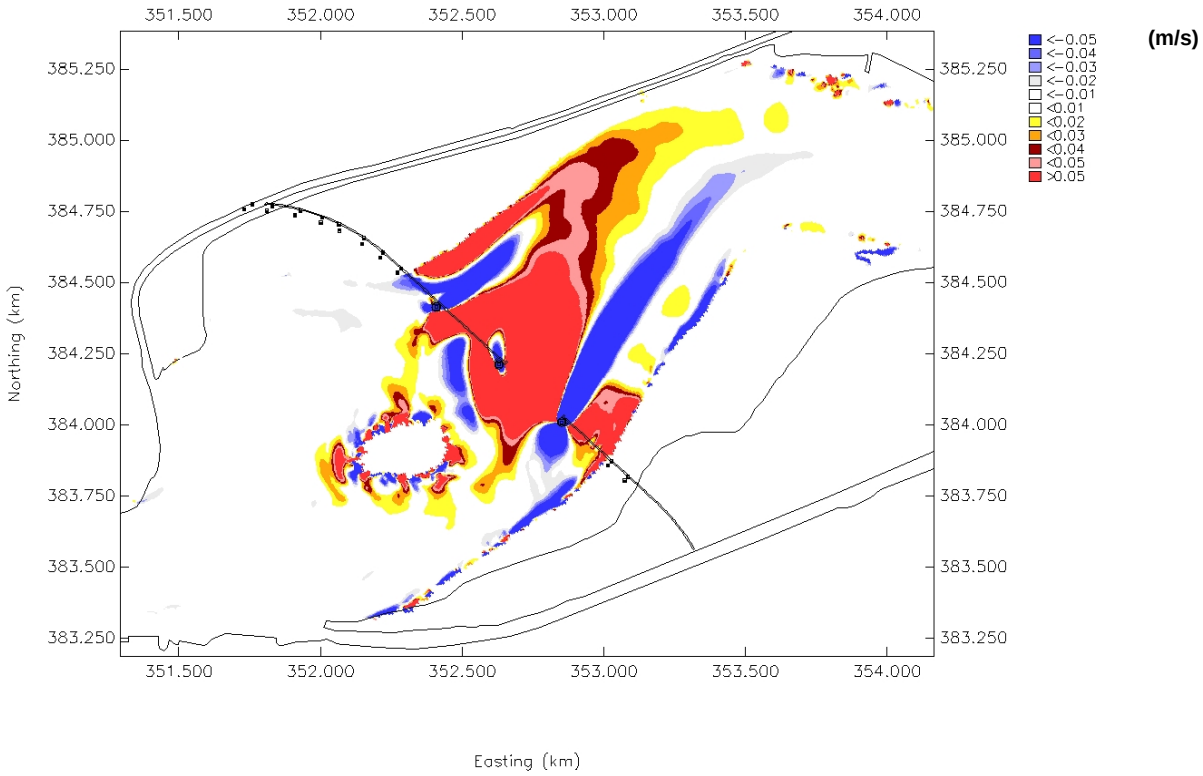

B.

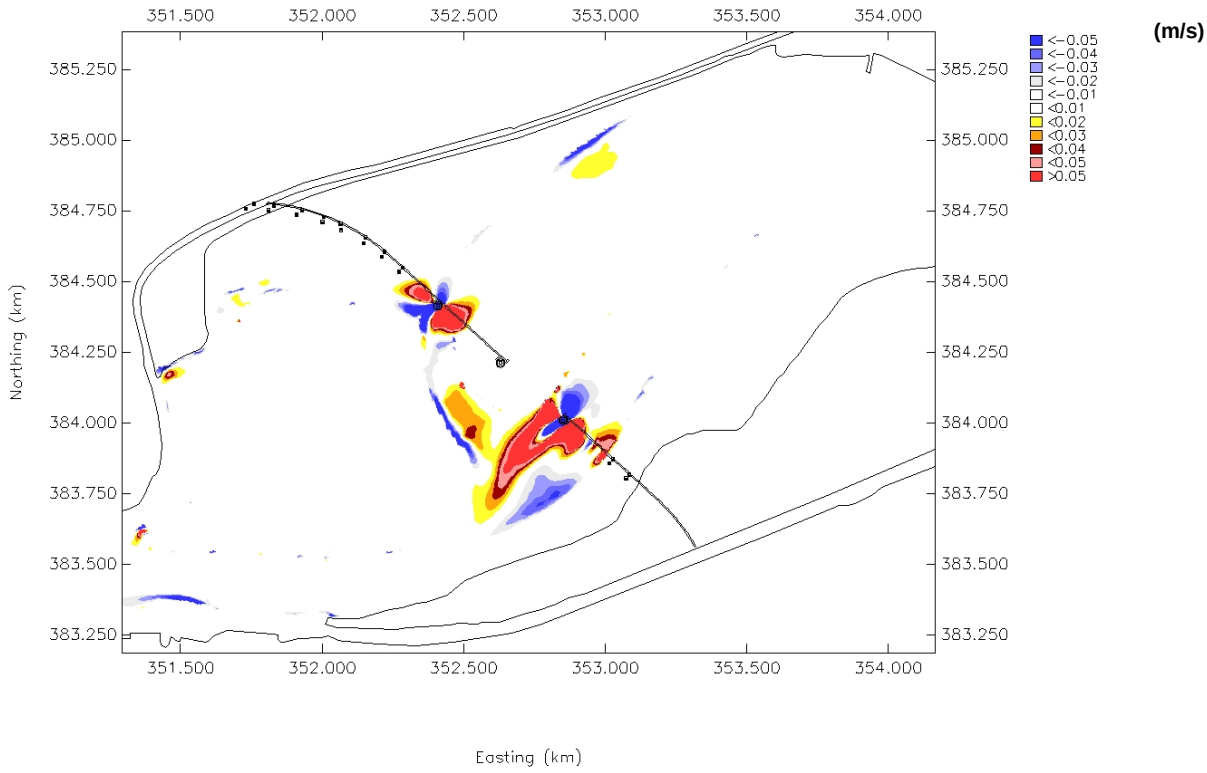

ABP mer marine environmental research

Differences in near-surface speed (m/s) between the Route 3A Preferred Option and the baseline case for high water (A) and peak ebb (B) on a spring tide (2005 bathymetry)

Figure A36

A.

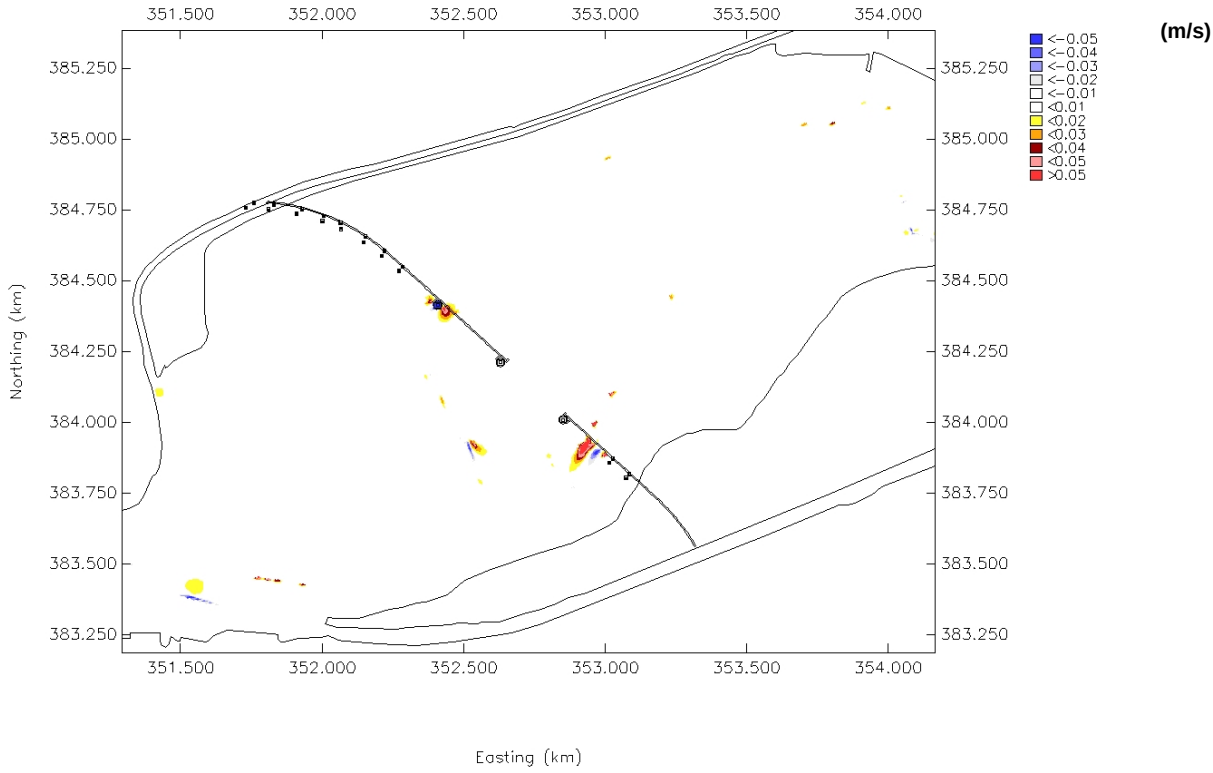

B.

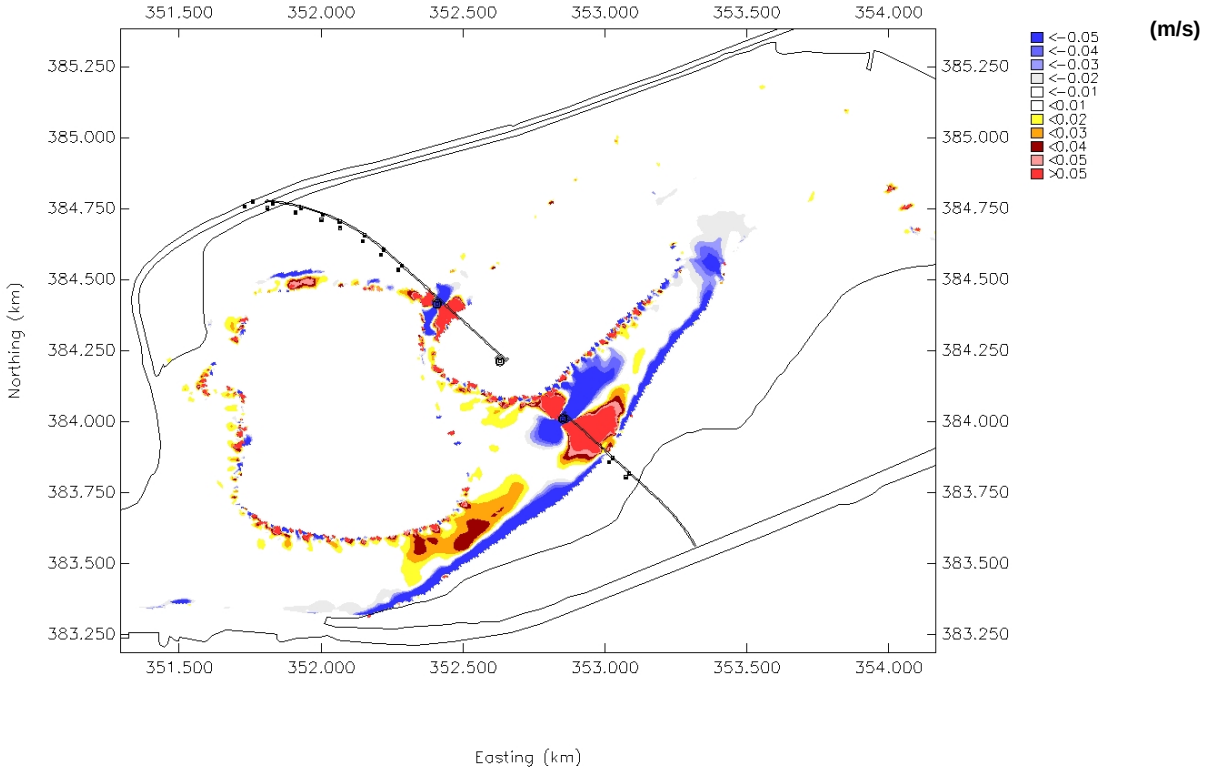

Differences in near-bed speed (m/s) between the Route 3A Preferred Option and the baseline case for low water (A) and peak flood (B) on a spring tide (2005 bathymetry)

Figure A37

A.

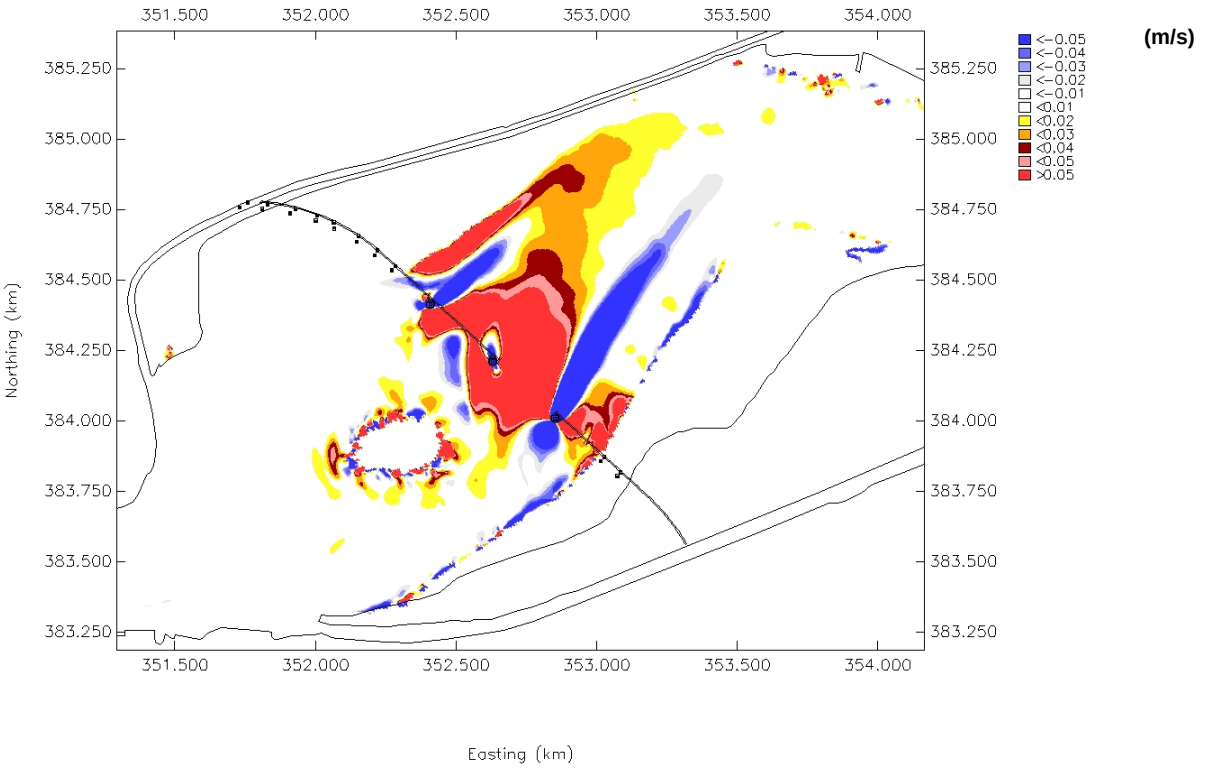

B.

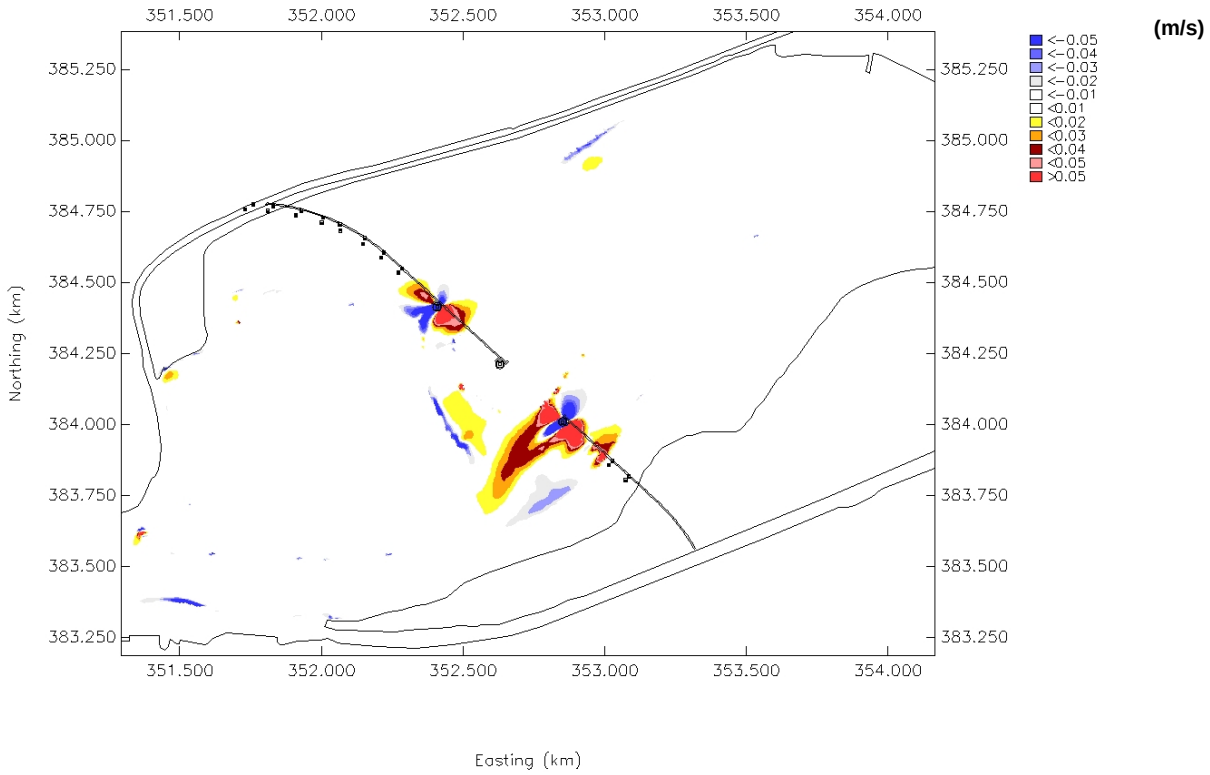

Differences in near-bed speed (m/s) between the Route 3A Preferred Option and the baseline case for high water (A) and peak ebb (B) on a spring tide (2005 bathymetry)

Figure A38

A.

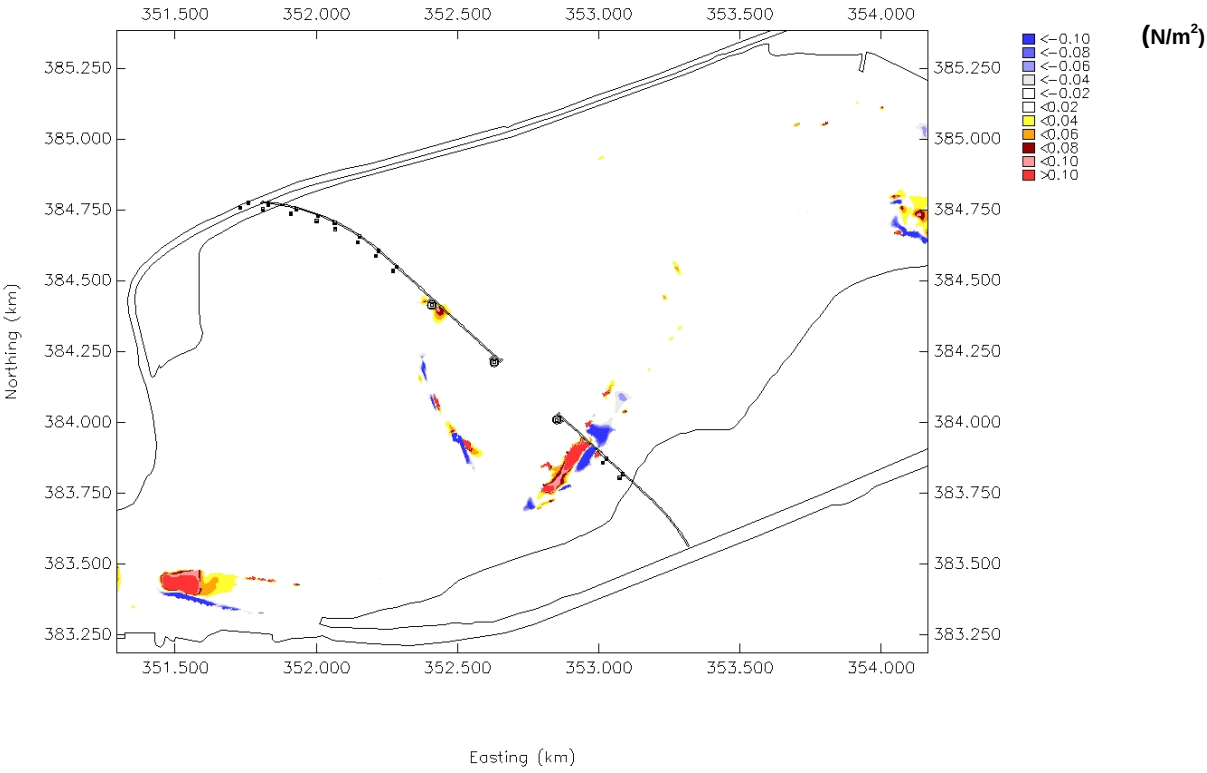

B.

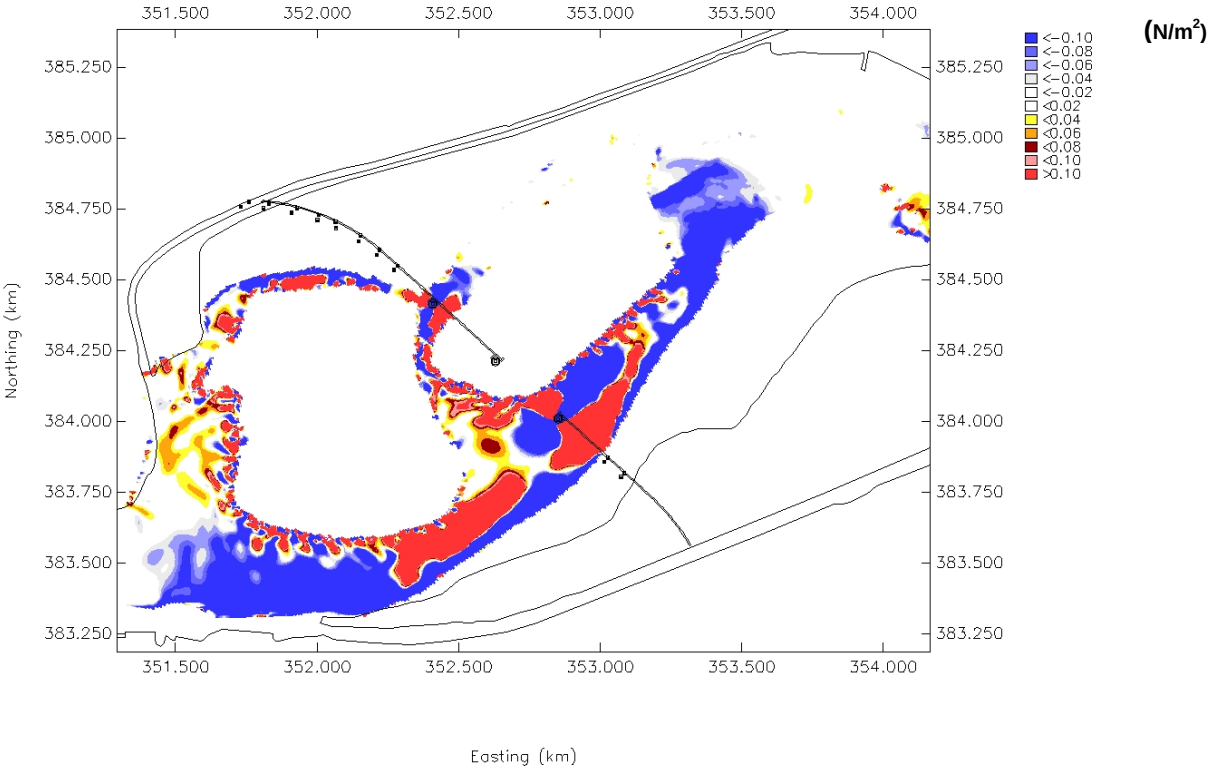

Differences in bed shear stress (N/m²) between the Route 3A Preferred Option and the baseline case for low water (A) and peak flood (B) on a spring tide. (2005 bathymetry)

Figure A39

A.

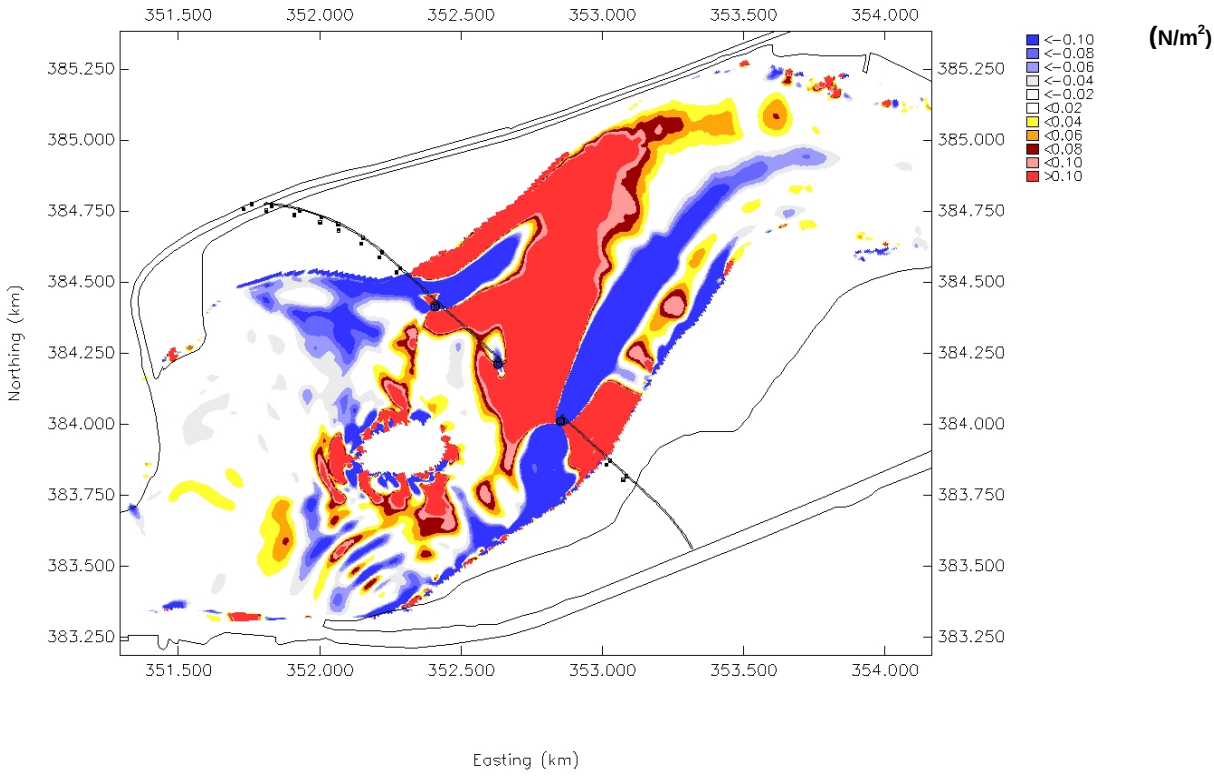

B.

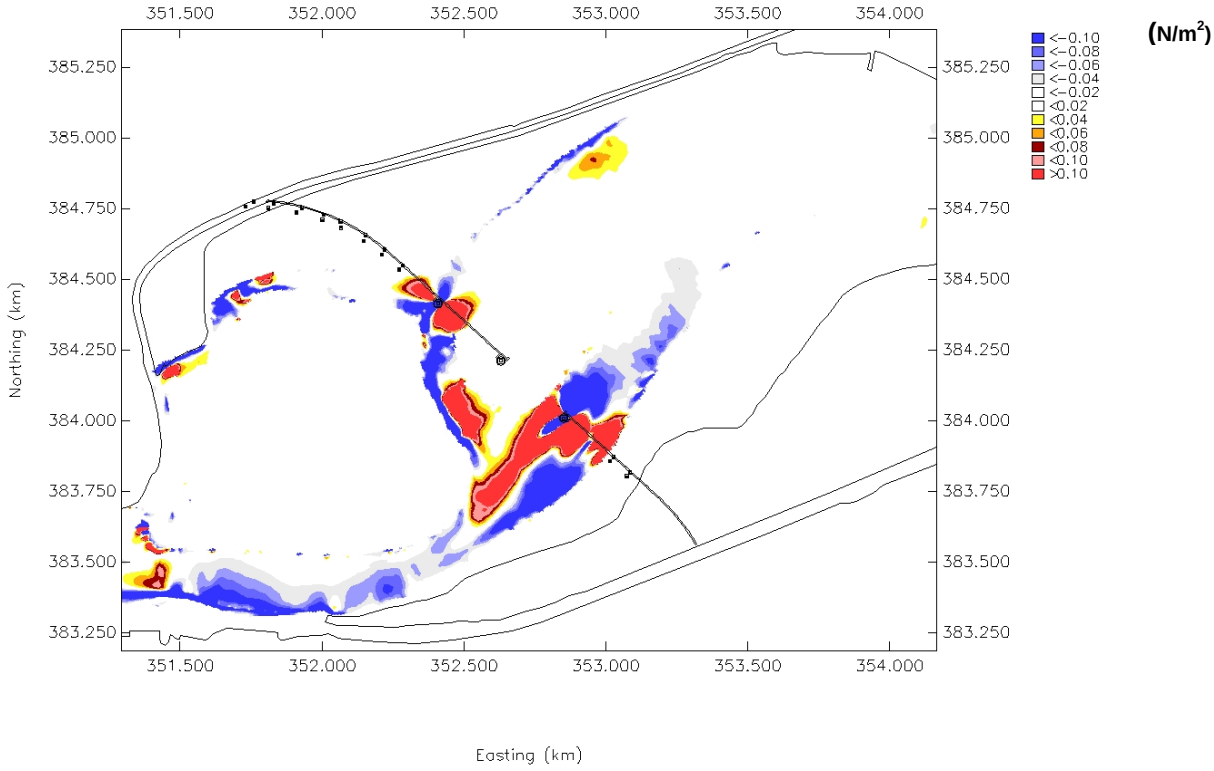

ABP mer marine environmental research

Differences in bed shear stress (N/m²) between the Route 3A Preferred Option and the baseline case for high water (A) and peak ebb (B) on a spring tide. (2005 bathymetry)

Figure A40

A.

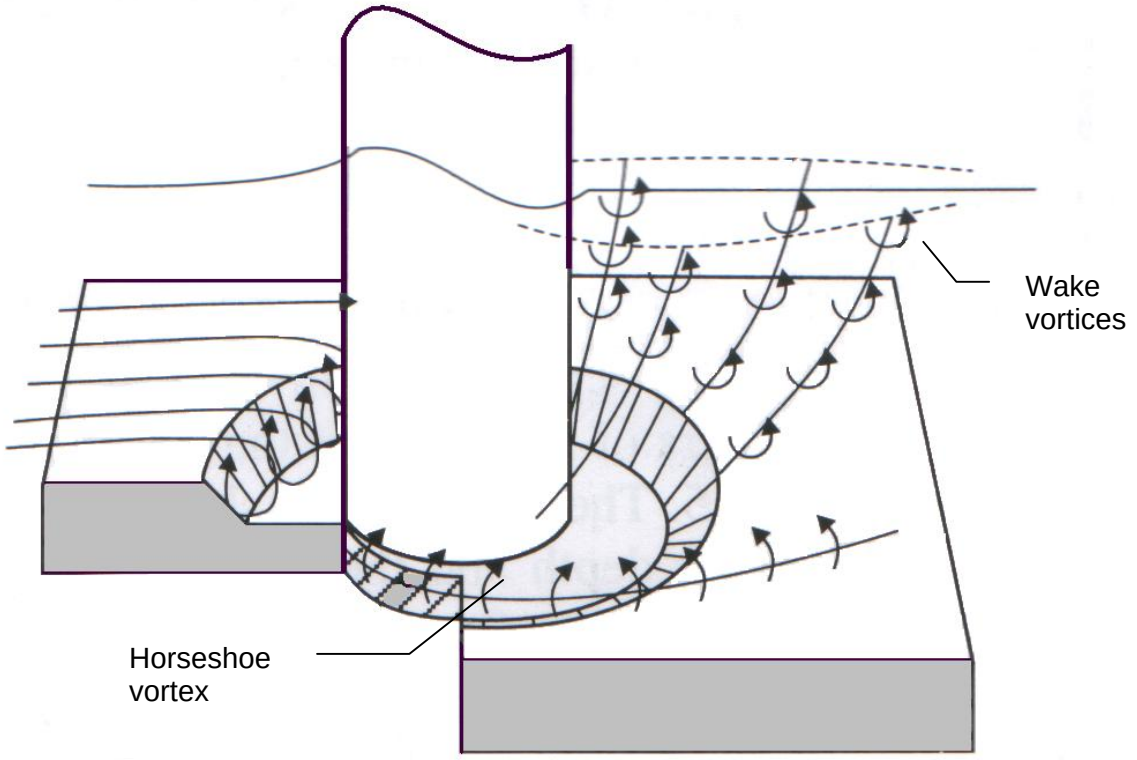

B.

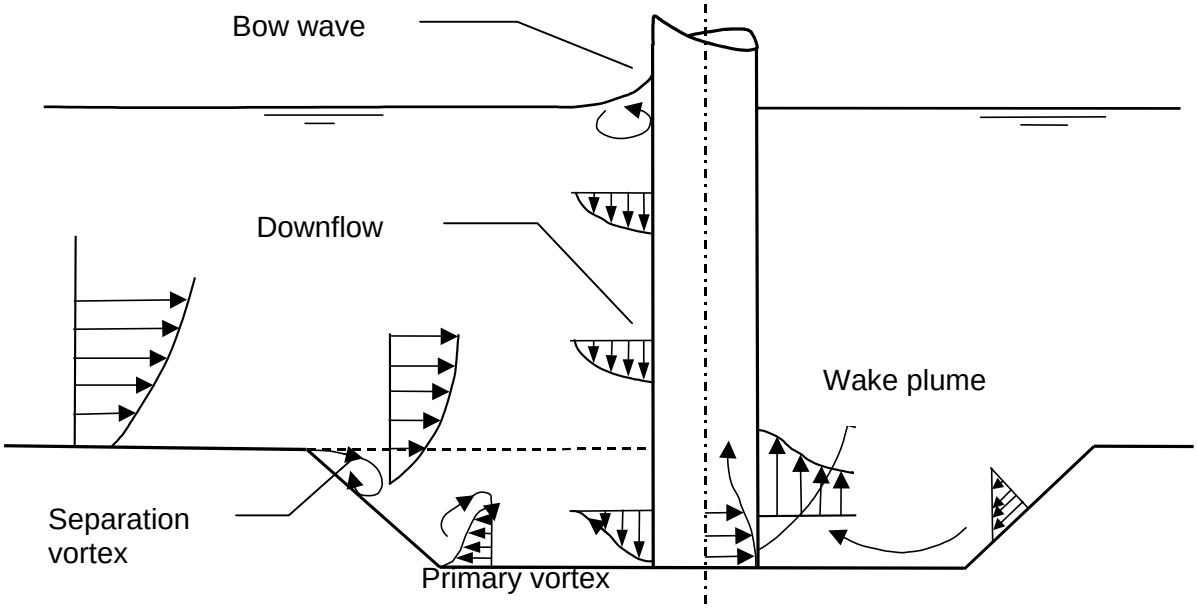

Flow pattern around a cylindrical pile
(after Herbich et al. 1984)

Figure A41

A.

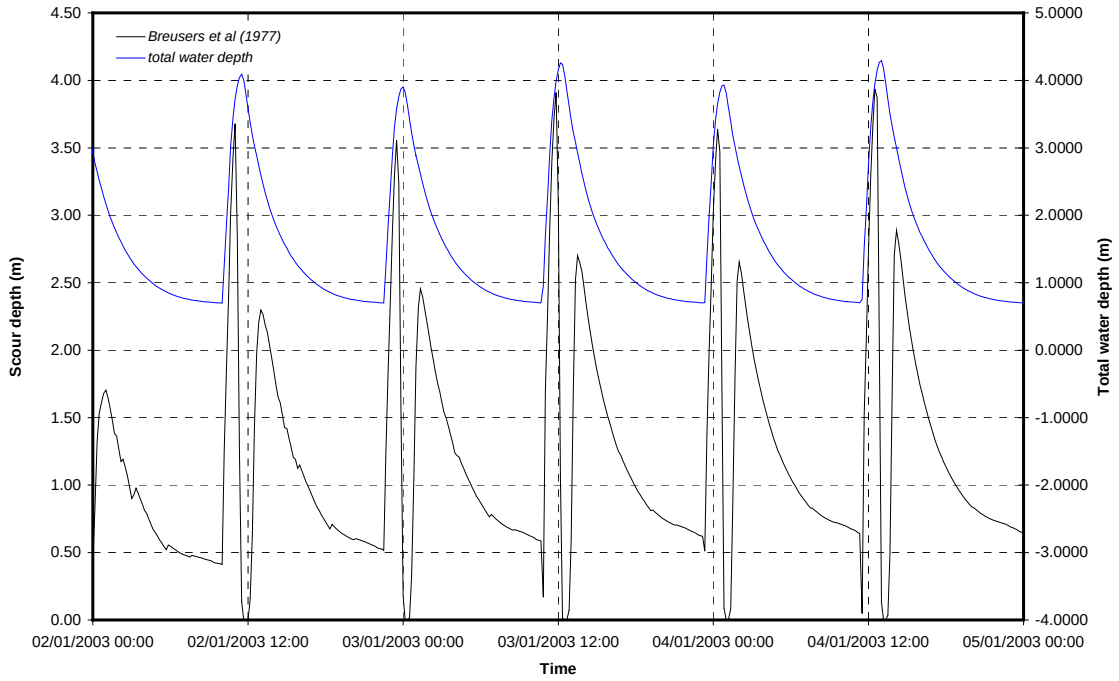

B.

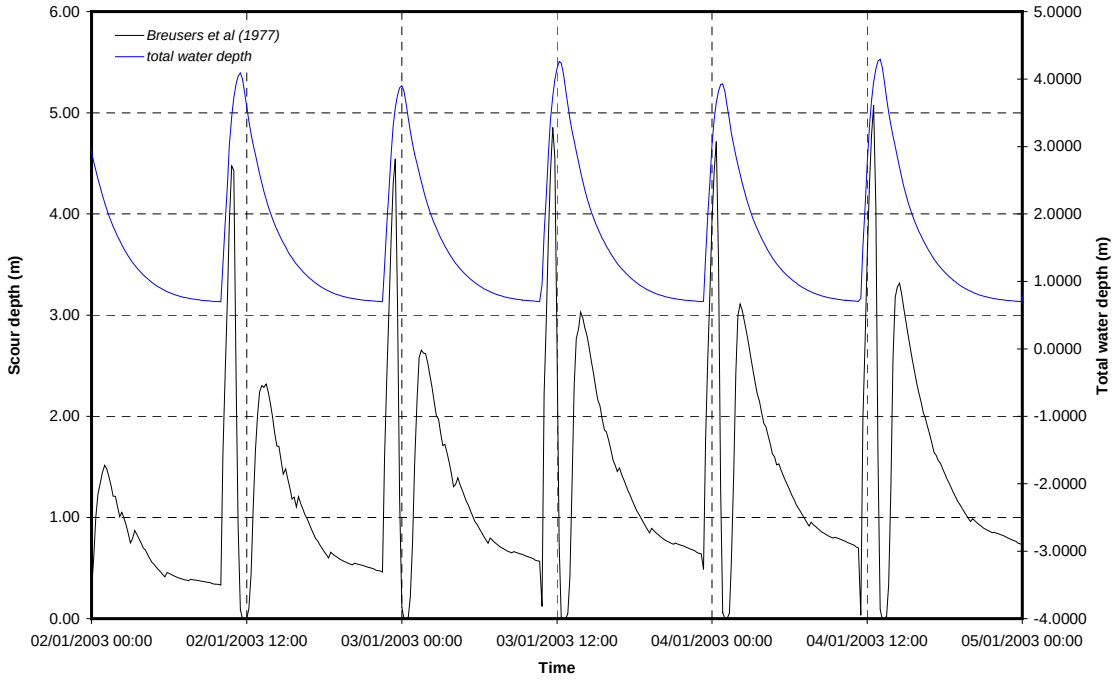

Predicted scour depth through time for a 30m diameter cofferdam (A) and a 60m square rock bund (B) over a spring tidal period. The equilibrium scour depth has been calculated using Breusers *et al*. (1977)

Figure A42

Appendix B

Morphological Modelling

Appendix B. Morphological Modelling

B1. Introduction

This appendix presents the results from the morphological numerical modelling undertaken to assess the impact of possible construction schemes with the preferred option as shown in drawing B4027/3/B/300 Rev. A.

- Route 3A preferred option (Drawing No. B4027/3/B/300 Rev. A):
  - Island construction scheme - Spring-neap cycle
  - Aligned jetty - Spring-neap cycle
  - Spike Island jetty - Spring-neap cycle
  - Aligned jetty - High fluvial (1:200 year event) and corresponding 1:200 year surge event
  - New bathymetry - aligned jetty spring-neap cycle
  - New bathymetry - aligned jetty High fluvial (1:200 year event) and corresponding 1:200 year surge event

As stated previously, the Route 3A preferred option has 3 main towers together with additional support piers for the bridge approaches. The bridge piers are octagonal (5m x 5m) and the towers are also octagonal (10m x 10m). As built the tower structures would all be located within the main body of the upper estuary whilst the pier groups would be located either on or above the intertidal area.

The morphological model uses a coarser grid resolution than the hydrodynamic model for the purpose of sensible run times. In the area of interest cell sizes are typically between 20m-30m. In the morphological simulations it was decided to adopt a conservative approach in that the 10m bridge towers were represented in the model by closing off a cell. Therefore, for the construction scenario with the cofferdams in place around the towers the closed off cell is the same as the operational case in the morphological model. However, the bridge piers and piles have been represented using added friction terms. In this manner there is an allowance for some flow transmission across the cell. It is accepted that this will lead to an over prediction in the impact of the scheme during the operational phase, but this was considered as a reasonable approach given the uncertainty in channel movement and position.

The morphological modelling of the Mersey Estuary has been undertaken using the predominant sediment type found across the study area (sand d50 = 150 um). The spatial results are presented as differences between the scheme and baseline conditions. The difference plots (Figures B1- B6) show changes in the thickness of sediment, and represent the change in actual thickness of sediment on the river bed. Positive values represent sediment deposition and negative values, sediment erosion. For each scenario two figures are presented at different scales to provide a greater overview of the scale of change. Figures labelled ‘A’ show ‘finer-scale’ changes within the limits $\pm$0.05m with a $\pm$0.01 cut-off. Figures labelled ‘B’

show the larger scale changes within the limits ±1.50m, but also have a ±0.01 cut-off so there is some level of correspondence with the finer-scale figures.

At each time-step the flow module calculates the change in the mass of bottom sediment that has occurred as a result of the sediment sink and source terms. This change in mass is then translated into a change in thickness of the bed sediment layer based on the density of the bed material. This change in thickness is equivalent to a change in bed elevation (i.e. erosion or deposition). The model is run for a spring-neap cycle with a morphological scale factor applied at each computational time-step, allowing the change in actual thickness of sediment on the river bed to be scaled to represent a 1-year simulation period (28 tides x 25 morphological scale factor). The period of investigation (spring-neap cycle) was selected based on high-water to high-water simulation where the high waters were equal in range, approximately.

B2. Island Construction Scheme

This section describes the morphological simulation undertaken for the Island construction scheme. The temporary island structure is rectangular in plan and surrounds the 30m diameter cofferdams. Further details are given in Section 2 of the main report.

Figure B1 shows the results of morphological change after one year for the island construction scheme. Changes (> 0.05m) are seen upstream of the proposed structures with an increase in sedimentation over the intertidal banks. There is a predicted increase in erosion adjacent to the island structures adjacent to the north and south channels (> 1.0m). The greatest extent of erosion occurs within the north channel. There is also some deposition predicted local to the temporary island structures.

In the vicinity of the Runcorn Gap and the existing bridge crossings there is a large area of erosion and deposition predicted to occur. The maximum rate of erosion in this area is predicted to be of the order of 1.2m, whilst along the northern side of the channel an area of deposition is predicted with a maximum value of 0.3m.

Within the main flood and ebb channels adjacent to the proposed crossing there is a slight change in sediment deposition along the margins of the order of ±0.02m.

B3. Aligned Jetty Construction Scheme

This section describes the morphological simulation undertaken for the aligned jetty construction scheme. The aligned jetty structure is in two sections, with one section extending from the southern bank and extending out to the southern most tower position and the second section extends from the northern bank out to the northern most and central tower positions. Each of the tower structures is surrounded by a 30m diameter cofferdam. Further details are given in Section 2 of the main report.

Figure B2 shows the results of morphological change after one year for the aligned jetty construction scheme. Erosion (≈ 1.4m) is predicted local to the north bank tower structure together with a corresponding area of accretion, (>0.05m) adjacent to the predicted erosion. The accretion round the northern most cofferdam extends over a larger area than that predicted for the erosion (3 - 4 times the area).

No change in bed elevation is predicted adjacent to the central cofferdam and the change in bed elevation in the vicinity of the southern most cofferdam is smaller in its extent and magnitude compared to the northern most structure. Local to the southern most cofferdam there is an area of erosion (<0.06m).

In general the increases in bed elevation (0.04m ±0.02m) upstream of the proposed bridge crossing are small. There are no significant changes are predicted downstream of the proposed bridge crossing.

B4. Jetty from Spike Island

This section describes the morphological simulation undertaken for the jetty construction scheme extending out from Spike Island. The temporary jetty structure is in one section, which extends from the Spike Island out to the northern most tower position and then across to the central tower and southern most tower positions. Each of the tower structures is surrounded by a 30m diameter cofferdam. Further details are given in Section 2 of the main report.

Figure B3 shows the results of morphological change after one year for the jetty from Spike Island. There is a predicted increase in erosion local to the cofferdam structures adjacent to the north and south channels (≈ 1.4m and 0.06m, respectively). The greatest extent of erosion occurs within the north channel and local to this area of erosion is a large area of accretion, (>0.05m) similar in extent to that predicted for the temporary jetty scheme.

There is no predicted change in bed elevation adjacent to the central cofferdam and changes in bed elevation (0.04m ±0.02m) upstream of the proposed bridge crossing are small. As for the temporary jetty construction scheme there are no significant changes predicted to occur downstream of the proposed bridge crossing.

B5. Aligned Jetty: Extreme Fluvial and Surge Event - 1:200 Return Period

This section describes the morphological simulation undertaken for the aligned jetty construction scheme simulated under extreme fluvial and surge events. The scenario applied corresponded to the extreme fluvial and surge event (with a 1:200 years return period) used previously and defined in Appendix B ABPmer (2004).

Figure B4 shows the results of the morphological model after a spring neap tidal cycle for the aligned jetty construction scheme. There is predicted accretion with an increase in bed elevation of 1.2m upstream and downstream of the north cofferdam. The extent of the accretion is limited to the immediate area around the cofferdam.

Figure B4 also shows clearly the large erosion local to the piers/cofferdams. The largest change in bed elevation (-1.8m) is adjacent to the cofferdam in the north channel and this is localised to the area around the cofferdam. More widespread erosion is predicted within the Widnes region and intermittently extending downstream up to but no further than Runcorn Gap. Upstream of the proposed crossing some erosion (≈ 1cm) is predicted along the margins of the main flood and ebb channels.

Considering the duration of the model simulation the changes in bed elevation are large relative to those predicted to occur in the normal spring-neap event. However, such extreme events are rare and would last only for a short period of time. These events are more likely the key drivers in any morphological response within the system.

B6. Aligned Jetty - New Bathymetry

This section describes the morphological simulation for the aligned jetty construction scheme. In early 2005 a limited survey of the estuary local to the proposed crossing was undertaken.

Figures B5 show the results of the morphological model after one year for the aligned jetty construction scheme. There is a predicted increase in erosion adjacent to the cofferdams within the north and south channels (≈ 1.3m and 1.4m, respectively). The largest area or erosion occurs forward and behind the southern cofferdam. Smaller areas of erosion are predicted adjacent to the north and central cofferdams. However, the spatial extent of this change is less than that predicted for the southern cofferdam.

An increase of (0.4m ±0.2m) in bed elevation is predicted along the margins of the south channel. This extends from Reed Island up to the proposed crossing site. The extent of change is slightly greater than predicted using the 2002 bathymetry (Figure B5). However, the change in bed elevation is not significantly different. An increase of 0.1m is predicted downstream of the central cofferdam. No difference in bed elevation is predicted downstream of the immediate areas of the proposed bridge crossing

Overall the estuary shows a similar morphological response in terms of predicted differences in bed elevation and the spatial extent of change, compared to the 2002 bathymetry simulation.

B7. Aligned Jetty - New Bathymetry: Extreme Fluvial and Surge Event - 1:200 Return Period

This section describes the morphological simulation undertaken for the aligned jetty construction scheme simulated under extreme fluvial and surge events.

Figure B6 shows the results of the morphological model after a spring-neap cycle for the aligned jetty modelled using the 2005 bathymetric dataset under an 'extreme' water level and discharge scenario. The results indicate an increase in bed elevation of 0.6m adjacent to the north channel cofferdam. A maximum reduction in bed elevation is also predicted adjacent the upstream face of the north channel cofferdam. The extent of the predicted areas of erosion is generally limited to the north and south cofferdams (Figure B6). Some accretion 0.1m ±0.05m is predicted along the margins of the main channel upstream of the proposed bridge crossing.

No difference in bed elevation is predicted outside the area of the proposed bridge crossing. Overall in comparison to the 2002 bathymetry extreme fluvial and surge simulation (Section B5), the estuary shows an almost identical morphological response in terms of predicted differences in bed elevation and spatial extent of change.

B8. Cross-Section Analysis - All Schemes (Spring-Neap Cycle)

Figure B7 shows the positions of the various cross-sections taken across the upper estuary. Whilst it has been attempted to locate these as close as possible to the position of the cross-section positions used in the Phase 1 modelling study, the change in the model grid has meant that this is not always practical. This difference in position is to allow for the greatest change in channel depth to be picked up in the particular cross-section.

Figure B8 shows the cross-sections at A and B. There is no discernible change in bed level between the baseline case and the 3 construction schemes at either cross-section.

Figure B9 shows the bed level changes for cross-sections C and D. At cross section C the aligned jetty scheme and the jetty from Spike Island scheme result in no noticeable difference in bed elevation. However, for the Island construction scheme erosion is predicted to occur across the intertidal bank in the central part of the channel (maximum erosion ≈ 0.3m). In addition, there is some accretion on the margin of the north channel (maximum accretion ≈ 0.14m). At cross-section D there is no perceptible change in bed elevation for the various construction schemes.

Figure B10 shows the bed level changes at cross-sections E and F. At cross-section E for the temporary island scenario there is some accretion predicted within the south channel (maximum ≈ 0.04m) and within the north channel some erosion on the upper slope of the channel side (≈ 0.06m) together with an area of accretion (≈ max 0.07m). For the two temporary jetty schemes the only perceptible change occurs within the north channel (accretion

≈ 0.02m) and some minor erosion (≈ 0.01m). At cross-section F the greatest changes are predicted to occur in the north channel. The two temporary jetty schemes show the greatest change with erosion within the channel of up to 1.4m. This cross-section is close to the temporary cofferdam. There is also some accretion predicted along the margins of the north channel with a maximum change of 0.3m, approximately. For the temporary island construction scheme there is some accretion of sediment along the margins of the north channel of the order of 0.35m -0.5m, approximately.

Figure B11 shows the cross-sections G and H. At cross-section G there is no perceptible change in the bed level in the southern channel for the two temporary jetty construction schemes and the baseline case. The modelling results for the temporary island construction scheme show some erosion on the shoulder of the south channel (maximum ≈ 0.05m). Within the north channel the island construction scheme shows both erosion of sediment (maximum ≈ 0.3m) and accretion (maximum ≈ 0.14m), whilst the two temporary jetty schemes show only accretion with a maximum reduction of 0.06m, approximately. In cross-section H the greatest changes are predicted to occur in the south channel. For the aligned jetty and the jetty from Spike Island construction schemes there is a reduction in bed elevation (≈ 0.3m) predicted to occur on the shoulder of the southern bank together with some accretion (max ≈ 0.09m). For the Island construction scheme there is accretion predicted to occur at the same location with a maximum rate of change of 0.08m - 0.11m, approximately. Within the north channel there is a small area of accretion in all three construction scenarios with a maximum increase in bed elevation for the island construction scheme and the two jetty construction schemes of 0.07m and 0.03m, respectively.

Figure B12 shows the cross-sections I and J. At cross-section I the modelling predicts a general pattern of accretion over much of the cross-section for all three of the construction schemes. For the island construction scheme there is a maximum increase in bed elevation of 0.05m - 0.17m. For the two temporary jetty construction schemes the maximum rate of accretion over the banks and channels is 0.01m - 0.07m, approximately. At cross-section J there is some slight erosion and accretion within the south channel in the temporary island construction scheme (maximum erosion ≈ 0.03m) and for the two jetty schemes (maximum erosion ≈ 0.01m). Within the north channel there are both areas of erosion and accretion for all three construction schemes. However, for the temporary island scheme the modelling suggests that there is some migration of the channel towards the north bank with maximum accretion of between 0.07m - 0.1m, approximately and maximum erosion of about 0.09m. For the two jetty schemes the maximum rate of erosion in the north channel is about 0.03m with maximum rates of accretion between 0.03m - 0.04m.

Table B1. Summary of cross-sectional bed level changes for the various construction schemes. Description of changes compared against the existing 'baseline' condition

Cross-Section	Preferred Option - Construction Scenarios		
	Temporary Island Scheme	Spike Island Jetty	Aligned Jetty
A	No Change	No Change	No Change
B	No Change	No Change	No Change
C	Erosion over intertidal bank (max ≈ 0.3m) and some accretion on margin of north channel (max ≈ 0.14m)	No Change	No Change
D	No Change	No Change	No Change
E	Slight accretion in south channel (max ≈ 0.04m) and some erosion (max ≈ 0.06m) and accretion (max ≈ 0.07m) within the north channel	Slight accretion (max ≈ 0.02m) and erosion (max ≈ 0.01m) in north channel	Slight accretion (max ≈ 0.02m) and erosion (max ≈ 0.01m) in north channel
F	Sedimentation along margins of north channel margin (max ≈ 0.35m -0.5m)	Erosion within north channel (max ≈ 1.4m) and some accretion along channel margin (max ≈ 0.3m)	Erosion within north channel (max ≈ 1.4m) and some accretion along channel margin (max ≈ 0.3m)
G	Slight erosion on shoulder of south channel (max ≈ 0.05m). In the north channel there is erosion (max ≈ 0.3m) and accretion (max ≈ 0.14m) predicted	Slight accretion in north channel (max ≈ 0.06m)	Slight accretion in north channel (max ≈ 0.06m)
H	Accretion (max ≈ 0.11m) at the shoulder of the south channel. Small area of accretion in north channel (max ≈ 0.07m)	Both erosion (max ≈ 0.3m) and accretion (max ≈ 0.09m) on shoulder of the south channel. Small area of accretion in north channel (max ≈ 0.03m)	Both erosion (max ≈ 0.3m) and accretion (max ≈ 0.09m) on shoulder of the south channel. Small area of accretion in north channel (max ≈ 0.03m)
I	General accretion over cross-section (max ≈ 0.17m)	General accretion over cross-section (max ≈ 0.07m)	General accretion over cross-section (max ≈ 0.07m)
J	Accretion and erosion in southern channel (max ≈ 0.03m). Migration of northern channel towards north bank with accretion (max ≈ 0.1m) and erosion (max ≈ 0.08m)	Accretion and erosion in southern channel (max ≈ 0.01m). Within the north channel modelling predicts both areas of erosion (max ≈ 0.03m) and accretion (max ≈ 0.04m)	Accretion and erosion in southern channel (max ≈ 0.01m). Within the north channel modelling predicts both areas of erosion (max ≈ 0.03m) and accretion (max ≈ 0.04m)
K	Some accretion in south channel (max ≈ 0.08m). Also accretion predicted in the north channel (max ≈ 0.06m)	Slight accretion in southern channel (max ≈ 0.01m). In addition some accretion in north channel (max ≈ 0.03m)	Slight accretion in southern channel (max ≈ 0.01m). In addition some accretion in north channel (max ≈ 0.03m)
L	Slight accretion in north channel (≈ 0.03m) and minor erosion on banks between north and south channels	Slight accretion in north channel (max ≈ 0.01m)	Slight accretion in north channel (max ≈ 0.01m)

Figure B13 shows the bed elevation for cross-sections K and L. For cross-section K all schemes show some accretion in both the south and north channels and again, the Island scheme shows the largest change. Within the southern channel the maximum increase in bed elevation for the island construction scheme and the two jetty construction schemes is 0.08m and 0.01m, respectively, whilst in the north channel this reduces to 0.06m and 0.03m, respectively. For all construction schemes there are no significant changes in bed elevation in cross-section L. For the island construction scheme there is some slight accretion in the north channel ($\approx$ 0.03m) and minor erosion on the banks between the north and south channels. For the two temporary jetty schemes there is slight accretion in the north channel (max $\approx$ 0.01m).

B9. Cross-Section Analysis - Aligned Jetty: Extreme Fluvial and Surge Event - 1:200 Return Period

As previously, Figure B7 shows the positions of the various cross-sections taken across the upper estuary.

Figure B14 shows the cross-sections at A and B. There is no discernible change in bed level between the baseline case and the construction scheme at these cross-sections.

Figure B15 shows the bed level changes for cross-sections C and D. At cross-section C there is some slight reduction in bed elevation across the central portion of the intertidal bank, with a maximum predicted change of 0.04m. Towards the edge of the bank there is some minor accretion (maximum change 0.02m). At cross-section D there is no perceptible change in bed elevation.

Figure B16 shows the bed level changes for cross-sections E and F. At cross-section E there is some minor erosion predicted to occur within the south channel (max = 0.03m). However, the greatest change is predicted to occur in the north channel with the model showing both accretion and erosion within the lower section of the channel (max accretion = 0.09m; max erosion = 0.24m). At cross-section F changes in the south channel are insignificant (max change = $\pm$0.01m). Within the north channel there is situated adjacent the north channel cofferdam the modelling exercise predicts a change in bed elevation of $\approx$ 0.5m and $\approx$ -1.5m. No change in sedimentation is predicted within the region of the south channel for this cross section.

The changes in bed level for cross-section G and H are shown in Figure B17. At cross-section G there is some slight erosion in the south channel (max = 0.06m) and deposition on the lower slope of the channel adjacent the intertidal bank (max = 0.32m). In the north channel there is some movement in channel position, with erosion (max = 0.48m) predicted along the side of the intertidal bank and deposition within the central part of the channel (max = 0.54m).

At cross-section H there is some erosion and deposition within the south channel with slight deepening of the channel along the shoreline (max = 0.11m) and accretion along the lower

slopes of the channel (max = 0.10m). Over the shoulder of the intertidal bank the modelling predicts a small area of deposition (max = 0.07m) and erosion (max =0.05m). In the north channel there is some erosion (max = 0.08m) and accretion (max = 0.03m) predicted.

Figure B18 shows the changes in bed level at cross-section I and J. Changes in bed level over cross-section I are small with maximum differences in deposition and erosion of ±0.03m. The largest changes are predicted to occur within the north channel. A similar level of change is predicted for cross-section J with minor erosion (max = 0.03m) and deposition (max = 0.02m) in both the south and north channels.

Figure B19 shows the change in bed level at cross-sections K and L. At cross-section K there is minor deposition predicted in the south channel (max = 0.03m) and over the intertidal bank (max = 0.02m). There are also some small areas of erosion over the banks (max = 0.02m). At cross-section L there is some slight accretion (max = 0.02m) and erosion (max = 0.03m) within the south channel. There is also erosion (max = 0.03m) and deposition (max = 0.02m) predicted within the north channel towards the intertidal bank.

Table B2. Summary of cross-sectional bed level changes for the Aligned Jetty: extreme fluvial and surge event - 1:200 return period. Description of changes compared against a comparable 'baseline' condition

Cross-Section	Preferred Option - Extreme Fluvial and Surge Event Scenario Aligned Jetty
A	No Change
B	No Change
C	Erosion over intertidal bank (max ≈ 0.04m) and some accretion on margin bank (max ≈ 0.02m)
D	No Change
E	Slight erosion in south channel (max ≈ 0.03m) and some erosion (max ≈ 0.24m) and accretion (max ≈ 0.09m) within the north channel
F	Within the north channel modelling predicts both areas of erosion (max ≈ 1. 8m) and accretion (max ≈ 0.9m). No significant change in bed elevation is predicted in the south channel.
G	There is some slight erosion in the south channel (max = 0.06m) and deposition on the lower slope of the channel adjacent the intertidal bank (max = 0.32m). within the north channel there is erosion (max = 0.48m) predicted along the side of the intertidal bank and deposition within the central part of the channel (max = 0.54m).
H	In the south channel there is a slight deepening of the channel along the shoreline (max = 0.11m) and accretion along the lower slopes of the channel (max = 0.10m). Some deposition (max = 0.07m) and erosion (max =0.05m) on shoulder of intertidal bank. In the north channel there is some erosion (max = 0.08m) and accretion (max = 0.03m) predicted.
I	Changes in bed level over cross-section are small with maximum differences in deposition and erosion of ±0.03m.
J	Changes in bed level over cross-section are small with maximum differences in deposition (max = 0.02m) and erosion of (max = 0.03m).
K	There is minor deposition predicted in the south channel (max = 0.03m) and over the intertidal bank (max = 0.02m). There are also some small areas of erosion over the banks (max = 0.02m).
L	There is some slight accretion (max = 0.02m) and erosion (max = 0.03m) within the south channel. There is also erosion (max = 0.03m) and deposition (max = 0.02m) predicted within the north channel towards the intertidal bank.

B10. Cross-Section Analysis - Aligned Jetty: New Bathymetry

As previously, Figure B7 shows the positions of the various cross-sections taken across the upper estuary.

Figure B20 shows the cross-sections at positions A and B. There is no discernible change in bed elevation between the baseline case and the construction scheme for each cross-section.

Figure B21 shows the bed level changes for cross-sections C and D. At cross-section C there is some minor deposition (max = 0.01m) and erosion (max = 0.01m) predicted over the intertidal bank and some slight erosion (max = 0.01m) within the north channel. At cross-section D there is no discernible change in bed elevation between the baseline case and the aligned jetty.

Figure B22 shows the changes in bed level for cross-sections E and F. At cross-section E there is no discernible change within the south channel. Towards the north channel there is some erosion over the intertidal bank (max = 0.01m). In the north channel deposition (max = 0.05m) is predicted.

At cross-section F there are small changes in bed level within the south channel (max deposition = 0.02m; max erosion = 0.02m) with some slight deepening of the channel and some erosion and deposition over the lower slopes of the channel, adjacent to the central intertidal bank. The greatest changes are predicted to occur within the north channel, with erosion (max = 1.01m) leading to a deepening of the channel and deposition (max = 0.35m) along the side of the channel. These large changes are due to the cross-section being close to the cofferdam/pier structure within the north channel.

Figure B23 shows the cross-sections at G and H and the corresponding bed level changes. At cross-section G there the model predicts both erosion and deposition in the south channel. Towards the shoreline there is some minor deepening of the channel (max = 0.03m) and towards the intertidal bank there is accretion (max = 0.02m). Along the flank of the bank there is some erosion (max = 0.06m), whilst over the top of the bank there is a change in profile with both erosion (max = 0.36m) and deposition (max = 0.21m) occurring. Within the north channel there is accretion occurring along the sides of the channel (max = 0.11m).

At cross-section H there is a change in profile within the south channel and along the flank of the intertidal bank. Towards the shoreline there is some deepening of the channel (max = 0.06m). Along the flank of the bank a small channel is formed (max erosion = 1.4m) and deposition along the shoulder of the bank (max = 0.6m). Within the north channel there is some erosion along the sides of the channel (max = 0.04m).

Figure B24 shows the cross-sections I to J. For cross-section I the modelling shows movement of the south channel profile with mostly deposition within the deep channel (max = 0.18m). Along the flanks of the intertidal bank there is erosion on the slopes forming a shallow channel

(max = 0.26m) then above this is an area of deposition (max =0.2m). Within the north channel the predicted changes are insignificant. At cross-section J the predicted changes are also confined the south channel. Within the deepest section of the channel there is deposition occurring (max = 0.3m). Then along the flank of the intertidal bank there is some erosion (max = 0.04m) and above this an area of accretion (max = 0.15m). Within the north channel the predicted changes are insignificant.

Table B3. Summary of cross-sectional bed level changes for the Aligned Jetty - 2005 bathymetry. Description of changes compared against a comparable 'baseline' condition

Cross-Section	Preferred Option - 2005 Bathymetry
	Aligned Jetty
A	No Change
B	No Change
C	Minor deposition (max = 0.01m) and erosion (max = 0.01m) predicted over the intertidal bank and some slight erosion (max = 0.01m) within the north channel.
D	No Change
E	Some erosion over the intertidal bank (max = 0.01m). Some deposition (max = 0.05m) in the north channel.
F	Small changes in south channel (max deposition = 0.02m; max erosion = 0.02m) with some slight deepening of the channel and some erosion and deposition over the lower slopes of the channel, adjacent to the central intertidal bank. Within the north channel there is erosion (max = 1.01m) and deposition (max = 0.35m).
G	In the south channel deepening of the channel (max = 0.03m) and accretion (max = 0.02m) on bank side. Along the flank of the bank there is some erosion (max = 0.06m). Over top of the bank there is a change in profile with erosion (max = 0.36m) and deposition (max = 0.21m) occurring. Within the north channel there is accretion occurring along the sides of the channel (max = 0.11m).
H	In south channel towards the shoreline there is deepening of the channel (max = 0.06m). Along the flank of the bank a small channel is formed (max erosion = 1.4m) and deposition along the shoulder of the bank (max = 0.6m). In the north channel there is some erosion along the sides of the channel (max = 0.04m).
I	Movement of the south channel profile deposition within the deep channel (max = 0.18m). Along the flanks of bank there is erosion on the slopes forming a shallow channel (max = 0.26m) then above this is an area of deposition (max =0.2m).
J	Deposition occurring in south channel (max = 0.3m). Along the flank of the intertidal bank there is some erosion (max = 0.04m) and above this an area of accretion (max = 0.15m).
K	In south channel there is accretion within the deepest section (max = 0.1m) and on the upper shoulder of the intertidal bank (max = 0.15m).
L	In south channel accretion close to the shoreline (max = 0.2m). Also, accretion over the side of the bank (max = 0.07m).

Figure B25 shows the cross-sections at K and L and the corresponding bed level changes. At section K the changes in bed level are confined to the south channel with accretion within the deepest section (max = 0.1m) and on the upper shoulder of the intertidal bank (max = 0.15m). Within the north channel any predicted changes are insignificant. At cross-section L, again the changes are confined to the south side of the channel with accretion close to the shoreline (max = 0.2m). The intertidal bank is much lower in profile at this section. The model shows

accretion over the side of the bank (max = 0.07m) whilst within the north channel there is no significant change.

B11. Cross-Section Analysis - Aligned Jetty: New Bathymetry: Extreme Fluvial and Surge Event - 1:200 Return Period

As previously, Figure B7 shows the positions of the various cross-sections taken across the upper estuary.

Figure B26 shows the cross-sections at positions A to B. There is no significant change in bed elevation between the baseline case and the aligned jetty under the extreme event for these sections.

Figure B27 shows the cross-sections at positions C to D. At cross-section C there is erosion and deposition predicted over the flanks and the top of the intertidal bank (max deposition = 0.05m; max erosion = 0.02m). Within the north channel there is erosion predicted in the deepest section (max = 0.02m). At cross-section D there is some minor erosion in the north channel (max = 0.02m).

Figure B28 shows the cross-sections at positions E to F. At cross-section E there is some erosion over the top of the intertidal bank (max = 0.02m) and some minor deposition (max = 0.04m) and erosion (max = 0.02m) within the north channel. At cross-section F the modelling predicts some movement in the profile of the south channel with a deepening of the channel towards the intertidal bank (max = 0.1m) and deposition (max 0.15m) and some erosion (max = 0.04m) along the lower flanks of the bank. The greatest changes occur in the north channel with a deepening of the channel (max = 1.2m) and deposition along the slopes of the channel (max = 0.7m).

Figure B29 shows the cross-sections at positions G to H and the corresponding bed level changes. At cross-section G there is change in the profile of the lower section of the south channel with some deepening of the channel (max = 0.2m) and deposition towards the intertidal bank (max = 0.25m). Over the top of the bank there is some minor erosion (max = 0.02m). Within the north channel there is erosion predicted (max = 0.04m) in the deep section and some deposition on the lower slopes of the channel (max = 0.01m).

Cross-section H also shows a similar pattern of change with movement in the profile of the south channel. There is deepening of the channel (max = 0.08m) an some deposition on the lower slope on the inshore side (max = 0.01m). On the flanks of the bank a shallow channel is forming (max erosion = 0.16m) with deposition either side (max = 0.37m). Within the north channel there is a reduction in the channel depth (max erosion = 0.04m) and some deposition on the lower slopes of the channel (max = 0.01m).

Table B4. Summary of cross-sectional bed level changes for the Aligned Jetty - 2005 bathymetry: extreme fluvial and surge event. Description of changes compared against a comparable 'baseline' condition

Cross-Section	Preferred Option - 2005 Bathymetry - Extreme Fluvial and Surge Event Scenario
	Aligned Jetty
A	No Change
B	No Change
C	Erosion and deposition predicted over the flanks and the top of the intertidal bank (max deposition = 0.05m; max erosion = 0.02m). Within the north channel there is erosion predicted in the deepest section (max = 0.02m).
D	Some minor erosion in the north channel (max = 0.02m).
E	Erosion over the top of the intertidal bank (max = 0.02m) and minor deposition (max = 0.04m) and erosion (max = 0.02m) within the north channel.
F	In the south channel a deepening of the channel towards the intertidal bank (max = 0.1m) and deposition (max 0.15m) and some erosion (max = 0.04m) along the lower flanks of the bank. In the north channel there is a deepening of the channel (max = 1.2m) and deposition along the slopes of the channel (max = 0.7m).
G	In the south channel there is deepening of the channel (max = 0.2m) and deposition towards the intertidal bank (max = 0.25m). Over the top of the bank there is some minor erosion (max = 0.02m). In the north channel there is erosion (max = 0.04m) in the deep section and deposition on the lower slopes of the channel (max = 0.01m).
H	Deepening of the south channel (max = 0.08m) and some deposition on the lower slope on the inshore side (max = 0.01m). On the flanks of the bank a shallow channel is forming (max erosion = 0.16m) with deposition either side (max = 0.37m). In the north channel there is a reduction in the channel depth (max erosion = 0.04m) and some deposition on the lower slopes of the channel (max = 0.01m).
I	Within the centre of the south channel is an area of deposition (max = 0.45m). On the lower flank of the intertidal bank is an area of erosion (max = 0.12m). Across the remaining part of the section differences in bed level are small (max erosion = 0.02m; max deposition = 0.01m).
J	Accretion within the south channel (max = 0.06m). Over the remaining part of the cross-section the changes are small (max erosion = 0.01m; max deposition = 0.03m).
K	Some erosion and deposition predicted in the north channel (max = $\pm$0.03m)
L	Some minor deposition (max = 0.02m) and erosion (max = 0.04m) in the south channel.

Figure B30 shows the cross-sections at positions I to J. At cross-section I there is still some adjustment occurring in the profile of the south channel. Within the centre of the deepest section is an area of deposition (max = 0.45m). On the lower flank of the intertidal bank is an area of erosion (max = 0.12m). Across the remaining part of the section differences in bed level are small (max erosion = 0.02m; max deposition = 0.01m). At cross-section J there is some accretion within the south channel (max = 0.06m). Over the remaining part of the cross-section the changes are small (max erosion = 0.01m; max deposition = 0.03m).

Figure B31 shows the cross-sections at K and L and the corresponding bed level changes. For cross-section K the modelling shows minor changes across the profile. There is some erosion and deposition predicted in the north channel (max = $\pm$0.03m). At cross-section L there is some minor deposition (max = 0.02m) and erosion (max = 0.04m) in the south channel. Elsewhere across the profile changes are not significant.

Appendix B
Figures

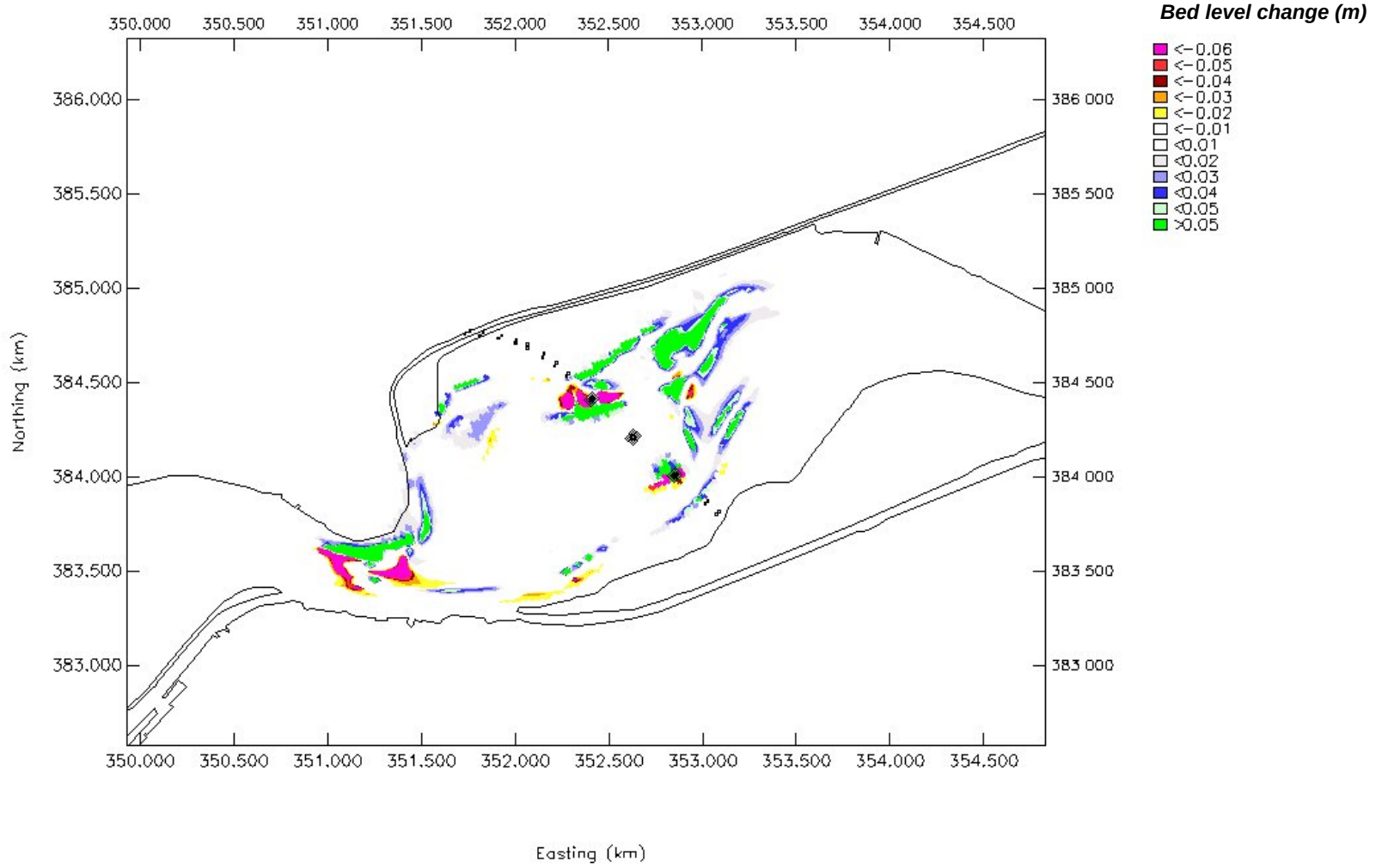

ABP mer marine environmental research	Morphological change (m) after a 1 year run. Island Construction Option	Figure B1a

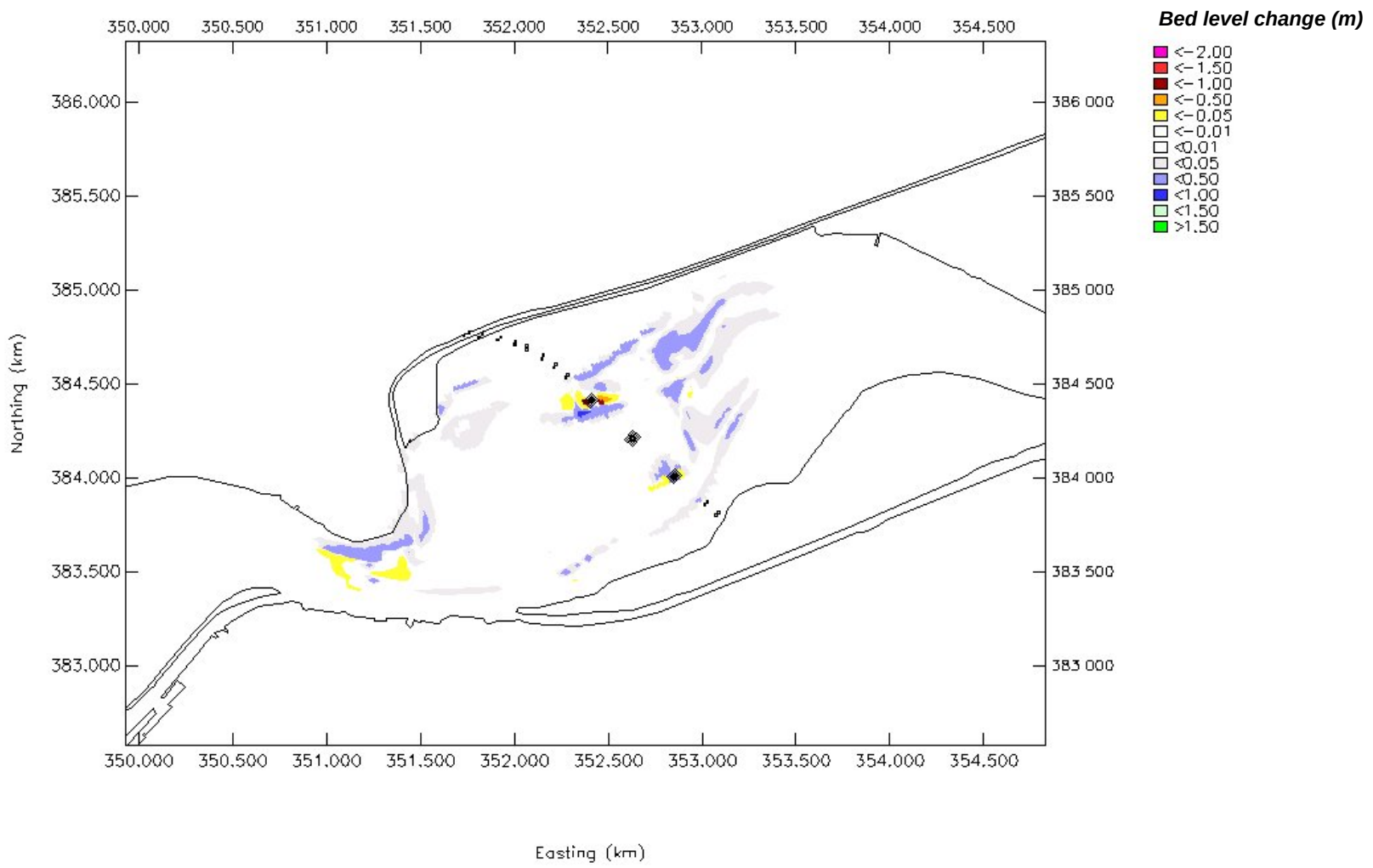

ABP mer marine environmental research	Morphological change (m) after a 1 year run. Island Construction Option	Figure B1b

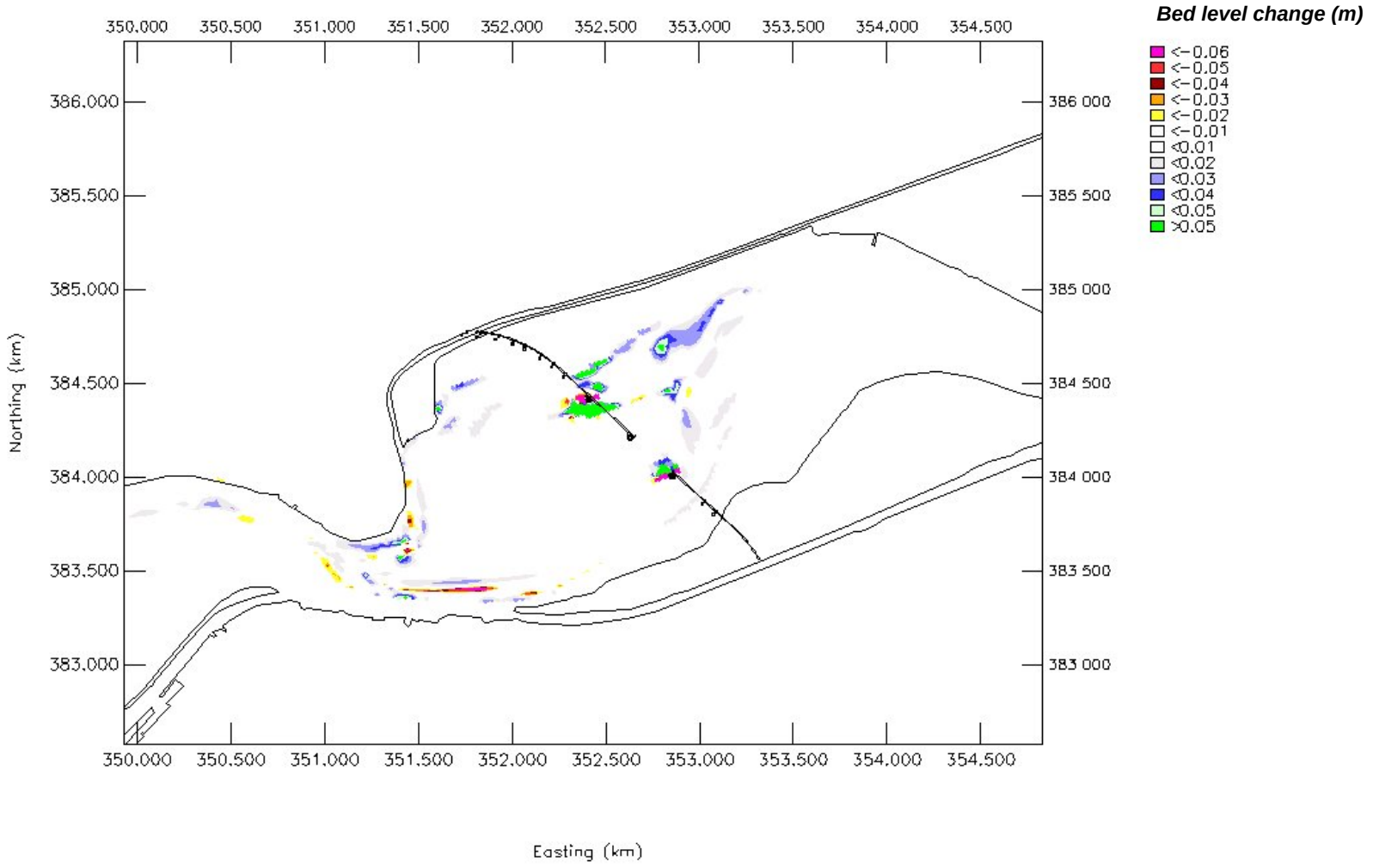

ABP mer marine environmental research	Morphological change (m) after a 1 year run. Aligned Jetty Construction Option	Figure B2a

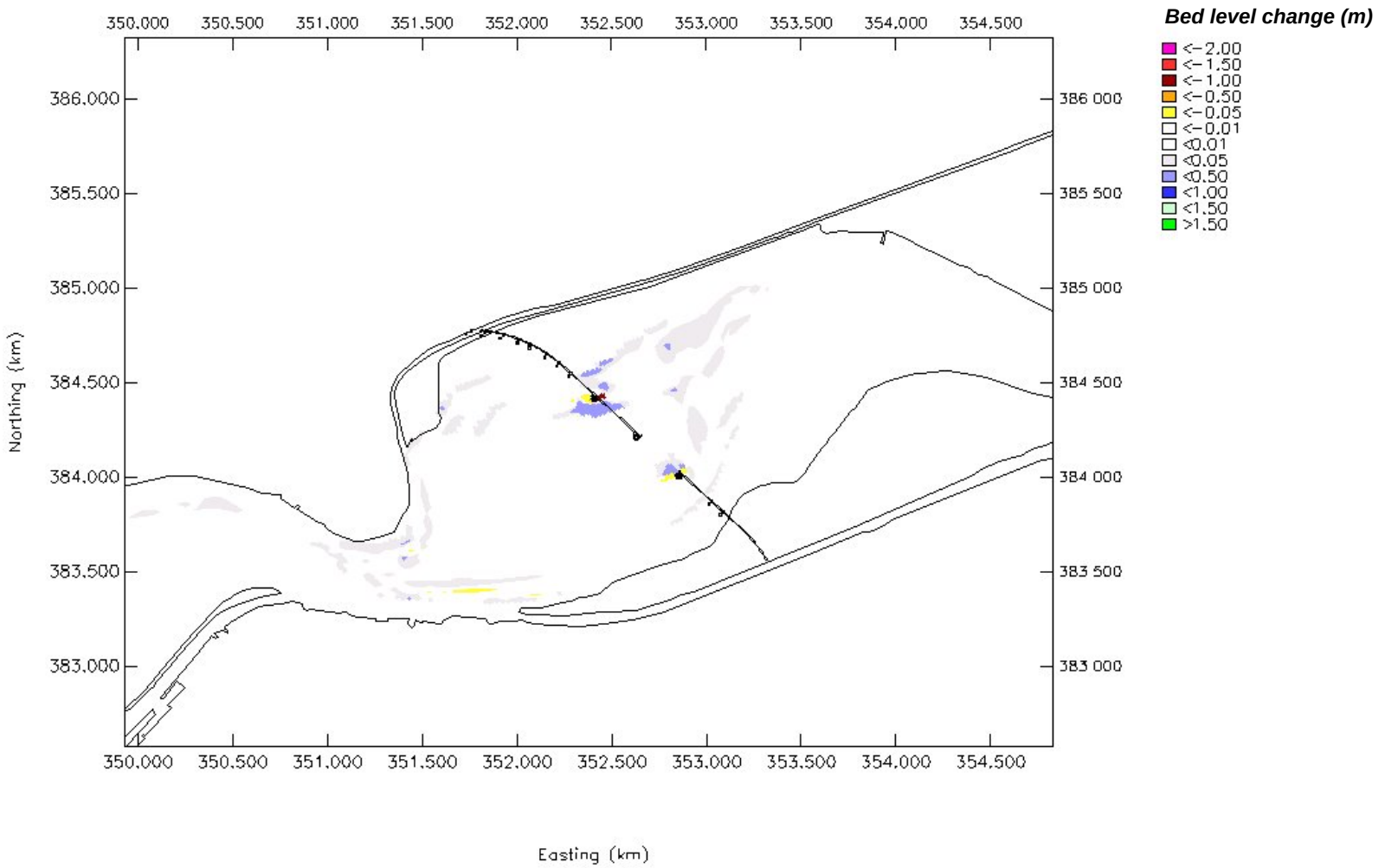

ABP mer marine environmental research	Morphological change (m) after a 1 year run. Aligned Jetty Construction Option	Figure B2b

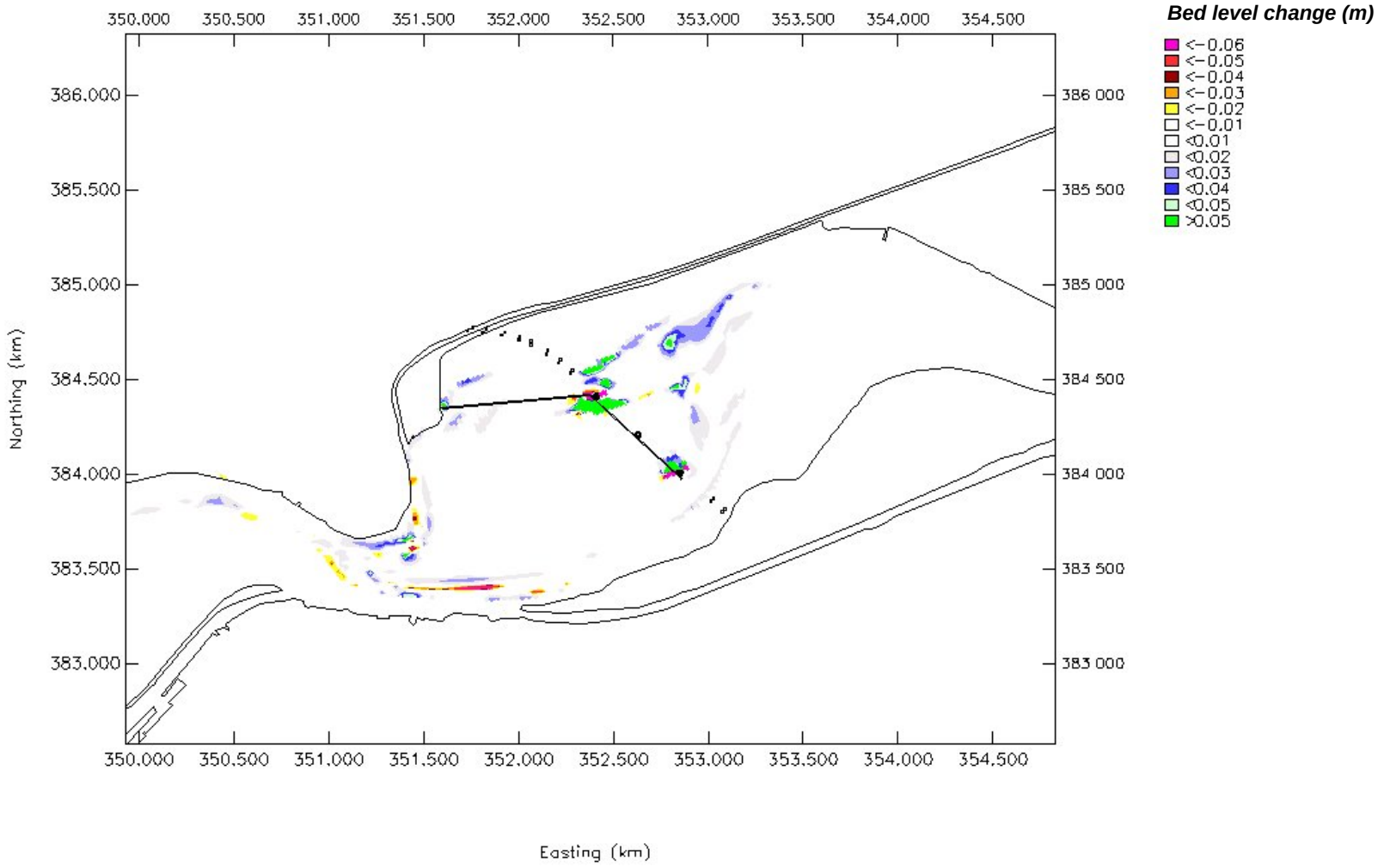

ABP mer marine environmental research	Morphological change (m) after a 1 year run. Spike Island Jetty Construction Option	Figure B3a

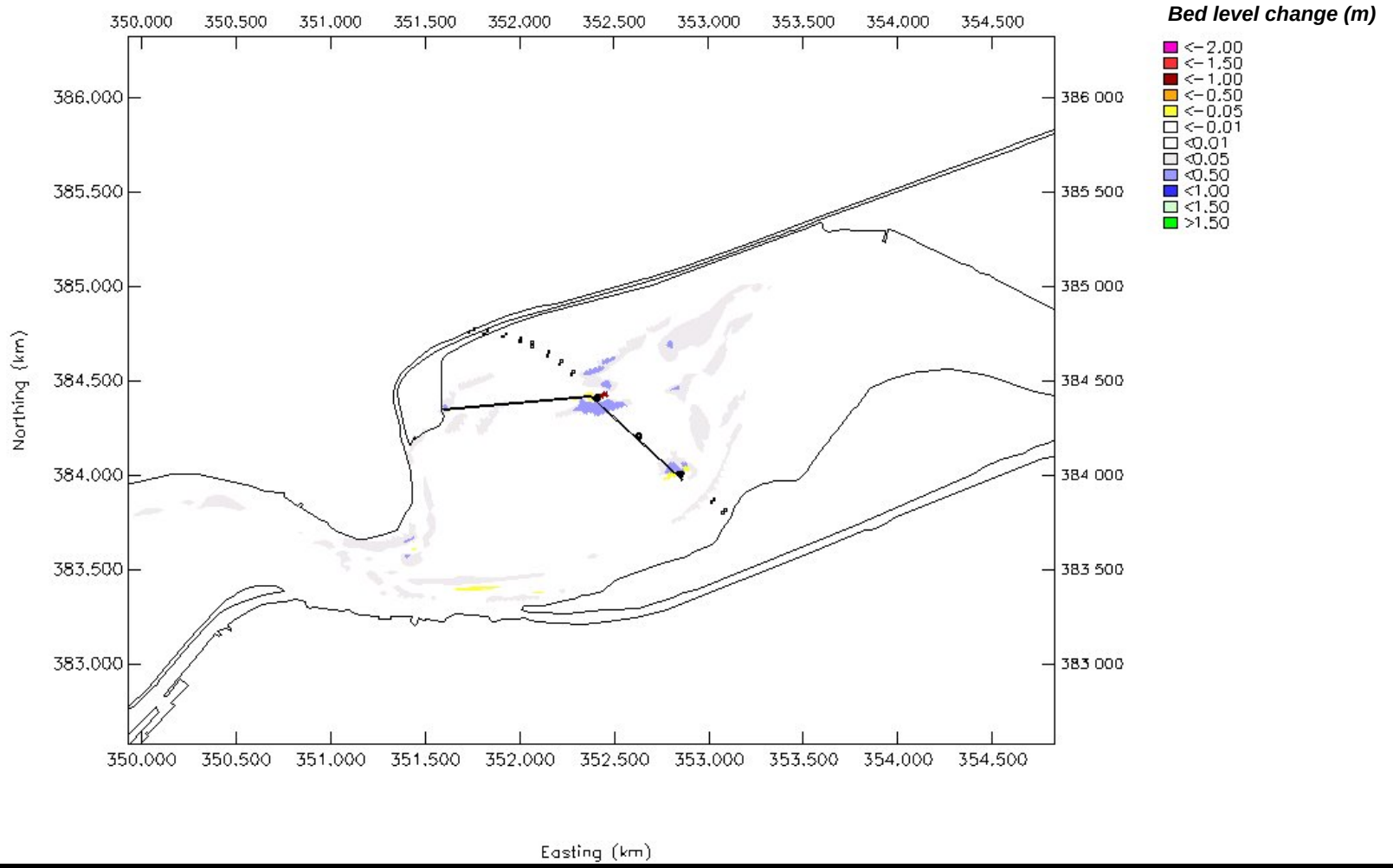

ABP mer marine environmental research	Morphological change (m) after a 1 year run. Spike Island Jetty Construction Option	Figure B3b

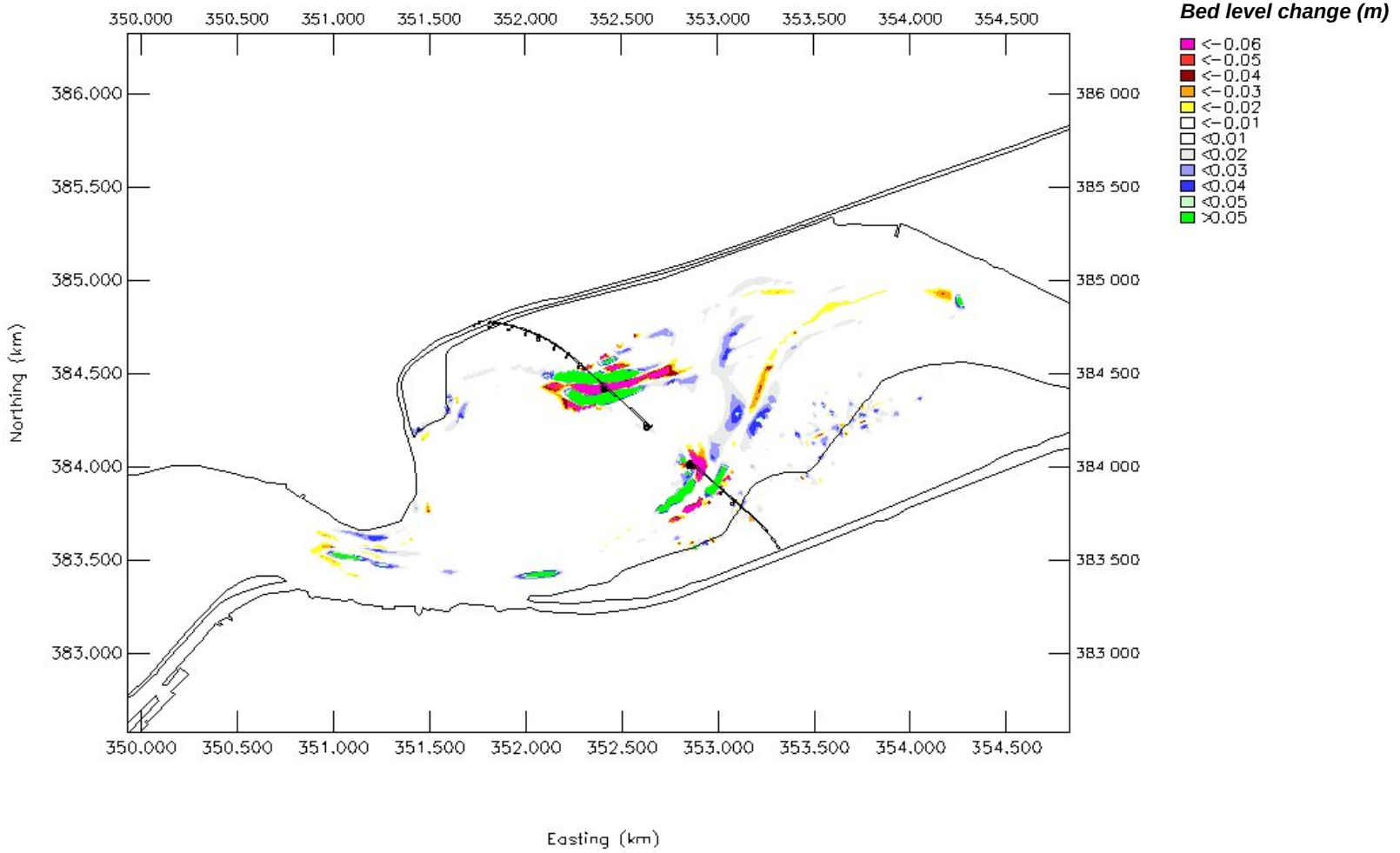

Morphological change (m) after spring neap run. Extreme Fluvial and Surge Event Scenario for Aligned Jetty with causeway

Figure B4a

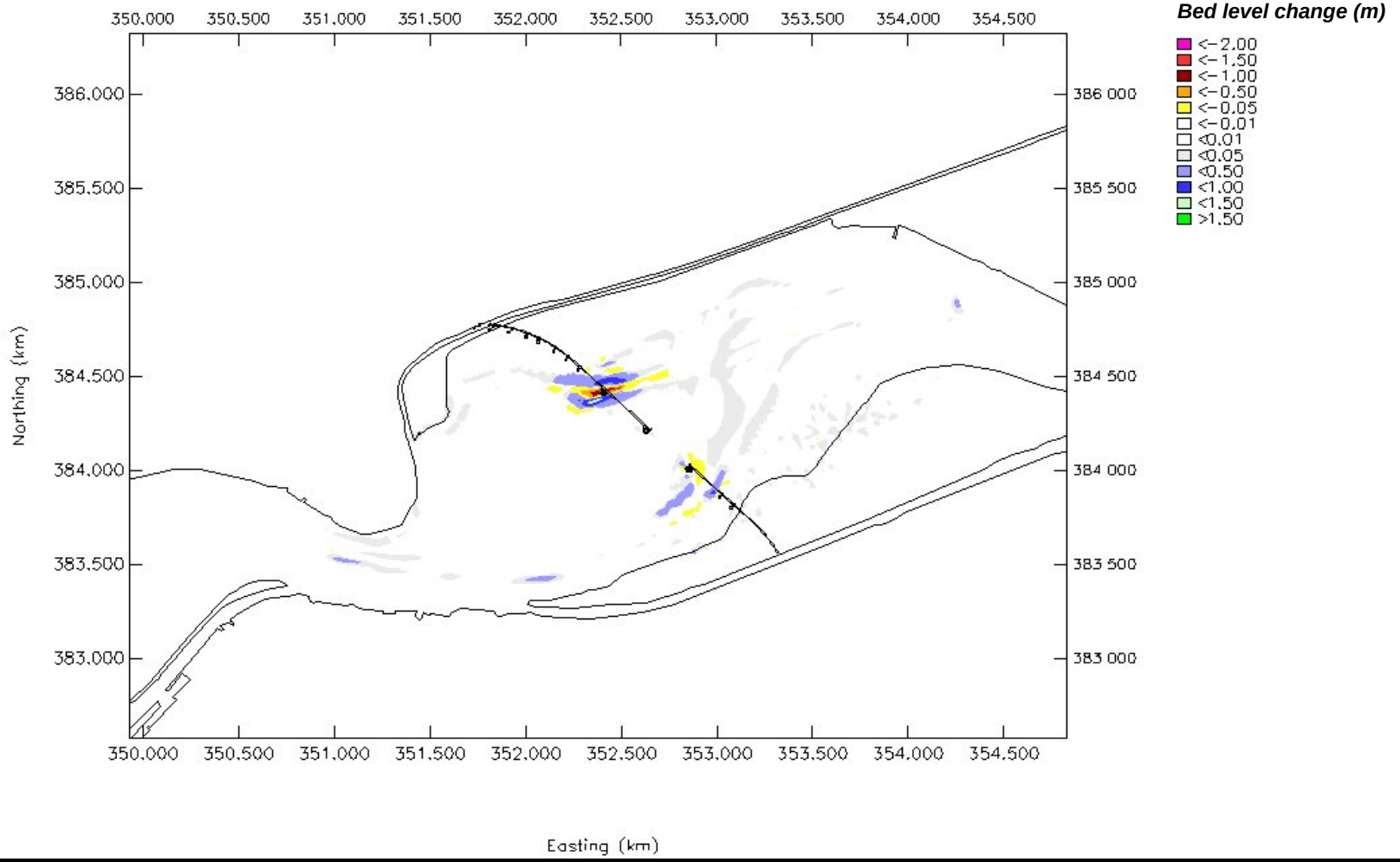

Morphological change (m) after spring neap run. Extreme Fluvial and Surge Event Scenario for Aligned Jetty with causeway

Figure B4b

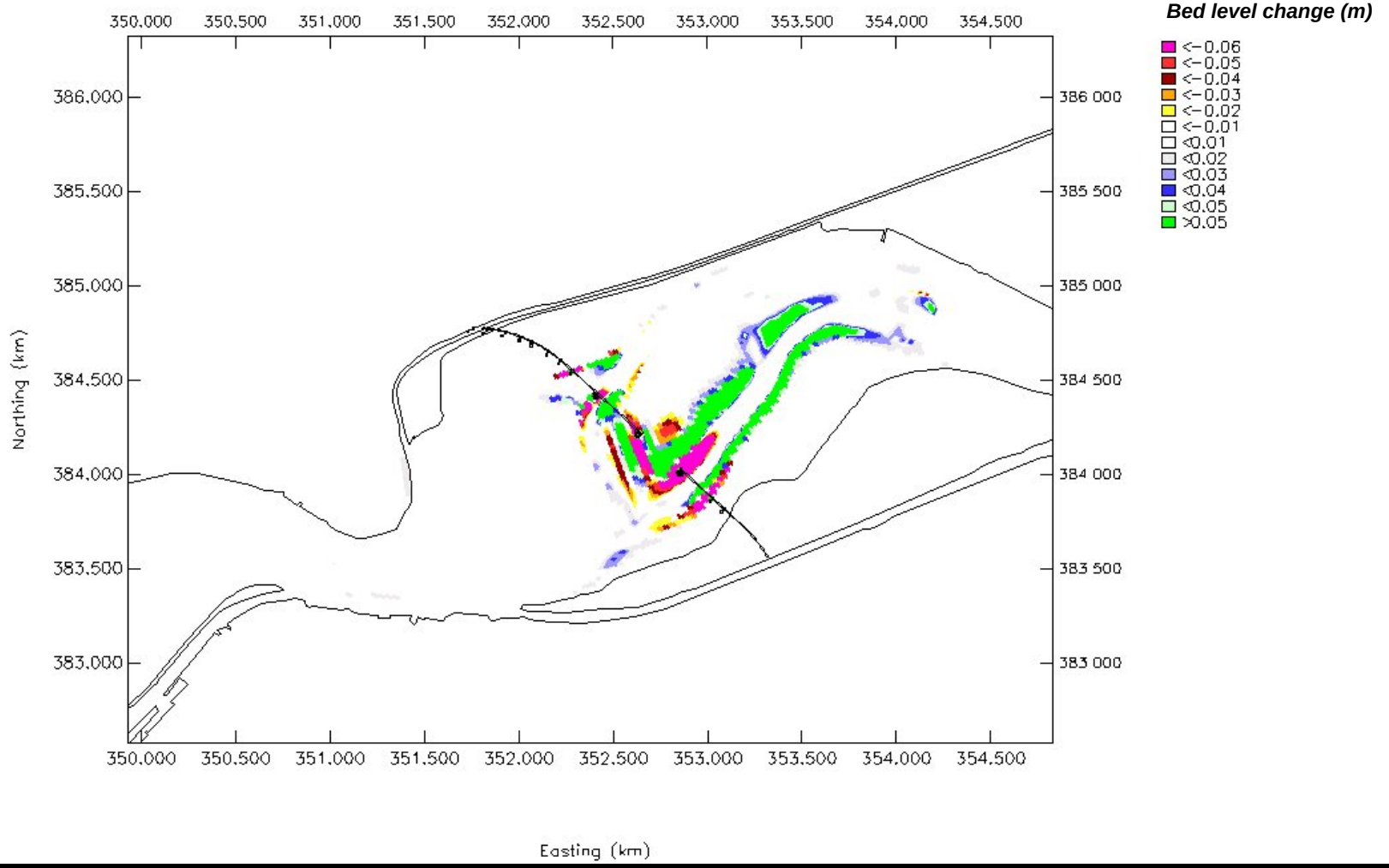

Morphological change (m) after a 1 year run. Aligned Jetty with causeway with 2005 bathymetry

Figure B5a

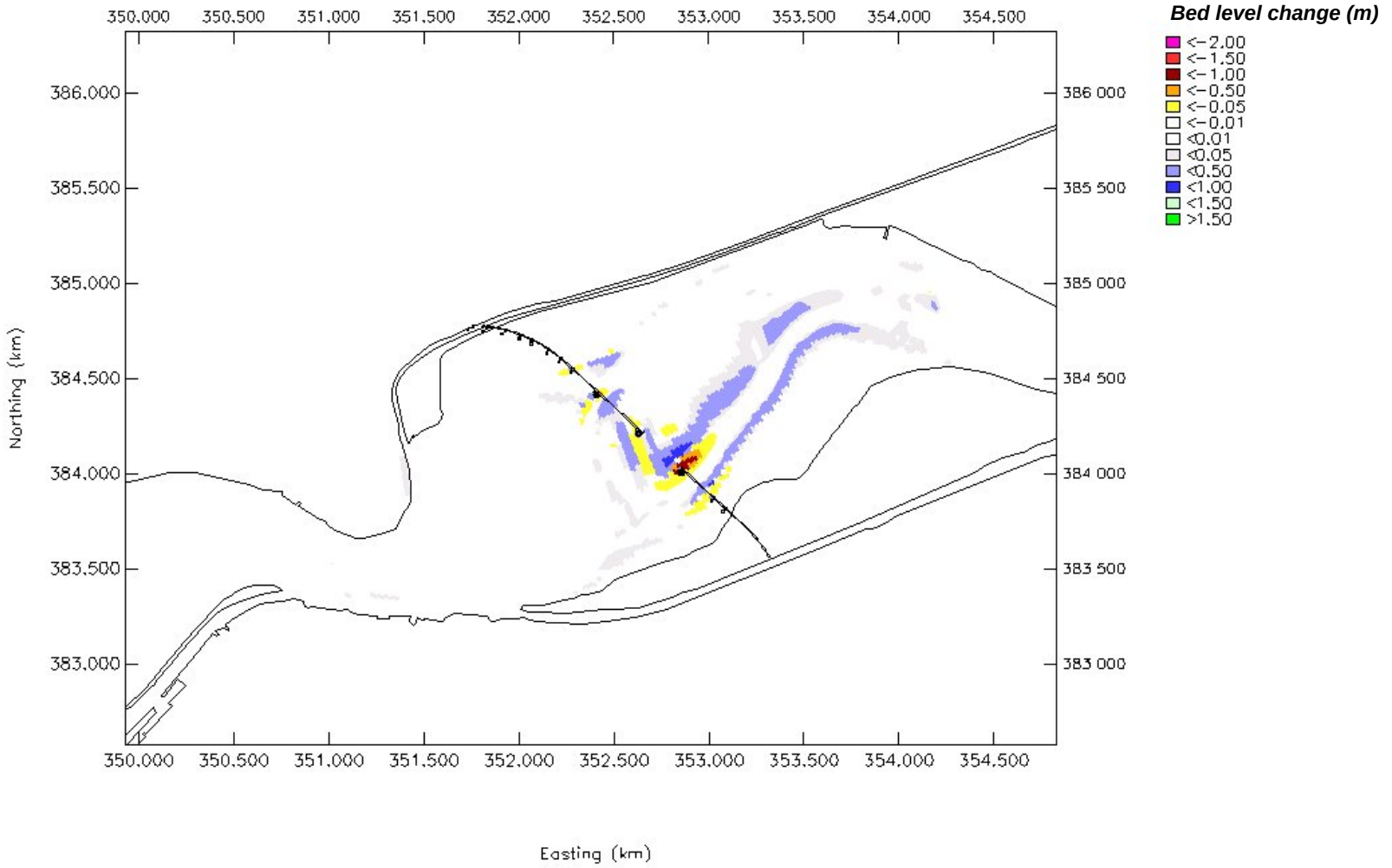

Morphological change (m) after a 1 year run. Aligned Jetty with causeway with 2005 bathymetry

Figure B5b

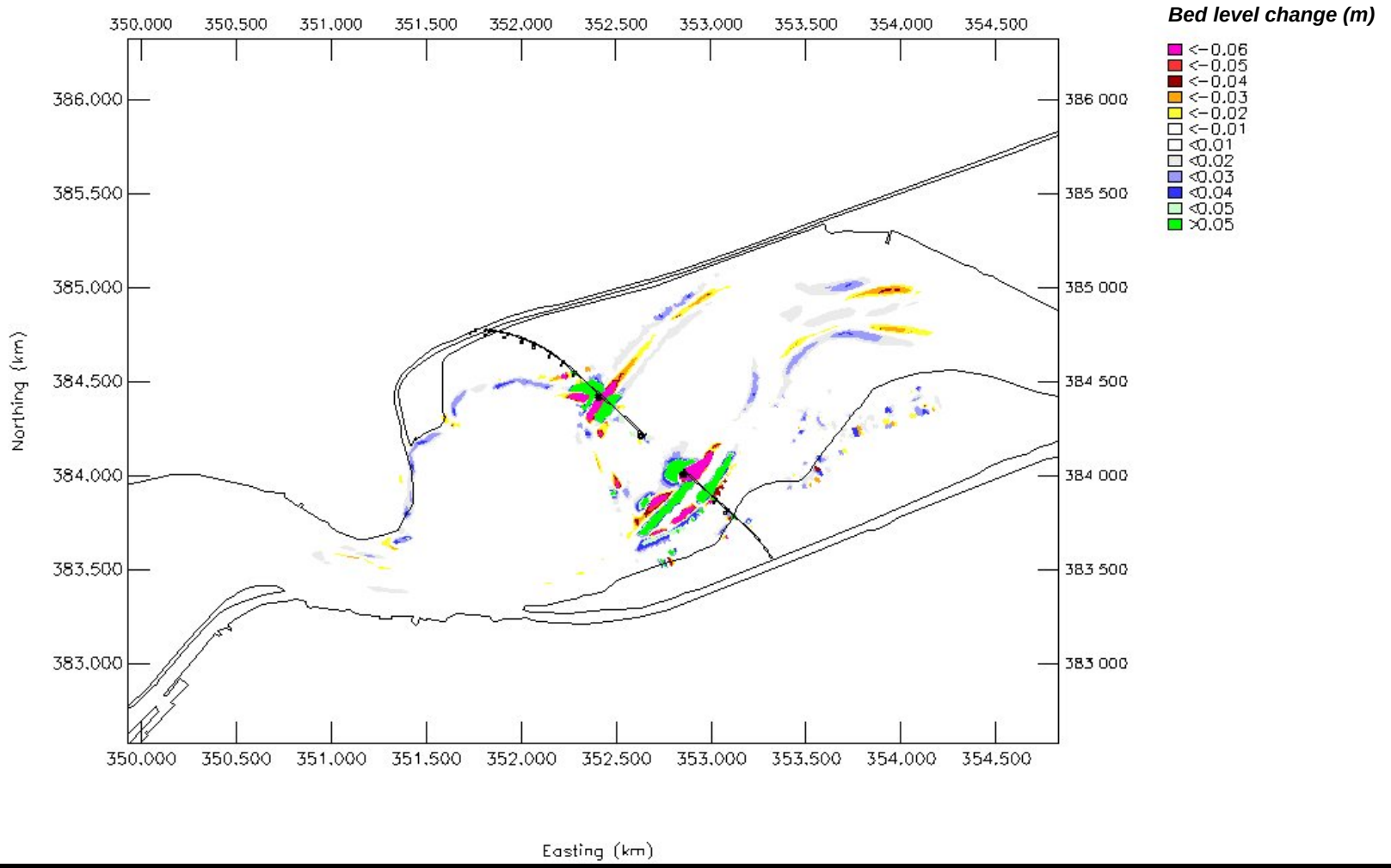

ABP mer marine environmental research	Morphological change (m) after spring neap run. Extreme Fluvial and Surge Event Scenario for Aligned Jetty with causeway with 2005 Bathymetry	Figure B6a

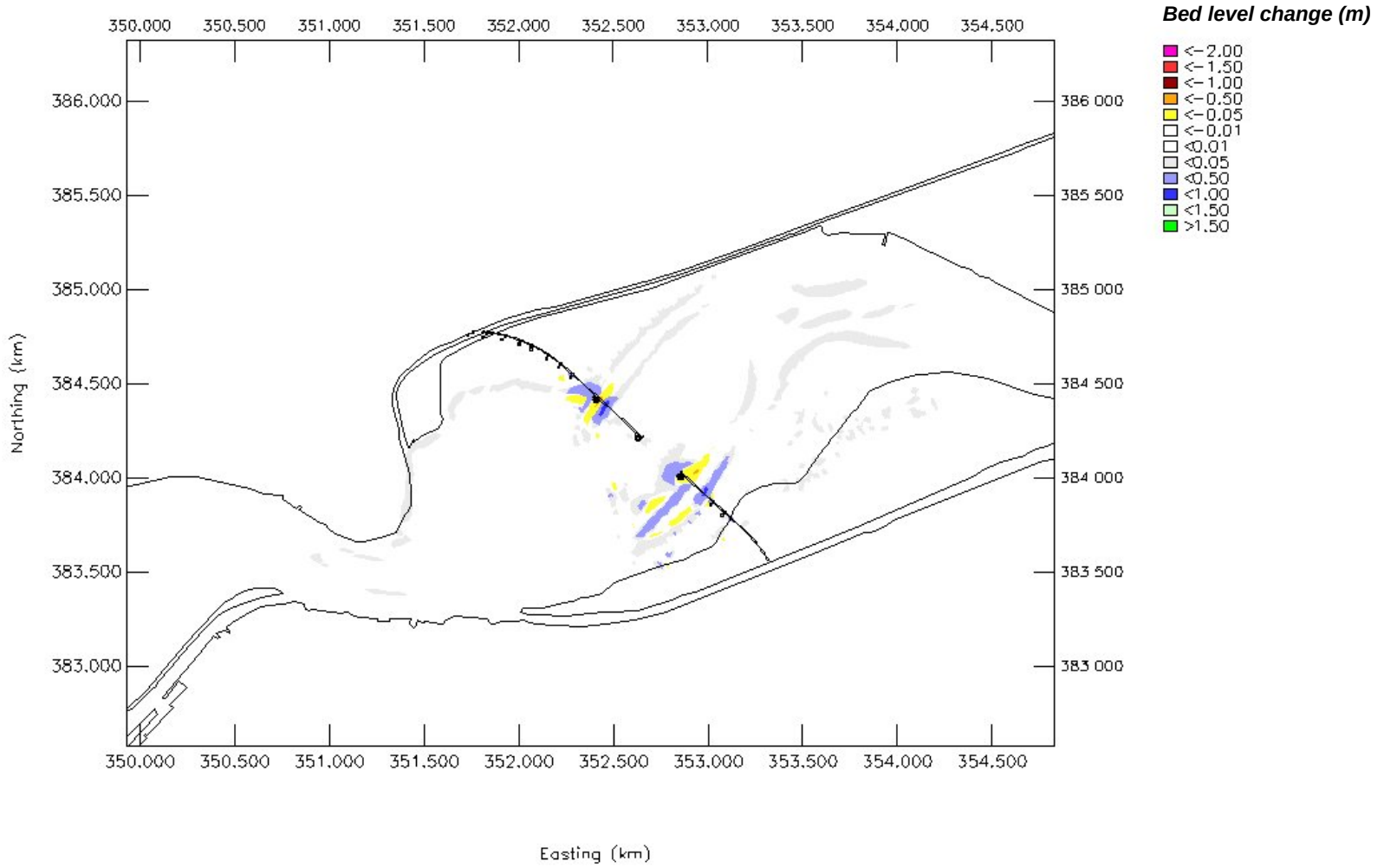

Morphological change (m) after spring neap run. Extreme Fluvial and Surge Event Scenario for Aligned Jetty with causeway with 2005 Bathymetry

Figure B6b

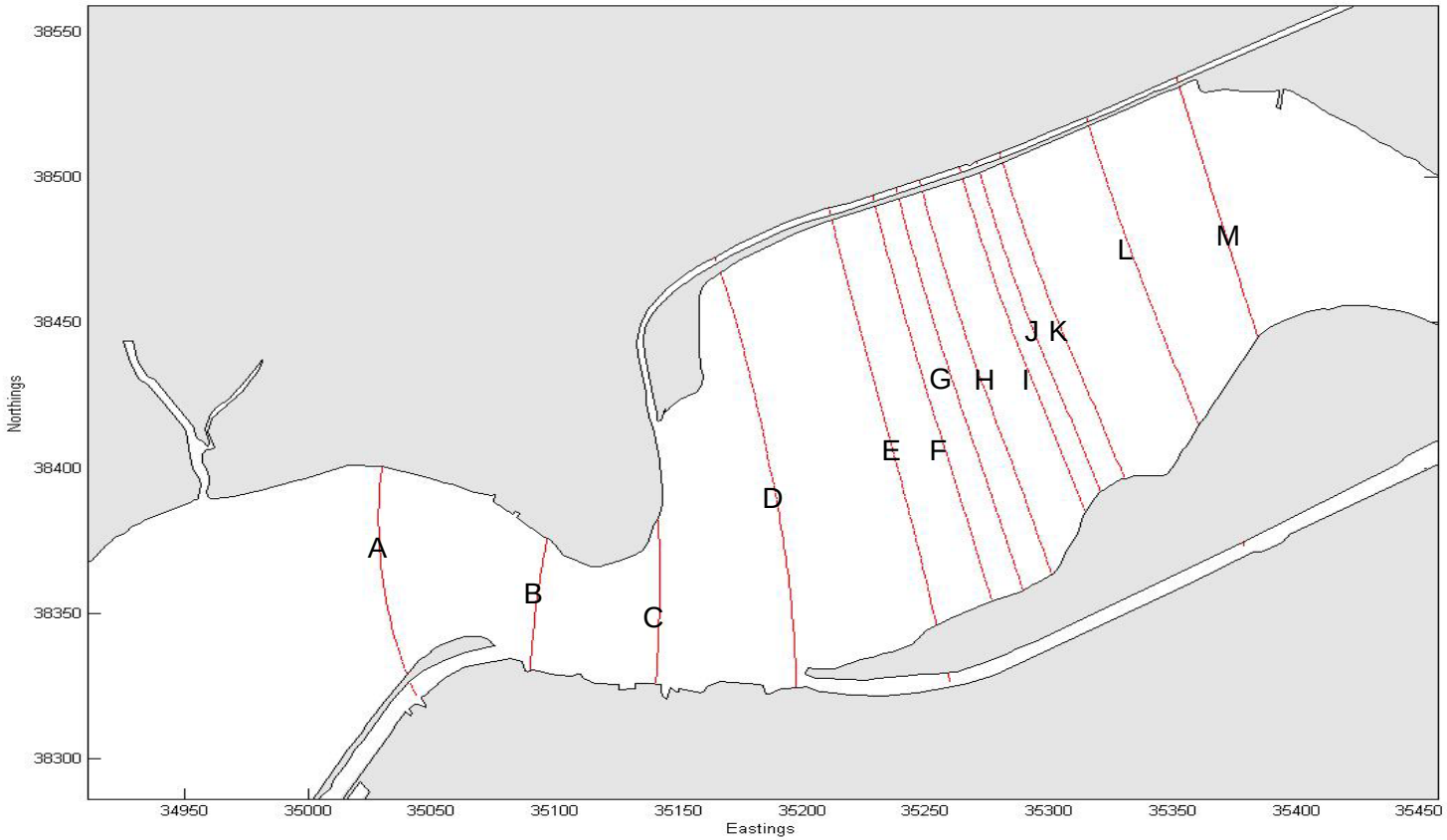

Locations of cross sections examined from the morphological model

Figure B7

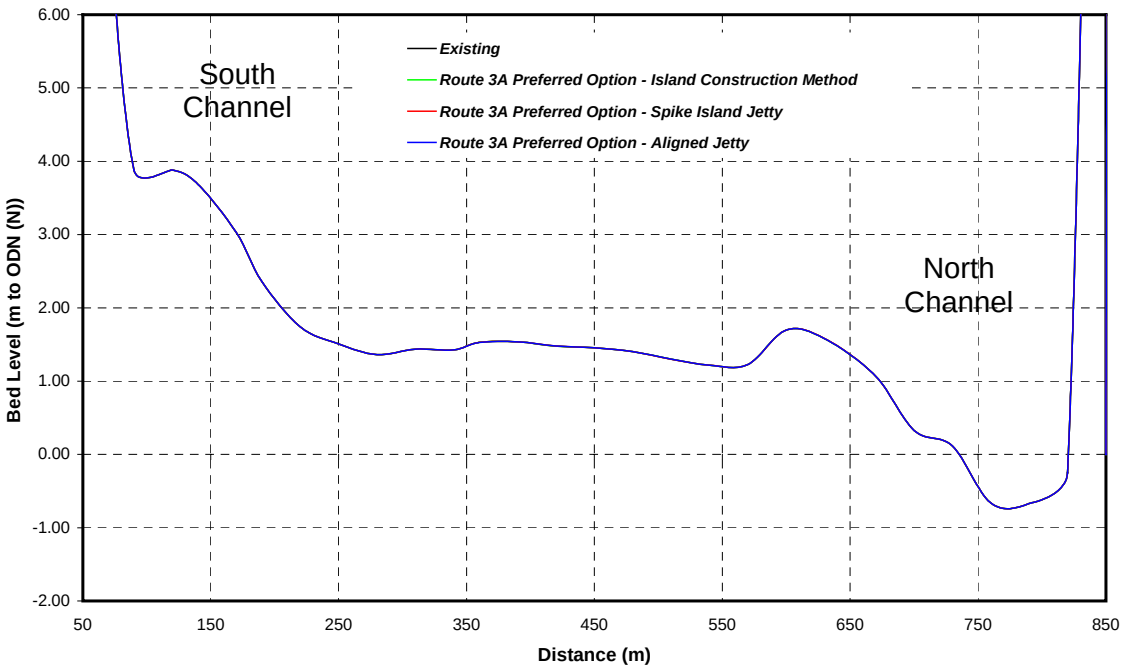

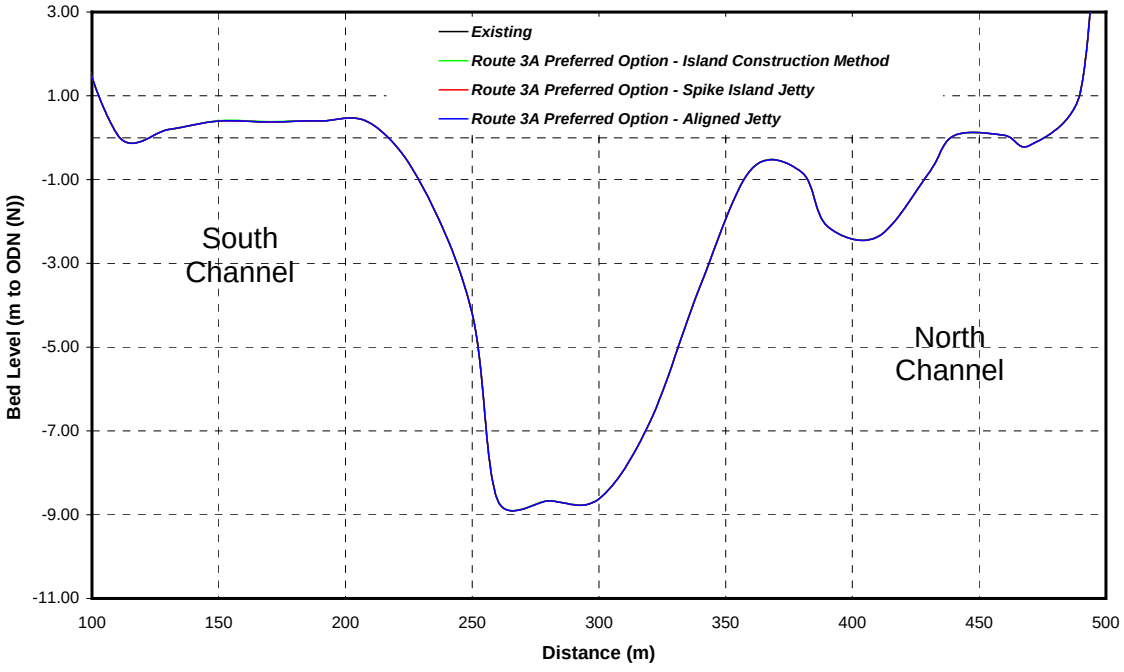

ABP mer marine environmental research

Cross–sections A and B for the three construction options over a spring-neap cycle

Figure B8

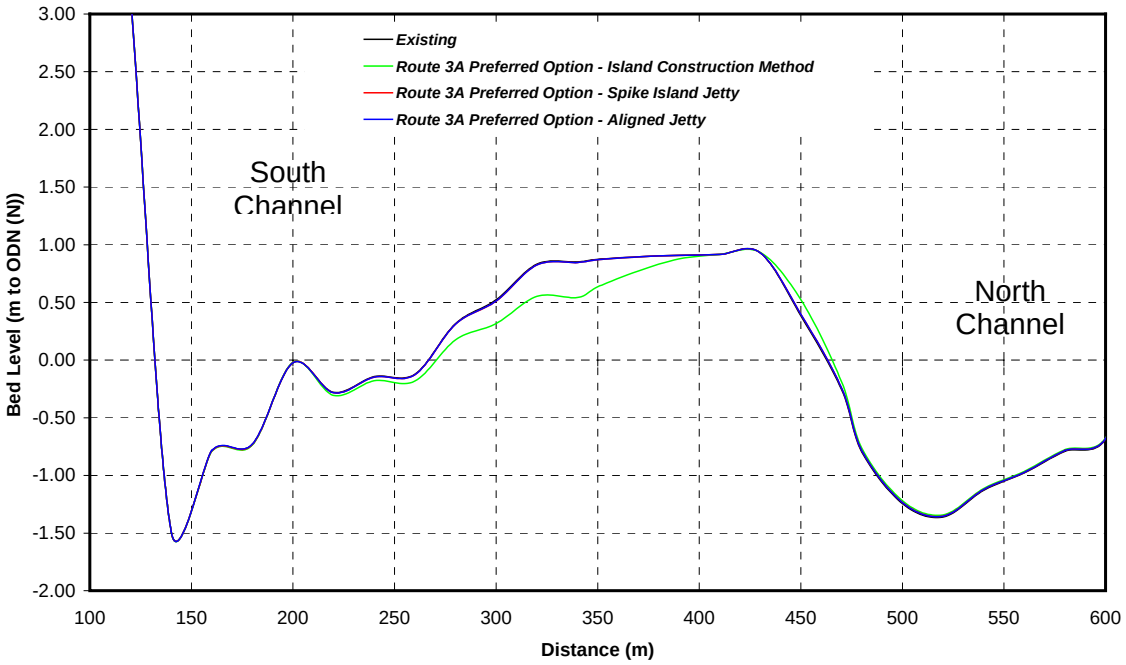

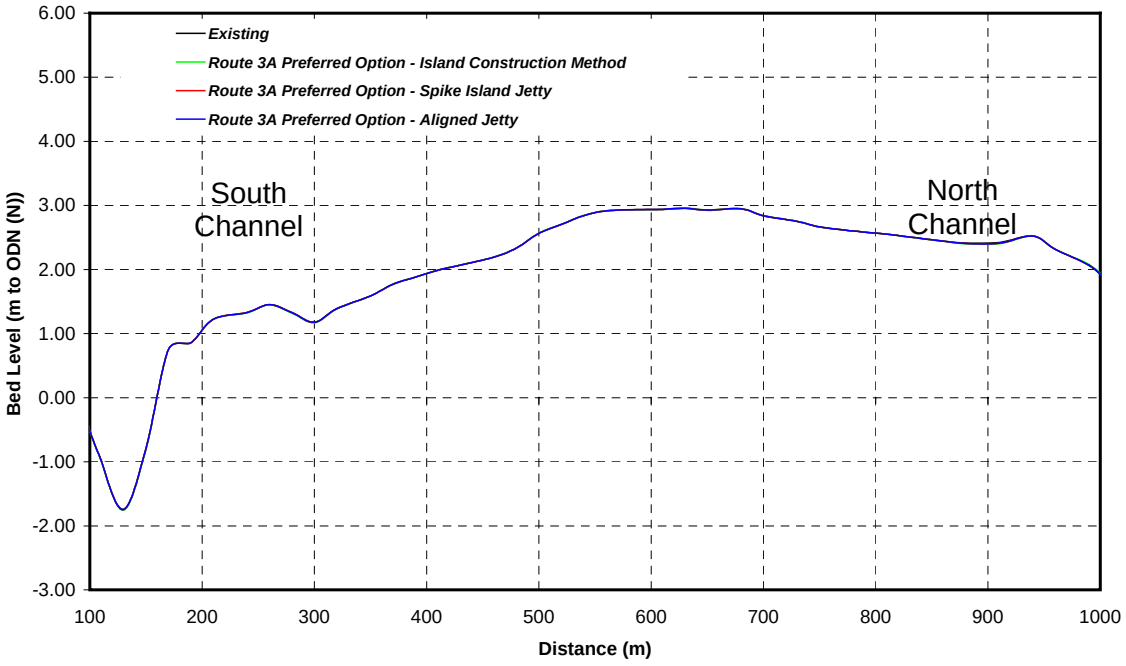

ABP mer marine environmental research	Cross–sections C and D for the three construction options over a spring-neap cycle	Figure B9

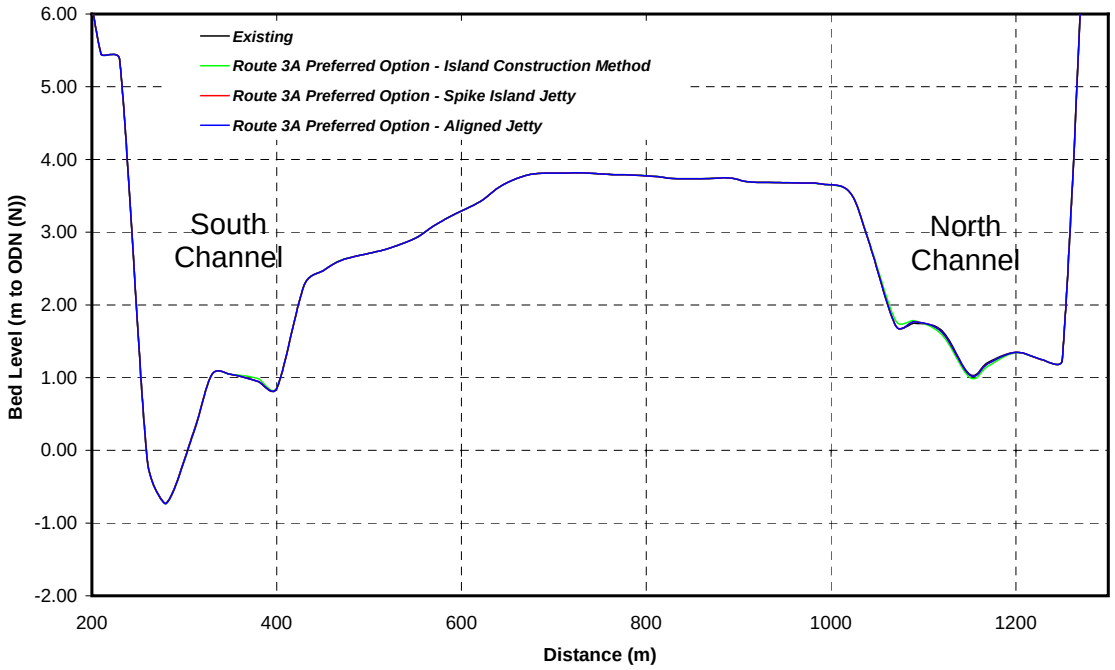

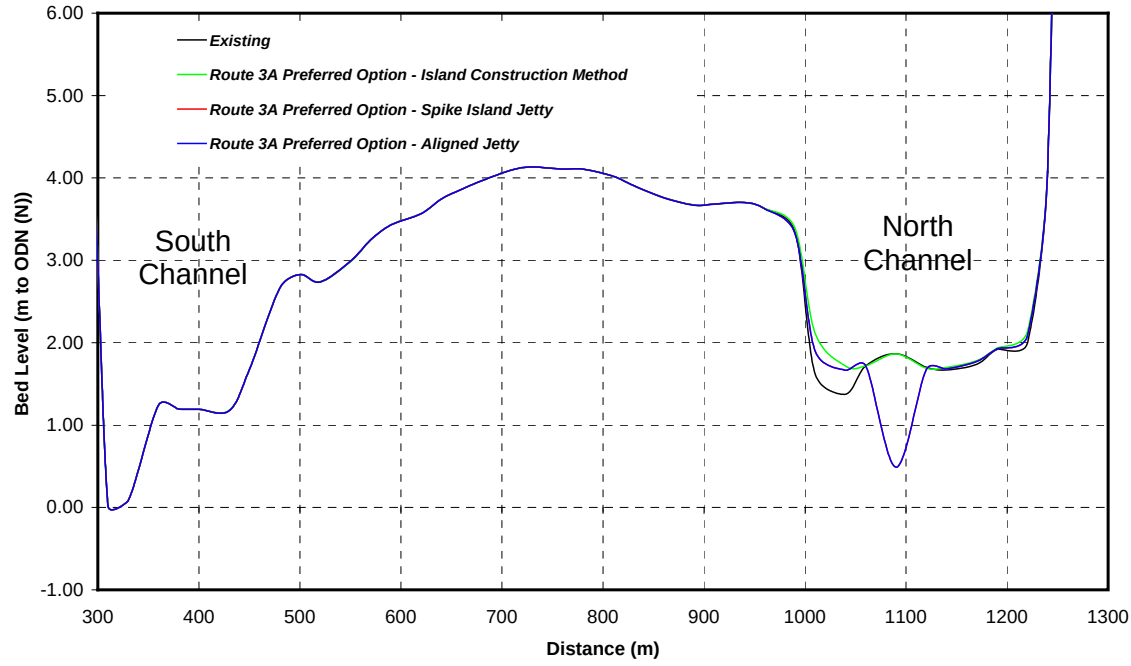

ABP mer marine environmental research	Cross–sections E and F for the three construction options over a spring-neap cycle	Figure B10

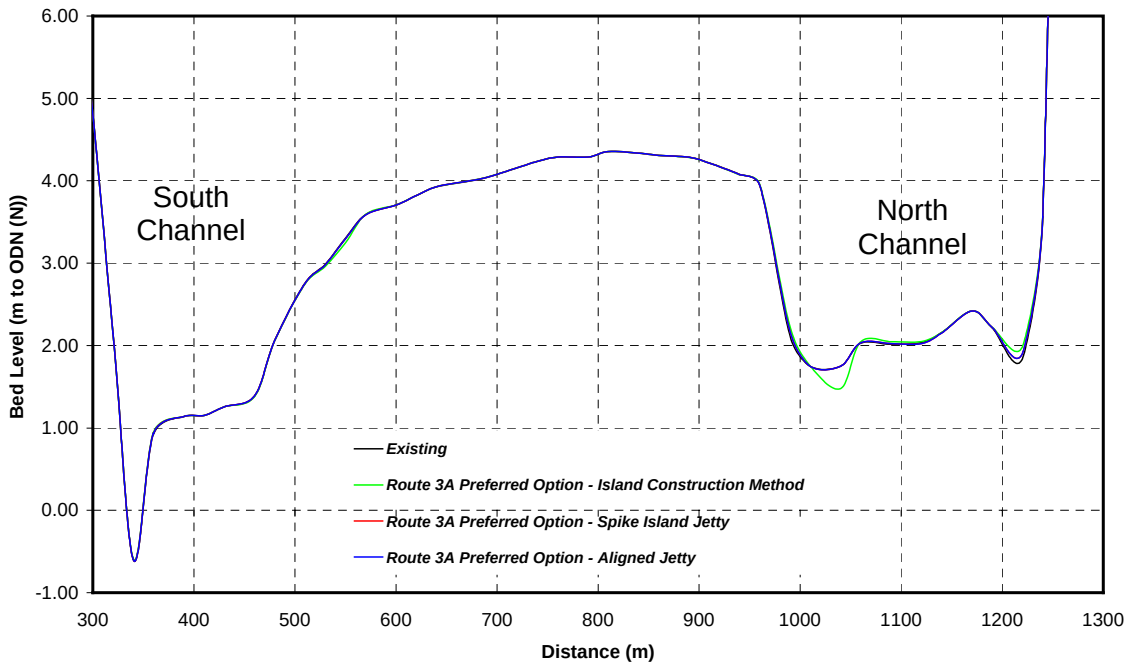

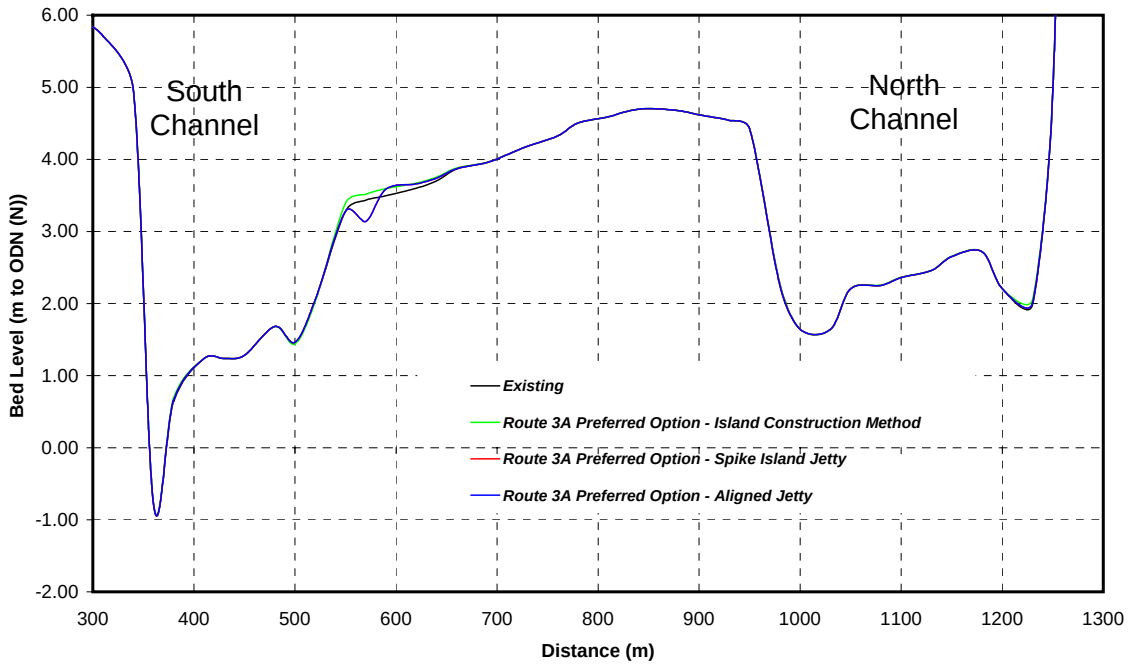

ABP mer marine environmental research	Cross–sections G and H for the three construction options over a spring-neap cycle.	Figure B11

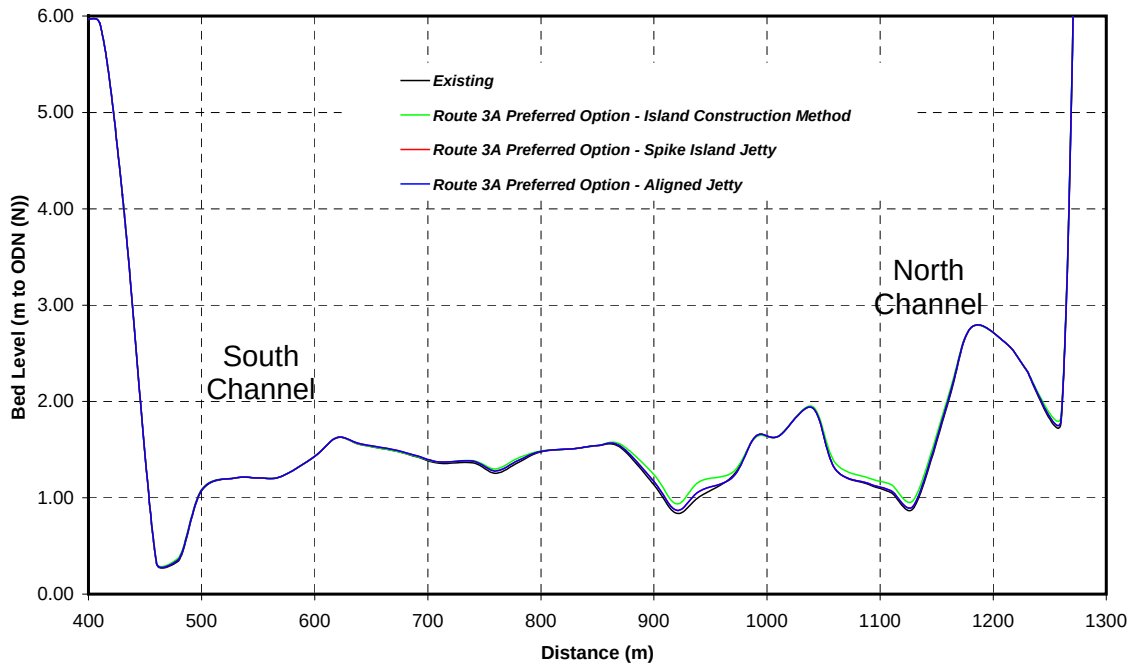

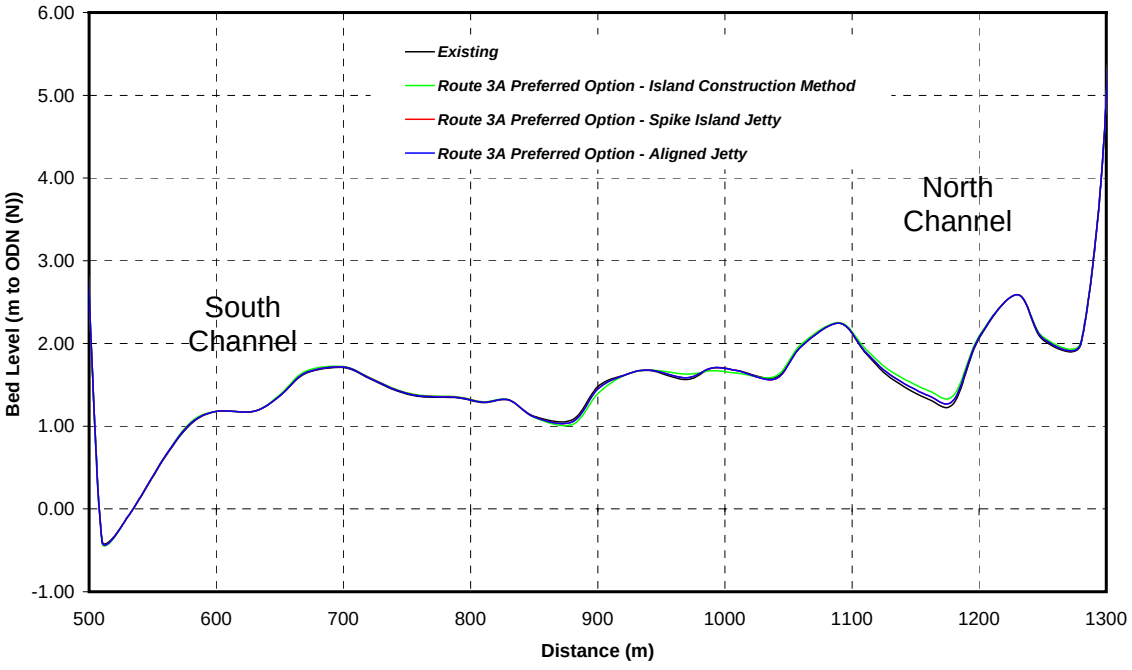

ABP mer marine environmental research	Cross–sections I and J for the three construction options over a spring-neap cycle	Figure B12

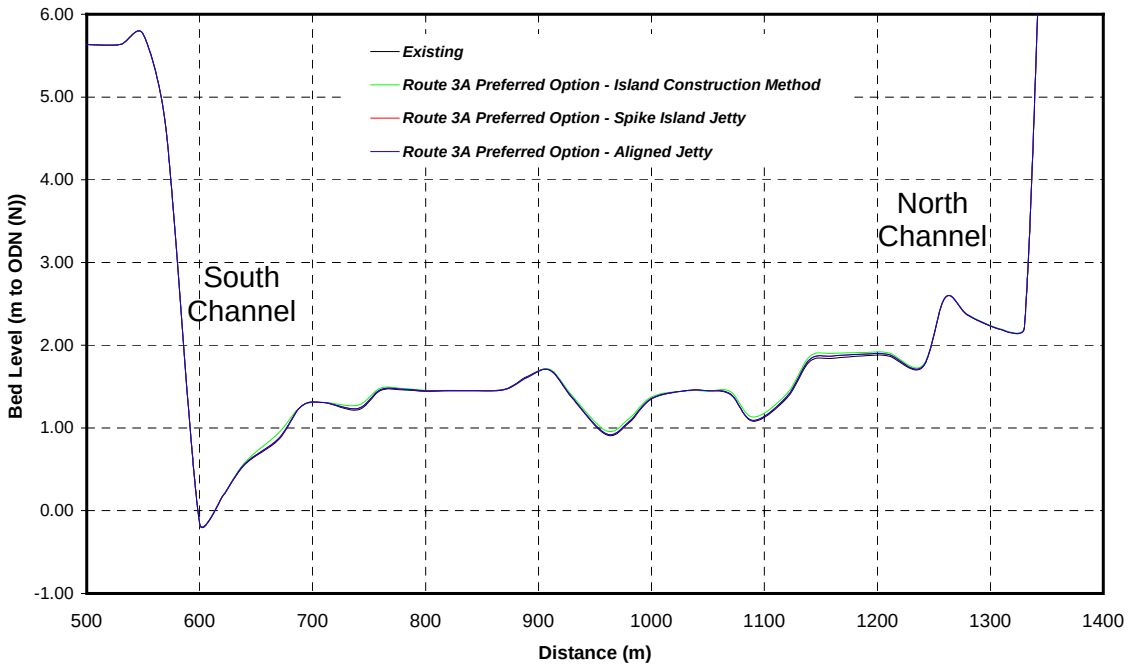

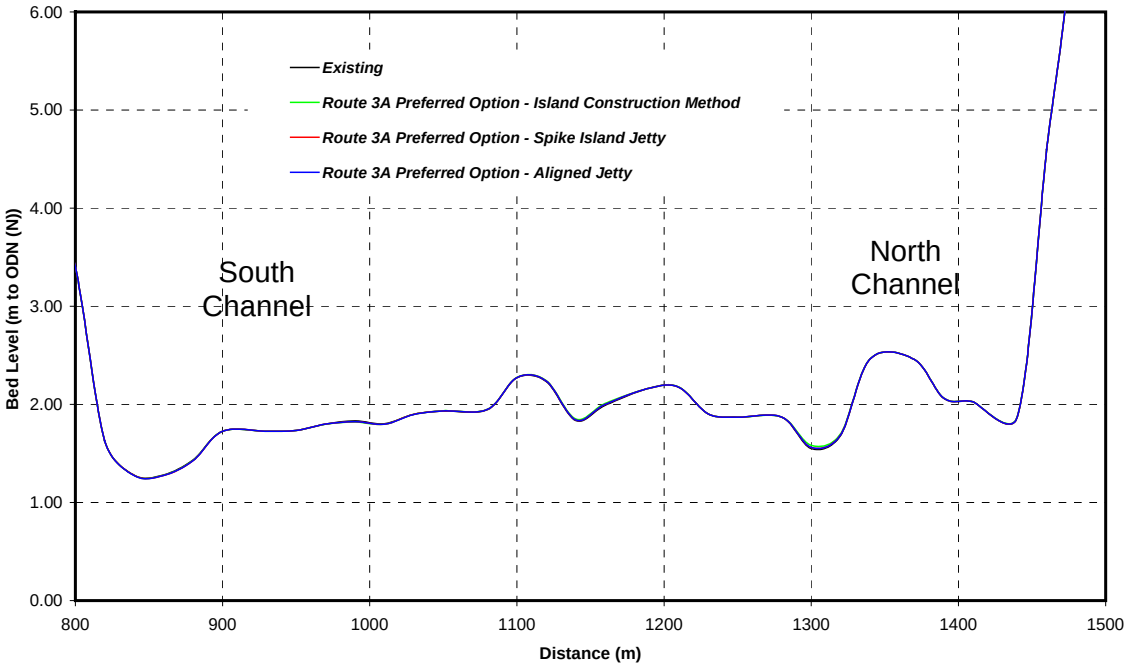

ABP mer marine environmental research

Cross–sections K and L for the three construction options over a spring-neap cycle

Figure B13

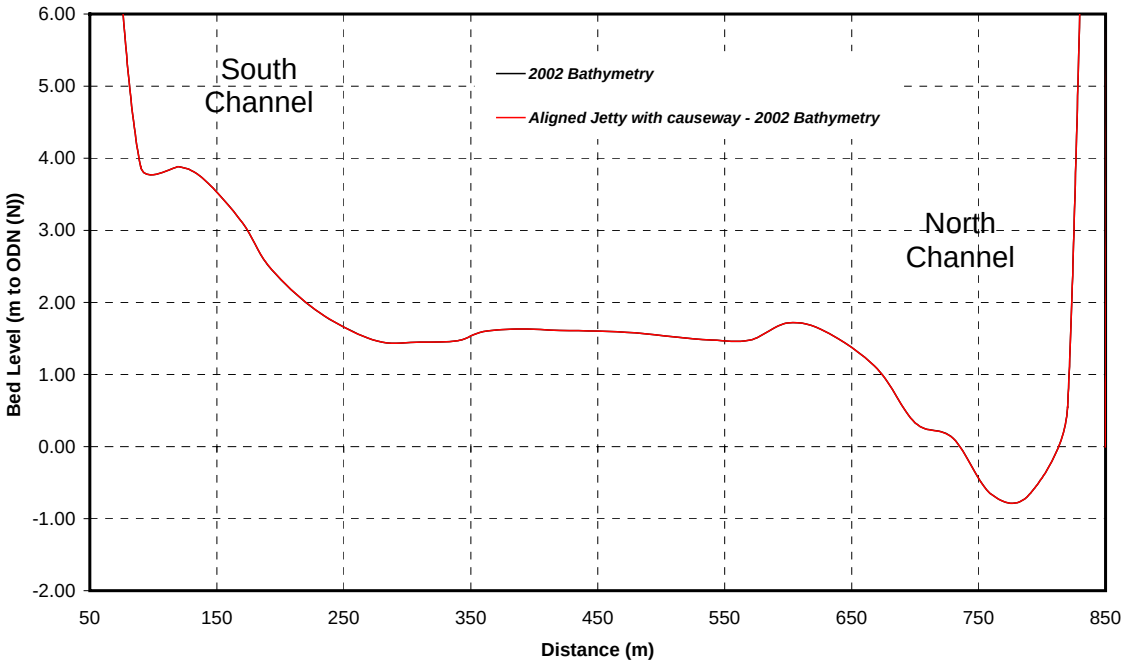

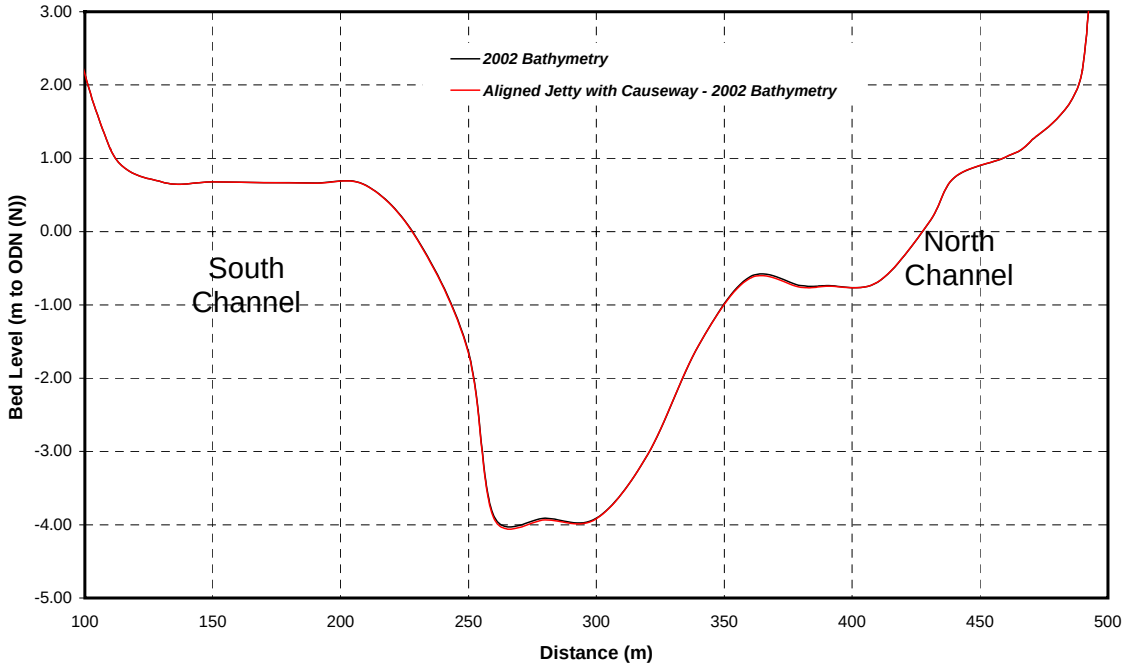

ABP mer marine environmental research	Cross–sections A and B for the aligned jetty with causeway for an extreme fluvial and surge event (1:200 years return period)	Figure B14

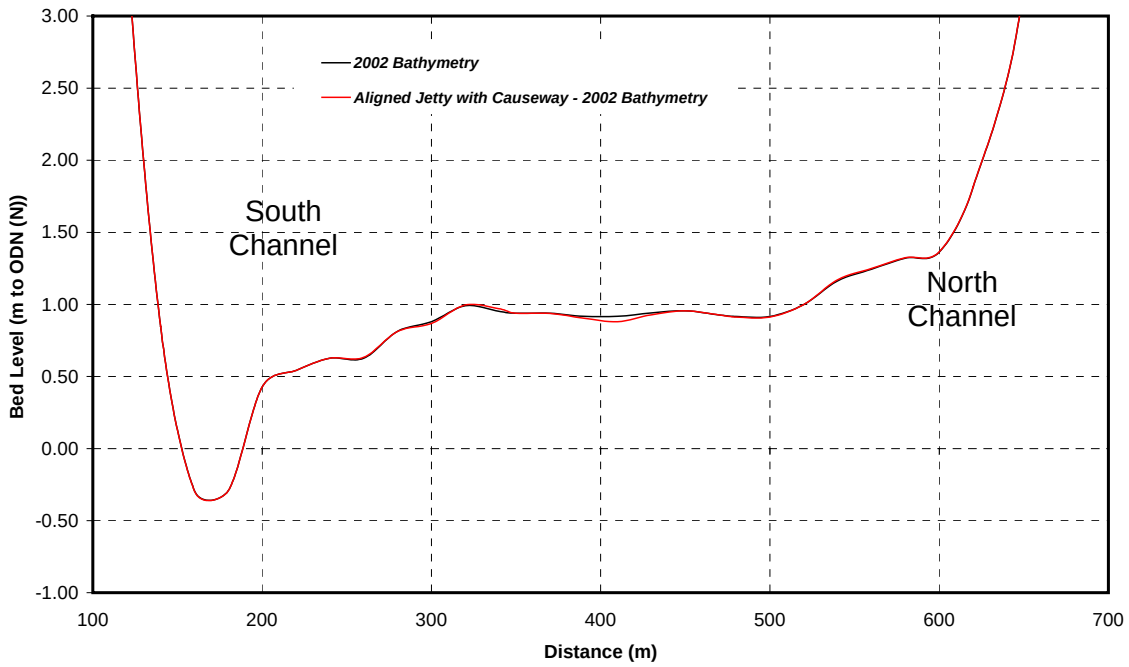

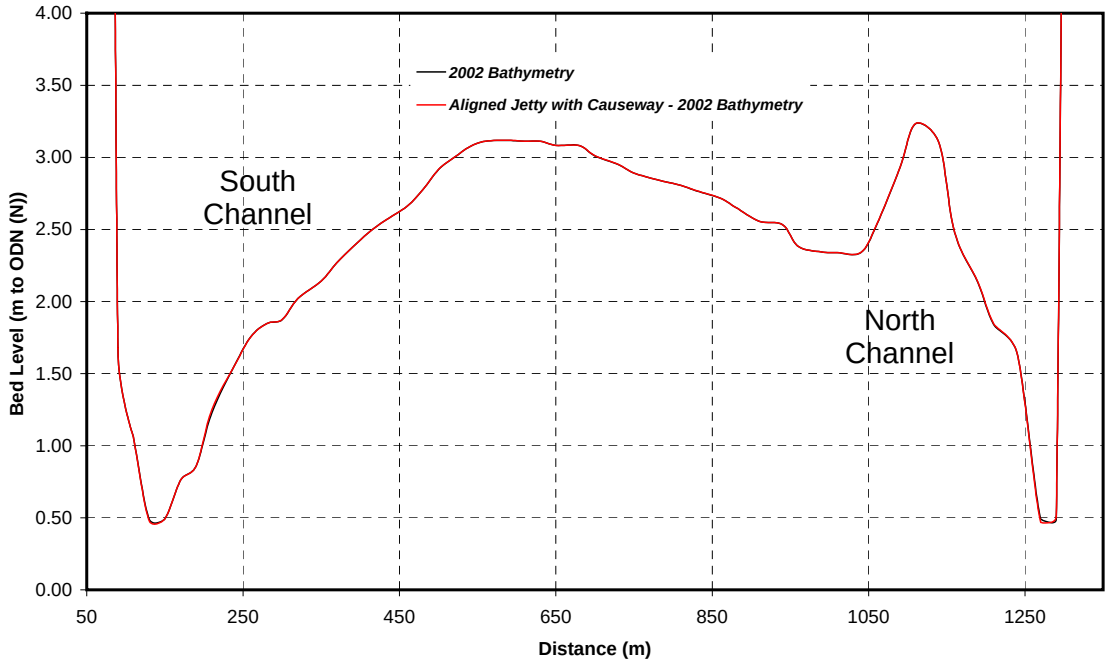

ABP mer marine environmental research	Cross–sections C and D for the aligned jetty with causeway for an extreme fluvial and surge event (1:200 years return period)	Figure B15

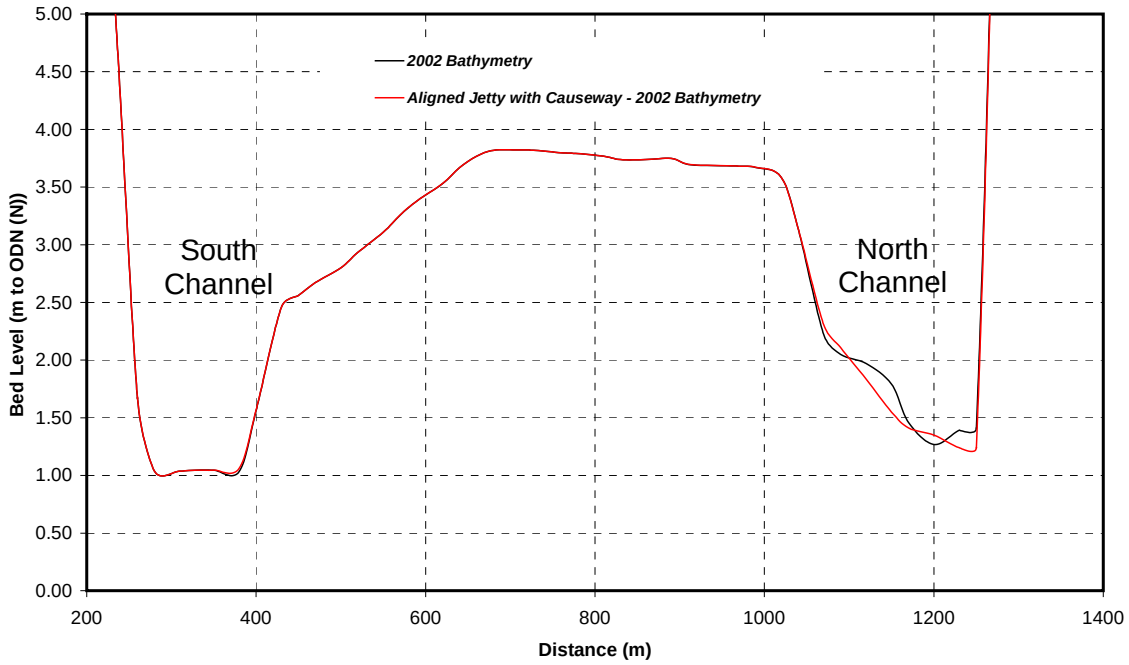

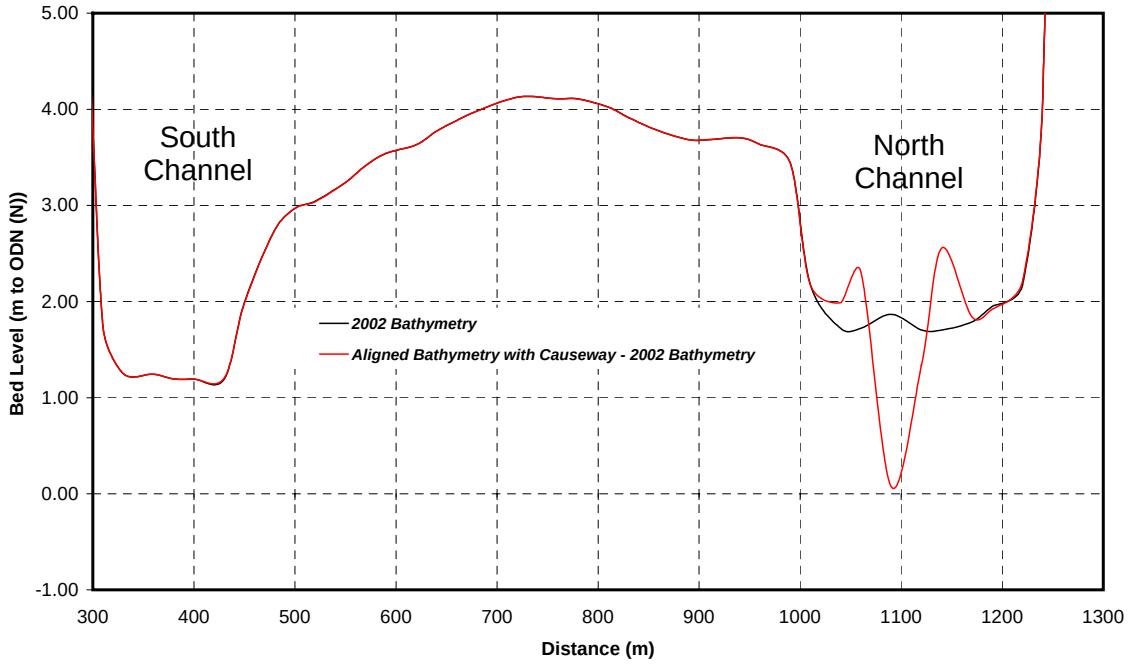

ABP mer marine environmental research	Cross–sections E and F for the aligned jetty with causeway for an extreme fluvial and surge event (1:200 years return period)	Figure B16

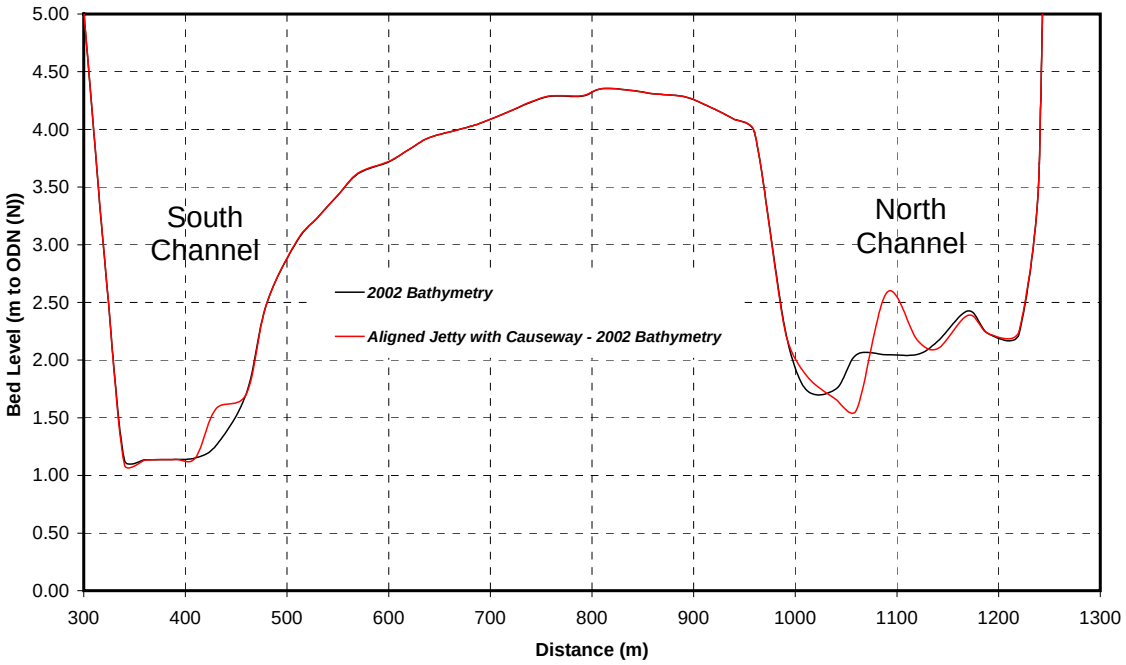

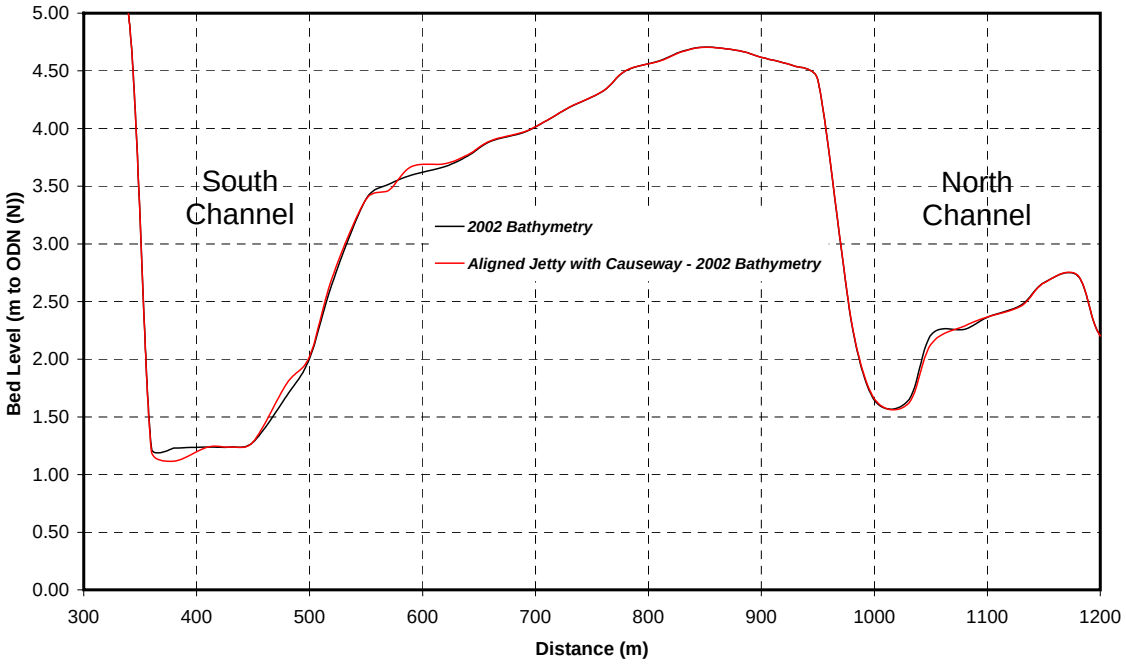

ABP mer marine environmental research	Cross–sections G and H for the aligned jetty with causeway for an extreme fluvial and surge event (1:200 years return period)	Figure B17

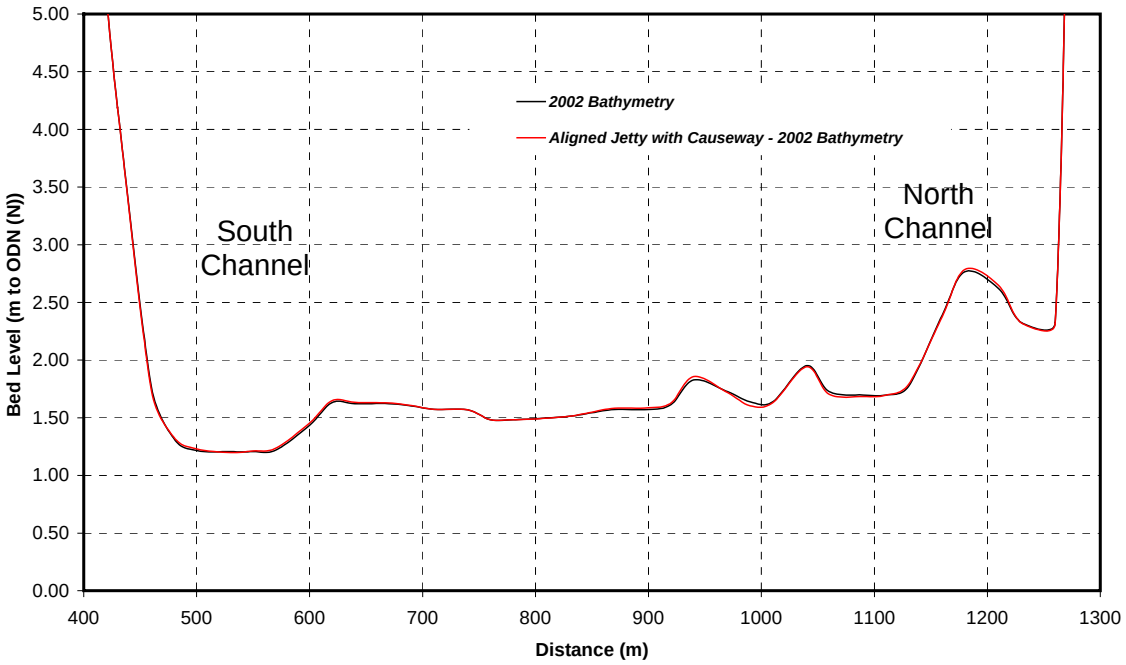

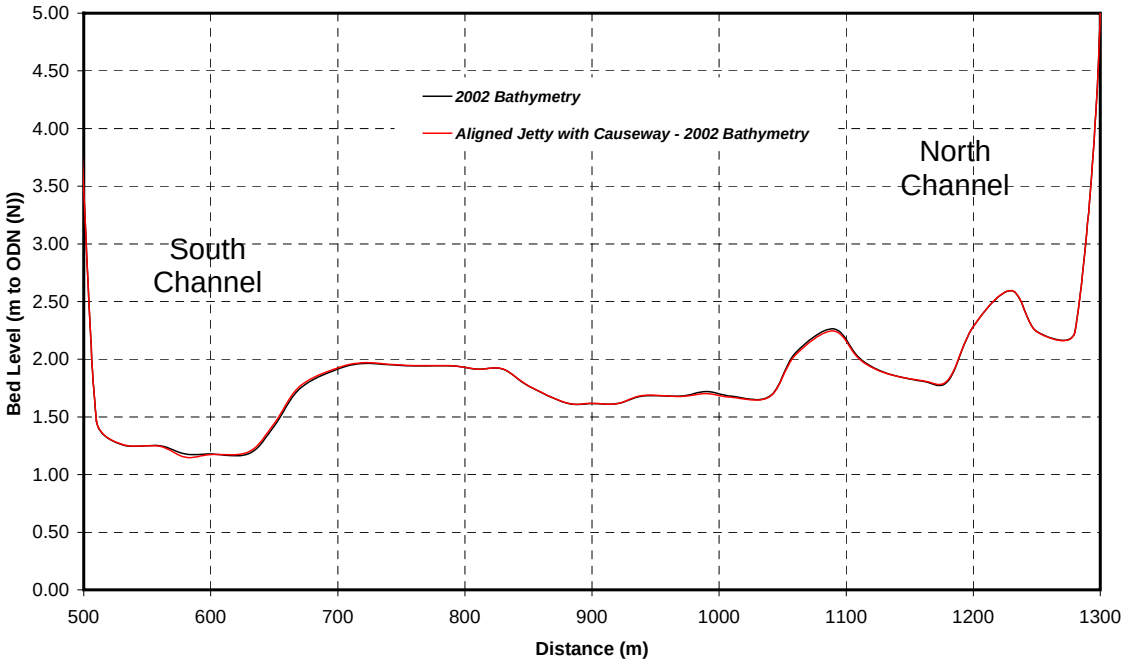

ABP mer marine environmental research	Cross–sections I and J for the aligned jetty with causeway for an extreme fluvial and surge event (1:200 years return period)	Figure B18

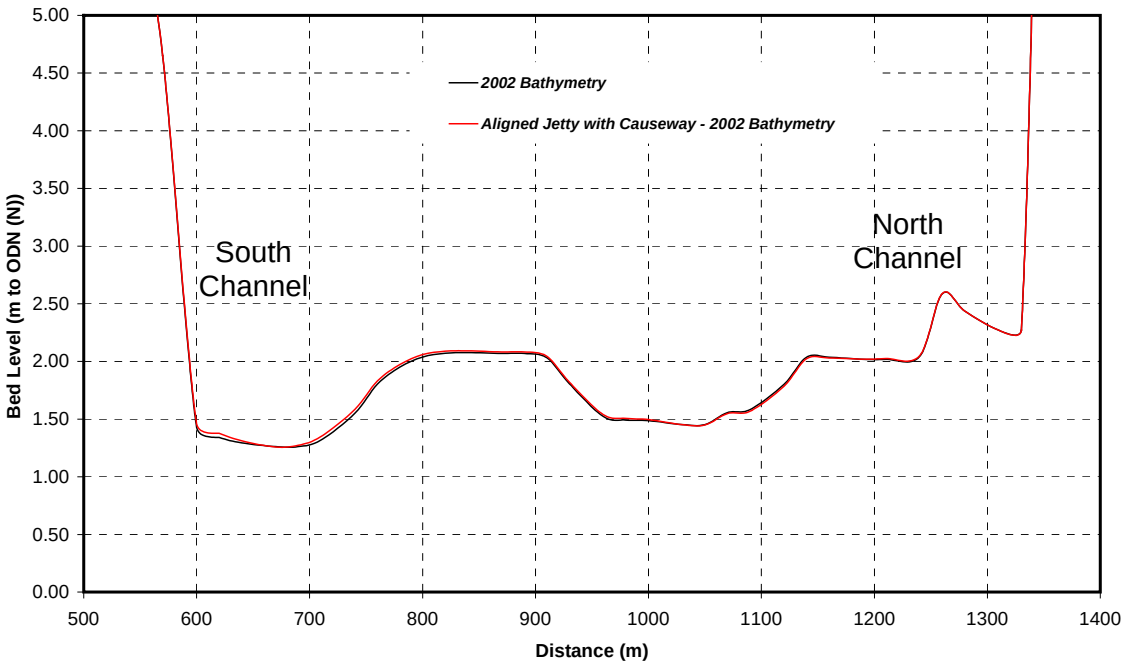

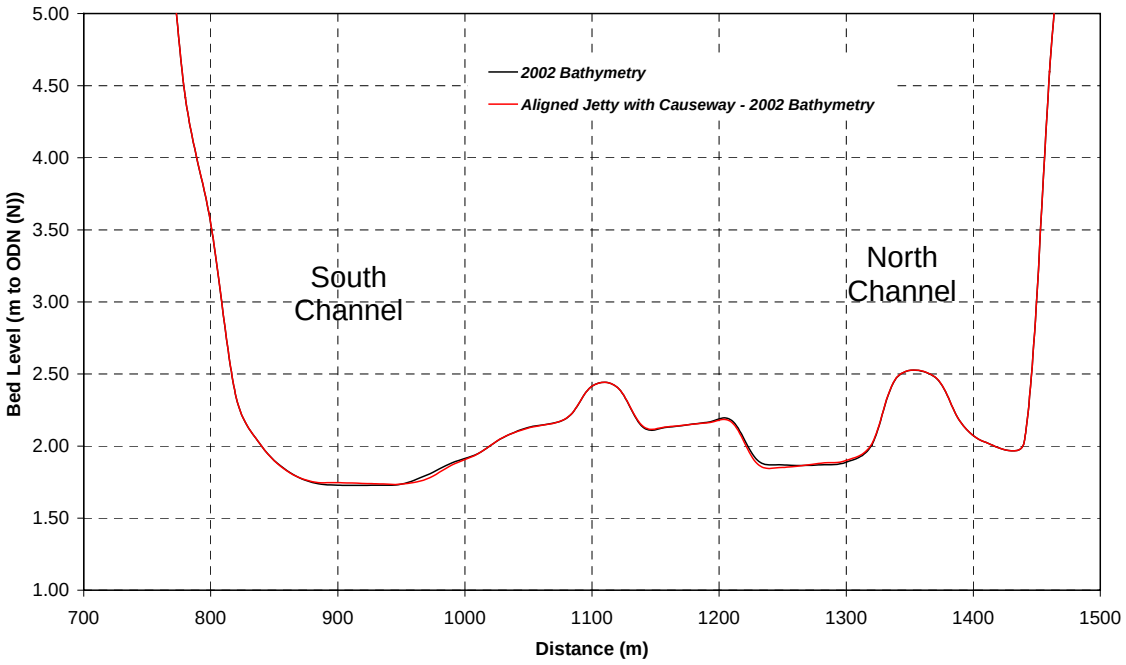

ABP mer marine environmental research	Cross–sections K and L for the aligned jetty with causeway for an extreme fluvial and surge event (1:200 years return period)	Figure B19

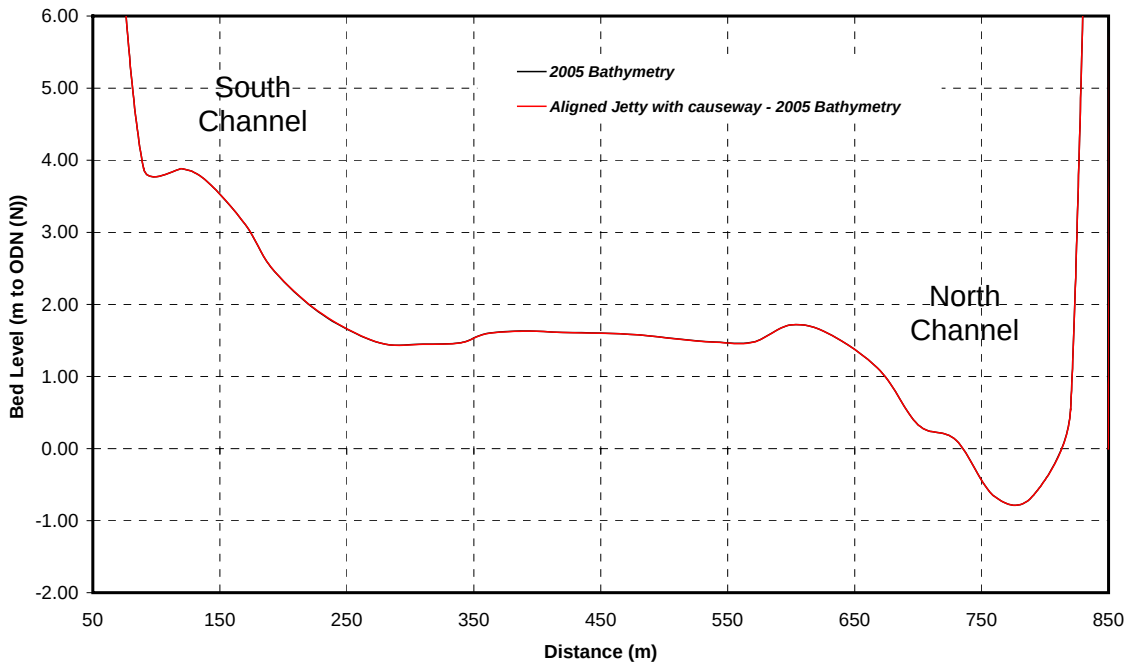

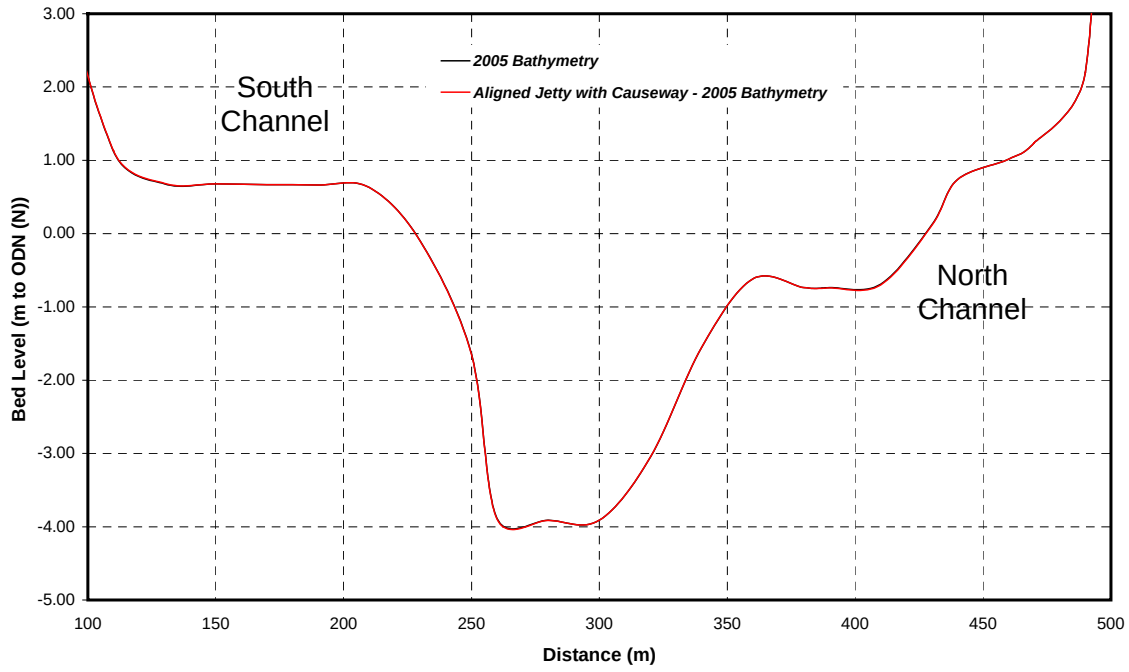

ABP mer marine environmental research	Cross–sections A and B for the aligned jetty with causeway for a spring-neap cycle and 2005 bathymetry	Figure B20

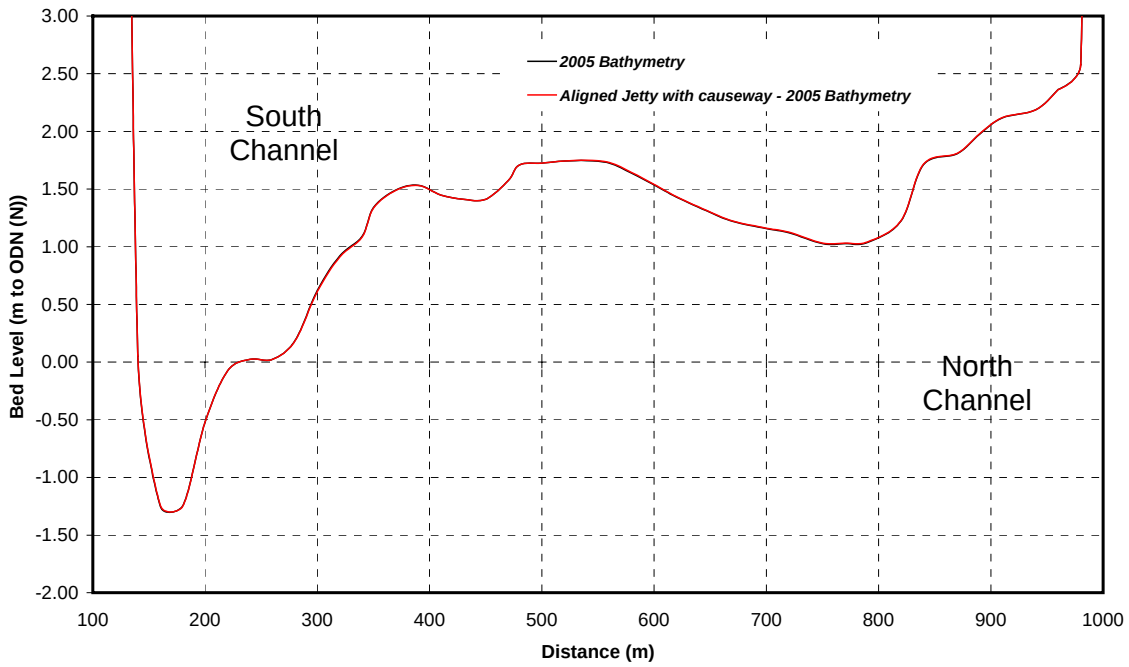

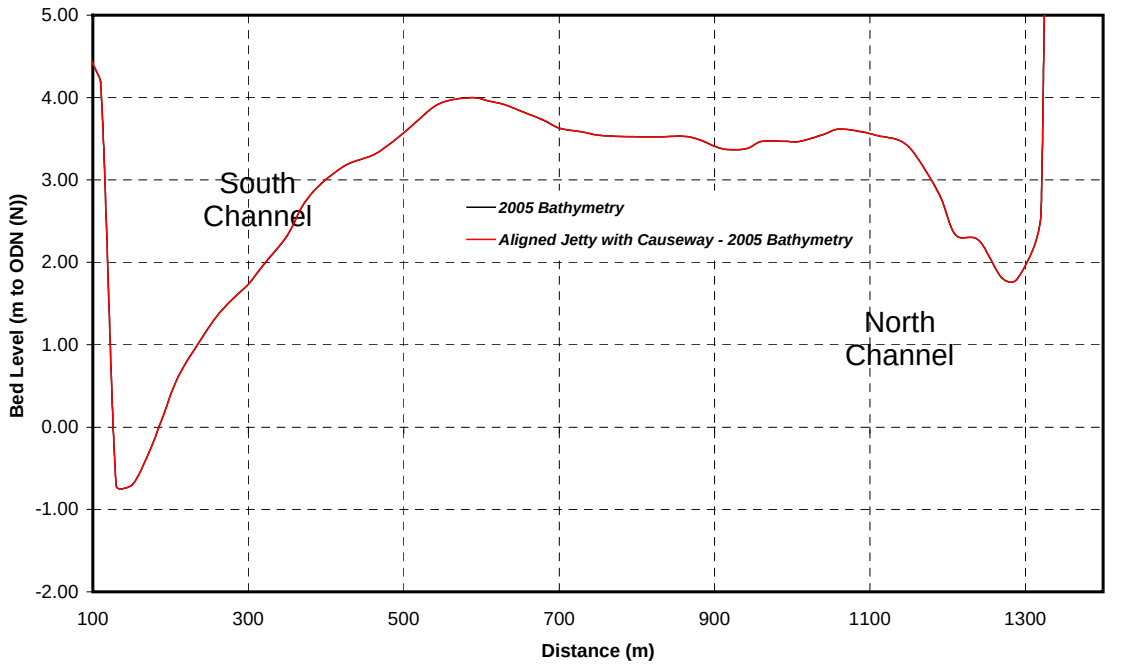

ABP mer marine environmental research	Cross–sections C and D for the aligned jetty with causeway for a spring-neap cycle and 2005 bathymetry	Figure B21

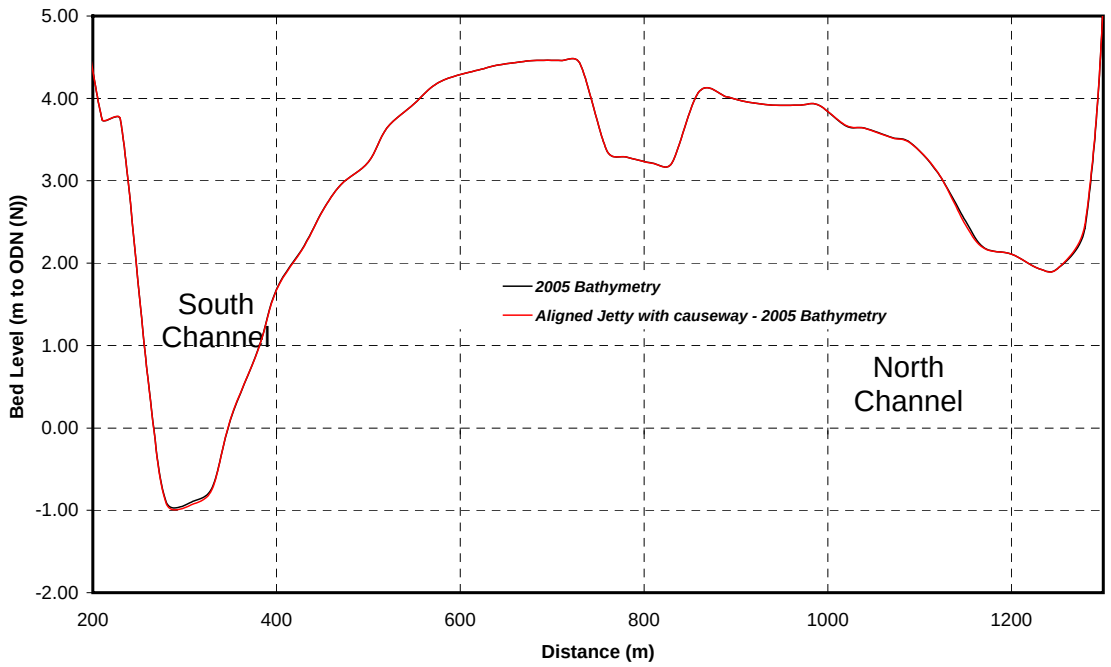

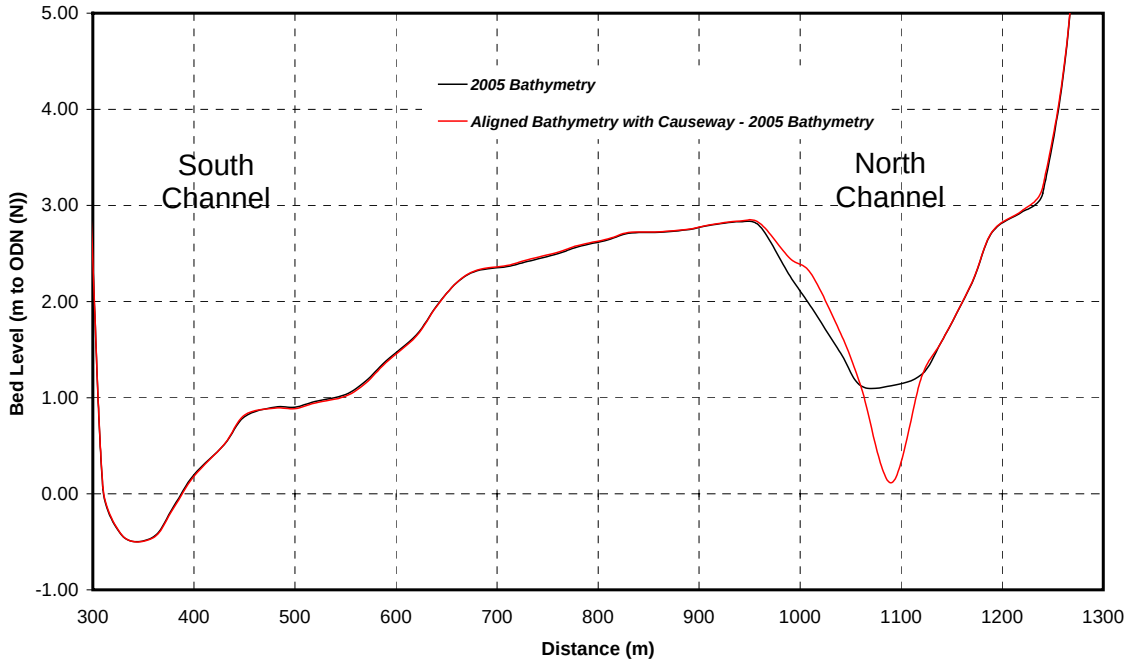

ABP mer marine environmental research	Cross–sections E and F for the aligned jetty with causeway for a spring-neap cycle and 2005 bathymetry	Figure B22

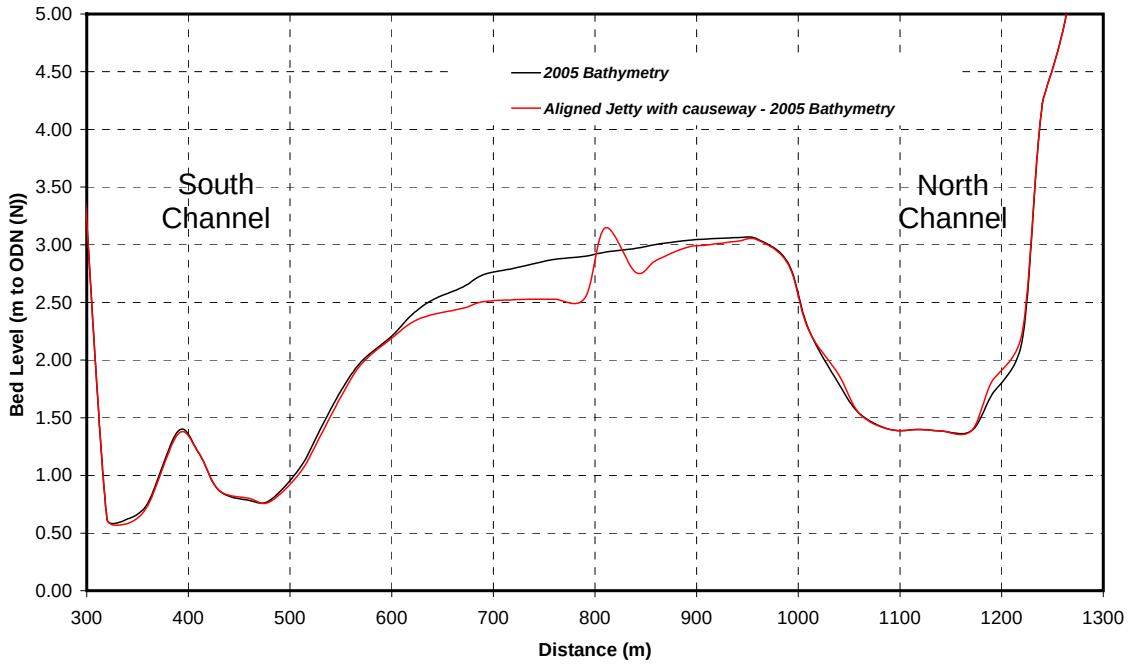

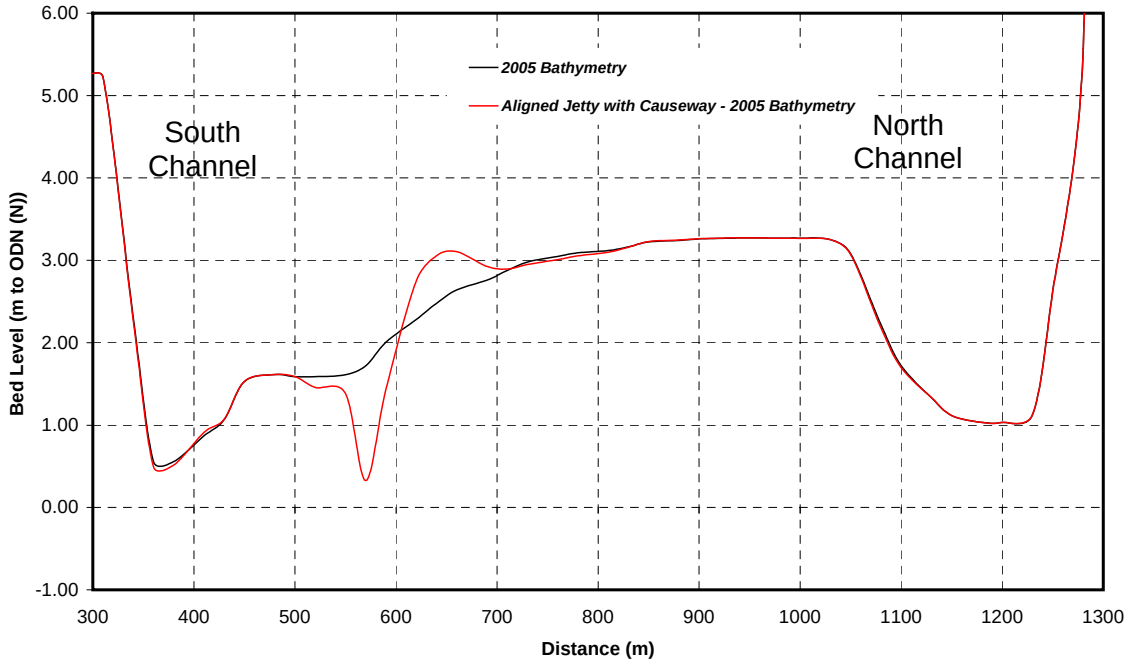

ABP mer marine environmental research	Cross–sections G and H for the aligned jetty with causeway for a spring-neap cycle and 2005 bathymetry	Figure B23

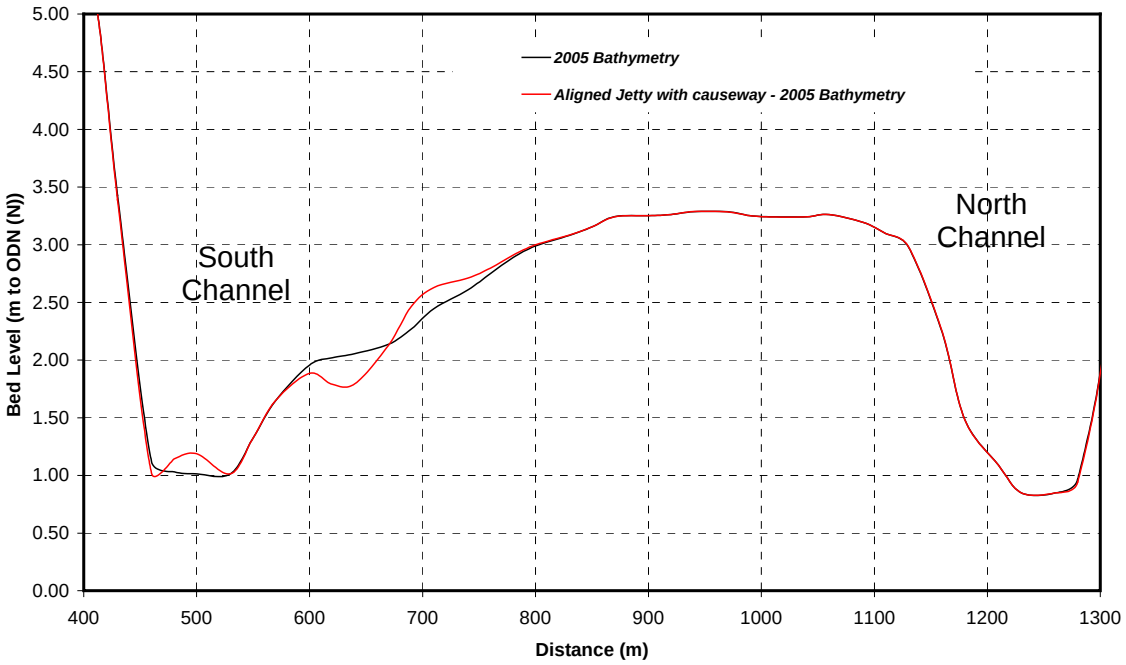

ABP mer marine environmental research

Cross–sections I and J for the aligned jetty with causeway for a spring-neap cycle and 2005 bathymetry

Figure B24

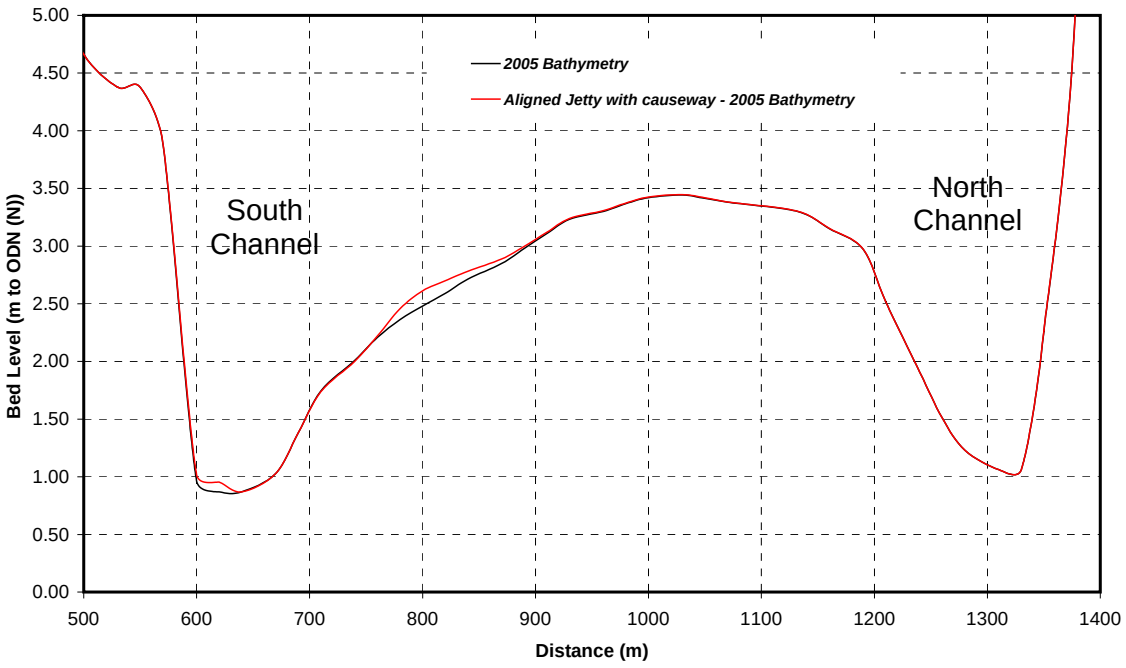

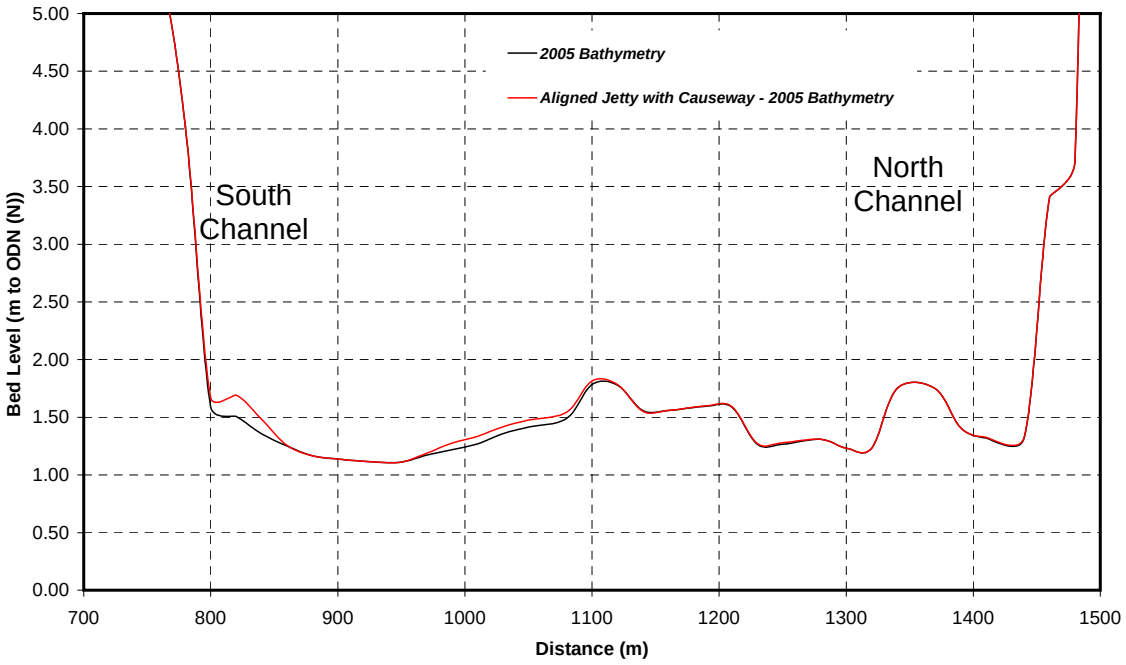

ABP mer marine environmental research	Cross–sections K and L for the aligned jetty with causeway for a spring-neap cycle and 2005 bathymetry	Figure B25

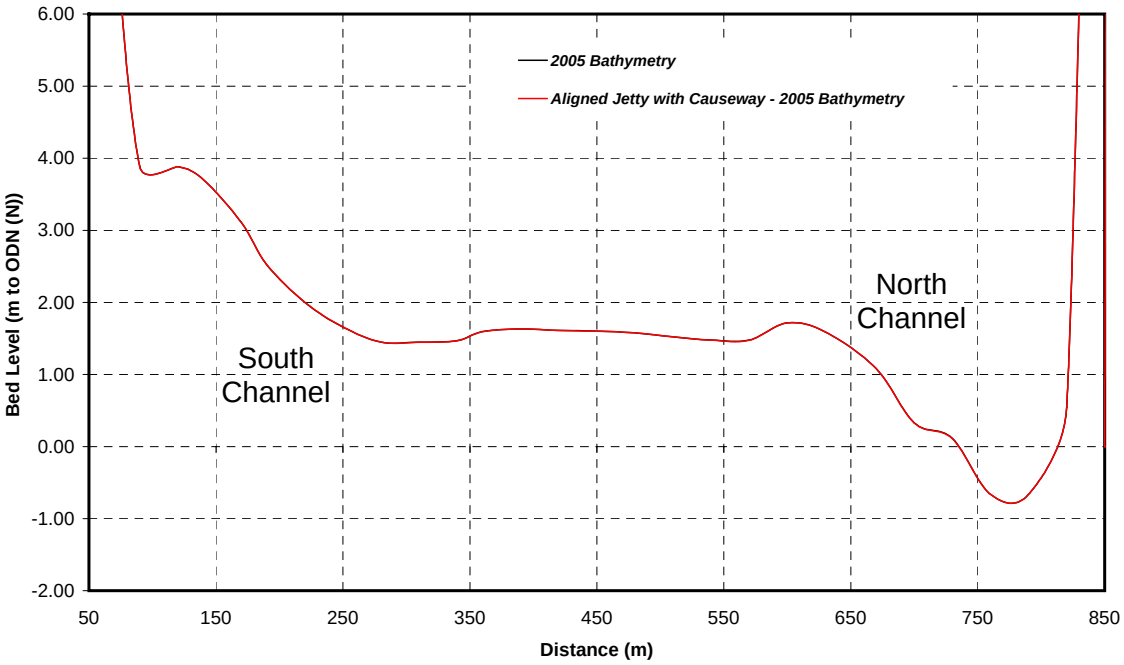

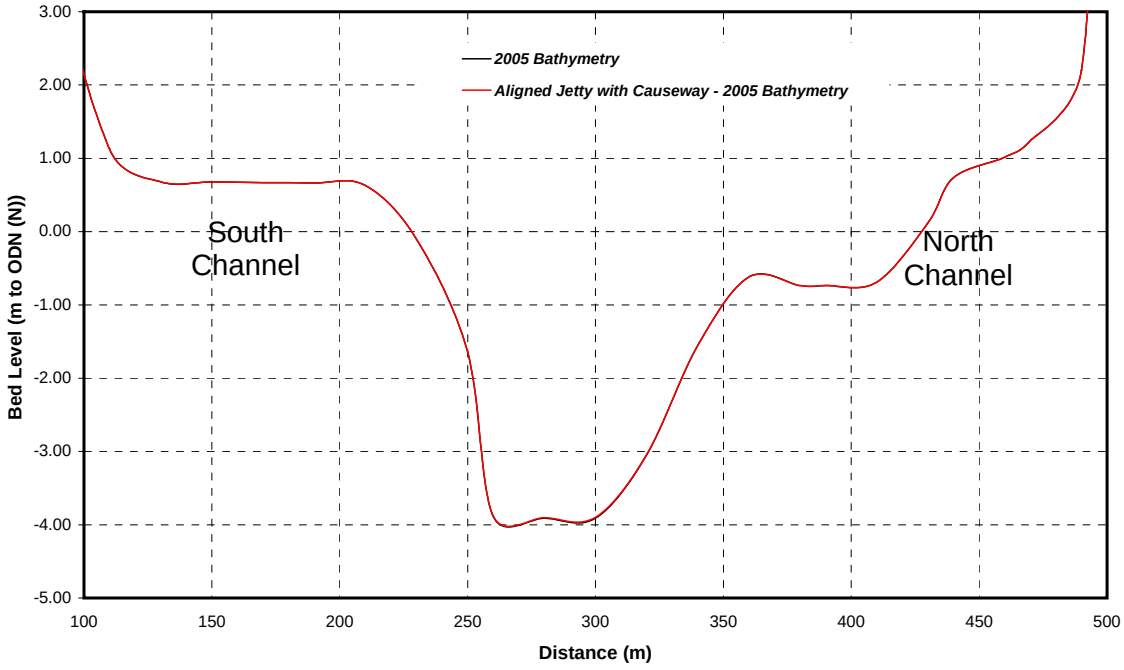

ABP mer marine environmental research

Cross–sections A and B for the aligned jetty with causeway for an extreme fluvial and surge event (1:200 years return period) using 2005 bathymetry

Figure B26

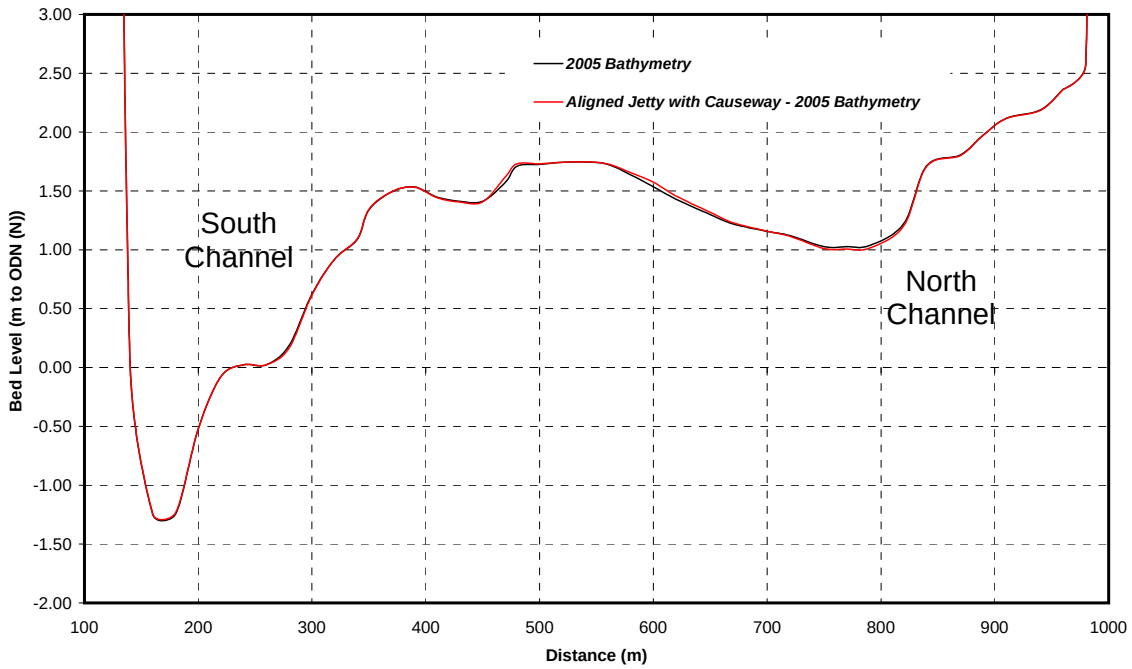

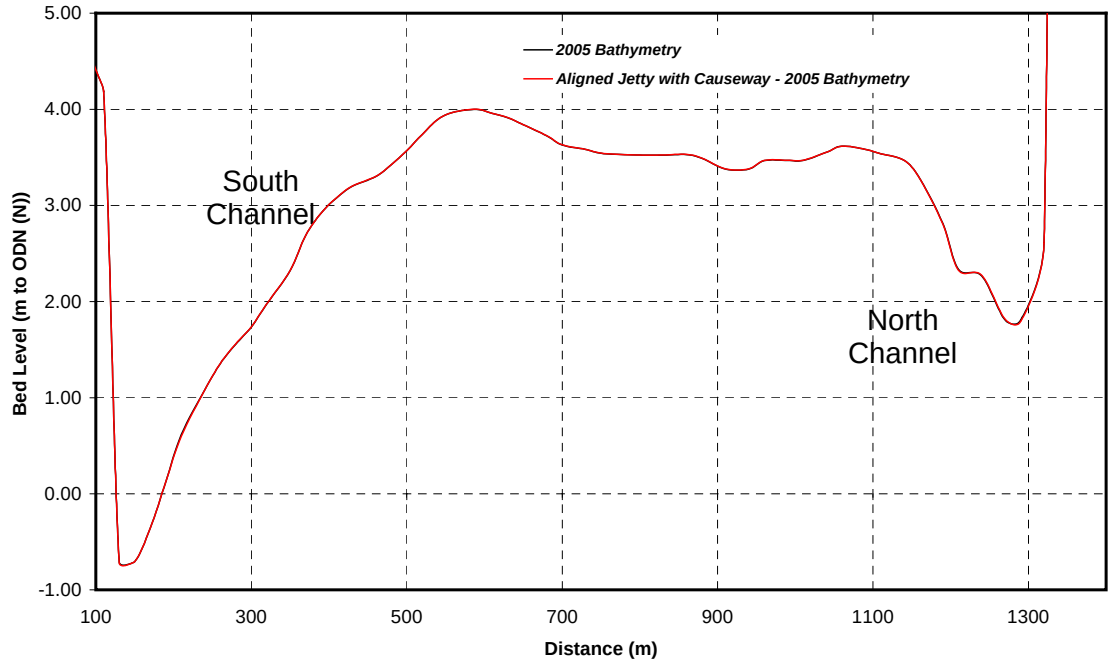

ABP mer marine environmental research	Cross–sections C and D for the aligned jetty with causeway for an extreme fluvial and surge event (1:200 years return period) using 2005 bathymetry	Figure B27

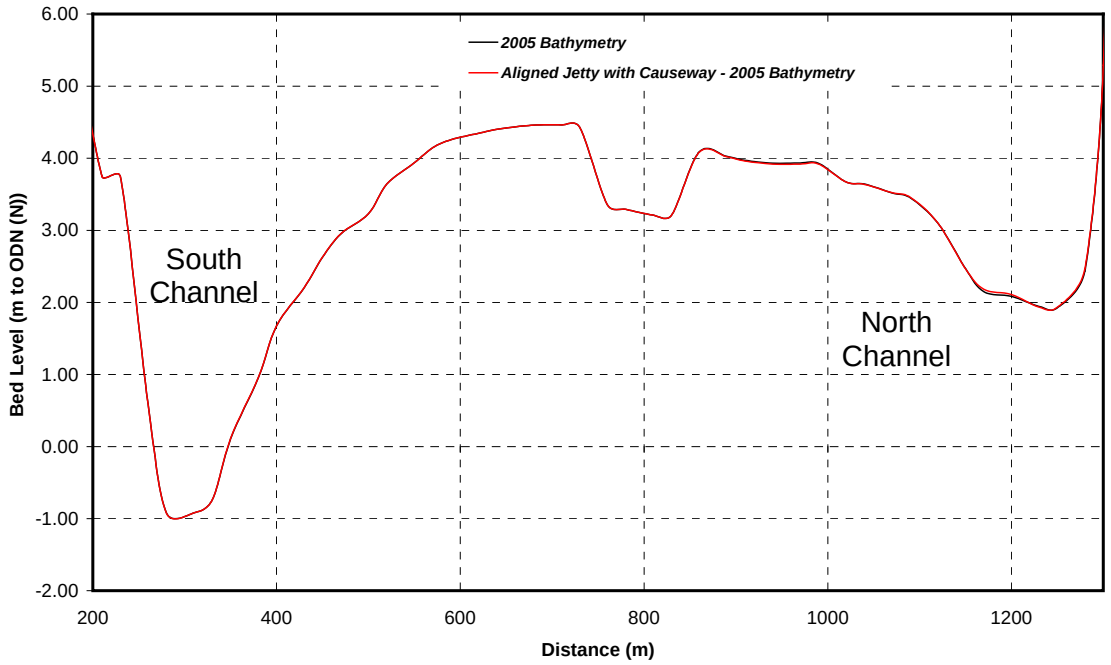

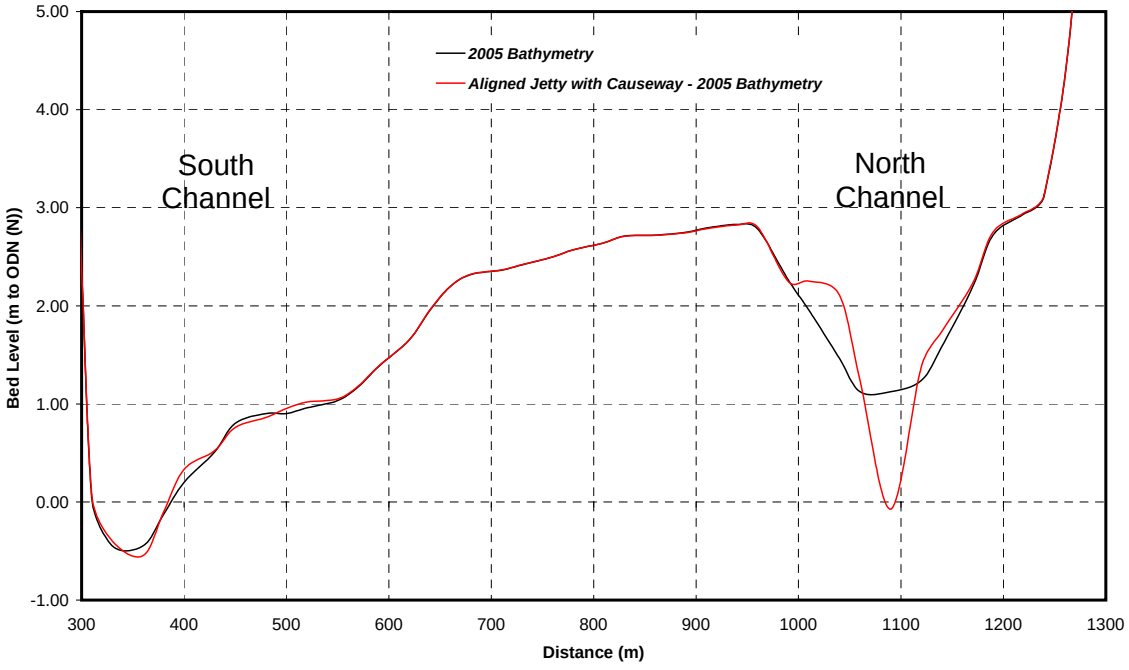

ABP mer marine environmental research	Cross–sections E and F for the aligned jetty with causeway for an extreme fluvial and surge event (1:200 years return period) using 2005 bathymetry.	Figure B28

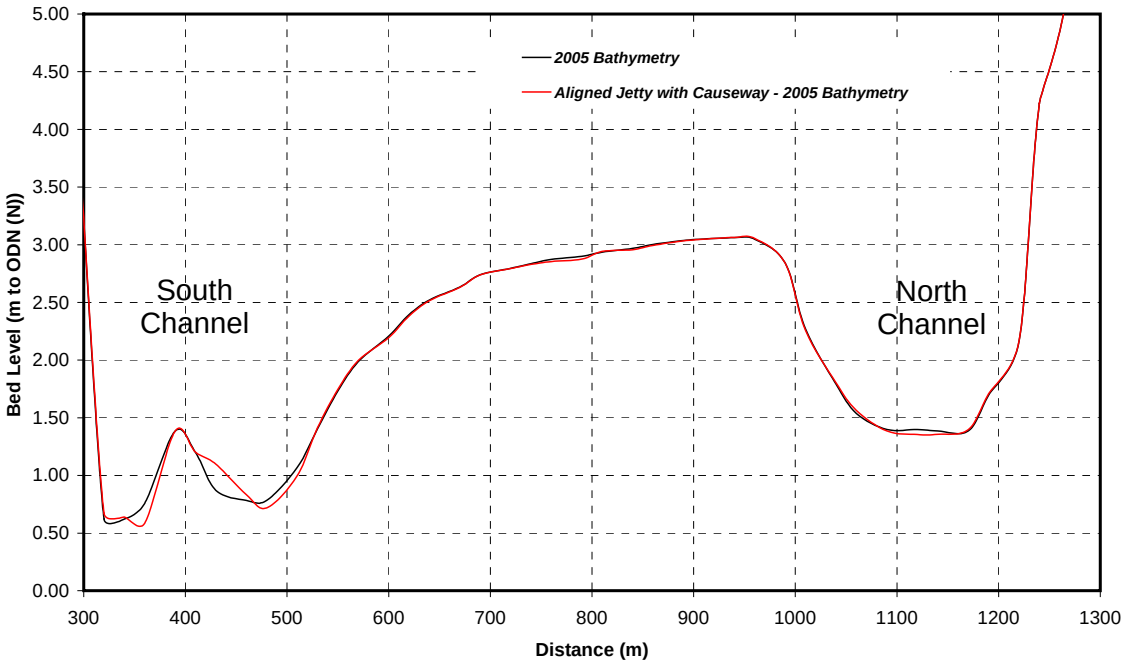

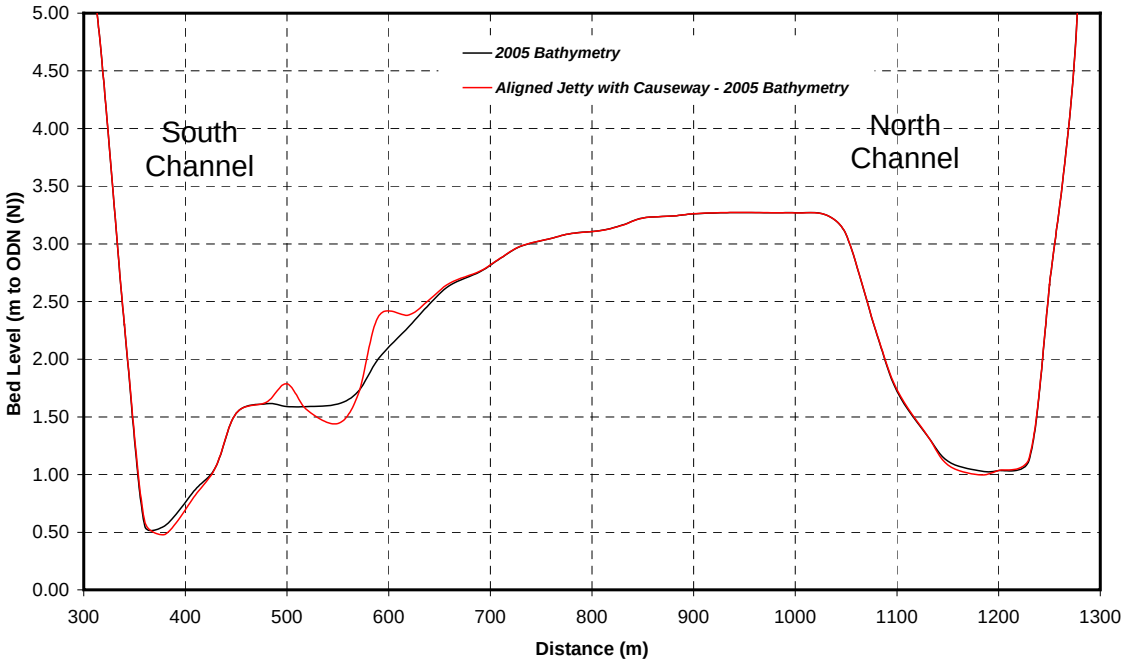

ABP mer marine environmental research	Cross–sections G and H for the aligned jetty with causeway for an extreme fluvial and surge event (1:200 years return period) using 2005 bathymetry.	Figure B29

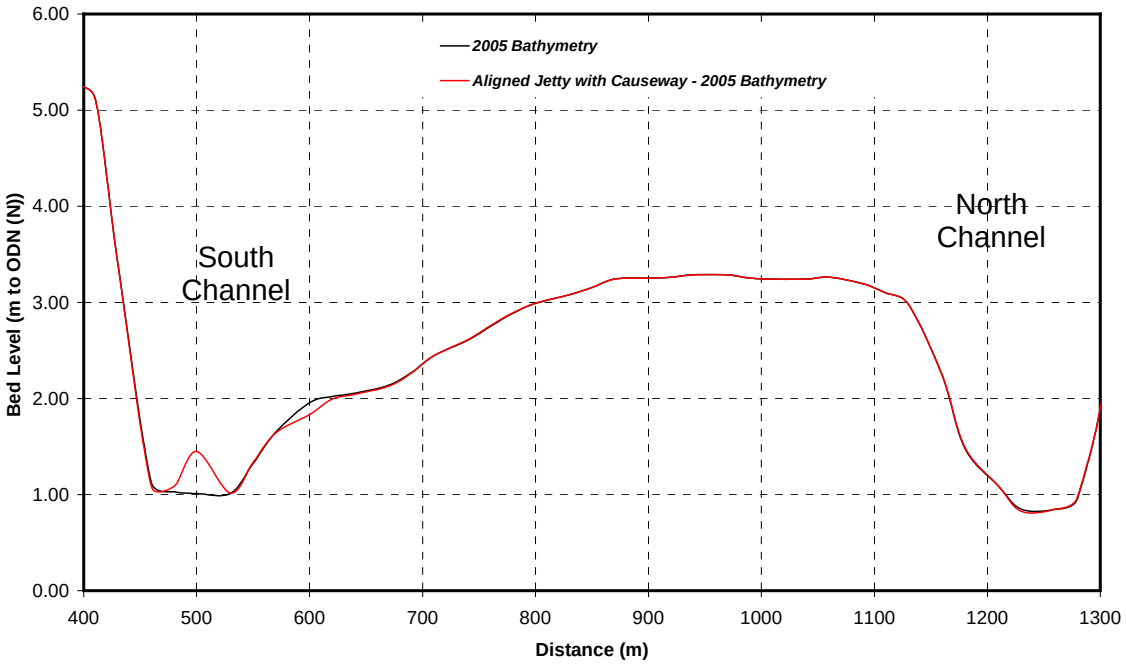

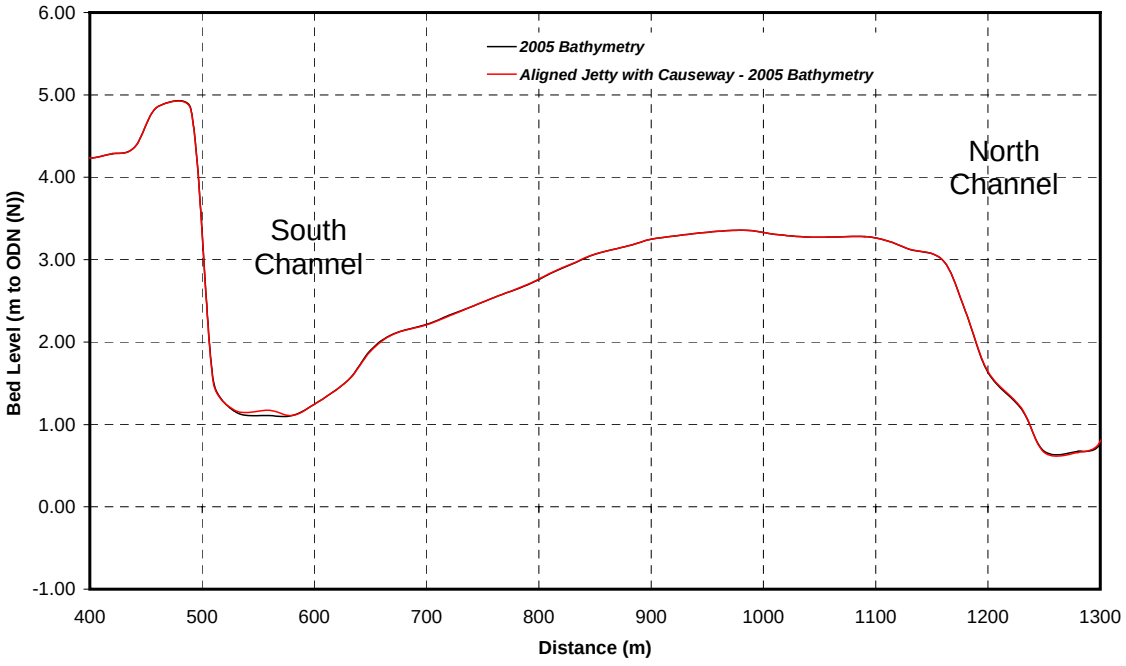

Cross–sections I and J for the aligned jetty with causeway for an extreme fluvial and surge event (1:200 years return period) using 2005 bathymetry

Figure B30

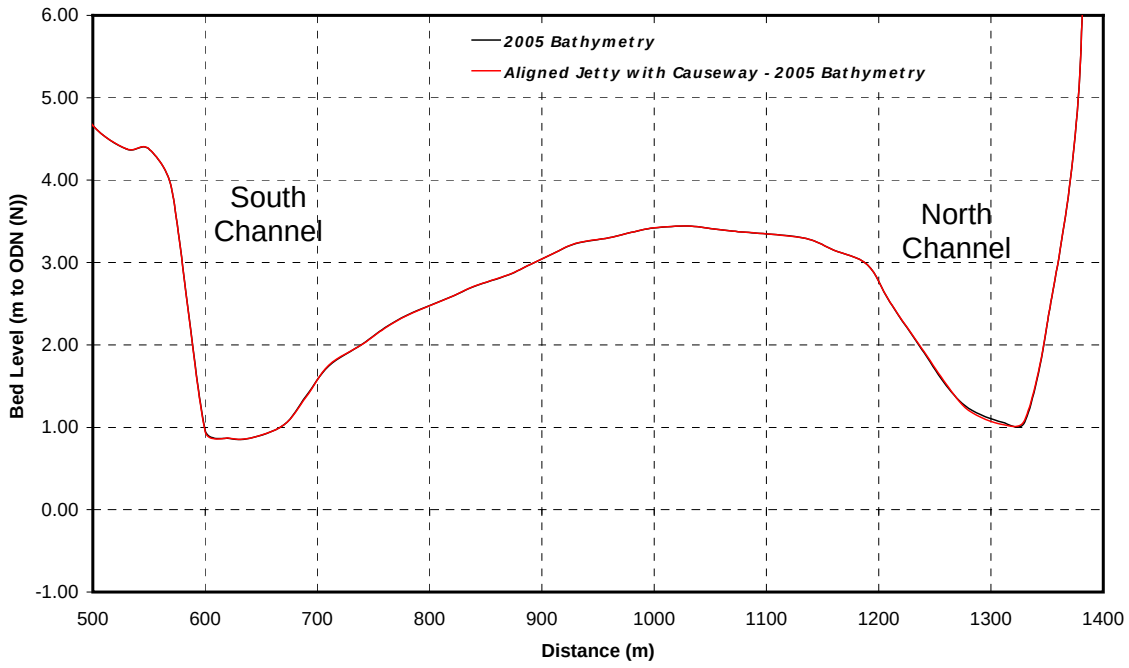

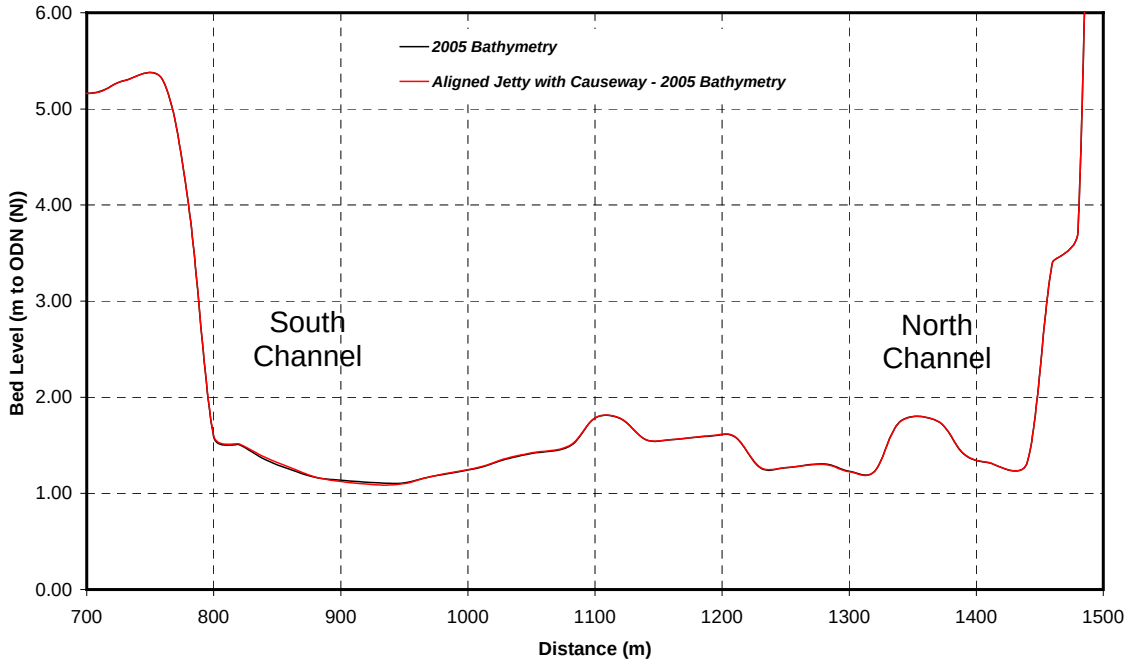

ABP mer marine environmental research	Cross–sections K and L for the aligned jetty with causeway for an extreme fluvial and surge event (1:200 years return period) using 2005 bathymetry	Figure B31

ABP Marine Environmental Research Ltd
Pathfinder House
Maritime Way
Southampton SO14 3AE

Tel: +44 (0)23 8033 8100
Fax: +44 (0)23 8033 8040

www.abpmer.co.uk

e-mail: enquiries@abpmer.co.uk